frontiers | Research Topics

Seascape ecology: From characterization to evaluation of state and change over time

Edited by
Monica Montefalcone and Carlo Nike Bianchi

Published in
Frontiers in Marine Science

FRONTIERS EBOOK COPYRIGHT STATEMENT

The copyright in the text of individual articles in this ebook is the property of their respective authors or their respective institutions or funders. The copyright in graphics and images within each article may be subject to copyright of other parties. In both cases this is subject to a license granted to Frontiers.

The compilation of articles constituting this ebook is the property of Frontiers.

Each article within this ebook, and the ebook itself, are published under the most recent version of the Creative Commons CC-BY licence. The version current at the date of publication of this ebook is CC-BY 4.0. If the CC-BY licence is updated, the licence granted by Frontiers is automatically updated to the new version.

When exercising any right under the CC-BY licence, Frontiers must be attributed as the original publisher of the article or ebook, as applicable.

Authors have the responsibility of ensuring that any graphics or other materials which are the property of others may be included in the CC-BY licence, but this should be checked before relying on the CC-BY licence to reproduce those materials. Any copyright notices relating to those materials must be complied with.

Copyright and source acknowledgement notices may not be removed and must be displayed in any copy, derivative work or partial copy which includes the elements in question.

All copyright, and all rights therein, are protected by national and international copyright laws. The above represents a summary only. For further information please read Frontiers' Conditions for Website Use and Copyright Statement, and the applicable CC-BY licence.

ISSN 1664-8714
ISBN 978-2-8325-3231-7
DOI 10.3389/978-2-8325-3231-7

About Frontiers

Frontiers is more than just an open access publisher of scholarly articles: it is a pioneering approach to the world of academia, radically improving the way scholarly research is managed. The grand vision of Frontiers is a world where all people have an equal opportunity to seek, share and generate knowledge. Frontiers provides immediate and permanent online open access to all its publications, but this alone is not enough to realize our grand goals.

Frontiers journal series

The Frontiers journal series is a multi-tier and interdisciplinary set of open-access, online journals, promising a paradigm shift from the current review, selection and dissemination processes in academic publishing. All Frontiers journals are driven by researchers for researchers; therefore, they constitute a service to the scholarly community. At the same time, the *Frontiers journal series* operates on a revolutionary invention, the tiered publishing system, initially addressing specific communities of scholars, and gradually climbing up to broader public understanding, thus serving the interests of the lay society, too.

Dedication to quality

Each Frontiers article is a landmark of the highest quality, thanks to genuinely collaborative interactions between authors and review editors, who include some of the world's best academicians. Research must be certified by peers before entering a stream of knowledge that may eventually reach the public - and shape society; therefore, Frontiers only applies the most rigorous and unbiased reviews. Frontiers revolutionizes research publishing by freely delivering the most outstanding research, evaluated with no bias from both the academic and social point of view. By applying the most advanced information technologies, Frontiers is catapulting scholarly publishing into a new generation.

What are Frontiers Research Topics?

Frontiers Research Topics are very popular trademarks of the *Frontiers journals series*: they are collections of at least ten articles, all centered on a particular subject. With their unique mix of varied contributions from Original Research to Review Articles, Frontiers Research Topics unify the most influential researchers, the latest key findings and historical advances in a hot research area.

Find out more on how to host your own Frontiers Research Topic or contribute to one as an author by contacting the Frontiers editorial office: frontiersin.org/about/contact

Seascape ecology: From characterization to evaluation of state and change over time

Topic editors

Monica Montefalcone — University of Genoa, Italy

Carlo Nike Bianchi — Retired, Italy

Citation

Montefalcone, M., Bianchi, C. N., eds. (2023). *Seascape ecology: From characterization to evaluation of state and change over time*. Lausanne: Frontiers Media SA. doi: 10.3389/978-2-8325-3231-7

Table of contents

frontiers | Frontiers in Marine Science

TYPE Editorial
PUBLISHED 27 July 2023
DOI 10.3389/fmars.2023.1254749

Check for updates

OPEN ACCESS

EDITED AND REVIEWED BY
Stelios Katsanevakis,
University of the Aegean, Greece

*CORRESPONDENCE
Monica Montefalcone
monica.montefalcone@unige.it

RECEIVED 07 July 2023
ACCEPTED 17 July 2023
PUBLISHED 27 July 2023

CITATION
Montefalcone M and Bianchi CN (2023) Editorial: Seascape Ecology: from characterization to evaluation of state and change over time. *Front. Mar. Sci.* 10:1254749. doi: 10.3389/fmars.2023.1254749

COPYRIGHT
© 2023 Montefalcone and Bianchi. This is an open-access article distributed under the terms of the Creative Commons Attribution License (CC BY). The use, distribution or reproduction in other forums is permitted, provided the original author(s) and the copyright owner(s) are credited and that the original publication in this journal is cited, in accordance with accepted academic practice. No use, distribution or reproduction is permitted which does not comply with these terms.

Editorial: Seascape Ecology: from characterization to evaluation of state and change over time

Monica Montefalcone[1,2]* and Carlo Nike Bianchi[3]

[1]Seascape Ecology Laboratory (SEL), Department of Earth, Environmental and Life Sciences (DiSTAV), University of Genoa, Genova, Italy, [2]National Biodiversity Future Center (NBFC), Palermo, Italy, [3]Department of Integrative Marine Ecology (EMI), Genoa Marine Centre (GMC), Stazione Zoologica Anton Dohrn - National Institute of Marine Biology, Ecology and Biotechnology, Genova, Italy

KEYWORDS

seafloor mapping, seagrass meadows, macroalgae, rocky reefs, rhodolith beds, vermetid reefs, biotic indices, bioconstruction

Editorial on the Research Topic

Seascape Ecology: from characterization to evaluation of state and change over time

Introduction

Landscape ecology was born in the 1930s when aerial photography was first adopted to study the spatial structure and heterogeneity of terrestrial ecosystems, in contrast to 'classical' ecology that tended to think in terms of populations and communities living in a homogeneous environment (Troll, 1939). It became a discrete, established discipline in the 1980s, with the founding of the International Association for Landscape Ecology (IALE). For long, landscape ecology remained a substantially terrestrial discipline, due to the lack of perception of submerged landscapes and the difficulty of considering the sea as territory (Bianchi et al., 2012). It has been necessary to wait for decades to see the transfer of landscape approaches and language to marine ecosystems: apart from early attempts (e.g., Cocito et al., 1991), seascape ecology became a recognized field of research only in the 2010s, when well-known marine ecological journals published Research Topics on seascape ecology (Pittman et al., 2011; Hidalgo et al., 2016), IALE chose seascape ecology as the main theme of one of its annual meetings (Liski et al., 2015) and two books dealing with seascape ecology were published (Musard et al., 2014; Pittman, 2018). Seascape is to be intended as the totality of natural and anthropogenic characters of a marine region.

As its terrestrial counterpart, seascape ecology deals with the spatial configuration of ecosystems and consider environmental heterogeneity and dynamics as the main subjects of study and the keys for ecosystem functioning and persistence. Of course, diversity patterns on land and in the sea are different (Boudouresque et al., 2014) and seascapes cannot be equated to landscapes (Manderson, 2016). Seascapes are often perceived to be in more natural conditions with respect to landscapes (Bianchi et al., 2005). However, integrated landscape-seascape spatial analyses are rarely attempted: in the case of the overcrowded Gulf of Naples (southern Italy), the landscape exhibits higher patch edge dimension, diversity and evenness, and a lower fractal dimension than the seascape (Appolloni et al., 2018). Through marine geospatial modelling, seascape approaches

represent an important decision-support tool for integrated coastal zone management (Parravicini et al., 2012).

Contributions

This Research Topic makes the point of an emerging discipline that is barely a decade old. The nine research articles here included illustrate some of the latest achievements in the field. Seascape ecology relies on special technologies such as remote sensing (either acoustic or optical), robotics, and scuba diving. Consistently, a majority of articles deal with recent advances in high-resolution marine habitat mapping. Józef et al. combined hydroacoustics and inspections to compare macroalgal meadows in two contrasting climate regimes in the Svalbards. Spyksma et al. applied diver-generated photomosaics to the temperate rocky reef ecosystems of north-eastern New Zealand. Photomosaics were an output of structure-from-motion photogrammetry, a technique that utilises numerous overlapping images, well established in terrestrial applications but still comparatively little employed in the sea. Ventura et al. integrated aerial and water surface low-cost drones for the cartography of coastal benthic habitats (beach wrack deposits, hard bottoms and seagrass meadows) in central Tyrrhenian Sea, Italy. Tomasello et al. employed photogrammetry by unmanned aerial vehicles to elaborate high-resolution digital elevation model of a giant beach wrack on the westernmost coast of Sicily, adjacent to one of the largest *Posidonia oceanica* meadows in the Mediterranean Sea. de Almeida et al. mapped mixed seagrass meadows in the Mexican Caribbean using satellite imagery and supervised classification based on sea truthing. The functioning of a mixed tropical seagrass meadow was studied by Cui et al., who analyzed the food web of the meadow composed of five species (*Enhalus acoroides*, *Thalassia hemprichii*, *Cymodocea rotundata*, *Halodule uninervis*, and *Halophila ovalis*) in South China Sea, using triple stable isotopes and fatty acid signatures.

Bioconstruction is a peculiar feature of the marine environment. Vermetid reefs are an outstanding example of bioconstruction that modify coastal seascapes forming platforms in the intertidal zone of rocky coasts; with their three-dimensional and seaward-expanding structure, they support high biodiversity levels and provide important ecological functions and ecosystem services. Picone and Chemello characterized a vermetid reef in Sicily (Italy) by means of unmanned aerial vehicle imagery.

Habitat characterization, to identify types, is the first phase of the process of environmental diagnostics, a typical application of seascape ecology; the second and final phase is evaluation, to define status and values. Ecological indices are a major tool to achieve the latter target. Astruch et al. developed an ecosystem-based index to assess the health status of coastal detritic bottoms, one of the most extensive habitats of the continental shelf worldwide, in the upper levels of the circalittoral zone. The index was tested in southern France, where rhodoliths (free living coralline algae) characterizes the seascape and might be an indicator of good environmental status for this kind of marine habitat. Thanks to the availability of a large dataset encompassing a wide array of descriptors, Oprandi et al. compared the performance of eleven indices relative to three habitats/biotic components (reefs, seagrass, and fish) in a marine protected area of Sardinia, Italy.

Perspectives

Efforts on seascape ecology like those in this Research Topic should be fostered, as the acceleration of environmental crises related to climate change, widespread sea pollution, and growing ocean overexploitation represent ever growing threats to marine ecosystems. In particular, future research should aim at increasing our understanding of seascape responses to environmental change, in order to offer information useful to develop tools to mitigate human impact on the marine environment.

Author contributions

MM: Writing – original draft, Writing – review & editing. CB: Writing – original draft, Writing – review & editing.

Acknowledgments

We thank the contributing authors, reviewers, and the Frontiers in Marine Science editorial staff for their support in producing this Research Topic.

Conflict of interest

The authors declare that the research was conducted in the absence of any commercial or financial relationships that could be construed as a potential conflict of interest.

Publisher's note

All claims expressed in this article are solely those of the authors and do not necessarily represent those of their affiliated organizations, or those of the publisher, the editors and the reviewers. Any product that may be evaluated in this article, or claim that may be made by its manufacturer, is not guaranteed or endorsed by the publisher.

References

Appolloni, L., Sandulli, R., Bianchi, C. N., and Russo, G. F. (2018). Spatial analyses of an integrated landscape-seascape territorial system: the case of the overcrowded Gulf of Naples, Southern Italy. *J. Environ. Accounting Manage.* 6 (4), 365–380. doi: 10.5890/JEAM.2018.12.009

Bianchi, C. N., Catra, M., Giaccone, G., and Morri, C. (2005). "Il paesaggio marino costiero: ambienti e diversità," in *Mediterraneo: Ambienti, Paesaggio, Diversità*. Eds. A. Cosentino, A. La Posta, A. M. Maggiore and N. Tartaglini (Milano: Téchne), 30–61.

Bianchi, C. N., Parravicini, V., Montefalcone, M., Rovere, A., and Morri, C. (2012). The challenge of managing marine biodiversity: a practical toolkit for a cartographic, territorial approach. *Diversity* 4, 419–452. doi: 10.3390/d4040419

Boudouresque, C. F., Ruitton, S., Bianchi, C. N., Chevaldonné, P., Fernandez, C., Harmelin-Vivien, M., et al. (2014). "Terrestrial versus marine diversity of ecosystems. And the winner is: the marine realm," in *Proceedings of the 5th Mediterranean symposium on marine vegetation*, (Tunis: UNEP/MAP–RAC/SPA) 11–25.

Cocito, S., Bianchi, C. N., Degl'Innocenti, F., Forti, S., Morri, C., Sgorbini, S., et al. (1991). "Esempio di utilizzo di descrittori ambientali nell'analisi ecologica del paesaggio sommerso marino costiero," *Atti della Società Italiana di Ecologia* 13, 65–68.

Hidalgo, M., Secor, D. H., and Browman, H. I. (2016). Introduction to the Themed Section: 'Seascape Ecology'. Observing and managing seascapes: linking synoptic oceanography, ecological processes, and geospatial modelling. *ICES J. Mar. Sci.* 73 (7), 1825–1830. doi: 10.1093/icesjms/fsw079

Liski, A., Metzger, M., and Wilson, M. (2015). "Seascape ecology: connecting land, sea and society," in *Proceedings of the 22nd IALE UK Conference (Edinburgh 7-9 September 2015)*. (United Kingdom: University of Edimburg), 9191.

Manderson, J. P. (2016). Seascapes are not landscapes: an analysis performed using Bernhard Riemann's rules. *ICES J. Mar. Sci.* 73 (7), 1831–1838. doi: 10.1093/icesjms/fsw069

Musard, O., Le Dû-Blayo, L., Francour, P., Beurier, J. P., Feunteun, E., and Talassinos, L. (2014). *Underwater Seascapes: from Geographical to Ecological Perspectives* (Cham, Switzerland: Springer), 291.

Parravicini, V., Rovere, A., Vassallo, P., Micheli, F., Montefalcone, M., Morri, C., et al. (2012). Understanding relationships between conflicting human uses and coastal ecosystems status: a geospatial modeling approach. *Ecol. Indic.* 19, 253–263. doi: 10.1016/j.ecolind.2011.07.027

Pittman, S. J. (2018). *Seascape Ecology* (Oxford: Wiley Blackwell), 501.

Pittman, S., Kneib, R., Simenstad, C., and Nagelkerken, I. (2011). Seascape ecology: application of landscape ecology to the marine environment. *Mar. Ecol. Prog. Ser.* 427, 187–302. doi: 10.3354/meps09139

Troll, C. (1939). Luftbildplan und ökologische Bodenforschung. *Z. der Gesellschaft für Erdkunde zu Berlin* 7/8, 241–298.

frontiers | Frontiers in Marine Science

ORIGINAL RESEARCH
published: 23 June 2022
doi: 10.3389/fmars.2022.903138

3D-Reconstruction of a Giant *Posidonia oceanica* Beach Wrack (*Banquette*): Sizing Biomass, Carbon and Nutrient Stocks by Combining Field Data With High-Resolution UAV Photogrammetry

Agostino Tomasello[1], Alessandro Bosman[2,3], Geraldina Signa[1,4]*, Sante Francesco Rende[3], Cristina Andolina[1,4], Giovanna Cilluffo[1,4], Federica Paola Cassetti[1], Antonio Mazzola[1,4], Sebastiano Calvo[1], Giovanni Randazzo[5], Alfonso Scarpato[3] and Salvatrice Vizzini[1,4]*

[1] Department of Earth and Marine Sciences (DiSTeM), University of Palermo, Palermo, Italy, [2] Institute of Environmental Geology and Geoengineering, National Research Council (CNR-IGAG), Rome, Italy, [3] Department for Environmental Monitoring and Protection and Biodiversity Conservation (BIO-DIR), National Institute for Environmental Protection and Research (ISPRA), Rome, Italy, [4] National Inter-University Consortium for Marine Sciences (CoNISMa), Rome, Italy, [5] Department of Mathematics and Computer Science, Physics and Earth Sciences, University of Messina, Messina, Italy

OPEN ACCESS

Edited by:
Monica Montefalcone, University of Genoa, Italy

Reviewed by:
Joseph Anthony Borg, University of Malta, Malta
Arnaldo Marín, University of Murcia, Spain

***Correspondence:**
Geraldina Signa
geraldina.signa@unipa.it
Alessandro Bosman
alessandro.bosman@cnr.it

Specialty section:
This article was submitted to Marine Ecosystem Ecology, a section of the journal Frontiers in Marine Science

Received: *23 March 2022*
Accepted: *26 May 2022*
Published: *23 June 2022*

Citation:
Tomasello A, Bosman A, Signa G, Rende SF, Andolina C, Cilluffo G, Cassetti FP, Mazzola A, Calvo S, Randazzo G, Scarpato A and Vizzini S (2022) 3D-Reconstruction of a Giant Posidonia oceanica *Beach Wrack (Banquette): Sizing Biomass, Carbon and Nutrient Stocks by Combining Field Data With High-Resolution UAV Photogrammetry. Front. Mar. Sci. 9:903138. doi: 10.3389/fmars.2022.903138*

Beach wracks are temporary accumulations of vegetal detritus that can be found along coastlines all over the world. Although beach wracks are often perceived as a nuisance for beach users, they play a crucial ecological role in carbon and nutrient connectivity across ecosystem boundaries, especially when they reach a relevant size, as in the case of the wedge-shaped seagrass accumulations called *banquette*. In this study, three-dimensional mapping of a giant *Posidonia oceanica banquette* was carried out for the first time using high-resolution UAV photogrammetry combined with field sampling and compositional and chemical analysis. The combined approach allowed a reliable estimation of the amount and spatial distribution of both vegetal biomass and sedimentary mass, as well as of total carbon, nitrogen and phosphorus content, revealing that i) *banquette* act as a sediment trap and represent hot spots of seagrass biomass and carbon accumulation; ii) *banquette* thickness, rather than the distance from the sea, influences the spatial distribution of all variables. Moreover, high-resolution digital elevation models (DEM) revealed discontinuous patterns in detritus accumulation resulting in an unknown *banquette* type here termed "Multiple Mega-Ridge *banquette*" (MMR *banquette*). On the one hand, this study highlighted the high potential of the UAV approach in very accurately 3D mapping and monitoring of these structures, with relevant implications for ecosystem service estimation and coastal zone management. On the other hand, it opened new questions about the role played by temporary beach wracks and, in particular, by *P. oceanica banquette* in the blue carbon exchange across land-ocean boundaries.

Keywords: blue carbon, nitrogen, drone, seascape, seagrass, litter, detritus, mega-ridge banquette

1 INTRODUCTION

Beach wracks are temporary accumulations of detached seagrasses and, to a lesser extent, macroalgae drifting along the shorelines, and they represent a significant fraction of primary production exported through waves and currents from blue carbon ecosystems (Duarte, 2017). They play a critical role in protecting the shoreline from coastal erosion (De Falco et al., 2008; Boudouresque et al., 2016). Being a temporary sink of biogenic carbon and nutrients (Mateo et al., 2003; Jiménez et al., 2017), beach wracks provide an important energy subsidy to adjoining coastal systems and dunes (Del Vecchio et al., 2013; Del Vecchio et al., 2017), supporting beach biodiversity and trophic webs (Lastra et al., 2008; Colombini et al., 2009; Beltran et al., 2020). However, in general, beach users consider these detrital accumulations a nuisance, prompting local administrators and beach managers to find sustainable solutions for their management (Mossbauer et al., 2012; Rotini et al., 2020). Because of the important implications for the connectivity between marine and terrestrial habitats, as well as coastal zone management, monitoring of beach wracks is a priority nowadays. To our knowledge, the first attempt in this direction was made along the Kenyan coast using a visual assessment technique, which required very time-consuming and demanding fieldwork (Ochieng and Erftemeijer, 1999) and produced highly uncertain outcomes, since beach wrack shapes are not comparable with standard geometric figures. At a later date, a video-monitoring and photo-shooting approach, using fixed cameras deployed on coastal beaches, was applied to seagrass wrack depositions along the German Baltic, Danish, Spanish and Italian coastlines (Mossbauer et al., 2012; Gómez-Pujol et al., 2013; Simeone et al., 2013; Pan et al., 2022). While this approach is certainly less expensive and time-consuming than a visual assessment, there are evident technical limitations, mainly related to the fixed position of the cameras.

In the last two decades, a new approach based on Unmanned Aerial Vehicles (UAVs) has been increasingly used for surveying and mapping terrestrial and coastal ecosystems. This approach bridges the gap between field assessment and traditional remote sensing while overcoming the logistic and economic constraints of both approaches (Anderson and Gaston, 2013). Briefly, the main advantages of UAVs stem from their low cost, small size, and lightweight, together with a high automation level and photographic accuracy (Remondino et al., 2011; Anderson and Gaston, 2013). UAVs fly at low altitudes even over remote and inaccessible areas (Castellanos-Galindo et al., 2019), providing rapid, cost-effective, and high-resolution topographic mapping and 3D-reconstructions (Remondino et al., 2011). These aspects make UAVs incredibly versatile and suitable for addressing many aspects of coastal zone monitoring and management, as recently reviewed by Adade et al. (2021). In more detail, the most frequent environmental UAV applications today are mapping and classification of sensitive ecosystems (e.g., Casella et al., 2017; Murfitt et al., 2017; Castellanos-Galindo et al., 2019; Tomasello et al., 2020), marine fauna (Schofield et al., 2019) and marine litter (Deidun et al., 2018), and monitoring of beach morpho-dynamics (Apostolopoulos and Nikolakopoulos, 2021 and references therein; Randazzo et al., 2021). UAVs were also used to map seagrass beach wracks by applying a two-dimensional mapping approach (Ventura et al., 2018; Pan et al., 2021), whereas, to our knowledge, three-dimensional mapping has never been carried out, although it is a necessary condition for obtaining good estimates of the volume and biomass of beach wracks, especially very large-sized ones.

Posidonia oceanica (L.) *Delile*, 1813 is an endemic seagrass of the Mediterranean Sea, where it plays key ecological roles and provides multiple ecosystem services (Vizzini, 2009; Campagne et al., 2014; Ondiviela et al., 2014). A large volume of seagrass biomass is seasonally detached from living plants by autumn and winter storms and reaches the coast where it may accumulate forming accumulations that vary from ephemeral and scattered small piles to much more compact structures up to several metres high (Gómez-Pujol et al., 2013; Boudouresque et al., 2016) that are known as *banquette* (Boudouresque and Meinesz, 1982; de Grissac, 1984). Due to a combination of hydrodynamic and geomorphological factors, sheltered beaches are particularly affected by the accumulation of seagrass litter occurring mainly from autumn to spring and characterised by marked spatial and temporal dynamics (Mateo, 2010; Simeone and De Falco, 2012; Simeone et al., 2013).

In light of the crucial ecological role played by seagrass beach wracks, as described above, and, in particular, of their function as a temporary sink/source of biogenic carbon and nutrients, we propose an innovative combined framework for estimating their size, along with biomass and nutrient bulk. More specifically, we show how the integration of high-resolution UAV photogrammetry with field sampling and laboratory analyses allows the estimation, with a high degree of accuracy, of the vegetal biomass, nutrient (carbon, nitrogen, and phosphorus) and sediment content of even very large seagrass beach wracks, such as, in this study, the largest *P. oceanica banquette* ever described.

2 MATERIALS AND METHODS

2.1 Study Area

The study was conducted at Faro beach within the area of Capo Feto, on the westernmost coast of Sicily, located between the towns of Mazara del Vallo and Marsala (**Figure 1**). Faro beach is a north-south oriented beach, about 600 m long, exposed to the west sectors where seagrass litter accumulates along the shore forming a wide *banquette* (**Figure 2A**). The back dune hosts an ecologically important wide salt marsh protected by several European Community regulations (Pernice et al., 2004) while offshore, the marine coastal area hosts a large *Posidonia oceanica* meadow growing on *matte* (Di Carlo et al., 2005), which is one of the largest *P. oceanica* meadows in the Mediterranean Sea (Calvo et al., 2010). *P. oceanica* also forms shallow barrier reefs that run parallel to the coastline and trap seagrass detritus (leaves, rhizomes and roots) that is then pushed toward the beach by strong winds and waves (Maccarrone, 2010).

Dominant westerly winter winds generate high-energy waves over the shallow seagrass meadows of Capo Feto (Di Carlo et al.,

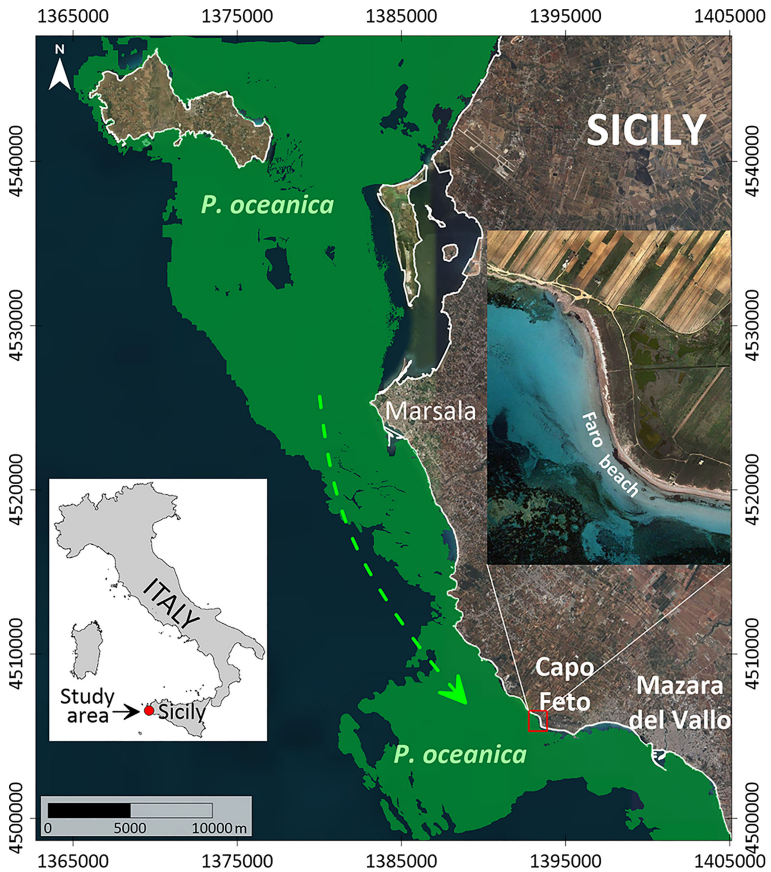

FIGURE 1 | Location of the study area in the western sector of Sicily Island and Faro beach within the Capo Feto area. The green area shows the distribution of *Posidonia oceanica*, green the white arrow indicates the prevalent direction of the littoral drift.

FIGURE 2 | **(A)** Aerial photograph of the *banquette* along the coast of Faro beach in the Capo Feto area. **(B)** Ground control point (GCP) measurement by GNSS receiver. **(C)** Detail of a *banquette* Mega-ridge.

2005). To describe in more detail the hydrodynamic regime in the study area, we used a hindcasting model provided by the NOAA (National Oceanic and Atmospheric Administration) (Chawla et al., 2013) and the new Climate Forecast System Reanalysis Reforecast (CFSRR) (https://polar.ncep.noaa.gov/waves/hindcasts/) of the National Center for Environmental Prediction (NCEP). The graph polar of wave climate (**Supplementary Figure 1A**) shows that the main storms come from the western sectors, while small storms come from the South-eastern (SE) slopes with frequencies lower than 8%. Indeed, a dominant wave climate comes predominantly from the WNW (between 280° and 300°) with maximum fetch available (**Supplementary Figure 1B**), open to the West (270°). This attack direction shows a general WNW - SES wave development and causes a general south-eastward littoral drift (Randazzo and Lanza, 2020).

2.2 Image Data Acquisition and Processing

2.2.1 Image Data Acquisition

An inspection of sequences of historical images from Google Earth enabled evaluation of the very high variability of the extent of seagrass litter accumulations in the area, which can range from 0 to about 100 m in width from the shoreline towards the sea. In particular, we surveyed the area both when the *banquette* was totally absent (here defined as pre-*banquette*) to collect data about the morphological structure of the beach, and when a large *banquette* was present (post-*banquette*) to calculate its magnitude. In this paper, we present data collected on 21 February 2019 and 05 December 2019, which represent the absence and presence of *banquette*, respectively (**Figures 3A, B**). To reconstruct the morphological features of the beach and the coastline before the deposition of the *banquette*, the first survey was conducted in three different sub-areas (**Figure 3A**), using a DJI Mavic 1 equipped with a camera with a frame 1/2.3 CMOS sized 12.35 Mpx sensor. The focal length was 26 mm (35 mm format equivalent) and the flight distance from the ground was 30 m, resulting in a ground sampling distance spanning from 1 cm/pixel.

We acquired 294 photos from three flights on 21 February 2019 (**Figure 3A**), between 11:51 and 13:36 CET and we processed the images of the UAV surveys using photogrammetry Pix4D mapper software (see below for the processing of collected data). The area of the reconstructed surface is 22,000 m^2, resulting in an average point density with equidistance of about 2 cm. For this first survey, no Global Navigation Satellite Systems (GNSS) Ground Control points (GCPs) were detected; however, the survey was corrected for the second survey (05 December 2019) using 40 homologous geo-referenced points.

To reconstruct the morphological structures of the *banquette*, on 05 December 2019 the second extensive survey was

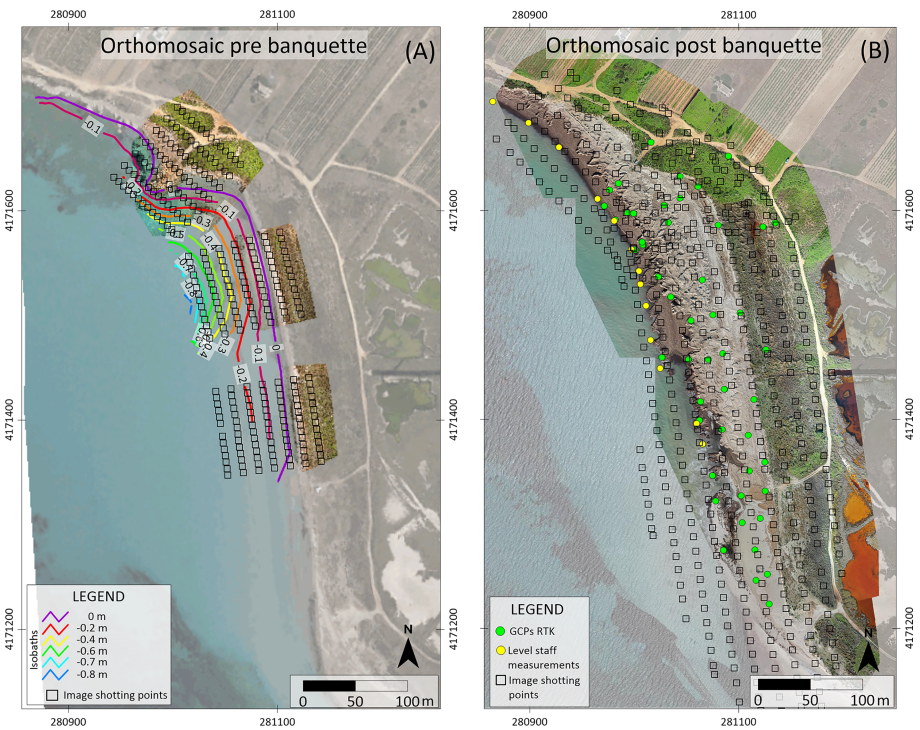

FIGURE 3 | Photogrammetric surveys of Capo Feto headland. **(A)** Orthomosaic map before (21 February 2019) the deposition of the *banquette* and location of image shooting points and isobaths reconstructed from the measurements made using a metric rod and photogrammetric survey in very shallow water; **(B)** Orthomosaic map after (05 December 2019) the deposition the *banquette*, location of Ground Control Points and level staff measurements.

conducted using a DJI Mavic 2 Pro equipped with a Hasselblad Camera with 1 "full-frame 20 Mpx CMOS sensor. Focal length was 10.26 mm (corresponding to 28 mm/35 mm equivalent focal lengths) and flight distances from the ground ranged between 45 m and 46 m, resulting in a ground sampling distance spanning from 1 cm/pixel. We acquired 900 photos from three flights on 05 December 2019 between 11:51 and 13:36 CET (**Figure 3B**), using Pix4D Capture software. In this case, Pix4D Mapper generated a point cloud composed of 37.5 × 106 vertices (**Figure 3B**). The area of the reconstructed surface was 113,500 m^2, resulting in an average point density with equidistance of about 3 cm. For these UAV flights, a topographic survey was carried out using a GNSS receiver. We measured 46 GCPs (**Figure 2B**) evenly distributed along the coast both on the *banquette* and on the road (**Figure 3B**) using a GNSS HiPerHR Topcon receiver in Real Time Kinematics (RTK afterwards) with sub-centimetric accuracy, which was used for model geo referencing. We used the Sicilian GNSS TOPCON network (GPS and GLONASS) for RTK corrections with a single base located 20 km away from the survey area. Furthermore, to check the depth of the *banquette* below the water in the outermost part of the accumulation, we made 13 measurements with a level staff and GNSS receiver (yellow points in **Figures 2C** and **3B**). These measurements were subsequently used to determine the maximum depth of the *banquette* in shallow water and the base area to be used for the estimation of volumes also below the coastline.

The alignment of the frames and their georeferencing were conducted using Pix4D mapper software, by inputting the measured coordinates of the GCPs identified along the coast. The main processing steps included: a) loading of survey frames; b) automatic key point generation at maximum frame resolution; c) import and manual assignment of GCPs (RTK) to the targets located on the ground including the *banquette*; d) point cloud generation considering half the frame resolution; e) generation of the Orthomosaic; f) Digital Elevation Model (DEM) reconstruction from the point cloud at 3 cm resolution (Rende et al., 2020).

Finally, the two datasets (pre- and post-*banquette* deposition) were compared in Global Mapper software using the LIDAR module to verify the accuracy of the elevations estimated at 10 cm. Since there was no *banquette* during the first survey, the difference between the two surfaces (pre- and post-*banquette* deposition) made it possible to estimate the total *banquette* volume. The analysis and interpretation of the digital cartographic data were carried out using DEMs and orthophotos at a resolution of 3 cm and 1 cm, respectively. The high-resolution gravimetric geoid of Italy ITG2009 ISG - International Service for the Geoid, was used for the transformation from ellipsoidal to orthometric elevation (https://www.isgeoid.polimi.it/Geoid/Europe/Italy).

2.2.2 Machine Learning and Image Classification

Object Base Image Analysis (OBIA) was used to discriminate the *banquette* from the surrounding environment. In particular, OBIA algorithms were combined with machine learning, using eCognition Developer software. The data input consisted of the orthomosaic obtained from the UAVs –integrated with RGB bands and a GSD (Ground Sample Distance) resolution of 1.5 cm. The EUNIS Habitat Classification nomenclature was used to map the *banquette*, according to the following four classes: 1) Facies of banks of dead leaves of *Posidonia oceanica* and other phanerogams (EUNIS habitat type code: A2.131); 2) Floating necromass of dead leaves (Walker et al., 2001); 3) Sand; 4) Water.

The segmentation algorithm chosen for this study is the Multi-resolution Segmentation which can create objects with as little internal heterogeneity as possible, representing significant elements of the territory. After creating the objects, 987 ground truth samples were used to train different types of classifiers available in the eCognition Developer software and classify the entire image. The results of 3 different classification algorithms were compared: Random Tree (RT), Support Vector Machine (SVM), and Kappa Nearest Neighbour (KNN). After classification, the vector of validation points was used to perform an accuracy assessment, again within eCognition Developer, which generates an error matrix. User's and Producer's accuracy, overall accuracy and the K index were therefore determined through 155 validation ground truth samples.

2.3 Sample Collection, Laboratory and Data Analysis

Sampling of the *banquette* was carried out in December 2019. To determine the structural complexity of the *banquette* and maximize its variation in terms of thickness and distance from the shoreline, three random transects were set perpendicularly to the coastline (**Supplementary Figure 2A**). At each transect, the following three stations were identified: inner edge (landward), middle point and outer edge (seaward) of the *banquette*. At each station, three surficial *banquette* samples were collected using a 20 x 20 cm frame; all material within the frame, to a depth of 20 cm, was collected using hand scissors. As the outer edge was characterised by variable and greater thickness, a further two samples were collected at increasing depth from the surface (depth differed among transects depending on the total height of the *banquette*) by digging horizontally from the vertical surface of the *banquette* to obtain cubic samples (20 cm sided) (**Supplementary Figure 2A**). Each sample was then stored at -20°C before analysis of i) *banquette* composition (density of vegetal and sediment components), ii) total organic carbon (TOC), total nitrogen (TN) and total phosphorous (TP) density.

At the laboratory, each sample was weighed whole and then divided into three sub-samples for i) determination of water content and, hence, dry weight, through oven-drying at 60°C until constant weight (*i.e.*, 24/48h), ii) compositional analysis, and iii) chemical analysis (TOC, TN, TP).

For the compositional analysis, the vegetal components (leaves, detritus, rhizomes, roots and *aegagropilae*) were separated from the sediment. The sediment was further separated into sand and mud through a 63 μm mesh sieve. Each vegetal and sediment component was individually oven-dried (60°C) to constant weight. Each component was expressed both as a percentage and density (kg m^{-3}). Moreover, the density of all components and only vegetal

components were summed to obtain respectively the total density and the biomass. For chemical analysis, subsamples were freeze-dried (ALPHA 1–4 LD plus, Martin Christ) and then ground to a fine powder (micromill Retsch MM20). TOC (on previously acidified samples through HCl 2N to remove carbonates) and TN were determined through an elemental analyser (Thermo Flash EA 1112). TP was analysed using inductively coupled plasma–optical emission spectroscopy (ICP-OES; Optima 8000, PerkinElmer) after sample mineralization. TOC, TN and TP were also expressed as density (kg m^{-3}).

Principal Component Analysis (PCA) was run based on the normalised total density, biomass, sand and mud density, as well as averaged TOC, TN and TP density to assess the differences between samples collected at different distances from the sea (inner edge, middle zone, outer edge) and depth from the *banquette* surface ranked according to four classes (0-20, 60-80, 100-120 and >160 cm) in order to take into account the different depth at which the samples were taken along the outer edge. In addition, after having identified, from the PCA, *banquette* depth as the main driver of the dataset variability, the relationship between depth and the other variables was individually tested using regression models. In particular, Linear Models (LM) were applied when the normality assumption was retained according to the Shapiro-Wilk test (Underwood, 1997); otherwise, Generalized Linear Models (GLM) were applied, since they allow the use of any distribution belonging to the Natural Exponential family (Lovison et al., 2011). Depth (cm) was used as the explanatory variable, whereas total density, biomass, sand, mud, TOC, TN and TP densities were used as response variables. PCA, and LM and GLM, were performed using PRIMER 6 v6.1.10 & PERMANOVA+ β20 (Anderson et al., 2008) and R v. 4.0.2 (R Core Team, 2018), respectively.

2.4 Mass Calculation

To calculate the total mass of the different components and nutrients in the *banquette*, the total volume obtained from the three-dimensional mapping (see *Image Data Acquisition*) was fractionated into N sub-units of columnar shape; the base of the column measured 20x20 cm, i.e., a surface (S) of 400 cm^2 and the height corresponding to the maximum thickness of the *banquette* (D_{max}) (**Supplementary Figure 2B**). For each sub-unit, the mass was calculated applying the formula $m = d_a V$, where d_a is the average density and $V = S\ D_{max}$. In turn, the d_a of each sub-unit was estimated, using the coefficients obtained by LM and GLM (see *Sample Collection, Laboratory and Data Analysis*), applying the formula $d_a = (d_{min} + d_{max})/2$, where d_{min} is the density at the surface corresponding to the intercept of the models and d_{max} is the density value estimated at the maximum thickness of the *banquette* (i.e. at its base) (**Supplementary Figure 2B**). Finally, the total mass of all the examined components was estimated by summing the mass (m) of all the sub-units. Since the relationship between sand and depth was not significant, estimates of its density were obtained from the difference between total density and biomass and mud.

3 RESULTS

3.1 Thematic Classification

The OBIA classification allowed us to obtain the highest overall accuracy for the KNN algorithm (92.28%) with a Kappa Index of Agreement of 0.90 (**Table 1**). The classification obtained with the Random Tree (RT) algorithm showed an overall accuracy of 90.31% and a Kappa Index of 0.86, while the SVM algorithm showed the worst result, 60.81% and 0.49 for overall accuracy and Kappa Index, respectively (**Table 1**). Consequently, the KNN results were chosen for the *banquette* map (**Figure 4** and **Supplementary Figures 3A, B**). According to KNN classification, the following thematic classes were covered: Facies of banks of dead leaves of *Posidonia oceanica* 2.18 ha, floating necromass of dead leaves 0.95 ha, sand 0.64 ha, and water surface 1.62 ha.

3.2 Morphological Characterization of the *Banquette*

The total area covered by the *banquette* at the time of the survey was approximately 3.1 ha, an underestimated value due to its further extension to the North where no photogrammetric surveys were carried out. The high-resolution ground and orthomosaic DEMs obtained from the photogrammetric restitution process showed an extensive distribution of the *banquette* along the coast. In particular, the coastline affected

TABLE 1 | Accuracy of the RT, SVM and KNN classification systems.

	RT		SVM		KNN	
	Overall accuracy: 90.31%		Overall accuracy: 58.00%		Overall accuracy: 92.28%	
	K = 0.86		K = 0.46		K = 0.90	
Class	**User's accuracy**	**Producer's accuracy**	**User's accuracy**	**Producer's accuracy**	**User's accuracy**	**Producer's accuracy**
Facies of banks of dead leaves of *Posidonia*	72.21%	87.08%	35.07%	81.94%	84.72%	78.91%
Floating necromass of dead leaves	87.13%	84.30%	88.00%	60.36%	87.61%	98.92%
Sand	99.18%	93.20%	87.00%	13.57%	97.30%	92.73%
Water	100.00%	95.70%	66.78%	97.81%	100.00%	97.28%

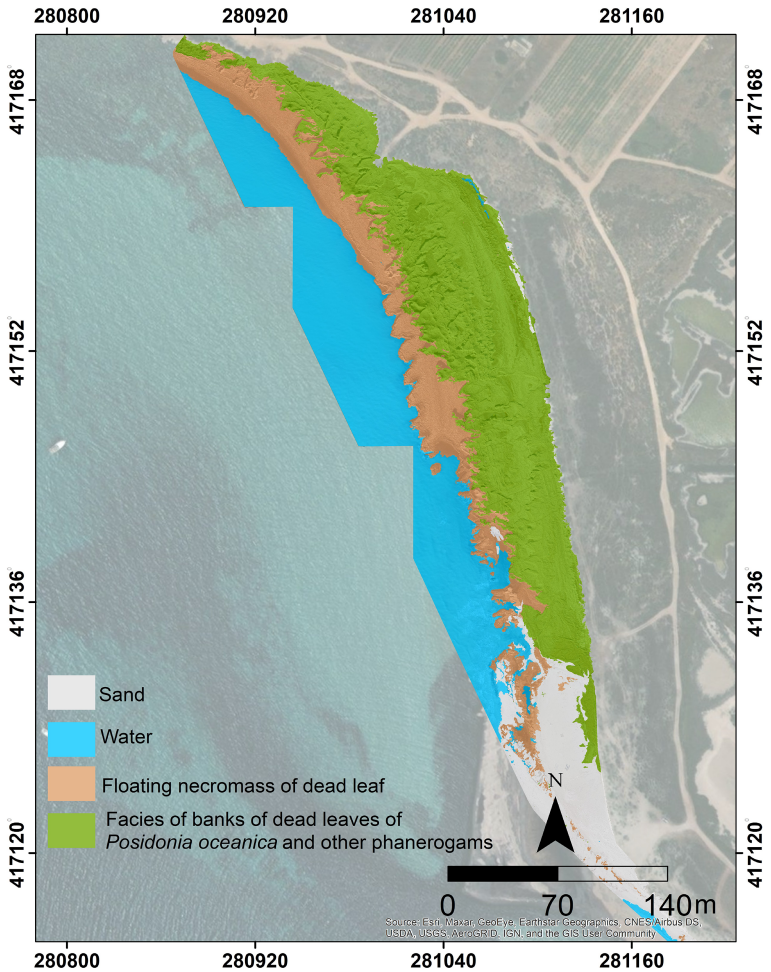

FIGURE 4 | Object-based Image Analysis (OBIA) classification results by means of Kappa Nearest Neighbour (KNN) filter for the Capo Feto area and thematic classes.

by the deposition of *banquette* was 600 m long and ranged from 24 m to 85 m in width (**Figure 5A**).

The *banquette* was mainly concentrated in the central part of the investigated area, which corresponds to the area of maximum curvature of the coastline (see the profiles in **Figure 5B**). The morphology of the *banquette* was not uniform but characterized by numerous cusps parallel to the coastline. The DEM showed the alignment of the cusps in several series, up to 6 cycles (**Figure 5B**), indicating more construction phases produced by the action of storm surges, mostly coming from the western sectors (**Figure 1**, **Supplementary Figure 1**). Near the sub-flat areas, the morphologies showed relatively low slopes (0.2°-2°) with a tendency to increase up to 90° near the cusps, generating sub-vertical fronts probably caused by the erosive action of waves that gradually push leaves towards the coast and at the same time erode the base of the existing accumulated mass. The high-resolution DEM and the map of difference show variable thicknesses, with a general seaward increase of up to about 3.40 m (**Figures 6A–C**).

The comparison of the two DEMs (pre and post *banquette* deposition) allowed estimation of the overall thickness and volume of the accumulated mass. The total estimated volume of the accumulated mass (vegetal and sedimentary) was about 20,009.6 m^3, while the thickness varied from a few decimetres to 3.10 m with respect to the hydrographic zero. However, if we consider the height with respect to the pre-deposition surface, the thickness increases up to 3.4 m. Overall, the greatest thickness was detected in the central sector of the deposition where there is the extension from the coast is the widest (**Figure 6A**).

3.3 Compositional and Chemical Characterization of the *Banquette*

The banquette was characterised by a clear dominance of leaf detritus (72.8 ± 12.5%, mean ± s.d.), followed by sand (10.0 ± 8.8%) and seagrass rhizomes (7.4 ± 8.1%), while aegagropilae, mud and fresh leaves were minor components (2.1 ± 3.8%, 2.0 ± 0.9% and 0.3 ± 0.4% respectively). Total density was 83.9 ±

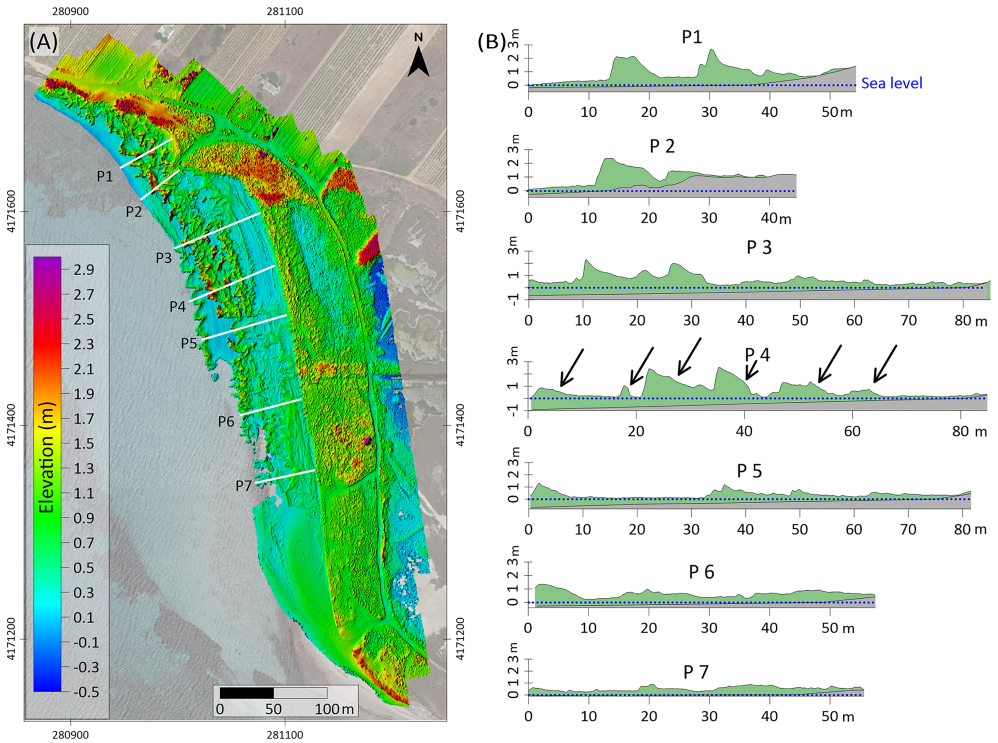

FIGURE 5 | **(A)** Digital elevation model (DEM) of the surveyed area and location of 7 sections encompassing the entire *banquette* extension from the coastline towards the sea. **(B)** The profiles show the accumulation of maximum seagrass accumulation cycles (arrows up to 6) with maximum thicknesses up to 3 m. The blue dotted horizontal line is the sea level at the time of image acquisition.

27.4 kg m^{-3}, of which 73.0 ± 22.3 kg m^{-3} were vegetal components, 9.8 ± 8.6 kg m^{-3} sand, and 1.7 ± 1.7 kg m^{-3} mud. TOC density was on average 19.35 ± 6.56 kg m^{-3}, while much lower values were found for TN (0.42 ± 0.14 kg m^{-3}) and TP (0.02 ± 0.01 kg m^{-3}). The first axis of the PCA ordination explained 74.7% of the variability and revealed a clear separation of the samples according to depth, while the second axis explained 16.3% of the variability, with the total for the two axes being 90.9%. Samples collected at greater depths clustered in the right part of the graph and showed the highest values of all variables. The deepest samples (> 160 cm) were characterised by the highest sand and mud density (**Figure 7**).

LM and GLM showed that all the variables considered significantly increased with increasing banquette depth (p value < 0.05) except for sand (p value > 0.05) (**Table 2**). The relationship between depth and total density showed the highest R^2 (0.66) followed by mud and biomass (R^2 = 0.57 and 0.47, respectively), indicating better goodness of fit for the regression analyses performed.

3.4 Data Integration and Mass Calculation

Overall, almost 700,000 volumetric subunits were generated *via* GIS model. Their average thickness and volume were 72.7 ± 47.3 cm and 29,097 ± 18,918 cm^3, respectively, totalling 20,009.6 m^3 (**Table 3**). The distribution of maximum density estimates for each variable at the base of all sub-units (*Dmax*) is shown in **Figure 8**; the highest value was observed for total density (200 kg dw m^{-3}). According to the calculations reported in section 2.4, the mass obtained for all the investigated variables ranged from 0.5 to 1,505.6 tons for TP and the vegetal component respectively, totalling 1,743 tons for the entire *banquette*.

4 DISCUSSION

4.1 *Banquette* Mapping, Volume Estimation and Morphological Traits

The high-resolution photogrammetric method applied in this study was reliable and powerful for measuring the three-dimensional extent of *Posidonia oceanica* litter accumulations even when reaching abnormal size, such as described here that, to our knowledge, represents the biggest ever analysed.

The use of this rapid and non-destructive approach also allowed obtaining very accurate quantitative information on the distribution of the various morphologies present. Previous studies have shown the potential of aerophotogrammetry in identifying and mapping seagrass detritus accumulated along the coasts (Ventura et al., 2018; Pan et al., 2021), but they were limited to two-dimensional mapping. In this study, for the first time, the images taken in suitable overlapping sequence

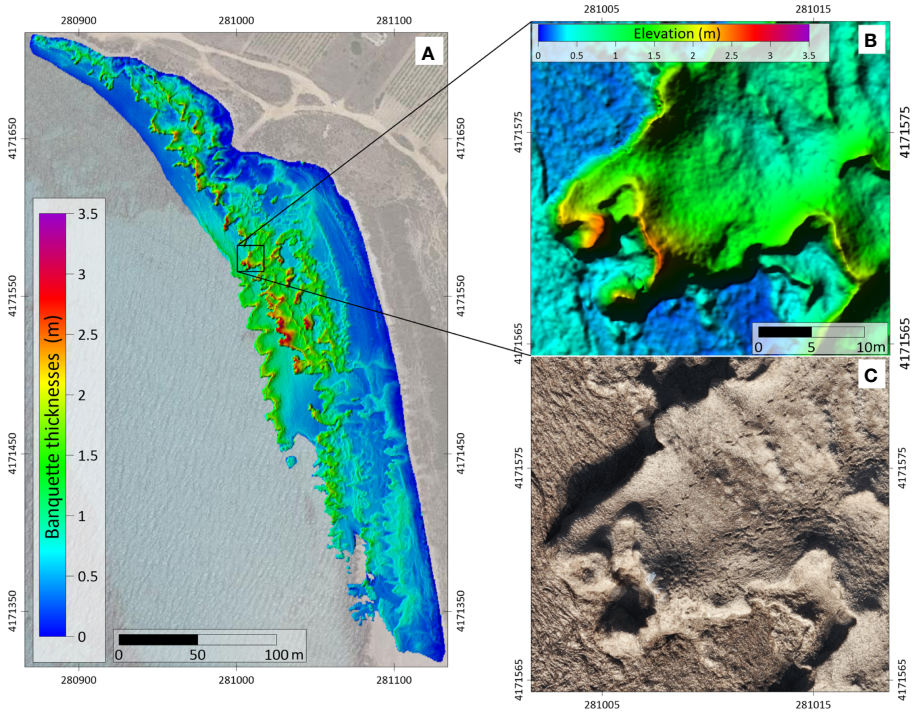

FIGURE 6 | **(A)** Map of difference between pre- and post-*banquette* deposition DEM; **(B)** Detail of post-*banquette* deposition DEM at 6 cm resolution; **(C)** Detail of orthomosaic map at 3 cm resolution.

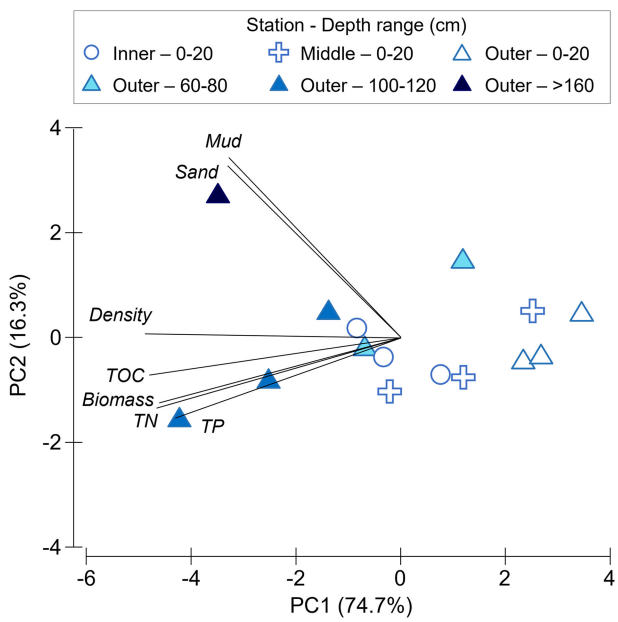

FIGURE 7 | Principal Component Analysis (PCA) ordination performed on total density, biomass, and sand, mud, TOC (Total Organic Carbon), TN and TP density data of the samples of the *banquette* collected from three stations (inner edge, middle zone and outer edge) along the transects, and at different depths. Vectors are overlayed based on the Pearson correlation r > 0.5.

demonstrated that UAVs are a very simple and, at the same time, cheap solution able to represent not only 2D detritus distribution but also its 3D architecture at centimetre-scale. This provided the opportunity to 3D reconstruct and map the seagrass meadows and the necromass structures, beached and submerged, characterised by very complex shapes across all geometric dimensions (Rende et al., 2020; Tomasello et al., 2020).

The availability of high-resolution orthomosaics and DEMs in a georeferenced environment using OBIA (Object-Based Image Analysis) classification techniques allows rapid and effective mapping of natural and physical habitats. Mapping and comparison of validated thematic maps (2D) (Rende et al., 2022) and volume estimates (3D) obtained from OBIA classification are also essential tools for environmental monitoring of medium and large-scale areas such as those of the Capo Feto area. This first high-resolution classification (**Figures 4**, **5**) compared with future surveys (time-lapse), will allow us to estimate the quantity of biomass and carbon accumulated or exported. The high-resolution DEM obtained for the study also allowed obtaining details of the morphologies present on the surface of the *banquette*, thereby permitting recognition of spatial cyclical trends in the variations of the thicknesses reached.

The analysis of these variations showed a general progressive increase in the thickness towards the sea. However, the analysis of the surface continuum in sections orthogonal to the coast allowed identification of repeated series of ridges, culminating in

TABLE 2 | Equation, R^2, F-value and p-value of the LM and GLM performed to assess the relationship between the depth (cm) of the *banquette* and total density, biomass, sand, mud, TOC, TN and TP density (kg m^{-3}).

Regression	Estimates	*SE*	*p-value*	R^2	*F-value*	*p-value*
density ~ depth				0.66	25.04	<0.05
Intercept	65.938	5.601	<0.05			
Slope	0.409	0.081	<0.05			
biomass ~ depth				0.47	11.49	<0.05
Intercept	60.701	5.679	<0.05			
Slope	0.281	0.082	<0.05			
sand ~ depth				0.26	5.12	<0.05
Intercept	5.320	1.757	<0.05			
Slope	0.081	0.053	ns			
mud ~ depth				0.58	20.807	<0.05
Intercept	1.072	0.137	<0.05			
Slope	0.013	0.004	<0.05			
TOC ~ depth				0.39	28.073	<0.05
Intercept	15.768	0.865	<0.05			
Slope	0.0812	0.175	<0.05			
TN ~ depth				0.30	18.79	<0.05
Intercept	0.353	0.023	<0.05			
Slope	0.001	0.003	<0.05			
TP ~ depth				0.23	12.71	<0.05
Intercept	0.021	1.607e-03	<0.05			
Slope	8.363e-05	2.346e-05	<0.05			

points of maximum height where the slope reverses interspersed with flat areas.

The entire *banquette* mass, especially the most seaward part, should be considered as a completely saturated floating element, which behaves like a dense fluid mass. Southward flux energy, without any confinement, tends to dissipate itself and confluence into the general littoral drift of the Physiographic Unit. Interestingly, the maximum heights of the series of ridges are located approximately in the centre-north of the beach because that is where maximum impact energy is, which then dissipates in both directions (north and south).

The "multi-ridge" nature of flat areas interspersed with giant accumulation ridges can be reasonably interpreted as the result of alternating phases of calmer seas and stormy seas respectively, responsible for an even more complex process of accumulation building than previously thought. Previous studies conducted in various regions of the Mediterranean have described the presence of typical wall delimiting seafront *banquette* with flat areas behind the beach (Roig Munar and Prieto, 2005; Simeone et al., 2013). However, this wall, despite being subject to continuous marine formation/erosion, has always been reported as a single structure. In fact, no explicit reference to the multiple presences of several walls running parallel to the coast had been ever made. For this reason, we propose the adoption of the term "multiple mega ridges *banquette*" (MMR *banquette*) to better identify the atypical *banquette* typology described in this study. Further studies will be needed to understand if and where MMR *banquette* occur along the Mediterranean coasts.

4.2 Compositional and Chemical Characteristics

This study showed that the large morphological variability of the *banquette* exerts a significant effect on the structure and compactness of the accumulation itself, with important implications for the estimation of the amount of the various

TABLE 3 | Number (Num), mean (± s.d.) thickness and volume and total volume of the GIS generated sub-units. Biomass, sediment (sand and mud), total organic carbon, and nutrient density estimated on average for the sub-units and total values.

Sub-units				*Banquette* components	Mean density (kg m^{-3})	Total mass (tons dw)	Shoreline concentration (ton dw m^{-1}) *
Num	Mean thickness (cm)	Mean volume (cm^3)	Total volume (m^3)				
687,693	72.7 ± 47.3	29.1 ± 18.9	20,009.6	**Biomass**	70.9 ± 6.7	1,505.6	2.5
				Sand	8.4 **	202.5 **	0.34 **
				Mud	1.5 ± 0.31	34.9	0.1
				TOC	17.9 ± 2.3	387.2	0.7
				TN	0.4 ± 0.0	8.1	0.01
				TP	0.02 ± 0.00	0.5	0.001
				Overall	80.8 ± 9.7	1,743	2.9

**Shoreline concentration was calculated by dividing total mass by 600 meters (length of the shoreline studied). **Sand mass per volume unit and total mass were estimated by subtracting biomass and mud from total density.*

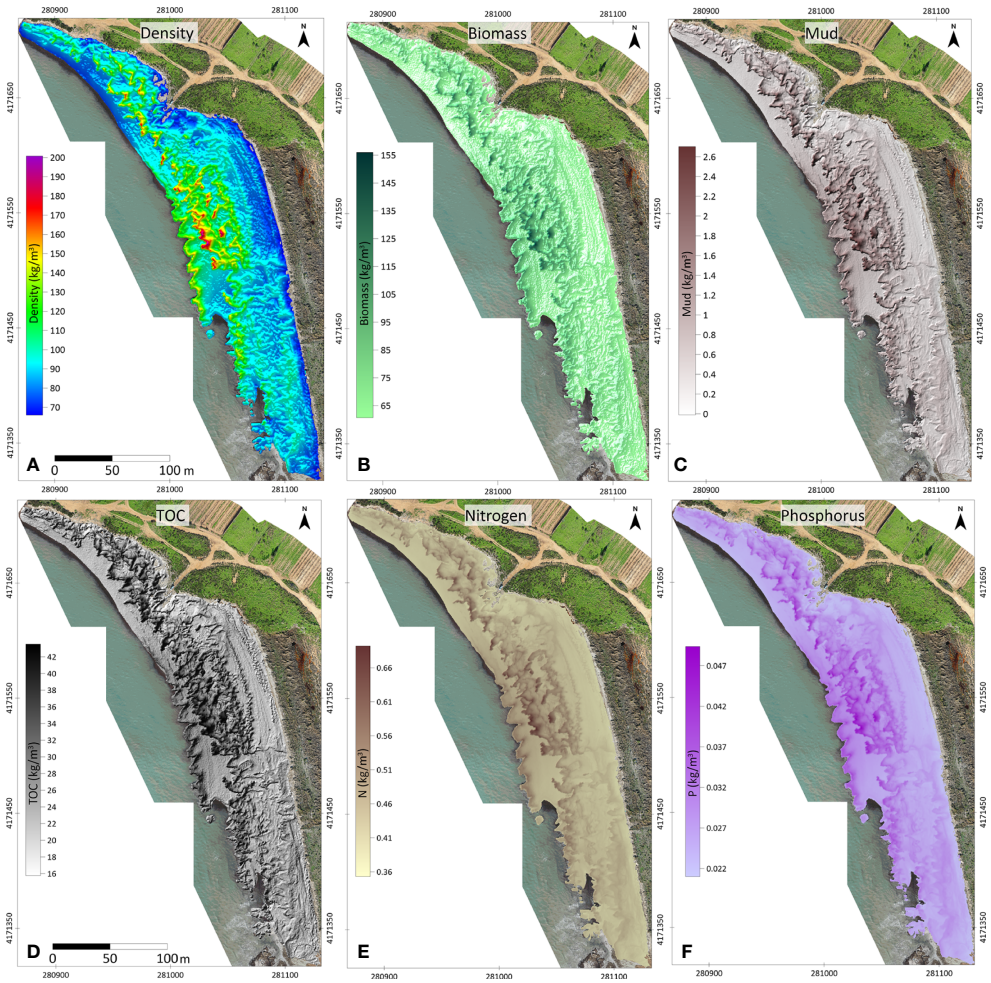

FIGURE 8 | Distribution maps of the maximum values estimated at the base of the Capo Feto *banquette* for: **(A)** total density, **(B)** biomass, **(C)** mud density, **(D)** TOC (Total Organic Carbon) density, **(E)** TN (Total Nitrogen) density, **(F)** TP (Total Phosphorus) density.

components. The evident causal relationship between depth and density of the *banquette* components has allowed us to model their variation along the *banquette* vertical profile. The banquette features, in terms of compositional and chemical variables, varied along the vertical profile, while the distance from the coast was not relevant. Excluding sand, which showed a high content at the inner edge as it is more exposed to the influence of the dune system behind it (Simeone and De Falco, 2012), total mass increases from 30 to 60% per unit volume for each meter below the *banquette* surface. Mateo et al. (2003) also observed a sharp increase in density from the surface to the base of the *banquette* due to a different degree of component compactness, suggesting that this is not a site-specific feature. The weight of the leaves determines a self-crushing effect that in turn produces the progressive expulsion of both air and interstitial water from the debris matrix. Although the density estimates were obtained from statistical models applied to field data collected up to 160 cm below the surface, it should be noted that this depth coincides with the 94th percentile of the almost 700,000 sub-units of depth measures generated *via* DEM and are, therefore, strongly representative of the entire *banquette* thicknesses pool.

4.3 Data Integration for Stock Calculation Upscaling

From a methodological point of view, this study demonstrated that the thickness of the *banquette* is an important covariate that clearly needs to be considered for a correct estimate of the carbon and nutrient stocks present in these structures. Moreover, the approach applied is relevant not only for purely geometric calculations of volumes *per se*, but also for those of a physical nature, given that the *banquette* has the characteristics of a variable-density body due to the intrinsic characteristics described above. If the effects associated with different thicknesses are ignored, the ability to make correct estimates of their mass can change dramatically. According to the literature, great variability in *banquette* thickness is due to coastal

morphology, hydrodynamic regime, distance and productivity of the adjacent seagrass meadows (e.g. Duong and Fairweather, 2011; Simeone and De Falco, 2012; Simeone et al., 2013; Jiménez et al., 2017). Since this is a natural phenomenon, particular attention should be paid to collection procedures in order to ensure that the depth of sampling can be determined and accounted for. We believe that the approach adopted here for studying a temporary and very unstable *banquette*, consisting of sampling along the sub-vertical fronts to characterize the deeper layers, represents a rapid and effective strategy and avoids more complex and time-consuming coring procedures, while reducing estimation errors relating to the compressive action induced by coring itself.

The results of the regression models incorporated in the volumetric *continuum* obtained by the superposition of the two DEMs, allowed sound determination of the total content of the various components throughout the study area. In more detail, the combined field and UAV photogrammetry approach revealed that *banquette*, although ephemeral, can accumulate huge amounts of vegetal biomass (i.e. about 1,500 tons dw) characterised by very high organic carbon and nitrogen content (i.e. about 390 and 8 tons dw, respectively). Although only smaller *banquette* have been studied so far, several studies have pointed out that the high biomass, carbon and nutrient accumulation makes seagrass beach wracks biochemical hotspots at the land-water interfaces (Coupland et al., 2007), critical sites involved in the coastal carbon and nutrient budget (Mateo et al., 2003; Mellbrand et al., 2011; Del Vecchio et al., 2013; Jiménez et al., 2017). The application of the approach to coastal areas with large and/or less accessible beach wracks described here will therefore clarify many still unclear aspects of their spatial and temporal dynamics and, especially if associated with flux estimates, their role in the exchange of carbon and across the land-ocean boundaries, a relevant and unexplored issue (Duarte, 2017).

The findings of this study also show that the *banquette* of Capo Feto traps large amounts of sand (almost 200 tons). This is of great relevance from both an ecological and management point of view. On the one hand, the sediment trapping ability of seagrass beach wracks and, especially, *banquette* protects beaches from coastal erosion, supports the formation of coastal dunes and prevents wind-induced sand transport (De Falco et al., 2008; Boudouresque et al., 2016). On the other hand, the widespread management practice of beach cleaning through beach wrack removal is associated with sediment subtraction that, in turn, contributes to beach erosion (De Falco et al., 2008; Mossbauer et al., 2012).

Given that the *banquette* studied formed within one year, it was possible to associate them with the primary production levels of the surrounding *Posidonia oceanica* meadow. Based on the available data, a vast meadow occupying about 8,300 ha of seabed from the surface (personal observations) to about 33 m (ROV inspections - AA.VV., 2002) is located in front of the Capo Feto coast (15,000 m long), in the middle of which lies the studied *banquette*. At a depth of 16 m, which corresponds to the average depth of *P. oceanica* in the area, total annual primary production (blades + sheaths + rhizomes) is estimated at 342.2 g dw m^{-2} y^{-1}, according to the general regression reported in Pergent et al. (1997). Considering that the *banquette* of this study consisted mainly of leaf detritus and that leaf blades account for 79% of total primary production (Pergent-Martini et al., 2021), we estimated the overall production of this tissue equalled 22,329 tons dw y^{-1}. Relating this value to coast length, we found that the adjacent meadow produces on average 1.5 ton dw m^{-1} y^{-1}, which corresponds to slightly more than half of the value we obtained for the *banquette* biomass (2.5 ton dw m^{-1}, **Table 3**). Assuming that the export of necromass from the seagrass meadows ranges between 10 and 55% of primary production and that shallow meadows are those most involved in the formation of beach wracks (Boudouresque et al., 2016), it follows that the *banquette* of Capo Feto is fed by seagrass detritus deriving also from other meadows located at greater distances, unlike the findings of Mateo et al. (2003). Leaf fall, which mainly occurs in late summer/autumn, is considered the main process responsible for carbon and nutrient loss from seagrasses (Romero et al., 2006). The TOC, N and P percentages estimated here (25.70, 0.54 and 0.03% respectively) in the Capo Feto *banquette* are consistent with the leaf litter nutrient content recorded by (Mateo et al., 2003; Mateo et al., 2006). Given that the export of blue carbon and nutrients from seagrass meadows toward other ecosystems follow parallel fluxes (*sensu* Mateo et al., 2006), the very high TOC, N and P bulk content found results from the high leaf primary production of the surrounding *P. oceanica* meadow conveyed at the Faro beach by the peculiar coastal morphology and hydrodynamic regime of the area. Considering that only a small portion of the *banquette* is thought to decompose on the beach, while most of it is exported inshore or offshore (Jiménez et al., 2017), new questions arise about the importance of such ephemeral systems as sinks/sources of organic matter, blue carbon and nutrients at regional or even global scale.

In conclusion, this study enabled us to estimate the amount and spatial distribution of both vegetal biomass and sedimentary mass, as well as blue carbon, nitrogen and phosphorus. On the one side, this study underlined the high potential of low-cost UAV surveys in 3D mapping and monitoring natural systems of high ecological importance and role, such as the "Multiple Mega-Ridge *banquette*". On the other side, the combination of high-resolution photogrammetry with a field-based analytical approach opens new scenarios, allowing us to understand the spatial and temporal dynamics of *banquette* formation and accumulation, with relevant implications for ecosystem service estimation and coastal zone management. *P. oceanica* provides the crucial regulating ecosystem service "coastal erosion protection", whose economic value of the associated goods and benefits for humans has been recently estimated as 188€/ha, corresponding to about 50% of the entire economic value of *P. oceanica* (Campagne et al., 2014). However, this is a cumulative value embedding the contribution of living meadows, *matte* and *banquette* ecosystem services, and therefore it is not possible to distinguish the specific contribution of the three different components. The relatively straightforward methodology

proposed here for accurately estimating the size and dynamics of the *banquette* will facilitate filling this gap. On the other hand, although beach wracks and *banquette* are included among the priority habitats to be preserved and protected in the Mediterranean area, according to the Barcelona Convention (UNEP/MAP, 2017), legislation about their management is still lacking in many Mediterranean countries, including Italy (Rotini et al., 2020). Under this framework, the methodology applied in this study may represent a valid approach supporting applications of National and European laws concerning the monitoring and management of *banquette* (MSFD EC, 2008; MATTM, 2019) and meeting the requirements of the Integrated Coastal Zone Management of the Mediterranean (ICZM) protocols. Moreover, as many sites along the Mediterranean coasts are affected by these short-term accumulation phenomena, the adoption of such effective tool to map them would also serve to quantify the blue carbon and nutrient exchange between the emerged and submerged coasts.

DATA AVAILABILITY STATEMENT

The raw data supporting the conclusions of this article will be made available by the authors, without undue reservation.

AUTHOR CONTRIBUTIONS

AT and SV conceived, designed, and supervised data integration and interpretation. AB and SR performed data processing, mapping, and geomorphological data interpretation. GR performed the remote sensing data planning and geomorphological interpretation. GS and CA analysed and interpreted compositional and chemical data. GC performed the statistical analysis. FC performed the field data sampling and analysis. AT, SR, GR, and AS funded the study. All authors contributed to the manuscript drafting and revision. All authors read and approved the submitted version.

FUNDING

This study was funded by the European Regional Development Fund (INTERREG Italia–Malta) under Projects: BESS - Pocket Beach Management and Remote Surveillance System (CUP B66C18000380005), Sea Forest LIFE 17CCM/IT 000121 project and MED Dé.Co.U. Plages project.

ACKNOWLEDGMENTS

The authors are grateful to Andrea Savona, Vincenzo Pampalone, Mario Vitti and Francesco Gregorio for their help in cartographic surveys and image acquisition. The authors are also grateful to Simona Noè and Silvia Chemello for the sampling activities and Cecilia Doriana Tramati, Adele Elisa Aleo and Lea Castellini for the laboratory activities. The authors are grateful to two reviewers for the comments that have improved the manuscript.

SUPPLEMENTARY MATERIAL

The Supplementary Material for this article can be found online at: https://www.frontiersin.org/articles/10.3389/fmars.2022.903138/full#supplementary-material

REFERENCES

AA.VV (2002). *Mappatura Delle Praterie Di Posidonia Oceanica Lungo Le Coste Della Sicilia E Delle Isole Circostanti* (Italy: Ministero dell'Ambiente – Servizio Difesa del Mare).

Adade, R., Aibinu, A. M., Ekumah, B., and Asaana, J. (2021). Unmanned Aerial Vehicle (UAV) Applications in Coastal Zone Management—a Review. *Environ. Monit. Assess.* 193, 154. doi: 10.1007/s10661-021-08949-8

Anderson, K., and Gaston, K. J. (2013). Lightweight Unmanned Aerial Vehicles Will Revolutionize Spatial Ecology. *Front. Ecol. Environ.* 11, 138–146. doi: 10.1890/120150

Anderson, M. J., Gorley, R. N., and Clarke, K. R. (2008). "PERMANOVA+ for PRIMER: Guide to Software and Statistical Methods," in *PRIMER-E* (UK: Plymouth), 1–214. doi: 10.13564/j.cnki.issn.1672-9382.2013.01.010

Apostolopoulos, D., and Nikolakopoulos, K. (2021). A Review and Meta-Analysis of Remote Sensing Data, GIS Methods, Materials and Indices Used for Monitoring the Coastline Evolution Over the Last Twenty Years. *Eur. J. Remote Sens.* 54, 240–265. doi: 10.1080/22797254.2021.1904293

Beltran, R., Beca-Carretero, P., Marbà, N., Jiménez, M. A., and Traveset, A. (2020). Spatio-Temporal Variation in Macrofauna Community Structure in Mediterranean Seagrass Wrack. *Food Webs.* 25, e00178. doi: 10.1016/j.fooweb.2020.e00178

Boudouresque, C. F., and Meinesz, A. (1982). Découverte De L'herbier De Posidonie. Parc National De Port-Cros. *Cahier* 4, 1–80.

Boudouresque, C. F., Pergent, G., Pergent-Martini, C., Ruitton, S., Thibaut, T., and Verlaque, M. (2016). The Necromass of the *Posidonia Oceanica* Seagrass Meadow: Fate, Role, Ecosystem Services and Vulnerability. *Hydrobiologia* 781, 25–42. doi: 10.1007/s10750-015-2333-y

Calvo, S., Tomasello, A., Di Maida, G., Pirrotta, M., Cristina Buia, M., Cinelli, F., et al. (2010). Seagrasses Along the Sicilian Coasts. *Chem. Ecol.* 26, 249–266. doi: 10.1080/02757541003636374

Campagne, C. S., Salles, J. M., Boissery, P., and Deter, J. (2014). The Seagrass *Posidonia Oceanica*: Ecosystem Services Identification and Economic Evaluation of Goods and Benefits. *Mar. pollut. Bull.* 97, 391–400. doi: 10.1016/j.marpolbul.2015.05.061

Casella, E., Collin, A., Harris, D., Ferse, S., Bejarano, S., Parravicini, V., et al. (2017). Mapping Coral Reefs Using Consumer-Grade Drones and Structure From Motion Photogrammetry Techniques. *Coral Reefs* 36, 269–275. doi: 10.1007/s00338-016-1522-0

Castellanos-Galindo, G. A., Casella, E., Mejía-Rentería, J. C., and Rovere, A. (2019). Habitat Mapping of Remote Coasts: Evaluating the Usefulness of Lightweight Unmanned Aerial Vehicles for Conservation and Monitoring. *Biol. Conserv.* 239, 108282. doi: 10.1016/j.biocon.2019.108282

Chawla, A., Spindler, D. M., and Tolman, H. L. (2013). Validation of a Thirty Year Wave Hindcast Using the Climate Forecast System Reanalysis Winds. *Ocean Model.* 70, 189–206. doi: 10.1016/j.ocemod.2012.07.005

Colombini, I., Mateo, M.Á., Serrano, O., Fallaci, M., Gagnarli, E., Serrano, L., et al. (2009). On the Role of *Posidonia Oceanica* Beach Wrack for

Macroinvertebrates of a Tyrrhenian Sandy Shore. *Acta Oecologica.* 35, 32–44. doi: 10.1016/j.actao.2008.07.005

Coupland, G. T., Duarte, C. M., and Walker, D. I. (2007). High Metabolic Rates in Beach Cast Communities. *Ecosystems* 10, 1341–1350. doi: 10.1007/s10021-007-9102-3

De Falco, G., Simeone, S., and Baroli, M. (2008). Management of Beach-Cast *Posidonia Oceanica* Seagrass on the Island of Sardinia (Italy, Western Mediterranean). *J. Coast. Res.* 24, 69–75. doi: 10.2112/06-0800.1

de Grissac, J. (1984). Effets des herbiers à Posidonia oceanica sur la dynamique marine et la sédimentologie littorale. In: Boudouresque, C.F., Jeudy de Grissac, A., and Olivier, J. (Eds.), *GIS Posidonie*. (Marseille, France: I-International Workshop on Posidonia oceanica bed. pp. 437–443.

Deidun, A., Gauci, A., Lagorio, S., and Galgani, F. (2018). Optimising Beached Litter Monitoring Protocols Through Aerial Imagery. *Mar. pollut. Bull.* 131, 212–217. doi: 10.1016/j.marpolbul.2018.04.033

Del Vecchio, S., Jucker, T., Carboni, M., and Acosta, A. T. R. (2017). Linking Plant Communities on Land and at Sea: The Effects of *Posidonia Oceanica* Wrack on the Structure of Dune Vegetation. *Estuar. Coast. Shelf Sci.* 184, 30–36. doi: 10.1016/j.ecss.2016.10.041

Del Vecchio, S., Marbà, N., Acosta, A., Vignolo, C., and Traveset, A. (2013). Effects of *Posidonia Oceanica* Beach-Cast on Germination, Growth and Nutrient Uptake of Coastal Dune Plants. *PLoS One* 8, e70607. doi: 10.1371/journal.pone.0070607

Di Carlo, G., Badalamenti, F., Jensen, A. C., Koch, E. W., and Riggio, S. (2005). Colonisation Process of Vegetative Fragments of *Posidonia Oceanica* (L.) Delile on Rubble Mounds. *Mar. Biol.* 147, 1261–1270. doi: 10.1007/s00227-005-0035-0

Duarte, C. M. (2017). Reviews and Syntheses: Hidden Forests, the Role of Vegetated Coastal Habitats in the Ocean Carbon Budget. *Biogeosciences* 14, 301–310. doi: 10.5194/bg-14-301-2017

Duong, H. L. S., and Fairweather, P. G. (2011). Effects of Sandy Beach Cusps on Wrack Accumulation, Sediment Characteristics and Macrofaunal Assemblages. *Austral Ecol.* 36, 733–744. doi: 10.1111/j.1442-9993.2010.02212.x

Gómez-Pujol, L., Orfila, A., Álvarez-Ellacuría, A., Terrados, J., and Tintoré, J. (2013). *Posidonia Oceanica* Beach-Cast Litter in Mediterranean Beaches: A Coastal Videomonitoring Study. *J. Coast. Res.* 165, 1768–1773. doi: 10.2112/si65-299.1

Jiménez, M. A., Beltran, R., Traveset, A., Calleja, M. L., Delgado-Huertas, A., and Marbà, N. (2017). Aeolian Transport of Seagrass (*Posidonia Oceanica*) Beach-Cast to Terrestrial Systems. *Estuar. Coast. Shelf Sci.* 196, 31–44. doi: 10.1016/j.ecss.2017.06.035

Lastra, M., Page, H. M., Dugan, J. E., Hubbard, D. M., and Rodil, I. F. (2008). Processing of Allochthonous Macrophyte Subsidies by Sandy Beach Consumers: Estimates of Feeding Rates and Impacts on Food Resources. *Mar. Biol.* 154, 163–174. doi: 10.1007/s00227-008-0913-3

Lovison, G., Sciandra, M., Tomasello, A., and Calvo, S. (2011). Modeling *Posidonia Oceanica* Growth Data: From Linear to Generalized Linear Mixed Models. *Environmetrics* 22, 370–382. doi: 10.1002/env.1063

Maccarrone, V. (2010). Determination of the Upper Boundary of a *Posidonia* Meadow. *Ecol. Inform.* 5, 267–272. doi: 10.1016/j.ecoinf.2009.11.001

Mateo, M. A. (2010). Beach-Cast *Cymodocea Nodosa* Along the Shore of a Semienclosed Bay: Sampling and Elements to Assess its Ecological Implications. *J. Coast. Res.* 26, 283–291. doi: 10.2112/08-1100.1

Mateo, M. A., Cebrián, J., Dunton, K., and Mutchler, T. (2006). "Carbon Flux in Seagrass Ecosystems," in *Seagrasses: Biology, Ecology and Conservation* (Dodrecht: The Nederlands: Springer), 159–162. doi: 10.1007/978-1-4020-2983-7_7

Mateo, M.Á., Sánchez-Lizaso, J. L., and Romero, J. (2003). *Posidonia Oceanica* "Banquettes": A Preliminary Assessment of the Relevance for Meadow Carbon and Nutrients Budget. *Estuar. Coast. Shelf Sci.* 56, 85–90. doi: 10.1016/S0272-7714(02)00123-3

MATTM (2019). Circular of Ministry of the Environment and Protection of the Territory and the Sea, n. 8838/2019 "gestione degli accumuli di *Posidonia oceanica*" spiaggiati.

Mellbrand, K., Lavery, P. S., Hyndes, G., and Hambäck, P. A. (2011). Linking Land and Sea: Different Pathways for Marine Subsidies. *Ecosystems* 14, 732–744. doi: 10.1007/s10021-011-9442-x

Mossbauer, M., Haller, I., Dahlke, S., and Schernewski, G. (2012). Management of Stranded Eelgrass and Macroalgae Along the German Baltic Coastline. *Ocean Coast. Manage.* 57, 1–9. doi: 10.1016/j.ocecoaman.2011.10.012

MSFD EC (2008). *Directive 2008/56/EC of the European Parliament and of the Council of 17 June 2008 Establishing a Framework for Community Action in the Field of Marine Environmental Policy* (Strasbourg, France: Marine Strategy Framework Directive), 19–40.

Murfitt, S. L., Allan, B. M., Bellgrove, A., Rattray, A., Young, M. A., and Ierodiaconou, D. (2017). Applications of Unmanned Aerial Vehicles in Intertidal Reef Monitoring. *Sci. Rep.* 7, 1–11. doi: 10.1038/s41598-017-10818-9

Ochieng, C. A., and Erftemeijer, P. L. A. (1999). Accumulation of Seagrass Beach Cast Along the Kenyan Coast: A Quantitative Assessment. *Aquat. Bot.* 65, 221–238. doi: 10.1016/S0304-3770(99)00042-X

Ondiviela, B., Losada, I. J., Lara, J. L., Maza, M., Galván, C., Bouma, T. J., et al. (2014). The Role of Seagrasses in Coastal Protection in a Changing Climate. *Coast. Eng.* 87, 158–168. doi: 10.1016/j.coastaleng.2013.11.005

Pan, Y., Ayoub, N., Schneider-Kamp, P., Flindt, M., and Holmer, M. (2022). Beach Wrack Dynamics Using a Camera Trap as the Real-Time Monitoring Tool. *Front. Mar. Sci.* 9. doi: 10.3389/fmars.2022.813516

Pan, Y., Flindt, M., Schneider-Kamp, P., and Holmer, M. (2021). Beach Wrack Mapping Using Unmanned Aerial Vehicles for Coastal Environmental Management. *Ocean Coast. Manage.* 213, 105843. doi: 10.1016/j.ocecoaman.2021.105843

Pergent-Martini, C., Pergent, G., Monnier, B., Boudouresque, C. F., Mori, C., and Valette-Sansevin, A. (2021). Contribution of *Posidonia Oceanica* Meadows in the Context of Climate Change Mitigation in the Mediterranean Sea. *Mar. Environ. Res.* 172, 105454. doi: 10.1016/j.marenvres.2020.105236

Pergent, G., Rico-Raimondino, V., and Pergent-Martini, C. (1997). Fate of Primary Production in *Posidonia Oceanica* Meadows of the Mediterranean. *Aquat. Bot.* 59, 307–321. doi: 10.1016/S0304-3770(97)00052-1

Pernice, G., Placenti, F., and Spina, A. (2004). Long-Term Analysis, (1863-2002) of Environmental Change in the Capo Feto Area (Mediterranean Sea). *Chem. Ecol.* 20, 37–41. doi: 10.1080/02757540410001665962

Randazzo, G., and Lanza, S. (2020). Regional Plan Against Coastal Erosion: A Conceptual Model for Sicily. *Land* 9, 1–14. doi: 10.3390/land9090307

Randazzo, G., Italiano, F., Micallef, A., Tomasello, A., Cassetti, F. P., Zammit, A., et al. (2021). WebGIS implementation for dynamic mapping and visualization of coastal geospatial data: A case study of BESS project. *Appl. Sci.* 11, 8233. doi:10.3390/app11178233

R Core Team (2018). *R: A Language and Environment for Statistical Computing* (Vienna, Austria: R Foundation for Statistical Computing). Available at: https://www.R-project.org/.

Remondino, F., Barazzetti, L., Nex, F., Scaioni, M., and Sarazzi, D. (2011). UAV Photogrammetry for Mapping and 3d Modeling – current status and future perspectives. *Int. Arch. Photogramm. Remote Sens. Spat. Inf. Sci.* XXXVIII-1/, 25–31. doi: 10.5194/isprsarchives-XXXVIII-1-C22-25-2011

Rende, S. F., Bosman, A., Di Mento, R., Bruno, F., Lagudi, A., Irving, A. D., et al. (2020). Ultra-High-Resolution Mapping of *Posidonia Oceanica* (L.) Delile Meadows Through Acoustic, Optical Data and Object-Based Image Classification. *J. Mar. Sci. Eng.* 8, 647. doi: 10.3390/JMSE8090647

Rende, S. F., Bosman, A., Menna, F., Lagudi, A., Bruno, F., Severino, U., et al. (2022). Assessing Seagrass Restoration Actions Through a Micro-Bathymetry Survey Approach (Italy, Mediterranean Sea). *Water* 14, 1285. doi: 10.3390/w14081285

Roig Munar, F. X., and Prieto, J.Á.M. (2005). Efectos De La Retirada De Bermas Vegetales De *Posidonia Oceanica* Sobre Playas De Las Islas Baleares: Consecuencias De La Presión Turística. *Investig. Geogr.* 52, 40–52. doi: 10.14350/rig.30080

Romero, J., Lee, K. S., Pérez, M., Mateo, M. A., and Alcoverro, T. (2006). "Nutrient Dynamics in Seagrass Ecosystems," in *Seagrasses: Biology, Ecology and Conservation* (Dodrecht: The Nederlands: Springer), 227–254. doi: 10.1007/978-1-4020-2983-7_9

Rotini, A., Chiesa, S., Manfra, L., Borrello, P., Piermarini, R., Silvestri, C., et al. (2020). Effectiveness of the "Ecological Beach" Model: Beneficial Management of Posidonia Beach Casts and Banquette. *Water (Switzerland)* 12, 1–16. doi: 10.3390/w12113238

Schofield, G., Esteban, N., Katselidis, K. A., and Hays, G. C. (2019). Drones for Research on Sea Turtles and Other Marine Vertebrates – A Review. *Biol. Conserv.* 238, 108214. doi: 10.1016/j.biocon.2019.108214

Simeone, S., and De Falco, G. (2012). Morphology and Composition of Beach-Cast *Posidonia Oceanica* Litter on Beaches With Different Exposures. *Geomorphology* 151–152, 224–233. doi: 10.1016/j.geomorph.2012.02.005

Simeone, S., De Muro, S., and De Falco, G. (2013). Seagrass Berm Deposition on a Mediterranean Embayed Beach. *Estuar. Coast. Shelf Sci.* 135, 171–181. doi: 10.1016/j.ecss.2013.10.007

Tomasello, A., Cassetti, F. P., Savona, A., Pampalone, V., Pirrotta, M., Signa, G., et al. (2020). The Use of Very High Resolution Images for Studying Posidonia Oceanica Reefs. *Vie Milieu* 70, 25–35.

Underwood, A. J (1997). *Experiments in Ecology: Their Logical Design and Interpretation Using Analysis of Variance* (UK: Cambridge University Press).

UNEP/MAP (2017). *Convention for the Protection of the Marine Environment and the Coastal Region of the Mediterranean* (Barcelona, Spain: Barcelona Convention) - UNEP(DEPI)/MED).

Ventura, D., Bonifazi, A., Gravina, M. F., Belluscio, A., and Ardizzone, G. (2018). Mapping and Classification of Ecologically Sensitive Marine Habitats Using Unmanned Aerial Vehicle (UAV) Imagery and Object-Based Image Analysis (OBIA). *Remote Sens.* 10, 1–23. doi: 10.3390/rs10091331

Vizzini, S. (2009). Analysis of the Trophic Role of Mediterranean Seagrasses in Marine Coastal Ecosystems: A Review. *Bot. Mar.* 52, 383–393. doi: 10.1515/bot.2009.056

Walker, D., Pergent, G., and Fazi, S. (2001). "Seagrass Decomposition," in *Global Seagrass Research Methods*. Eds. F. Short and R. Cole (Amsterdam, Netherlands: Elsevier).

Conflict of Interest: The authors declare that the research was conducted in the absence of any commercial or financial relationships that could be construed as a potential conflict of interest.

Publisher's Note: All claims expressed in this article are solely those of the authors and do not necessarily represent those of their affiliated organizations, or those of the publisher, the editors and the reviewers. Any product that may be evaluated in this article, or claim that may be made by its manufacturer, is not guaranteed or endorsed by the publisher.

Copyright © 2022 Tomasello, Bosman, Signa, Rende, Andolina, Cilluffo, Cassetti, Mazzola, Calvo, Randazzo, Scarpato and Vizzini. This is an open-access article distributed under the terms of the Creative Commons Attribution License (CC BY). The use, distribution or reproduction in other forums is permitted, provided the original author(s) and the copyright owner(s) are credited and that the original publication in this journal is cited, in accordance with accepted academic practice. No use, distribution or reproduction is permitted which does not comply with these terms.

frontiers | Frontiers in Marine Science

TYPE Original Research
PUBLISHED 26 July 2022
DOI 10.3389/fmars.2022.953191

Check for updates

OPEN ACCESS

EDITED BY
Monica Montefalcone,
University of Genoa, Italy

REVIEWED BY
Stanislao Bevilacqua,
University of Trieste, Italy
Sante Francesco Rende,
Istituto Superiore per la Protezione e la Ricerca Ambientale (ISPRA), Italy

*CORRESPONDENCE
Arie J. P. Spyksma
arie.spyksma@auckland.ac.nz

SPECIALTY SECTION
This article was submitted to Marine Ecosystem Ecology, a section of the journal Frontiers in Marine Science

RECEIVED 25 May 2022
ACCEPTED 27 June 2022
PUBLISHED 26 July 2022

CITATION
Spyksma AJP, Miller KI and Shears NT (2022) Diver-generated photomosaics as a tool for monitoring temperate rocky reef ecosystems.
Front. Mar. Sci. 9:953191.
doi: 10.3389/fmars.2022.953191

COPYRIGHT
© 2022 Spyksma, Miller and Shears. This is an open-access article distributed under the terms of the Creative Commons Attribution License (CC BY). The use, distribution or reproduction in other forums is permitted, provided the original author(s) and the copyright owner(s) are credited and that the original publication in this journal is cited, in accordance with accepted academic practice. No use, distribution or reproduction is permitted which does not comply with these terms.

Diver-generated photomosaics as a tool for monitoring temperate rocky reef ecosystems

Arie J. P. Spyksma[1,2]*, Kelsey I. Miller[2] and Nick T. Shears[2]

[1]New Zealand Geographic, Auckland, New Zealand, [2]Leigh Marine Laboratory, Institute of Marine Science, University of Auckland, Auckland, New Zealand

Robust monitoring data provides important information on ecosystem responses to anthropogenic stressors; however, traditional monitoring methodologies, which rely heavily on time in the field, are resource intensive. Consequently, trade-offs between data metrics captured and overall spatial and temporal coverage are necessary to fit within realistic monitoring budgets and timeframes. Recent advances in remote sensing technology have reduced the severity of these trade-offs by providing cost-effective, high-quality data at greatly increased temporal and spatial scales. Structure-from-motion (SfM) photogrammetry, a form of remote sensing utilising numerous overlapping images, is well established in terrestrial applications and can be a key tool for monitoring changes in marine benthic ecosystems, which are particularly vulnerable to anthropogenic stressors. Diver-generated photomosaics, an output of SfM photogrammetry, are increasingly being used as a benthic monitoring tool in clear tropical waters, but their utility within temperate rocky reef ecosystems has received less attention. Here we compared benthic monitoring data collected from virtual quadrats placed on photomosaics with traditional diver-based field quadrats to understand the strengths and weaknesses of using photomosaics for monitoring temperate rocky reef ecosystems. In north-eastern New Zealand, we evaluated these methods at three sites where sea urchin barrens were prevalent. We found key metrics (sea urchin densities, macroalgae canopy cover and benthic community cover) were similar between the two methods, but data collected *via* photogrammetry were quicker, requiring significantly less field time and resources, and allowed greater spatial coverage than diver-based field quadrats. However, the use of photomosaics was limited by high macroalgal canopy cover, shallow water and rough sea state which reduced stitching success and obscured substratum and understory species. The results demonstrate that photomosaics can be used as a resource efficient and robust method for effectively assessing and monitoring key metrics on temperate rocky reef ecosystems.

KEYWORDS

urchin barren, underwater photogrammetry, structure from motion, survey technique, benthic monitoring, photomosaic, seascape

1 Introduction

Globally, human activities are increasingly shaping ecosystems, though direct and indirect pathways such as climate change, species invasion, habitat modification, and harvest. Well-designed monitoring programmes can evaluate key ecosystem trends and inform management, conservation and restoration initiatives (Lovett et al., 2007; Lindenmayer and Likens, 2010; Mihoub et al., 2017). Traditionally, ecosystem monitoring has involved manual data collection in the field, which provides high quality data, but typically at low spatial and temporal scales due to the high effort and acquisition costs required. This creates data collection trade-offs (Braunisch and Suchant, 2010; Del Vecchio et al., 2019; D'Urban Jackson et al., 2020). For example, increasing the spatial scale may require reducing the amount of data collected at each site. Thus, alternative methods of data collection have been sought.

Recent developments in cost effective remote sensing techology such as high resolution satellites and unmanned aerial vehicles (UAVs) have revolutionised many forms of ecological monitoring, particularly in terrestrial environments (Aplin, 2005; Klemas, 2015; Yao et al., 2019). Imagery from these technologies, coupled with powerful computing software, allow rapid data collection and analysis over greater spatial scales and improved access to remote and less accessible locations (Klemas, 2015). The speed, access, and image quality can help to alleviate some of the trade-offs between monitoring effort and data quality and quantity that arise from traditional in-field data collection methods, enabling a better understanding of environmental change by allowing larger quantities of detailed data to be collected or over larger spatial scales during the same time frame.

Marine ecosystems are typically difficult to access and expensive to monitor. The impacts of human activities are acutely felt in coastal and nearshore marine regions (Halpern et al., 2008) where the cumulative effects of climate change, overfishing and terrestrial runoff result in large-scale ecosystem degradation and collapse (Halpern et al., 2019). Benthic ecosystems are particularly vulnerable as many species are sessile or have limited mobility and are unable to avoid disturbance (Solan et al., 2004). Nearshore, shallow subtidal benthic ecosystems have traditionally been monitored through *in situ* observations made by SCUBA divers with tools such as quadrats and transect tapes. These methods are time consuming and consequently spatially limited, and are prone to observer variability (Pizarro et al., 2017; Marre et al., 2020). Alternatively, aerial imagery and remote sensing data from satellite and UAVs can increase the spatial coverage, but often lack the resolution required to detect fine scale benthic patterns (Mizuno et al., 2017) and are restricted by water clarity, tides and meterological conditions, limiting their usefulness to very clear water habitats (Casella et al., 2017) or shallow depths, such as near surface kelp cover (Bennion et al., 2019; Tait et al., 2019; Cavanaugh et al., 2021).

Underwater structure-from-motion (SfM) photogrammetry presents a useful middle ground, allowing rapid, fine scale benthic observations to be made over larger spatial scales than are possible using traditional methods. Imagery for underwater SfM photogrammetry can be collected by divers with handheld cameras (Bayley and Mogg, 2020), by systems towed behind a vessel (Fakiris et al., 2022) and using remotely operated vehicle (ROV) or autonomous underwater vehicle (AUV) technology (Ling et al., 2016; Teague and Scott, 2017). While the extraction of benthic data from underwater photos, photo-quadrats and video (photogrammetry) is not new (Bohnsack, 1979; Logan et al., 1984; Roberts et al., 1994; Preskitt et al., 2004), improvements in computing power and photogrammetric software have allowed SfM to become a powerful, flexible tool for benthic monitoring and research, providing more methodological options for collecting data that fits intended study aims. SfM photogrammetry reconstructs a three-dimensional (3D) scene or feature from a series of overlapping two-dimensional (2D) images (Bayley and Mogg, 2020). Underwater SfM image acquisition of large areas is rapid (110 m^2 can be covered in approximately 15 min by a diver [Pizarro et al., 2017]), can be collected with low-cost camera equipment (Raoult et al., 2016) and resulting reconstruction resolution can be cm - mm per pixel due to the proximity of image capture (Marre et al., 2019). Reconstructions can also be orthorectified (correctly scaled) by using ground control points, scale references and/or GPS, allowing for standardised, accurate measurements (Burns et al., 2015; Teague and Scott, 2017; Marre et al., 2019; Nocerino et al., 2020). The SfM process produces a range of 2D or 3D outputs including photomosaics, digital elevation models, 3D meshers and point clouds. Photomosaics, 2D data, allow extraction of biological metrics such as species counts and cover percentages which can be used for calulating community composition, density and diversity (Raoult et al., 2016; Mizuno et al., 2017; Marre et al., 2019). 3D data can also provide information on structural complexity, species morphometrics and biomass (Palma et al., 2018; Bayley et al., 2019), which are frequently used for ecosystem monitoring. Machine learning classifiers, such as object based image analysis (OBIA), can further enhance the utility of these data formats by allowing the semi- or fully automatic classification of features (De Oliveira et al., 2021; Ternon et al., 2022).

Despite the surge in popularity of diver-based SfM photogrammetry for gathering benthic data in shallow water tropical ecosystems, similar examples from temperate regions remain limited. Temperate nearshore subtidal ecosystems are typically turbid environments when compared to their tropical counterparts making SfM image capture a greater challenge (Lochhead and Hedley, 2022; Ternon et al., 2022). Wave action is particularly problematic on rocky reefs dominated by kelp or other algae. These non-rigid taxa will continuously move in relation to water motion which has the potential to hinder the

SfM reconstruction process, as has been shown in terrestrial systems when surveying vegetation in windy conditions (Dandois et al., 2015; Fraser and Congalton, 2018). Diver-based SFM photogrammetry work on algal dominated rocky reefs has to date been limited in spatial scale and focussed on measuring a single metric such as reef rugosity (Monfort et al., 2021), substrate composition (Ternon et al., 2022) or quantifying crustose coralline algae cover underneath kelp canopies (Smale et al., 2020). The potential for using SfM photogrammetry for collecting data from temperate rocky reef ecosystems, particularly as an alternative to, or supplement to traditional SCUBA-based methods for benthic monitoring, requires further investigation.

Here we assess the use of diver-generated photomosaics, a 2D SfM photogrammetry output, for extracting biotic data used for ecosystem monitoring from subtidal rocky reefs along the north-eastern coastline of New Zealand. This coastline has been subjected to significant commercial and recreational fishing pressure since the early 1900s which has resulted in significant declines in the abundance of predatory snapper (*Chrysophrys auratus*) and lobster (*Jasus edwardsii*; Francis and McKenzie, 2015; Webber et al., 2018). Without top-down predatory pressure, overgrazing by the sea urchin *Evechinus chloroticus* has transformed areas of productive *Ecklonia radiata* kelp forest to relatively impoverished urchin barren (Shears and Babcock, 2002). Consequently, urchin barrens are now commonly found on rocky reefs between 2 – 9 m deep along much of the north-eastern New Zealand coastline (Shears and Babcock, 2004). Benthic monitoring within these ecosystems has traditionally been carried out by divers using field quadrats, which is resource and time intensive resulting in limited spatial and temporal sampling. To assess the potential of photomosaics as a monitoring tool we compared data collected from photomosaics to that of traditional quadrats surveys at three sites primarily characterised by urchin barrens within north-eastern New Zealand. At each site SCUBA divers surveyed transects across the reef using quadrats. At the same time, overlapping imagery of the surveyed reef areas was collected and photomosaics created. From these mosaics sea urchin densities, benthic community composition and macroalgae canopy cover, primary metrics recorded in traditional field quadrats, were extracted for comparison. Data collection time for these metrics from both methods was also noted. We discuss these findings along with the strengths and weaknesses of using photomosaics as a monitoring tool within temperate rocky reef ecosystems.

2 Methods and materials

2.1 Field sites

The three sites selected for this study were within within Tıkapa Moana Hauraki Gulf north-eastern New Zealand (Figure 1). All sites were gradually sloping rock reefs that had been significantly impacted by sea urchin overgrazing. The reefs were characterised by a narrow band of mixed algae in the shallows (~ 0-2 m, mostly *E. radiata* and *Carpophyllum* spp.), extensive sea urchin barrens and a deeper *E. radiata* kelp forest. These sites also spanned an environmental gradient of increasing wave exposure and decreasing sedimentation from inner to outer Gulf (Seers and Shears, 2015). As such the lower depth range of the urchin barrens, which is influenced by wave action (Shears and Babcock, 2004), varied from 5–7 m at Leigh, (sheltered bay) to 8-9 m at Hauturu-o-Toi (the most exposed site with the clearest water).

At each site, line transects were laid out perpendicular to the shoreline on a fixed bearing (Figure 1). These ran from the upper limits of the subtidal zone (mean low water [MLW]), through the extent of the urchin barren (the primary area of monitoring focus) to the shallow edge of the kelp forest, sand, or approximately 100 m (~10 m depth), whichever came first. Markers were present every five meters along each transect line. Photogrammetric scale bars (25 cm x 12.5 cm) were placed along the transect length to aid the 3D model reconstruction process. Each scale bar had six visible markers, with exact distance between marker used for accurate scale during the photomosaic processing. Start and end points for each transect were marked by GPS and with heavy weights with subsurface floats. Five transects were surveyed at Leigh and Ōtata, and six surveyed at Hauturu-o-Toi (Table 1).

Data on macroalgae canopy cover, sea urchin density and benthic community composition were collected at Ōtata in November 2020 and at Hauturu-o-Toi in March 2021. Macroalgal cover and benthic community composition data was collected at Leigh in April 2021 however, sea urchin density data was only collected from two transects (C1 and C2; Figure 1, Table 1). This was because sea urchins had been removed from T1 – T3 prior to the benthic survey for a simultaneous project.

Here benthic community composition refers to the sessile biotic taxa and abiotic substrates occupying space on the rocky reef. Benthic community composition categories were selected *a priori*, with the same categories used in the traditional and photogrammetric surveys for consistency (Table S1).

2.2 Traditional field quadrat surveys

A team of two divers collected benthic information along each transect line at 5 m marked intervals, adapted from methods in Shears and Babcock (2004). At each interval, a 1 m^2 quadrat was placed on the reef to assess *in situ* macroalgae canopy cover, sea urchin densities, and the benthic community composition. Canopy cover of large brown macroalgae (by species) and benthic community composition categories were visually estimated and expressed as percent covers. To provide an overview of each quadrat a photo was captured using a GoPro Hero 7. The total time taken for each dive team to collect this information from each transect

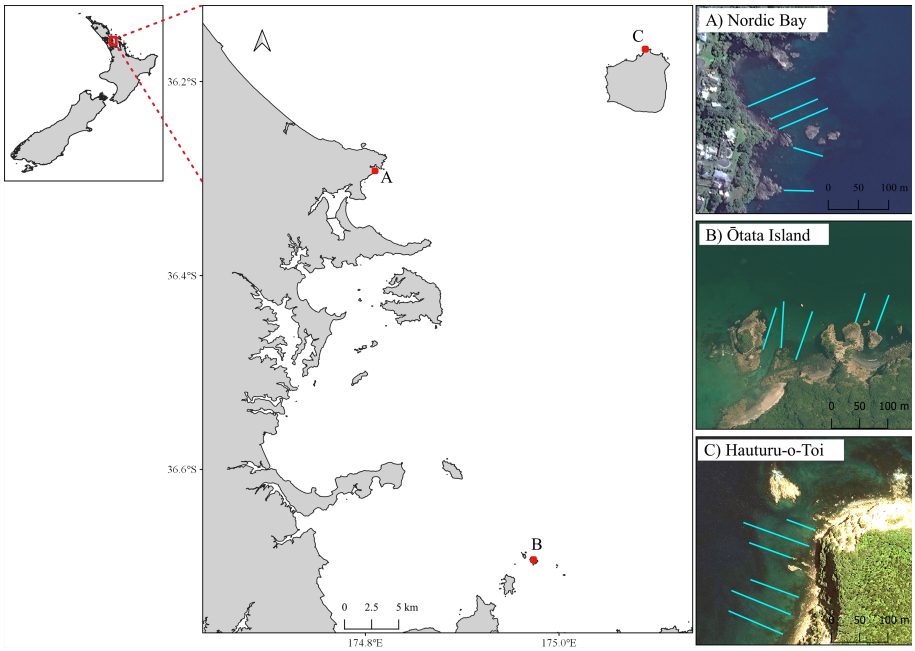

FIGURE 1
Map of Hauraki Gulf in north-eastern New Zealand, with three benthic monitoring sites: **(A)** Leigh, **(B)** Ōtata (inner Gulf); and **(C)** Hauturu-o-Toi (offshore island). Turquoise lines show approximate transect location.

was recorded. Additional information collected by divers but not compared with photomosaic survey include general habitat category, substrate type, depth, abundance and size categories of laminarian (to 25 cm) or fucoid kelps (< or > 25 cm), abundance of large mobile invertebrates, and size categories (to 20 mm) and behaviour of sea urchins. The time taken to collect this additional information was not included into the data collection time analysis, however it was estimated to add an additional 10-20% to the total time taken to collect data from within field quadrats at each site.

2.3 Photomosaic survey

2.3.1 Image collection

Concurrent with the field quadrat surveys, a diver carried out a photographic survey of each transect using methods adapted from previous papers such as Suka et al. (2019) which have collected imagery suitable to produce photomosaics (Figure 2A). Using a wide-angle underwater camera (Nikon Z6 with 14 mm rectilinear lens) the diver slowly swam (~14 m/min) a single pass over each transect line at a distance of 1 – 1.5 m above the benthos. Imagery geospatial information (longitude, latitude and depth) was collected along each transect using an ultra-short baseline underwater geolocation system (UWIS®, x,y absolute accuracy ± 2.5 m). Total time taken to collect the images per dive was recorded after each transect. The camera was orientated directly downward and recorded an image every second, resulting in ~80% overlap between sequential images. Camera settings were aperture priority (f8) with ISO 800 – 3200. These settings allowed for consistent lighting across the length of the each transect, while enabling a high enough shutter speed to counter the effects of motion blur.

2.3.2 Photomosaic assembly

Using the neutral grey tone of the scale bars, image sets for each transect were batch processed to correct for white balance in Adobe Lightroom before being imported into Agisoft Metashape (Professional V1.7) to create the photomosaics (Figure 2B). This was deemed a more appropriate method for ensuring correct colour within the image set than setting the white balance manually in the field as it avoided the need to stop and adjust white balance as depth changed over the length of the transect. Photomosaics were produced using a process similar to that outlined in Bayley and Mogg (2020). Imagery was first aligned (Accuracy = High, Generic preselection, Tie point limit = 70,000, Key point limit = 7,000), creating a sparse point cloud. Model accuracy was refined using the gradual selection tool to remove points with high reconstruction uncertainty, high projection error and poor projection accuracy (Threshold values of 20, 0.5 and 4 respectively). Each sparse cloud was then scaled using image geospatial reference information, checked using the photogrammetric scale bars placed along the transect line and refined using between marker distances.

TABLE 1 Key comparison metrics for each transect between SfM photomosaics and field quadrats. Data collection times are highlighted in red if they were slower, green if faster and blue if the same.

Transect	Site	Sea State	Field Transect Length	Photomosaic Transect Length	Percentage of total transect length covered by photomosaic	Total Number Quadrats assessed	Data collection time photogrammetry method - minutes per quadrat	Data collection time field methodlogy - minutes per quadrat	Number of quadrats compared for macroalgae canopy cover	Number of quadrats compared for substratum cover	Percentage of quadrats assessed for canopy cover and benthos
C1	Otata	<0.5 m	5-65 m	5-55 m	83	11	3.5	8.3	11	11	100
C2	Otata	<0.5 m	0-90 m	10-80 m	78	15	3.3	4.4	15	15	100
T1	Otata	<0.5 m	0-100 m	0-85 m	85	17	3.2	5.0	17	16	94
T2	Otata	<0.5 m	0-100 m	0-100 m	100	21	3.0	8.1	21	21	100
T3	Otata	<0.5 m	0-95 m	0-85 m	89	18	2.8	7.6	18	18	100
C1	Hauturu-o-Toi	<1.0m	0-85 m	0-50 m, 60-75 m	76	15	3.1	6.3*	15	7	47
C2	Hauturu-o-Toi	<1.0m	0-75 m	0-75 m	100	16	3.1	3.6	16	9	56
C3	Hauturu-o-Toi	<1.0m	0-105 m	0-70 m	67	15*	2.8	3.2	15	8	53
T1	Hauturu-o-Toi	<1.0m	0-85 m	10-85 m	88	15	3.4	6.6*	15	10	67
T2	Hauturu-o-Toi	<1.0m	0-110 m	0-110 m	100	23	3.0	6.0	23	16	70
T3	Hauturu-o-Toi	<1.0m	0-100 m	0-95 m	95	17	2.9	2.5	17	16	94
C1	Leigh	<1.0 m	0-85 m	35-85 m	59	11	3.4	3.4	11	11	100
C2	Leigh	<0.5 m	15-35 m	15-35 m	100	5	3.4	3.8	5	5	100
T1	Leigh	<1.0 m	0-90 m	5 -75 m	78	15	3.0	3.1	15	13	87
T2	Leigh	<0.5 m	0-90 m	0-90 m	100	18	2.6	3.5	18	15	83
T3	Leigh	<0.5 m	0-100 m	0-95 m	95	19	2.8	3.7	19	18	95

*Time values considered to be outliers and removed from analysis.

10.3389/fmars.2022.953191

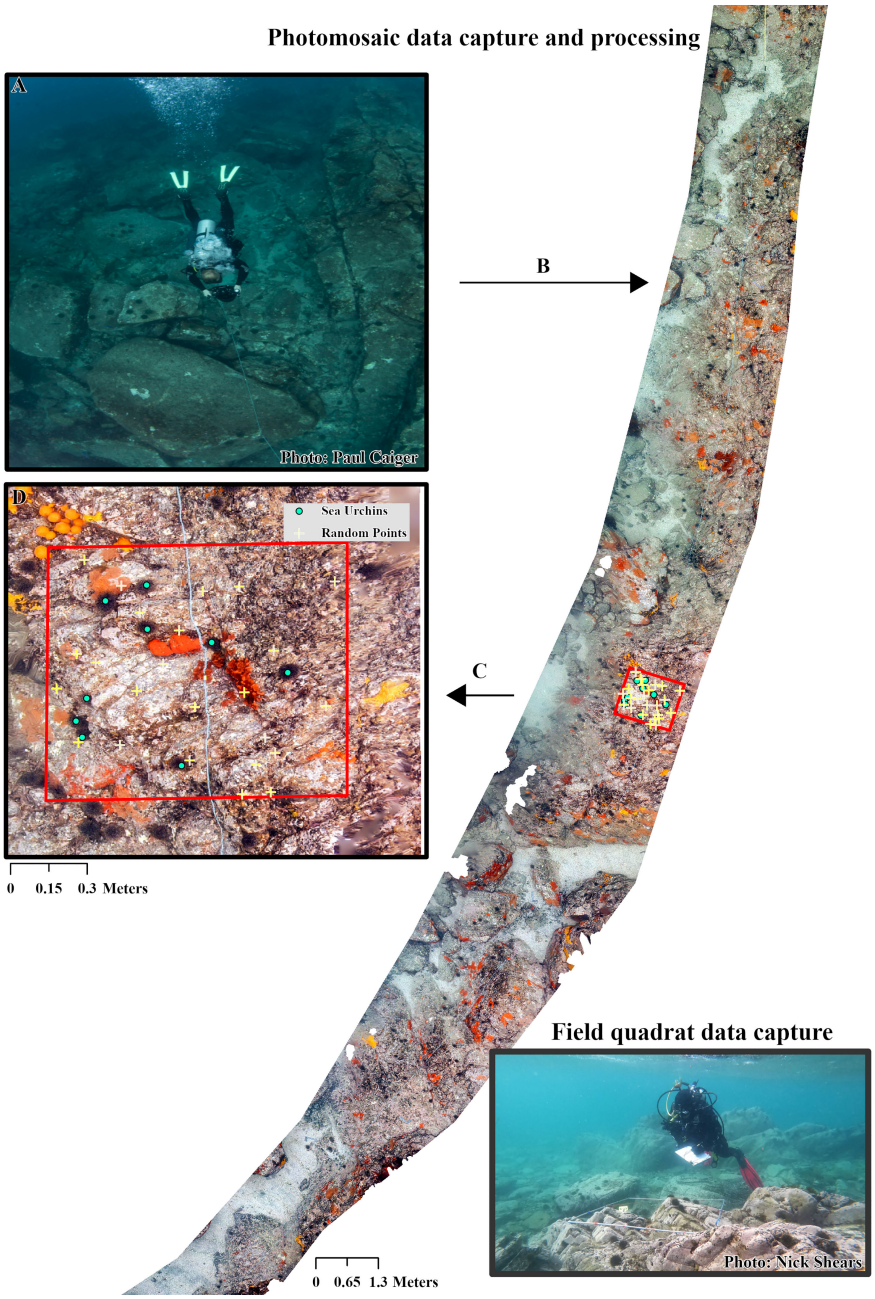

FIGURE 2
Photomosaic data capture and processing. **(A)** Capture of raw imagery in the field, **(B)** image processing and creation of photomosaic, **(C)** transfer of photomosaic raster into GIS software and **(D)** placement of virtual quadrats, annotation of random benthic community points and marking of sea urchins. Transect line is visible crossing through the quadrat position. Insert Diver collecting data from field quadrat.

The sparse cloud was re-optimised, and a dense cloud created (Quality = High, Depth filtering = Mild). A digital elevation model (DEM) was produced from the point cloud which then allowed for the photomosaic to be created (Surface = DEM, blending mode = Mosaic, Hole filling and ghosting filter enabled). As with Raoult et al. (2016) photomosaic assembly time was not included in the data collection time analysis because much of this process is automated. Additionally, the total processing time is dependent on camera image resolution, the number of images being processed and computing power available for use (Bayley and Mogg, 2020; Couch et al., 2021).

2.3.3 Data extraction

Photomosaics were imported into ArcGIS Pro (V2.8) for data extraction (Figures 2C, D). Metrics extracted from the mosaics were: sea urchin density, large brown macroalgae canopy cover and benthic community composition (later two expressed as a percentage). These metrics were assessed at every 5 m interval that could be positively matched to the corresponding 5 m interval recorded during the field survey. Data was extracted from within a 1 m^2 virtual quadrat, created using the feature envelope to polygon tool around a 0.5 m circular buffer centred on each interval marker. Virtual quadrats were populated with 25 randomly placed points using the generate random points tool. Each point was assigned a cover type following the coral point count method (Kohler and Gill, 2006). Cover fell into three broad categories: large brown macroalgae (three types), benthic community composition (twenty-five types – including biotic and abiotic covers) and unclassified for all points which could not be positively identified (four types; Table S1). Following this, all sea urchins were identified and marked within each virtual quadrat. The total time taken to extract the above information was recorded. At Leigh, the time taken to record sea urchin densities along three of the transects was estimated (from the pooled average per quadrats time for all transects across the three sites) due to the absence of sea urchins following removal prior to the survey (see **Section 2.1**).

A percentage value was calculated for macroalgae types and benthic community composition categories recorded within each virtual quadrat. Points classified as shadow/blur were excluded from macroalgae canopy cover calculations as these represented points where the presence or absence of macroalgae could not clearly be determined. All macroalgae and unclassified cover types were excluded from benthic community composition calculations as these represented points where the underlying benthic canopy type could not be accurately defined. Any virtual quadrats where more than eight individual points could not be used towards a cover percentage conversion were discarded from the comparison analysis (Table 1).

To test the effect of reducing number of random points assigned to each transect on overall benthic community composition the first 15 points from each quadrat were selected and compared to the results from 25 points. For this comparison, any quadrat where more than five individual points could not be used towards a percentage conversion were discarded from the comparison analysis.

Because field quadrats were placed on 3D surfaces, while virtual quadrats were placed in 2D space, slight differences in quadrat placement were likely to have occurred between the two methods. While not an issue for cover percentages, which were an estimate for both methods, this would likely impact comparisons of sea urchin counts. To account for this, five intervals were randomly selected from each transect. At each a virtual quadrat was drawn out to match the alignment of the field quadrats. The photographs taken during the field quadrat survey was used to guide virtual quadrat placement. All visible sea urchins were then recorded for comparison. Due to camera issues at Leigh (field quadrat survey), sea urchin densities comparisons were made from photomosaics and field quadrat data of transects C1 and C2 collected from a previous survey in August 2020.

2.3.4 Data analysis

Binomial logistic regression was used to assess the probability of successfully stitching a five-metre section of photomosaic (success = yes or no) relative to three variables: biological habitat type, depth and wave action. Each section was categorised as: barren (no macroalgae canopy), mixed (sparse macroalgae canopy present) or macroalgae (dense macroalgae cover present) and depth bracket (<3 m, 3 – 5.9 m, 6+ m). Wave action (<0.5 m, 0.5 – 1.0 m) was applied to each transect based on swell conditions on the day (Table 1). The optimal model was selected through backwards elimination of non-significant interaction terms. This resulted in the final model with one interaction term (Biological habitat type*Wave action).

Two-way ANOVA was used to investigate any differences in data collection time between data collection methods (Photogrammetry, Field Quadrats), site (Leigh, Ōtata, Hauturu-o-Toi), and this interaction. Time was standardised to data collection time per quadrat and log transformed to meet the assumptions of normality and equal variance (Shapiro-Wilks and Levene's Tests respectively). Time values for two Hauturu-o-Toi transects (Field Quadrats) were considered outliers and were removed, along with the times for the corresponding photogrammetry transects from analysis. As a significant interaction was found, *post hoc* t-tests for time differences between data collection methods were performed for each site.

Two-way ANOVA was used to investigate any differences in sea urchin densities and large brown macroalgae cover, for two groups (*Ecklonia radiata* and *Sargassum sinclairii*), between data collection methods (Photogrammetry, Field Quadrats), site (Leigh, Ōtata, Hauturu-o-Toi) and the interaction. As all three metrics meet the assumptions of normality and equal variance (Shapiro-Wilks and Levene's Tests respectively) two-way ANOVA tests were performed on untransformed data. Data on fucoid canopy cover failed to meet the assumptions of normality and equal variance, even after being square root transformed. Fucoid canopy cover differences between data collection methods (Photogrammetry, Field Quadrats), site (Leigh, Ōtata, Hauturu-o-Toi) and the interaction were therefore investigated using univariate PERMANOVA. Univariate PERMANOVA was chosen because it is robust against the non-normality and heterogeneity of variance that are often associated with ecological data (Anderson, 2014). This test was performed on untransformed transect averaged data.

Multivariate PERMANOVA was used to compare benthic community composition data between the two survey methods. The test was performed on square-root transformed transect

averaged data in PRIMER-e (V7) using Bray-Curtis dissimilarity matrices. This tested the main effects of method (Photogrammetry, Field Quadrats), site (Leigh, Ōtata, Hauturu-o-Toi), and their interaction. Down-weighting the importance of the most abundant species, through the square-root transformation, was considered appropriate to ensured that less common species also contributed towards similarity calculations within the data matrix (Clarke et al., 2014). Nonmetric multidimensional scaling (nMDS) was then used to visualise dissimilarity in benthic community composition between the survey methods at each site. To understand which benthic community composition categories contributed most to observed dissimilarity between data collection methodologies at each site, similarity percentage (SIMPER) breakdowns were undertaken. At each site, the benthic community composition categories that accounted for the greatest dissimilarity between methodologies (to an accumulated 70% of the observed dissimilarity) were identified.

An additional multivariate PERMANOVA analysis was undertaken to assess differences in the data between photogrammetry point counts based on 25 random points and 15 random points. This tested for main effects of method (Photogrammetry 25 pts, Photogrammetry 15 pts), site (Leigh, Ōtata, Hauturu-o-Toi) and their interaction.

3 Results

3.1 Photogrammetry metrics

A high resolution photomosaic was successfully created for each of the 16 transects assessed. Thirteen photomosaics had sub-millimetre image resolution, with the lowest quality resolution being 1.4 mm/pixel. Photomosaic coverage across the total transect length was high, averaging (± SE) 87 ± 1% (Table 1). The probability of stitching success was typically greater than 90% within areas of barren across all depths and levels of wave action (Table 2). The lowest probability (85%) of success for barren areas was seen in less than 3 m of water where wave action was 0.5 - 1.0 m. Stitching success in areas of mixed barren/macroalgae showed a similar trend to barrens and was typically high (> 88%) except for in areas less than 3 m deep when wave action was 0.5 - 1.0 m. Here the probability of success fell to 67%. Stitching success was lowest in biological habitats classified as macroalgae (10% – 83%), with the lowest probability of success in shallow water. However, for macroalgae we found that overall success rates rose when wave action was greater (Table 2).

We found that failed image alignment was the primary cause of poor stitching success of kelp in deeper water. Image alignment, the first step of the SfM reconstruction process, requires the precise 3D coordinates for a feature (e.g. a corner or edge) to be calculated across multiple overlapping images (Sieberth et al., 2014). A lack of accurately mapped features may result in the failure to correctly align subsequent images, limiting image reconstruction. In very shallow water, failed image alignment also contributed to the poor stitching success of areas of both mixed and macroalgae; however, the impracticality of capturing imagery in very shallow water meant that in some instances imagery from the upper extent of a transect was simply not available for alignment and subsequent stitching.

Macroalgae canopy cover could be evaluated for all virtual quadrats (Table 1). In contrast, benthic community composition could only be calculated for an average of 84 ± 4% of virtual quadrats on each transect (Table 1), which varied between sites. For Leigh and Ōtata, the average number of quadrats where benthic community composition could be determined be made was above 90%. Virtual quadrats that could not be assessed were those with high (> 50%) macroalgae canopy cover. Consequently, not enough points were classified as a benthic community composition type. For Hauturu-o-Toi, the average number of virtual quadrats able to be assessed for benthic community composition was noticeably lower (64 ± 7%.) While high macroalgae canopy cover limited assessment for some quadrats, the primary cause of low benthic assessment rates was due to a filamentous algae bloom. It was extremely difficult to accurately quantify benthic community composition types in both methodological approaches where high densities of overlying filamentous algae were present.

TABLE 2 Results from logistic regression assessing the probability of successfully stitching a section of photomosaic at different depths, within different habitat types and under differing wave conditions.

Variables	Coefficient	SE	*Z*	*p*	Odds ratio
Intercept	2.31	0.49	4.75	0.00	10.09
Depth (3–5.9 m)	1.78	0.51	3.50	0.00	5.91
Depth (6+ m)	1.34	0.58	2.30	0.02	3.84
Habitat (macroalgae)	-4.43	0.96	-4.61	0.00	0.01
Habitat (mixed)	14.33	1429.39	0.01	0.99	>100
Wave action (0.5–1 m)	-0.56	0.66	-0.85	0.40	0.57
Macroalgae x Wave action (0.5–1.0 m)	2.50	1.14	2.20	0.03	12.18
Mixed x Wave action (0.5–1.0 m)	-15.35	1429.39	-0.01	0.99	0.00

In the model the intercept represents barren (Habitat) in <3 m of water (Depth) when wave action was <0.5 m (Wave action).

3.2 Data collection

Photogrammetry data collection was faster than field quadrat data collection at Ōtata and Leigh but not Hauturu-o-Toi (Figure 3A, Table 3A). On average (± SE) traditional field quadrat data collection took 4.7 ± 1.9 min/quadrat while photogrammetric data collection took 3.1 ± 0.1 min/quadrat, approximately 1 minute and 44 seconds faster per quadrat. Time spent in the field accounted for 100% of the total data collection time for field quadrats, whereas field time only accounted for ~10% of the total data collection time for the photogrammetry method (Figure 3B). This equated to roughly 5 – 6 minutes of

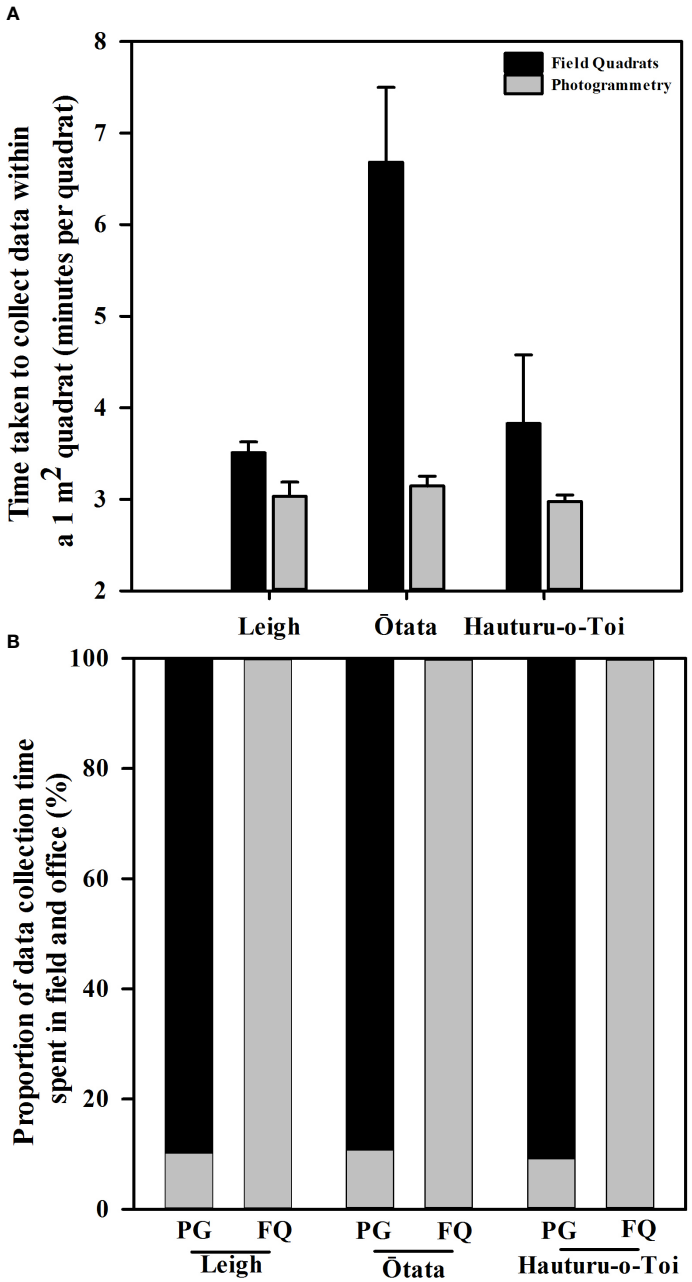

FIGURE 3
(A) Mean (+ SE) time taken per 1m^2 quadrat to collect data from virtual photogrammetry quadrats (grey bars) and *in situ* field quadrats (black bars) at each of the three monitoring sites. **(B)** Proportion of total data collection time spent in the field (grey bars) and in the office (black bars) for virtual photogrammetry quadrats (PG) and field quadrat (FQ) at each of the three monitoring sites.

TABLE 3 Results of two-way ANOVA tests on (A) data collection time, (B) sea urchin densities, (C) canopy cover of *Ecklonia radiata* and, (D) canopy cover of *Sargassum sinclairii*, (E) a univariate PERMANOVA test on canopy cover of fucoid algae, (F) a multivariate PERMANOVA test on the difference between photogrammetry and field quadrats, and (G) a multivariate PERMANOVA test on the difference in substratum covers between 25 and 15 random points.

A)	Data collection time		
Coefficient	Df	F	*p*
Method x Site	2	7.08	**0.00**
Residual	22		

B)	Sea urchin densities		
Coefficient	Df	F	*p*
Method	1	0.01	0.91
Site	2	2.12	0.12
Method x Site	2	0.16	0.85
Residual	124		

C)	*Ecklonia* cover		
Coefficient	Df	F	*p*
Method	1	0.47	0.50
Site	2	18.00	**0.00**
Method x Site	2	0.40	0.68
Residual	26		

D)	*Sargassum* cover		
Coefficient	Df	F	*p*
Method	1	0.90	0.36
Site	2	12.25	**0.00**
Method x Site	2	0.17	0.84
Residual	26		

E)	Fucoid cover		
Coefficient	Df	F	*p*
Method	1	0.20	0.66
Site	2	9.03	**0.00**
Method x Site	2	0.10	0.91
Residual	26		

F)	Photogrammetry vs Field Quadrats		
Coefficient	Df	F	*p*
Method	1	8.94	**0.00**
Site	2	21.84	**0.00**
Method x Site	2	1.29	0.23
Residual	26		

G)	Photogrammetry point comparison		
Coefficient	Df	F	*p*
Method	1	0.19	0.95
Site	2	38.58	**0.00**
Method x Site	2	0.05	1.00
Residual	26		

Significant p values are bold. Main test p values omitted where a significant interaction term exists.
Each test for the main effects of Method, Site and Method x Site.

time collecting the required imagery per transect or ~19 sec/quadrat.

3.3 Sea urchin densities

Mean sea urchin densities did not differ significantly between data collection methodologies, nor was there an interaction between methodology and site (Figure 4A, Table 3B). However, at Leigh, the photomosaics showed non-significant lower densities of sea urchins. This was likely due to higher densities of small (<40 mm test diameter) cryptic sea urchins that were harder to detect within the mosaic.

3.4 Macroalgae cover

Mean canopy cover for all macroalgae groups (*Ecklonia radiata*, *Sargassum sinclairii* and fucoids) did not differ significantly between data collection methodologies nor were there interactions between methodology and site (Figures 4B–D, Tables 3C–E).

3.5 Benthic community composition

Results from the multivariate PERMANOVA showed a difference in benthic community composition between the two methodological approaches (Table 3F). SIMPER analysis found that at all sites sediment cover was a primary contributor to the observed methodological differences and that broadly consistent benthic community compositions, with low levels of average dissimilarity, were recorded between the methods (Figure 5, Table 4). At Leigh and Hauturu-o-Toi sediment was the greatest contributor to overall dissimilarity; sediment cover was four to five times higher within field quadrats than in virtual quadrats. This is highlighted in the nMDS plots for both sites where there is clear separation between the methodologies in the direction of sediment (Figure 6). At Ōtata, recorded sediment cover was approximately three times higher

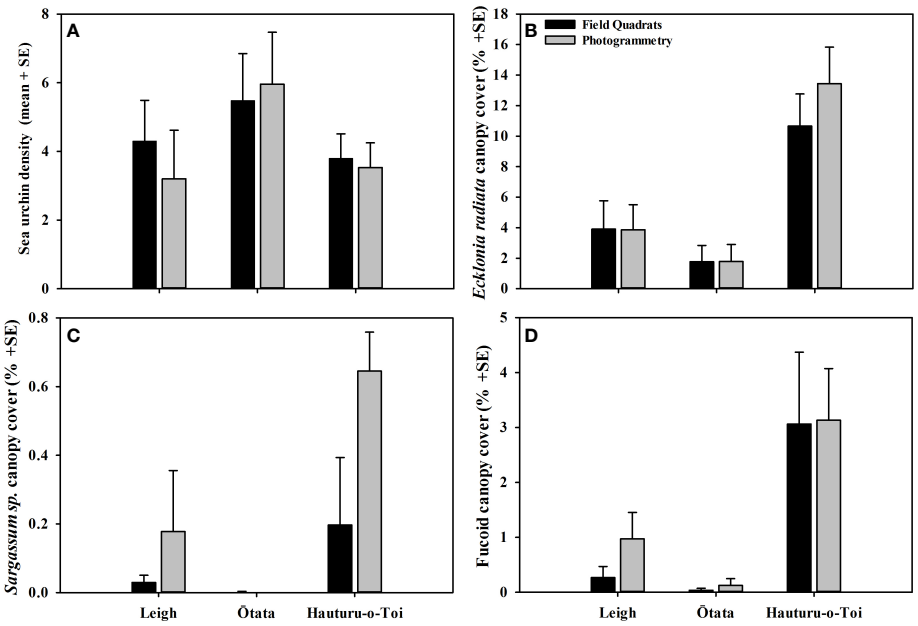

FIGURE 4
(A) Mean (+SE) sea urchin density, **(B)** mean *Ecklonia radiata* canopy cover, **(C)** mean *Sargassum sinclairii* canopy cover and **(D)** mean fucoid canopy cover recorded in virtual photogrammetry quadrats (grey) and field quadrats (black) at each of the three monitoring sites.

within field quadrats than in virtual photogrammetry plots; however, recorded brown encrusting algae (BEA) cover was approximately four times higher in the virtual photogrammetry quadrats than in the field quadrats (Figure 5). Both contribute equally to overall dissimilarity and nMDS plots show methodological separation, primarily in the direction of sediment/BEA (Figure 6).

Within virtual quadrats for the photomosaics, we found that the use of 25 random points per quadrat did not yield significantly different overall substratum coverage percentages than 15 random points per quadrat, nor was there any interaction between the number of points and sites surveyed (Figure 5, Table 3G).

4 Discussion

In this study we compared commonly used ecosystem monitoring metrics on temperate rocky reefs dominated by urchin barrens between data extracted from high-resolution, SfM derived, photomosaics and traditional diver-based field quadrats. Primary survey metrics, including sea urchin densities, kelp canopy cover and benthic community composition data, were similar between the two methodologies, consistent with other papers comparing benthic data collected by photography with traditional methods (Dodge et al., 1982; Preskitt et al., 2004; Parravicini et al., 2009; Jokiel et al., 2015) and more specifically comparing the use of photomosaics with traditional methods (Ling, et al., 2016; Raoult et al., 2016; Burns et al., 2020; Barrera-Falcon et al., 2021; Couch et al., 2021). Photogrammetric data collection required minimal in-field time, and can increase the potential survey area. However, not all habitats are suitable, as reconstruction success was hindered in areas of very shallow waters and/or areas where high macroalgal canopy cover existed. High macroalgal canopy cover and the presence of seasonal algal growth restricted the ability to extract benthic community composition information from photomosaics. A wider range of data metrics were able to be collected from field quadrats than photomosaics across all habitat surveyed. Overall we found that high resolution photomosaics were a quick, efficent way of collecting robust data on basic moniroting metrics from temperate rocky reefs with low macroalgae canopy cover, whilst also providing a permanent visual record of the site. In areas where macroalgae cover was high, traditional diver-based field quadrat surveys yielded more comprehensive data as sampling under the canopy remained possible, whereas photomosaics only provided information on macroalgae canopy cover. Decisions regarding the level of detail, and consequently time and resources required for in-field data collection, will ultimately depend on the aims of any study. The strengths and limitations of photomosaics as a tool for monitoring temperate rocky reef ecosystems are discussed below (Table 5).

4.1 Strengths and limitations

Data collection from SfM derived photomosaics was generally more time efficient than in-water monitoring using

10.3389/fmars.2022.953191

TABLE 4 SIMPER analysis results at (A) Leigh, (B) Ōtata and (C) Hauturu-o-Toi showing average site dissimilarity between data collection methods (photogrammetry, field quadrats) and key benthic community composition categories contributing towards overall dissimilarity.

A)	Leigh Average Dissimilarity 20.6%	
Benthic Community Cover Categories	**Individual Contribution (%)**	**Cumulative Contribution (%)**
Sediment	21.6	21.6
Crustose coralline algae (CCA)	14.77	36.37
Red foliose turf	9.75	46.12
Red/Green Turf (RGT)	9.03	55.15
Brown encrusting algae (BEA)	8.53	63.68
Sponge	6.99	70.67
B)	**Ōtata**	
	Average Dissimilarity 25.0%	
Benthic Community Cover Categories	**Individual Contribution (%)**	**Cumulative Contribution (%)**
BEA	15.9	15.9
Sediment	14.46	30.36
Bare rock (BR)	11.29	41.65
Coralline turf (CT)	7.54	49.19
Sand, shell, gravel (SSG)	7.48	56.67
Anemone	7.43	64.1
CCA	6.95	71.05
C)	**Hauturu-o-Toi**	
	Average Dissimilarity 23.3%	
Benthic Community Cover Categories	**Individual Contribution (%)**	**Cumulative Contribution (%)**
Sediment	21.59	21.59
BR	11.63	33.22
CCA	10.41	43.63
SSG	9.94	53.57
RT	9.65	63.22
BEA	9.41	72.62

Benthic community composition categories up to a cumulative total of 70% of the average dissimilarity have been included.

field quadrats. It should however be noted that more data metrics were able to be recorded (and were recorded in this study) within field quadrats than photomosaics, such as specific measurements and invertebrate records. Although this additional data was not considered in the time analysis, some metrics such as recording kelp abundance can be time consuming, and would further increase the overall time taken per field quadrat. The amount of time required for these metrics varied greatly depending on density of invertebrates, macroalgae, etc., but was estimated at roughly 10-20% additional time. Within urchin barrens, where this comparison was primarily conducted and where macroalgae was absent or sparse, the additional time required to make algal and invertebrate measurements was minimal. In this study, where four to six divers conducting multiple dives were required to collect the field quadrat data at each site, a single diver could capture the required photogrammetric imagery within two dives. Importantly, SfM methodolgy conferred the additional advantage of only one tenth of the total data collection time occuring underwater. Monfort et al. (2021) discussed similar findings where rugosity measured from SfM derived 3D point clouds was quicker than *in situ* 'chain and tape' measurements, while Couch et al. (2021) found that photomosaics yeilded similar coral colony data to *in situ* data collection, but reduced field time by 55%. This reduction in field time is consistent with the use of other photographic techniques, such as photo-quadrats, over field quadrats (Preskitt et al., 2004). Using SfM photogrammetry can significantly reduce the field time and resources required to collect benthic monitoring data and thus can capture more data spatially, albiet from a more limited range of data metrics, in restricted field seasons or windows. While capturing photographic data requires the additional expenses of camera equipment, a number of studies have found that low cost cameras performs well for creating photomosaics (Raoult et al., 2016; Neyer et al., 2019; Nocerino et al., 2019) and that initial costs associated with purchasing equipment are quickly offset by

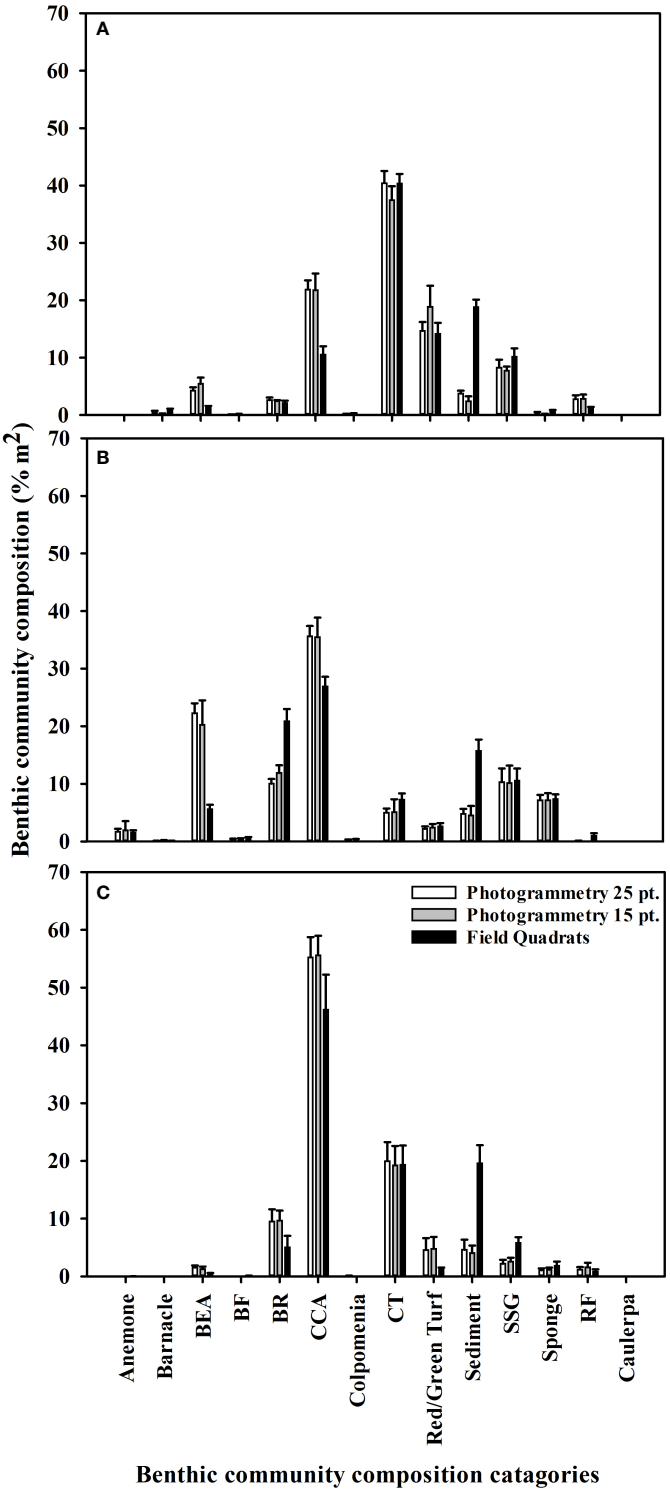

FIGURE 5
Mean (+SE) benthic community composition percentage covers recorded at **(A)** Leigh, **(B)**, Ōtata and **(C)** Hauturu-o-Toi using virtual photogrammetry quadrats with 25 random points (white), virtual photogrammetry quadrats with 15 random points (grey) and field quadrats (black). For display purposes only benthic community composition categories with a mean cover greater than 1% are included.

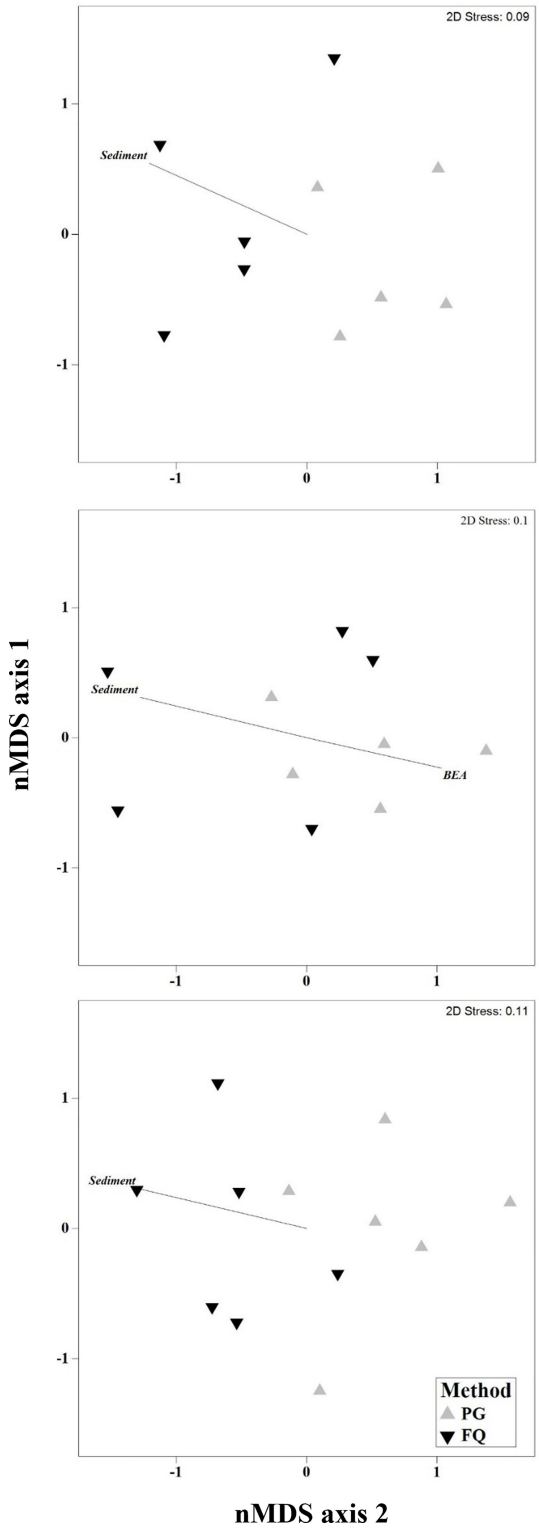

FIGURE 6
Non-metric multidimensional scaling (nMDS) plots of dominant benthic community composition categories at **(A)** Leigh, **(B)** Ōtata and **(C)** Hauturu-o-Toi as recorded within virtual photogrammetry quadrats (PG, grey) and field quadrats (FQ, black). nMDS plots based on Bray-Curtis distance matrices constructed from square-root transformed transect centroid data. Black lines show directional influence of key benthic community composition categories from SIMPER analysis.

TABLE 5 Comparative strength and weaknesses of field quadrats and photomosaics within temperate rocky reef ecosystems.

Metric	Method	
	Field quadrats	Photomosaics
Data extraction	Moderate	Fast
In-water data extraction component	100%	10 - 15%
Dive team required (per site)	4 - 6 divers	1- 2 divers
Area coverage (per dive)	15 - 25 m^2	300+ m^2
Permanent visual record	Limited	Yes
Visual perspective	3D in field	2D digital image
Level of detail within areas of low macroalgae cover	High	High
Level of detail within areas of high macroalgae cover	High	Low
Ability to identify cryptic species	Easy	Difficult
Feasibility in very shallow water	Yes	Yes, but difficult in areas of shallow mixed algae
Feasibility in rough conditions	Feasible within all habitat types but strenuous	Only feasible over areas of low macroalgae cover
Quality control	Relies on well trained field team and accurate in-field data entry	High, can re-evaluate data and confer with others at leisure
Processing time	~2 hours per transect.	~3 – 4 hours per transect. ~1.5 hours per transect of manual input; remainder is automated

the cost-savings made from reduced field and resources requirements (Jokiel et al., 2015).

The consistency between data collected from the two methods suggests both provide robust forms of benthic monitoring data for key metrics. We did, however, find two notable differences in the datasets. Firstly, sediment cover was consistently higher in field quadrats than in the photomosaic data. This was largely due to different methods for benthic community composition estimates: visual (for field quadrats) and point count (photomosaic) estimates. Visual estimates tease out sediment bound within other substrate types, increasing sediment cover while decreasing other cover types (particularly encrusting and turfing algae). In the point count method, only points where a substrate type could not be identified due overlying sediment were recorded as sediment, resulting in lower sediment estimates. Secondly, brown encrusting algae cover (BEA) was consistently higher in photomosaics at Ōtata. Larger field teams require more training and increase the risk of inter-observer variation and errors. Surveyor experience can play an important role in the quality of collected data (Bernard et al., 2013) and an individuals interpretation of a given classification type, can result in substantial differences from one recorder to another (Cherrill and McClean, 1999; Beijbom et al., 2015). Observer error was considered the likely cause for this differences in BEA cover at Ōtata. Many encrusting algae look superficially similar and different interpretation of BEA between divers may have resulted in misclassificaion. This would result in consistency issues when trying to compare results with future monitoring data. In contrast, extracting data from the photomosaics required a single desk-based annotator who could rest when fatigued, could revisit sections of the imagery if discrepancies were picked up, and could confer with other ecologists for identification, reducing overall error and increasing quality control.

With SfM photogrammetry, a significant time investment is required to process the imagery into usable formats such as photomosaics (Couch et al., 2021). However, once processed, a photomosaic represents a permanent visual archive of a study area that can be repeatedly returned to without the need for further field time. It also allows for a significantly greater area of reef to be surveyed. Where 15 – 20 m^2 of data was collected from a transect using field quadrats as much as 100 m^2 was available for data extraction from the photomosaics. These benefits need to be carefully considered against the costs associated with the lengthy processing times required to create these and other SfM outputs. In this study photomosaic processing time was roughly 3 – 4 hours per transect. We did not include photomosaic processing as part of the 'timed' data collection because processing timeframes can vary signficantly with image resolution, the number of images being processed and available computing power (Bayley and Mogg, 2020; Couch et al., 2021). Overall processing time will increase with image resolution, larger areas, number of images and less computing power. However, much of the process is fully automated, with batch processing allowing simultaneous processing requiring only periodic manual intervention. For this study the manual processing components included image georeferencing and white balancing, intial workflow set up within Metashape and scaling/refining the sparse cloud. The time taken for this was relatively consistent across transects (~1.5 hours) and accounted

for at most 50% of the total photomosaic processing time. In contrast, data recorded from field quadrats does not require computer-orientated post processing but does require transcription into a digital format for analysis. For this study this included copying field data into a digital spreadsheet, labelling and validating photos for each quadrat and data quality checks. This can be slowed or compromised by transcription errors, illegible handwriting or reliance on individuals recollections if data does not make sense. As with photomosaic processing we did not include this transcription into the 'timed' data collection processed however this accounted for roughly 2 hours per transect. While overall photomosaic processing time was approximately twice as long as the field quadrat data transcription process, the manual processing time was similar for both methods. Thus, we constrained the activities for time comparison to include data collection only (field and data extraction).

The number of sampling points within a given area can affect both precision and sampling time. We found that reducing the number of sampled points from 25 to 15 did not alter the overall breakdown of substratum covers within a 1 m^2 quadrat but decreases the time required to analyse a virtual quadrat. Perkins et al. (2016) found the precision of targeted monitoring species, when analysing benthic imagery, was increased by increasing the number of images sampled, as opposed to increasing sampling rate within images. However, the appropriate number of points per unit area will depend on the distribution and abundance of the species of interest (Pante and Dustan, 2012). For comparitive purposes this study only examined point count data within 1 m^2 quadrats, however the methodological approaches for data extraction from photomosaics are highly varied. In the case of community composition data, this could have also been collected across the length of our transects by hand-drawing polygons around various community catagories (Urbina-Barreto et al., 2021), or with the aid of machine learning classification algorithms (Mohamed et al., 2020; Ternon et al., 2022). This affords researchers the choice of selecting different data extraction method to best meet study aims as well as the ability to use the same underlying data set, but different methodological approaches for data extraction if new questions arise.

Despite increased sampling availabilty within a given photomosaic, reconstructing the entire transect was not always possible. Coverage in the shallowest areas (<1.5 m) was often impractical, while areas of dense macroalgae (typically the upper and lower extents of a transect) suffered from image alignment issues. Image misalignment was likely caused by macroalagal movement between images due to wave action and/or because dense macroalgae represents a homogenous, low contrast surface where the feature matching algorithms failed to pick out distinct points (Mancini et al., 2013). Vegetation movement, caused by high wind speeds, can cause feature mismatches and poor image alignment in UAV forest surveys (Dandois et al., 2015; Fraser and Congalton, 2018). Similarly, water motion can cause macroalgal movement between images, also resulting in feature mismatches and a failure to properly align images. In terrestrial systems, these alignment issues can be overcome by flying at greater altitiudes (Fraser and Congalton, 2018), which increases the area available in each image to detect features and reduces perspective distortion between images. We recommend that underwater imagery for SfM processing over macroalgae be captured at least 1 m above the benthos to improve the chances of success. Alternatively, issues matching homogeneous, low contrast features might explain why images over dense monospecific stands of macroalgae failed to align while areas along the same transect, surveyed under the same sea state conditions and dominated by a mixture of dense turfing and foliosed algae along with juvenile macroalgae, were able to be aligned. Overall, we found photomosaics provided limited monitoring information over areas of dense macroalgae cover.

Dense macroalgal canopies conceal underlying substratum, thereby reducing the utility of the imagery for substratum assessment (Tait et al., 2019). Where field quadrats can access under the kelp canopy and collect underlying benthic data, the photomosaics were only able to provide basic macroalgae canopy cover data. Seasonal filamentous algal blooms also caused data collection issues for photogrammetry and to a lesser extent for field quadrats. Where possible, imagery collections should occur outside of key growth periods for filamentous algae. Although not a major issue for this study, 2D imagery, such as photomosaics and photo-quadrats, are limited in their ability to detect organisms or substrate types occupying in deep cracks or overhangs (Jokiel et al., 2015; Couch et al., 2021). We found that photomosaics were less able to detect small sea urchins (<40 mm) hidden in cracks and crevices. Similarly, Ling et al. (2016) found that daytime density estimates of the sea urchin *Centrostephanus rodgersii*, which preferentially occupy crevices during the day, were lower in photomosaics than estimates from divers who were able to inspect crevices as they surveyed the area. While this study was designed to investigate data captured from 2D photomosaics, three-dimensional forms of photogrammetry data, such as point clouds and 3D meshes, may be able to be utilised to gather additional data from highly complexity reefs.

It has been suggested in tropical systems that there is unlikely to be a single method that can be considered the 'gold standard' for benthic monitoring (Burns et al., 2020; Couch et al., 2021). This appears true within temperate rocky reef ecosystems as well. As SfM derived photogrammetry has increased in popularity, and data derived from photogrammetry can be standardised with that collected from more traditional means (Jokiel et al., 2015), researchers have the ability to select and develop monitoring approaches that draw upon the strengths of different combinations of traditional and emerging techniques. For example, a study could incorporate field quadrat-based approaches in very shallow or highly layered habitats but using SfM photogrammetry in areas with low macroalgal cover, or a broad-scale SfM photogrammetry across a large area with fine detail collected from a smaller number of field quadrats. The ability to use

diverse and perhaps complementary techniques will allow benthic ecologists to maximise data collection across the spectrum of habitat types present throughout an ecosystem within realistic time and resource constraints.

5 Conclusion

The results from this study build our understanding of the strengths and weakness of utilising diver-generated photomosaics, a form of SfM derived photogrammetry, for monitoring temperate rocky reefs. Photomosaics provide robust, spatially extensive data for a number of key rocky reef metrics, but is limited with respect to cryptic or understory species. Photogrammetry data collection is generally more time efficient than *in situ* field quadrat monitoring and requires minimal dive time. It also provides a permanent record of a site which can be reinvestigated without more time in the field. Their utility is lessened in areas of high macroalgae canopy cover, very shallow water or heightened sea state. Thus diver-generated photomosaics are a valuable monitoring tool in areas of low macroalgae cover, such as urchin barrens, but of limited value within kelp forests. As with comparative studies in tropical systems, highlighting the strengths and weakness of different data collectiong methodolgies reveals there is unlikely to be a 'gold standard' for monitoring temperate rocky reef ecosystems. Instead developing flexible monitoring programmes that utilise a range of techniques, including photogrammetry and more traditional methods, will result in the greatest level of data capture and spatial coverage, while reducing in-field resource and time related costs.

Data availability statement

The datasets presented in this study can be found in online repositories. The names of the repository/repositories and accession number(s) can be found below: https://figshare.com/projects/Divergenerated_photomosaics_as_a_tool_for_monitoring_temperate_rocky_reef_ecosystems/140110.

Author contributions

AS and KM conceived the ideas and designed methodology. AS and KM collected the data. AS analysed the data. AS led the writing of the manuscript. All authors contributed critically to the drafts and gave final approval for publication.

Funding

Funding for this project was provided by Live Ocean Charitable Trust, New Zealand Geographic, Foundation North: GIFT, and University of Auckland Doctoral Scholarship (awarded to KM).

Acknowledgments

Thanks to James Frankham for ongoing encouragement and support for the project; thanks to staff and students at the Leigh Marine Laboratory for assistance with field work. Thanks to two reviewers for their helpful feedback and improvements to this manuscript.

Conflict of interest

The authors declare that the research was conducted in the absence of any commercial or financial relationships that could be construed as a potential conflict of interest.

Publisher's note

All claims expressed in this article are solely those of the authors and do not necessarily represent those of their affiliated organizations, or those of the publisher, the editors and the reviewers. Any product that may be evaluated in this article, or claim that may be made by its manufacturer, is not guaranteed or endorsed by the publisher.

Supplementary material

The Supplementary Material for this article can be found online at: https://www.frontiersin.org/articles/10.3389/fmars.2022.953191/full#supplementary-material

References

Anderson, M. J. (2014). *Permutational multivariate analysis of variance (PERMANOVA)* (John wiley & sons, Inc. Hoboken, New Jersey: Wiley statsref: statistics reference online), 1–15.

Aplin, P. (2005). Remote sensing: ecology. *Prog. Phys. Geogr.* 29, 104–113. doi: 10.1191/030913305pp437pr

Barrera-Falcon, E., Rioja-Nieto, R., Hernández-Landa, R. C., and Torres-Irineo, E. (2021). Comparison of standard Caribbean coral reef monitoring protocols and underwater digital photogrammetry to characterize hard coral species composition, abundance, and cover. *Front. Mar. Sci.* 8, 722569. doi: 10.3389/fmars.2021.722569

Bayley, D., and Mogg, A. (2020). A protocol for the large-scale analysis of reefs using structure from motion photogrammetry. *Methods Ecol. Evol.* 11, 1410–1420. doi: 10.1111/2041-210X.13476

Bayley, D. T., Mogg, A. O., Koldewey, H., and Purvis, A. (2019). Capturing complexity: field-testing the use of 'structure from motion' derived virtual models

to replicate standard measures of reef physical structure. *PeerJ* 7, e6540. doi: 10.7717/peerj.6540

Beijbom, O., Edmunds, P., Roelfsema, C., Smith, J., Kline, D., Neal, B., et al. (2015). Towards automated annotation of benthic survey images: Variability of human experts and operational modes of automation. *PLoS One* 10, e0130312. doi: 10.1371/journal.pone.0130312

Bennion, M., Fisher, J., Yesson, C., and Brodie, J. (2019). Remote sensing of kelp (Laminariales, ochrophyta): monitoring tools and implications for wild harvesting. *Rev. Fish. Sci. Aquacult.* 27, 127–141. doi: 10.1080/23308249.2018.1509056

Bernard, A. T., Götz, A., Kerwath, S. E., and Wilke, C. G. (2013). Observer bias and detection probability in underwater visual census of fish assemblages measured with independent double-observers. *J. Exp. Mar. Biol. Ecol.* 433, 75–84. doi: 10.1016/j.jembe.2013.02.039

Bohnsack, J. A. (1979). Photographic quantitative sampling of hard-bottom benthic communities. *Bull. Mar. Sci.* 29, 242–252.

Braunisch, V., and Suchant, R. (2010). Predicting species distributions based on incomplete survey data: the trade-off between precision and scale. *Ecography* 33, 826–840. doi: 10.1111/j.1600-0587.2009.05891.x

Burns, J. H., Delparte, D., Gates, R. D., and Takabayashi, M. (2015). Integrating structure-from-motion photogrammetry with geospatial software as a novel technique for quantifying 3D ecological characteristics of coral reefs. *PeerJ* 3, e1077. doi: 10.7717/peerj.1077

Burns, J., Weyenberg, G., Mandel, T., Ferreira, S., Gotshalk, D., Kinoshita, C., et al. (2020). A comparison of the diagnostic accuracy of in situ and digital image-based assessments of coral health and disease. *Front. Mar. Sci.* 7, 304. doi: 10.3389/fmars.2020.00304

Casella, E., Collin, A., Harris, D., Ferse, S., Bejarano, S., Parravicini, V., et al. (2017). Mapping coral reefs using consumer-grade drones and structure from motion photogrammetry techniques. *Coral Reefs* 36, 269–275. doi: 10.1007/s00338-016-1522-0

Cavanaugh, K. C., Cavanaugh, K. C., Bell, T. W., and Hockridge, E. G. (2021). An automated method for mapping giant kelp canopy dynamics from UAV. *Front. Environ. Sci.* 8, 58735. doi: 10.3389/fenvs.2020.587354

Cherrill, A., and McClean, C. (1999). The reliability of 'Phase 1'habitat mapping in the UK: the extent and types of observer bias. *Landscape urban Plann.* 45, 131–143. doi: 10.1016/S0169-2046(99)00027-4

Clarke, K. R., Gorley, R. N., Somerfield, P. J., and Warwick, R. M. (2014). *Change in marine communities: an approach to statistical analysis and interpretation, 3rd edition* (Plymouth: PRIMER-E).

Couch, C., Oliver, T., Suka, R., Lamirand, M., Asbury, M., Amir, C., et al. (2021). Comparing coral colony surveys from in-water observations and structure-from-Motion imagery shows low methodological bias. *Front. Mar. Science.* 8, 657943. doi: 10.3389/fmars.2021.647943

D'Urban Jackson, T., Williams, G. J., Walker-Springett, G., and Davies, A. J. (2020). Three-dimensional digital mapping of ecosystems: a new era in spatial ecology. *Proc. R. Soc. B* 287, 20192383. doi: 10.1098/rspb.2019.2383

Dandois, J. P., Olano, M., and Ellis, E. C. (2015). Optimal altitude, overlap, and weather conditions for computer vision UAV estimates of forest structure. *Remote Sens.* 7, 13895–13920. doi: 10.3390/rs71013895

Del Vecchio, S., Fantinato, E., Silan, G., and Buffa, G. (2019). Trade-offs between sampling effort and data quality in habitat monitoring. *Biodiv. Conserv.* 28, 55–73. doi: 10.1007/s10531-018-1636-5

De Oliveira, L. M. C., Lim, A., Conti, L. A., and Wheeler, A. J. (2021). 3D classification of cold-water coral reefs: A comparison of classification techniques for 3D reconstructions of cold-water coral reefs and seabed. *Front. Mar. Sci.* 8, 640713. doi: 10.3389/fmars.2021.640713

Dodge, R. E., Logan, A., and Antonius, A. (1982). Quantitative reef assessment studies in Bermuda: a comparison of methods and preliminary results. *Bull. Mar. Sci.* 32, 745–760.

Fakiris, E., Papatheodorou, G., Kordella, S., Christodoulou, D., Galgani, F., and Geraga, M. (2022). Insights into seafloor litter spatiotemporal dynamics in urbanized shallow Mediterranean bays. an optimized monitoring protocol using towed underwater cameras. *J. Environ. Manage.* 308, 114647. doi: 10.1016/j.jenvman.2022.114647

Francis, R. I. C. C., and McKenzie, J. R. (2015). "Assessment of the SNA 1 stocks in 2013," in *New Zealand fisheries assessment report 2015/76*, (Wellington, New Zealand: Ministry of Primary Industries) 82 p.

Fraser, B. T., and Congalton, R. G. (2018). Issues in unmanned aerial systems (UAS) data collection of complex forest environments. *Remote Sens.* 10, 908. doi: 10.3390/rs10060908

Halpern, B., Frazier, M., Afflerbach, J., Lowndes, J., Micheli, F., O'Hara, C., et al. (2019). Recent pace of change in human impact on the world's ocean. *Sci. Rep.* 9, 1–8. doi: 10.1038/s41598-019-47201-9

Halpern, B. S., Walbridge, S., Selkoe, K. A., Kappel, C. V., Micheli, F., D'Agrosa, C., et al. (2008). A global map of human impact on marine ecosystems. *Science* 319, 948–952. doi: 10.1126/science.1149345

Jokiel, P. L., Rodgers, K. S., Brown, E. K., Kenyon, J. C., Aeby, G., Smith, W. R., et al. (2015). Comparison of methods used to estimate coral cover in the Hawaiian islands. *PeerJ* 3, e954. doi: 10.7717/peerj.954

Klemas, V. V. (2015). Coastal and environmental remote sensing from unmanned aerial vehicles: An overview. *J. Coast. Res.* 35, 1260–1267. doi: 10.2112/JCOASTRES-D-15-00005.1

Kohler, K. E., and Gill, S. M. (2006). Coral point count with excel extensions (CPCe): A visual basic program for the determination of coral and substrate coverage using random point count methodology. *Comput. geosci.* 32, 1259–1269. doi: 10.1016/j.cageo.2005.11.009

Lindenmayer, D. B., and Likens, G. E. (2010). The science and application of ecological monitoring. *Biol. Conserv.* 143, 1317–1328. doi: 10.1016/j.biocon.2010.02.013

Ling, S. D., Mahon, I., Marzloff, M. P., Pizarro, O., Johnson, C. R., and Williams, S. B. (2016). Stereo-imaging AUV detects trends in sea urchin abundance on deep overgrazed reefs. *Limnol. Oceanogr.: Methods* 14, 293–304. doi: 10.1002/lom3.10089

Lochhead, I., and Hedley, N. (2022). Evaluating the 3D integrity of underwater structure from motion workflows. *Photogrammetr. Rec.* doi: 10.1111/phor.12399

Logan, A., Page, F. H., and Thomas, M. L. (1984). Depth zonation of epibenthos on sublittoral hard substrates off deer island, bay of fundy, Canada. *Estuarine Coast. Shelf Sci.* 18, 571–592. doi: 10.1016/0272-7714(84)90091-X

Lovett, G., Burns, D., Driscoll, C., Jenkins, J., Mitchell, M., Rustad, L., et al. (2007). Who needs environmental monitoring? *Front. Ecol. Environ.* 5, 253–260. doi: 10.1890/1540-9295(2007)5[253:WNEM]2.0.CO;2

Mancini, F., Dubbini, M., Gattelli, M., Stecchi, F., Fabbri, S., and Gabbianelli, G. (2013). Using unmanned aerial vehicles (UAV) for high-resolution reconstruction of topography: The structure from motion approach on coastal environments. *Remote Sens.* 5, 6880–6898. doi: 10.3390/rs5126880

Marre, G., Deter, J., Holon, F., Boissery, P., and Luque, S. (2020). Fine-scale automatic mapping of living posidonia oceanica seagrass beds with underwater photogrammetry. *Mar. Ecol. Prog. Ser.* 643, 63–74. doi: 10.3354/meps13338

Marre, G., Holon, F., Luque, S., Boissery, P., and Deter, J. (2019). Monitoring marine habitats with photogrammetry: a cost-effective, accurate, precise and high-resolution reconstruction method. *Front. Mar. Sci.* 6, 276. doi: 10.3389/fmars.2019.00276

Mihoub, J. B., Henle, K., Titeux, N., Brotons, L., Brummitt, N. A., and Schmeller, D. S. (2017). Setting temporal baselines for biodiversity: the limits of available monitoring data for capturing the full impact of anthropogenic pressures. *Sci. Rep.* 7, 1–13. doi: 10.1038/srep41591

Mizuno, K., Asada, A., Matsumoto, Y., Sugimoto, K., Fujii, T., Yamamuro, M., et al. (2017). A simple and efficient method for making a high-resolution seagrass map and quantification of dugong feeding trail distribution: A field test at Mayo bay, Philippines. *Ecol. Inf.* 38, 89–94. doi: 10.1016/j.ecoinf.2017.02.003

Mohamed, H., Nadaoka, K., and Nakamura, T. (2020). Towards benthic habitat 3D mapping using machine learning algorithms and structures from motion photogrammetry. *Remote Sens.* 12, 127. doi: 10.3390/rs12010127

Monfort, T., Cheminée, A., Bianchimani, O., Drap, P., Puzenat, A., and Thibaut, T. (2021). The three-dimensional structure of Mediterranean shallow rocky reefs: Use of photogrammetry-based descriptors to assess its influence on associated teleost assemblage. *Front. Mar. Sci.* 8, 924. doi: 10.3389/fmars.2021.639309

Neyer, F., Nocerino, E., and Grün, A. (2019). Image quality improvements in low-cost underwater photogrammetry. international archives of the photogrammetry. *Remote Sens. Spatial Inf. Sci.* 42, 135–142. doi: 10.3929/ethz-b-000343605

Nocerino, E., Menna, F., Gruen, A., Troyer, M., Capra, A., Castagnetti, C., et al. (2020). Coral reef monitoring by scuba divers using underwater photogrammetry and geodetic surveying. *Remote Sens.* 12, 3036. doi: 10.3390/rs12183036

Nocerino, E., Neyer, F., Grün, A., Troyer, M., Menna, F., Brooks, A., et al. (2019). Comparison of diver-operated underwater photogrammetric systems for coral reef monitoring. SPRS-international archives of the photogrammetry. *Remote Sens. Spatial Inf. Sci.* XLII-2/W10, 143–150. doi: 10.5194/isprs-archives-XLII-2-W10-143-2019

Palma, M., Rivas Casado, M., Pantaleo, U., Pavoni, G., Pica, D., and Cerrano, C. (2018). SfM-based method to assess gorgonian forests (Paramuricea clavata (Cnidaria, octocorallia)). *Remote Sens.* 10, 1154. doi: 10.3390/rs10071154

Pante, E., and Dustan, P. (2012). Getting to the point: Accuracy of point count in monitoring ecosystem change. *J. Mar. Biol.* 2012, 1–7. doi: 10.1155/2012/802875

Parravicini, V., Morri, C., Ciribilli, G., Montefalcone, M., Albertelli, G., and Bianchi, C. N. (2009). Size matters more than method: visual quadrats vs photography in measuring human impact on Mediterranean rocky reef communities. *Estuarine Coast. Shelf Sci.* 81, 359–367. doi: 10.1016/j.ecss.2008.11.007

Perkins, N. R., Foster, S. D., Hill, N. A., and Barrett, N. S. (2016). Image subsampling and point scoring approaches for large-scale marine benthic monitoring programs. *Estuarine Coast. Shelf Sci.* 176, 36–46. doi: 10.1016/j.ecss.2016.04.005

Pizarro, O., Friedman, A., Bryson, M., Williams, S. B., and Madin, J. (2017). A simple, fast, and repeatable survey method for underwater visual 3D benthic mapping and monitoring. *Ecol. Evol.* 7, 1770–1782. doi: 10.1002/ece3.2701

Preskitt, L. B., Vroom, P. S., and Smith, C. M. (2004). A rapid ecological assessment (REA) quantitative survey method for benthic algae using photoquadrats with scuba. *Pacific Sci.* 58, 201–209. doi: 10.1353/psc.2004.0021

Raoult, V., David, P. A., Dupont, S. F., Mathewson, C. P., O'Neill, S. J., Powell, N. N., et al. (2016). GoPros™ as an underwater photogrammetry tool for citizen science. *PeerJ* 4, e1960. doi: 10.7717/peerj.1960

Roberts, D. E., Fitzhenry, S. R., and Kennelly, S. J. (1994). Quantifying subtidal macrobenthic assemblages on hard substrata using a jump camera method. *J. Exp. Mar. Biol. Ecol.* 177, 157–170. doi: 10.1016/0022-0981(94)90234-8

Seers, B. M., and Shears, N. T. (2015). Spatio-temporal patterns in coastal turbidity–long-term trends and drivers of variation across an estuarine-open coast gradient. *Estuarine Coast. Shelf Sci.* 154, 137–151. doi: 10.1016/j.ecss.2014.12.018

Shears, N. T., and Babcock, R. C. (2002). Marine reserves demonstrate top-down control of community structure on temperate reefs. *Oecologia* 132, 131–142. doi: 10.1007/s00442-002-0920-x

Shears, N. T., and Babcock, C. R. (2004). *Community composition and structure of shallow subtidal reefs in northeastern new Zealand* (Wellington, New Zealand: Department of Conservation).

Sieberth, T., Wackrow, R., and Chandler, J. H. (2014). Influence of blur on feature matchin and a geometric approach for photogrammetric deblurring. *Int. Arch. Photogrammetr. Remote Sens. Spatial Inf. Sci.* XL-3, 321–326. doi: 10.5194/isprsarchives-XL-3-321-2014

Smale, D. A., Epstein, G., Hughes, E., Mogg, A. O., and Moore, P. J. (2020). Patterns and drivers of understory macroalgal assemblage structure within subtidal kelp forests. *Biodiv. Conserv.* 29, 4173–4192. doi: 10.1007/s10531-020-02070-x

Solan, M., Cardinale, B. J., Downing, A. L., Engelhardt, K. A., Ruesink, J. L., and Srivastava, D. S. (2004). Extinction and ecosystem function in the marine benthos. *Science* 306, 1177–1180. doi: 10.1126/science.1103960

Suka, R., Asbury, M., Gray, A. E., Winston, M., Oliver, T., and Couch, C. S. (2019). *Processing photomosaic imagery of coral reefs using structure-from-MotionStandard operating procedures* (Honolulu: U.S: Department of Commerce, National Oceanic and Atmospheric Administration).

Tait, L., Bind, J., Charan-Dixon, H., Hawes, I., Pirker, J., and Schiel, D. (2019). Unmanned aerial vehicles (UAVs) for monitoring macroalgal biodiversity: comparison of RGB and multispectral imaging sensors for biodiversity assessments. *Remote Sens.* 11, 2332. doi: 10.3390/rs11192332

Teague, J., and Scott, T. (2017). Underwater photogrammetry and 3D reconstruction of submerged objects in shallow environments by ROV and underwater GPS. *J. Mar. Sci. Res. Technol.* 1, 005.

Ternon, Q., Danet, V., Thiriet, P., Ysnel, F., Feunteun, E., and Collin, A. (2022). Classification of underwater photogrammetry data for temperate benthic rocky reef mapping. *Estuarine Coast. Shelf Sci.* 270, 107833. doi: 10.1016/j.ecss.2022.107833

Urbina-Barreto, I., Garnier, R., Elise, S., Pinel, R., Dumas, P., Mahamadaly, V., et al. (2021). Which method for which purpose? a comparison of line intercept transect and underwater photogrammetry methods for coral reef surveys. *Front. Mar. Sci.* 8, 636902. doi: 10.3389/fmars.2021.636902

Webber, D. N., Starr, P. J., Haist, V., Rudd, M., and Edwards, C. T. T. (2018). "The 2017 stock assessment and management procedure evaluation for rock lobsters (Jasus edwardsii) in CRA 2," in *New Zealand fisheries assessment report 2018/17*, 87 p.

Yao, H., Qin, R., and Chen, X. (2019). Unmanned aerial vehicle for remote sensing applications–a review. *Remote Sens.* 11, 1443. doi: 10.3390/rs11121443

frontiers | Frontiers in Marine Science

TYPE Original Research
PUBLISHED 09 November 2022
DOI 10.3389/fmars.2022.1021675

Check for updates

OPEN ACCESS

EDITED BY
Monica Montefalcone,
University of Genoa, Italy

REVIEWED BY
Peter M. J. Herman,
Delft University of Technology, Netherlands
Carlo Nike Bianchi,
Retired, Genoa, Italy

*CORRESPONDENCE
Józef M. Wiktor Jr
wiktor_jr@iopan.pl

SPECIALTY SECTION
This article was submitted to Marine Ecosystem Ecology, a section of the journal Frontiers in Marine Science

RECEIVED 17 August 2022
ACCEPTED 20 October 2022
PUBLISHED 09 November 2022

CITATION
Wiktor JM Jr, Tatarek A, Kruss A, Singh RK, Wiktor JM and Søreide JE (2022) Comparison of macroalgae meadows in warm Atlantic versus cold Arctic regimes in the high-Arctic Svalbard. *Front. Mar. Sci.* 9:1021675. doi: 10.3389/fmars.2022.1021675

COPYRIGHT
© 2022 Wiktor, Tatarek, Kruss, Singh, Wiktor and Søreide. This is an open-access article distributed under the terms of the Creative Commons Attribution License (CC BY). The use, distribution or reproduction in other forums is permitted, provided the original author(s) and the copyright owner(s) are credited and that the original publication in this journal is cited, in accordance with accepted academic practice. No use, distribution or reproduction is permitted which does not comply with these terms.

Comparison of macroalgae meadows in warm Atlantic versus cold Arctic regimes in the high-Arctic Svalbard

Józef M. Wiktor Jr[1]*, Agnieszka Tatarek[1], Aleksandra Kruss[2], Rakesh Kumar Singh[3], Józef M. Wiktor[1] and Janne E. Søreide[4]

[1]Institute of Oceanology Polish Academy of Sciences (PAN), Marine Ecology Department, Sopot, Poland, [2]NORBIT Subsea, Trondheim, Norway, [3]Département de Biologie, Chimie et Géographie, Rimouski, QC, Canada, [4]The University Centre in Svalbard, Department of Arctic Biology, Longyearbyen, Norway

A warmer Arctic with less sea ice will likely improve macroalgae growth conditions, but observational data to support this hypothesis are scarce. In this study, we combined hydroacoustic and video inspections to compare the depth of growth, density and thickness of macroalgae (>10 cm) meadows in two contrasting climate regimes in Svalbard 1) the warm, ice free, Atlantic influenced West Spitsbergen and 2) the cold, Arctic and seasonal ice covered East Spitsbergen. Both places had similar insolation and comparable turbidity levels. Macroalgae communities at both places were similar and were formed mainly by common north Atlantic kelp species: *Saccharina latissima, Alaria esculenta, Laminaria digitata* and *L. hyperborea*. However, the density of the bottom coverage and thalli condition were strikingly different between the two sites. Algae at the warmer site were intact and fully developed and occupied most of the available hard substrate. At the colder site, only patchy macroalgae canopies were found and most thallies were physically damaged and trimmed at a uniform height due to physical ice scouring. These differences in macroalgal density and thalli condition were only found at depths down to 5 m. Deeper, no distinct differences were observed between the warm and cold sites. Sea urchins were only observed at the warm site, but in few numbers with no visible negative top-down control on macroalgae growth.

KEYWORDS

kelp forest, hydroacoustic, ice-scouring, Arctic, climate change

1 Introduction

Arctic coastal ecosystems are transforming as the climate warms and human activities in the region increase. The Arctic is characterized by an extensive coastline, constituting up to 1/3 of the global coastline. Coastal waters are vital for breeding and foraging for many fishes, birds and mammals, and provide important ecosystem services for human settlements and businesses. The rapid warming reduces the amount of sea ice, increase coastal erosion and increase river run-off and sediment loads that physically change the nearshore bottom habitats and, thus, the biodiversity and biomass of these regions. Those changes may have with potential drastic effects on existing food webs (Byrnes et al., 2011; Krumhansl et al., 2016; Pörtner et al., 2022).

Macroalgae are dominant primary producers in Arctic fjords: up to 50% of the organic carbon available to zoobenthos originates from macrophytes' production (Renaud et al., 2015). In favorable conditions, macroalgae form dense canopies referred to as kelp forests, which play an important role in coastal ecosystems as a carbon source, as well as a habitat for other species (Włodarska-Kowalczuk et al., 2009; Smale et al., 2013). Most of this production is exported to surrounding ecosystems — only about 2% of the macroalgae carbon is disposed on the site where it originated (Filbee-Dexter et al., 2018). The remaining part is transported into deeper waters and buried there, or released into the pelagial and subsequently built into the pelagic food chain (von Biela et al., 2016), as well as being deposited on land (Buchholz and Wiencke, 2016). Kelp forest presence also positively affects productivity of phytoplankton in adjacent waters (Miller et al., 2011). Along with the ongoing change in the global climate (Pörtner et al., 2022), sea ice is strongly declining in the Arctic (Stroeve et al., 2007). Ice cover is known to be one of the most important environmental drivers shaping the kelp forest in the Arctic (Krause-Jensen et al., 2012), so we expect that the decline in sea ice extent and duration will positively affect kelp forests, and subsequently the entire arctic coastal ecosystem.

In this study we compared macroalgae communities at the same latitude (~78°N) in the Svalbard Archipelago but with marked differences in sea temperatures and sea ice characteristics: (**i**) the cold coast of Storfjorden (eastern Svalbard) with seasonal ice cover and (**ii**) the warm coast of Isfjorden (western Svalbard) under the influence of Atlantic waters and no sea ice formation. Acoustic methods are particularly efficient in the assessment of benthic habitats (Blondel and Murton, 1997; Brown et al., 2011) especially in polar environments where direct sampling or diving is difficult. Acoustic methods provide a large amount of spatial data for modelling and monitoring of marine environments, particularly when applied to turbid waters (Anderson et al., 2008; Kruss et al., 2017). In this work we used acoustical mapping devices, single and multibeam echosounders, to find differences in local algae distribution along the depth gradient. We obtained a broad and continuous image of the bottom and, when present, of a canopy surface.

Most macroalgae require attachment to a firm substrate and are therefore limited to areas where rocks, boulders or exposed bedrock are present (Kruss et al., 2008; Kruss et al., 2019). Their vertical distribution is linked to light availability, which varies depending on the position of the Sun above the horizon and water transparency. In the most favourable conditions (in the most transparent tropical waters) macroalgae are observed as deep as 100 m (Markager and Sand-Jensen, 1992). In the Arctic, depending on the region and light penetration, macroalgae can be found down to ca. 60 m in the clear waters of Greenland (Boertmann et al., 2013). In highly turbid waters of the West Spitsbergen fjords (Kruss et al., 2008; Tatarek et al., 2012) hardly any macrophytes are observed below 40 m, with an exception of encrusted Rhodophyta that can be found as deep as 60 m. Distribution of kelps in Kongsfjorden (Spitsbergen) has been reported to reach down to 18 m for the foliose algae species (Bischof et al., 2019a).

Optimal temperature for kelps' growth is between 5 °C and 15 °C, although it varies depending on species: optimum growth occurs in temperatures around 5 °C in case of species associated with cold waters: *Laminaria solidungula*, *L. hyperborea* and *Desmarestia aculeata* and 15 °C for *Laminaria digitata, L. saccharina latissima* and *Alaria esculenta*. Deviation from the optimal temperature results in significant decrease in growth rates (Fortes and Lüning, 1980). The exception is *Laminaria solidungula*, an Arctic endemic species, which is extremely well adapted to low temperatures — its growth rate is reduced only by 50% at 0 °C compared to the one in its optimal temperature, while other species nearly stop growing in such low temperatures (Wiencke and Tom Dieck, 1990; Tom Dieck (Bartsch), 1992; Andersen et al., 2013).

In general, macroalgae are expected to populate any available hard substratum in the littoral zone such as rocks, boulders, stones or even rough gravel. Their survival, however, is influenced by a number of environmental stressors. In places exposed to waves, entire patches of kelp forests are often destroyed over the winter (Bekkby et al., 2014). On the other hand, in places of less extreme environment, kelp grazers – mostly sea urchins – can thrive and limit macroalgae distribution (Scheibling et al., 1999). At Svalbard there are many tidewater glaciers with calving icebergs and growlers in the water. This free-floating ice scours the bottom in shallow water areas when put in motion by wind and water currents, removing everything that was attached to the bottom. Sea ice also has a significant effect on the macroalgae and shapes their local distribution — in places where it is present, macroalgae

living in shallow water get frozen into the bottom of the ice sheet and often are stripped from the substrate and transported further from the shore (Minchinton et al., 1997) adding carbon to benthic food chains or being deposited as blue carbon (Pedersen et al., 2020).

Sea-ice affects light transmission through the water surface — it reflects and attenuates most of the radiation, limiting how deep it penetrates the water column. For macroalgal development, the total amount of available photosynthetically active radiation (PAR) during the growth season is important, as it determines the amount of energy for new growth. In the Arctic, sufficient sunlight is available only from March to October, during the Polar Day (Wiencke et al., 2007). Kelps have very low compensation points in order to start accumulating resources as quickly as possible, maximizing the time before they are overshadowed by organisms in the water column above. The most efficient in harvesting light is *Laminaria solidungula*, its compensation point is as low as 0.5-3.0 μE. Such a low value is exceptional — this is another adaptation for growing in the high Arctic conditions, other species are less efficient. Common kelp occurring in the Atlantic Arctic — *L. digitata* needs at least 6 μE of PAR, while *Saccharina latissima* even more – 9 μE. This adaptation allows kelps to thrive in areas where yearly doses of PAR can be as low as 45 — 71 mol m^{-2} yr^{-1} (Bonsell and Dunton, 2018). When ice cover shadows the water column, benthic algae cannot use that advantage. As soon as the ice is gone, pelagic species proliferate quickly, cutting benthic species off from light by attenuating and using all light that enters the water column. Thus the number of days with sunlight and with ice cover in a given place is a key factor that affects suitability to host a macroalgal canopy (Krause-Jensen et al., 2012).

Spring bloom quickly depletes nutrients recycled from the bottom during winter storms and water becomes transparent again in the summer. Rising temperature causes high meltwater runoff that introduces vast amounts of suspended matter into the water – a common phenomenon in the Svalbard fjords (Kruss et al., 2008; Tatarek et al., 2012; Ronowicz et al., 2013), where well-developed laminarian forests were observed in completely murky waters during summer. Kelps being adapted to low light levels can use nutrients introduced by meltwater facilitating their growth even in such conditions.

Current data describing kelp distribution in the Arctic/Svalbard area are scarce and scattered, usually with poor vertical resolution. The lack of high-resolution data gives only limited insight into the current state of the Arctic coastal environments. Generating such high-resolution, reliable data will allow us to make predictions and develop environmental models of the changes in coastal regions. In this work, we provide a detailed, quantitative description of the local distribution of macroalgae in two contrasting environmental regimes in terms of sea ice conditions: one where sea ice is still present, and one where it is not occurring anymore. By comparing those regions we show possible evolution of the Arctic coastal regions prone to decline in sea ice due to rise in global temperatures.

2 Materials and methods

2.1 Study area

For this study, two contrasting habitats were selected: one in Isfjorden (Bohemanneset, referred as Warm Arctic – WA) which is influenced by the warm West Spitsbergen Current (Skogseth et al., 2020) and is situated on the west coast, and (2) in Storfjorden (Agardhbukta, referred to as Cold Arctic CA), which is fed with cold current from the Arctic Ocean (Skogseth et al., 2005). Different characteristics of water masses in both regions result in variations in habitat conditions.

In the WA area, the average annual water temperature has not dropped below freezing point in the last 30 years, so the sea does not freeze in this area at all or at most sporadically. In CA, on the eastern coast there is sea ice and fast ice regularly for some part of the year. For instance, in 2019 sea ice was present from the end of January (permanent ice cover was preceded by drifting sea ice at the end of December 2018) and lasted until 11 May, with drifting pack ice being present until 23 May.

Both selected study localisations are situated at similar latitude and both have similar south-east exposition (104° at WA and 113° at CA). That ensures comparable insolation, which is one of the key factors shaping living conditions for autotrophic organisms. The amount of radiation reaching the sea surface would be affected solely by local cloud cover, which is similar in both investigated regions (Figure 1). On the way through the water column to the bottom, sunlight might be partially attenuated by the sea ice cover (Perovich et al., 1993) and absorbed by particles suspended in the water (Castellani et al., 2022). At the CA site, turbidity is slightly higher than at the WA site, possibly due to higher meltwater runoff, yet differences are not very pronounced. For that reason, we assume that ice would be the main reason for the difference in macroalgal canopy between study sites due to both attenuation properties and potential for scouring the bottom.

2.2 Data acquisition

2.2.1 Positioning and survey

All acoustic data were collected from small boats with side poles mounting of single beam (SBES) and multibeam (MBES) echosounders on port and starboard side, respectively. There

were also two separate positioning systems. A single GNSS antenna was mounted on the top of the SBES pole, while two Trimble antennas were attached along the MBES pole with 2 m separation to secure precise positioning. Due to problems with receiving RTK corrections in remote Arctic areas, we decided to record all navigation and motion data and process them later using Applanix PosPac PP-RTX technology to achieve centimetric horizontal and vertical positioning accuracy. Data were collected from both instruments simultaneously. Survey lines were planned along the shore line starting from the deeper part towards shallower to avoid underwater obstacles such as rocks. Line spacing was adjusted to assure full bottom coverage by the multibeam wide swath system.

2.2.2 Single beam echosounder

Previous theoretical (Carbó and Molero, 1997; Shenderov, 1998) and experimental studies (Sabol et al., 2002; Kruss et al., 2008; Kruss et al., 2017) show that the SBES echo envelopes recorded over rocky, sandy or muddy bottom and seafloor covered by macrophytes are considerably different. Habitats classification based on acoustic mapping from SBES is already a well established technique with efficient and reliable results (Brown et al., 2011).

Acoustic data were recorded at 420kHz frequency by Biosonics DTX split beam echosounder. This echosounder collects data with a swath perpendicular to the bottom with an opening angle of 5.2°. Echoes received come from a round shape area interacting with the incident wave. The deeper it is, the bigger the footprint becomes. This kind of survey gives information from the seabed below the instrument and along the boat track. Data were recorded by Biosonic's Visual Acquisition software, which stored a full echo signal envelope for each ping as volume backscattering strength values (SV). Based on that, we could analyze bottom reflection and water column reverberations at the same time. Pulse length used was 0.1 ms, giving 2 cm vertical resolution of the data.

Parametrization and classification of seabed substrata was possible due to differences in signal response values and echo shapes originating from different bottom types and habitats (Lurton, 2002; Jackson and Richardson, 2007). Echo signal was corrected for signal losses due to the water, to enable it to estimate the influence of bottom hardness and detect macrophytobenthos growing on it, and to compare the data from different depths.

2.2.3 Multibeam echosounder

We used a high resolution integrated multibeam echosounder Norbit iWBMSh. The instrument was equipped with a motion sensor and set to operate at 360 kHz, with a swath opening of 140° across track, and 1.9° along track. Each swath comprises 512 beams and outputs a point cloud of bottom detections, allowing centimetric resolution of the seabed surface. A range of intensity values were recorded for each beam (snippet) as well, producing a high-resolution backscatter mosaic image (showing how strong the bottom is reflecting acoustic signals). The great advantage of using MBES for habitat mapping is wide coverage while keeping high resolution of the mapped seafloor areas.

Data were collected using QPS QINSy software that records but also visualizes the preliminary results and supports navigation during the survey. Post-processing was made in QIMERA for bathymetry and FMGT for backscatter.

The pre-processed data set gathered by single beam echosounder consists of 69468 observations at the WA and 86126 at the CA. SBES parameters were smoothed with a rolling filter calculating mean, median and extremes of each variable. This dataset was then aggregated into values representing averaged algae and bottom descriptors derived from SBES rasterized into 25 cm x 25 cm 'pixels' (0.0625 m^2) matching the underlying bathymetric grid (for illustration see Supplementary Figure S1). The value associated with each pixel is determined by calculating statistics for all observations falling within its area. This resulted in 64553 observations at WA (19706 with algae canopy) and 59513 at Cold Site (12062 with algae canopy). Resulting dataset covered area of 3720 m^2 at CA and 4035 m^2 at WA.

2.2.4 Video footage

Ground-truthing was accomplished by inspecting video footage recorded by a submersible camera. Two different systems were used. The CA site was inspected by a drop camera unit consisting of two small sport cameras and diving spotlight attached to a self-made rack constructed from PVC pipes equipped with stabilizing fins. In the WA area, pictures were recorded using a towable platform equipped with a camera, LED lights, depth sensor, altimeter and PAR sensor. Due to that, spatial coverage of ground-truthing points in CA is smaller compared to the other site (Figure 2).

In total, 4868 seconds of video footage was recorded for ground-truthing of echograms: 788 s at the CA site and 4080 s at the WA, all along with single beam echosounder (SBES) acquisition which was to improve their positioning and validating classification results.

When the canopy was dense, the bottom type was not visible. In such cases, we assumed it was a hard substrate. When hard substrate was mixed with soft sediments, barren spots could be observed, revealing its nature.

Observations included a coverage, taxonomic composition of visible algae, type of bottom, presence of sea urchins and singular features (like single kelp, rock on a sandy bottom and other objects clearly visible on the echograms; those observations help in future alignment of data acquired by camera with the ones captured with SBES). Spatial information of observations were fitted by aligning them with SBES datasets using reading closest in time to the given observation.

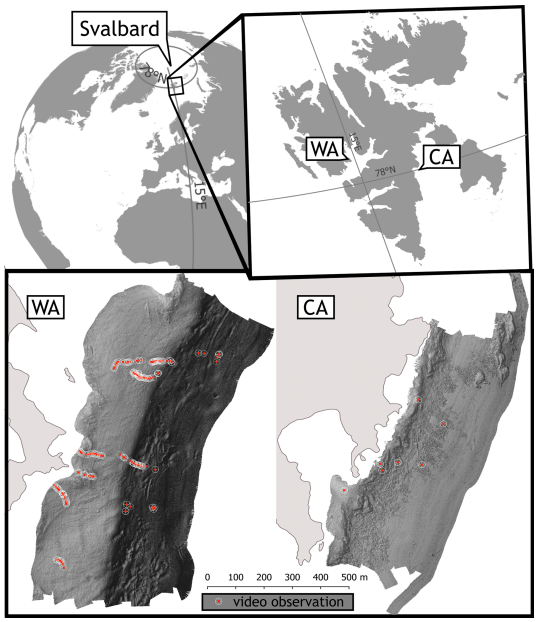

FIGURE 1
Localization of hydroacoustic study area and ground-truthing data (open circles) over reliefs of surveyed polygons in Isfjorden (Bohemanneset) in West Spitsbergen referred to as Warm Arctic (WA) and in Storfjorden (Agardhbukta) East Spitsbergen referred to as Cold Arctic (CA).

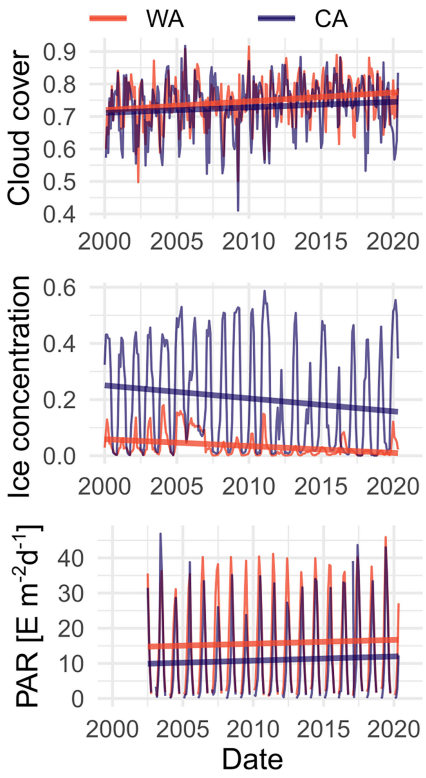

FIGURE 2
Spatially averaged cloud cover, monthly ice concentration (a fraction of water surface covered by sea ice according to the MERRA-2 model) and Photosynthetically Active Radiation (PAR) in areas surrounding study sites: Warm Arctic (WA) in West Spitsbergen and Cold Arctic (CA) in East Spitsbergen in years 2000-2020 (data used for plotting were obtained using the Giovanni online data system, developed and maintained by the NASA GES DISC). Thick lines show the trend of the value in each place.

2.2.5 Remote data

Turbidity, diffuse attenuation coefficient for PAR (Kd) and chlorophyll *a* data presented were based on MODIS-Aqua data provided by NASA OB.DAAC (NASA's Ocean Biology Distributed Active Archive Center), processed using SeaDAS v2021.1; developed and maintained by NASA Ocean Biology Processing Group (OBPG) (Baith et al., 2001). SeaDAS was modified to use Spectral Shape Parameter (SSP) aerosol correction (Singh et al., 2019). Suspended particulate matter (SPM) were estimated as described in (Nechad et al., 2010) using water-leaving reflectance (ρ_w) at a 667 nm band generated from MODIS-Aqua data using SeaDAS.

Giovanni interface (Beaudoing et al., 2020) was used to acquire data describing environmental conditions in areas around sampling sites (Figure 1). All data used in our research are monthly values, area-averaged in respective areas representing sampling polygon's surroundings. Cloud cover, expressed as cloud fraction (The fraction of the sky that is covered by clouds) and PAR (4 km resolution) are based on The Level-3 (L3) MODIS Atmosphere Monthly Global Product MYD08_M3 (NASA Goddard Space Flight Center et al., 2018) and ice concentration (sea-ice covered fraction of tile) are based on MERRA-2 product: tavgM_2d_flx_Nx (Global Modeling and Assimilation Office (GMAO), 2015).

2.3 Data processing

2.3.1 SBES data analysis

The database with algae detections from each SBES ping was translated into a spatial database using the raster package (Hijmans and van Etten, 2016) in the R environment. Point data were rasterized using MBES bathymetry as a reference grid with basic resolution of 25 cm (Supplementary Figure S1).

Small boats, like the one used as a platform to collect the presented data, are prone to unpredictable movements due to wave, wind and on-board operations. This influences SBES echoes, as this instrument was not attached to advanced positioning (as it was in a case of MBES using Real Time Kinematic) corrections or motion sensor data. To compensate for the unexpected movement effect, each calculated parameter was smoothed with a median walking window filter (window width = 100 pings).

The echo signal is automatically corrected for transmission loss in the Biosonic's software, full echograms were output as Matlab (Mathworks) input files for further analysis. Macroalgae detection was performed by procedures developed by Kruss et al. (2017).

Having "roots" (a base of the canopy; depth at which holdfasts are attached to the bottom) and "tops" of macroalgae (the depth of the surface of algal canopy) we could calculate the macroalgae layer thickness expressed in SBES samples, which was subsequently recalculated to be expressed in meters.

Due to a changing velocity of the boat during a data acquisition, the number of pings per output cell varied. To maintain a high quality of the statistical analysis, cells with less than 50 pings were removed. Rasterization processes were performed using a number of aggregating functions: (1) coverage (expressed as number of positive algae detections/all pings within a cell), (2) median canopy thickness, (3) canopy type: 5 categories of canopy described in Table 1.

2.3.2 Bottom type classification

Not every substrate is suitable for algae to grow — it must provide a secure and stable surface to attach to. Herein, we categorized substrates into two categories: hard (including bedrock, boulders and big rocks) and soft (loose sediments like sand and small gravel). In many cases, mixtures of them are observed: e.g. rock on sand etc. Different levels of disturbance would display as different fractions of a potential niche that are actually used by algae (realized niche): the greater the disturbance, the more likely that the canopy would be detached or damaged. In order to compare canopy in two distinct sites, we limit our analysis to hard substrates only.

Seabed classification based on SBES combined with ground truth data is a complex task. We used well established parametric methods based on echo shape descriptions (van Walree et al.,

TABLE 1 Description of canopy categories in the current study.

ID	Coverage	Canopythickness	Description
1	0	0	none
2	<50%	<0.5 m	Low canopy, patchy distribution
3	≥50%	<0.5 m	Low canopy, continuous
4	<50%	≥0.5 m	Continuous, small
5	≥50%	≥0.5 m	Continuous, high

2005; Michaels, 2007; Anderson et al., 2008; Kruss et al., 2017) to estimate bottom hardness and type. These parameters were calculated for each echo envelope (e.g. mean, length, kurtosis, skewness, center of gravity).

We also used a very crude method to discriminate between bottom types. First, mean signal strength of the bottom was calculated for each reading. Those values were then pooled together, and 10000 random values were sampled and fed into a k-means procedure looking for two distinct groups of values (hard and soft bottom). The histogram of SV was clearly bimodal, so doing that would produce results good enough for further analyses (Supplementary Figures S2, S3).

2.3.3 Multibeam data processing and terrain analysis

Norbit multibeam data were treated in QPS QIMERA (multibeam processing software) using processed positioning data with centimetric precision. Together with motion unit data we could compensate for the output bathymetry for all vertical and horizontal artefacts that come from boat movement and refer to this layer to mean water level for the region. Backscatter mosaic was created in QPS FMGT software based on registered snippets. This software automatically corrects transmission losses of the signal and angular dependency of signal reflection, which makes mosaics homogenous and removes artefacts.

Bathymetry was created with 25 cm resolution, keeping sufficient point density per cell. This layer was the basis for further calculation of roughness, slope and aspect as derivatives of bottom morphology.

3 Results

Investigated locations differ by the dose of PAR reaching the bottom. It is a result of the ice cover presence/absence in spring, and the higher concentration of mineral particles associated with the runoff of discharge waters reaching the littoral zone either directly from the glaciers or through the river (Agardhelva), carrying a significant load of suspensions (3.7 mg L^{-1} TSS) (van Winden, 2016). Such a load reduces the transparency of the water in CA (in most sites inspected with the camera, visibility was very low). WA, on the other hand, is located far from glaciers, so suspended matter in the water was already significantly diluted by the waters of the open sea penetrating the Isfjorden. At the CA the bottom remains flat below the depth of 20 m what facilitates resuspension of the fine material, what is not a case at the WA where the bottom drops steeply to a depth where the influence of the waves causing the re-suspension of the bottom sediments is negligible.

3.1 Remote sensing of the optical parameters of the water in investigated areas

Concentrations of particulate matter were higher at CA for most of the time reaching a value of 20 g m^{-2}, while in WA this occasionally reached ca. 17 g m^{-2}, but generally stayed below 8 g m^{-2} (Figure 3). Particulate matter was the main driver of overall diffuse attenuation coefficient (K_d) variability, as the chlorophyll

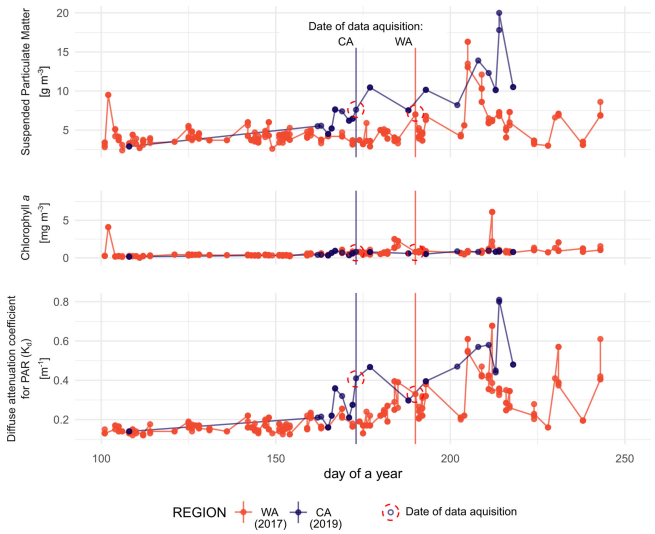

FIGURE 3
Time series of remotely derived parameters related to water transparency. Each series shows values from the year when the area was surveyed (2017 for WA and 2019 for CA). Day when *in situ* data were collected are indicated by vertical lines. Lack of data in case of CA in the spring is due to the ice and clouds obstructing the view.

TABLE 2 Geographical position and physical information of the two study sites Warm Arctic (WA) and Cold Arctic (CA) in respective West and East Spitsbergen.

	Warm Arctic (WA)	Cold Arctic (CA)
Geographical name	Bohemanneset, Isfjorden	Agardhbukta, Storfjorden
Date of observation	2017-07-09	2019-06-22
Top left corner of the area	14.767°E; 78.381°N	18.458°E; 78.381°N
Bottom right corner of the area	14.805°E; 78.370°N	18.490°E; 77.952°N
Length along the coast [m]	1347	1394
Width across depth gradient [m]	636	479
Surface area (planimetric)	624177 m^2	378721 m^2
Bottom landscape surface area	645950 m^2	396224 m^2
Area of SBES data	4035 m^2	3720 m^2
Area of hard substrate	3393 m^2	2488 m^2
Global aspect	107°	113°
Depth range [m]	2.4-45.7	0.9-14.3
Mean Depth (median) [m]	16.7	11.2

a concentrations were similar in both cases. Overall, transparency in both regions was similar (Figure 3).

3.2 Background bathymetry

Planimetric areas (measured along sea surface) of 624 327 m^2 at the WA and 379 000 m^2 at the CA were surveyed (Table 2). It corresponded with sea floor areas (bottom landscape surface) of 645 950 m^2 at WA and 396 224 m^2 at WA.

3.3 Single beam echosounder observations

The best split between hard and soft spatially averaged bottom reflectivity calculated by k-means for two groups performed on the results of rasterization of the local median value of SV was -7.406. Using this criterion most of the hard and soft substrate was correctly classified. Mixed substrates that included soft sediments were also assigned to the soft substrate class using this model (Table 3).

At the WA 84% of all SBES readings indicated presence of the hard substrate, while in the CA this share was lower — 67%. As data represents averaged values in 25 cm x 25 cm quadrants it corresponded to the areas of 2488 m^2 in CA (out of total 3720 m^2) and 3393 m^2 in WA (out of total 4035 m^2).

More than half of both areas were not inhabited by algae (58% in WA and 59% in CA; Table 4). The most prominent canopy type (continuous and thick) occupied 1[0-9] % of the WA bottom, while it was present only at 2% of a suitable bottom at the CA.

In both cases, continuous low canopy comprised nearly 25% of the total area of inhabitable bottom (26% vs 21% WA and CA respectively). Patchy low canopy was nearly as common as the continuous one (19%) at CA site, while being limited to 9% at WA.

At the WA site, macroalgal canopies occupied the available bottom to a larger extent compared to CA: at the WA site over 50% of suitable bottom was covered with macrophytes in waters shallower than 6 m, reaching up to 80% at 3 m depth. At CA, it never exceeds 50%, with the peak coverage of 45% at 5 m (Figure 4).

Canopies at both sites extended down to 13 m under water surface (coverage >5%). Occasionally some fronds were observed deeper.

Observed canopy thickness ranged between 0.1 m and 1 m (Figure 5). At CA, average canopy thickness was fairly constant throughout the depth range (thickness of 0.25 m - 0.3 m) reaching maximum thickness in the 6 m bin. At WA, peak average canopy thickness was 50 cm reaching maximum thickness in the 4 m depth bin, decreasing to 25-30 cm thickness at 7 m depth. At both study sites the thickest canopy was observed at about 4 m - 5 m depth where values as high as 1 m were recorded (Figure 6).

The canopy was the thickest on average at depth between 3 m – 5 m extending more than 30 cm from the bottom, reaching as much as 50 cm at 4 m (Figure 6). At the CA site, the mean macrophyte canopy layer did not exceed 25 cm at any depth and was constant more or less even down to 7 m.

At WA (Figures 7A–F), continuous high canopy is present whenever there are boulder/rock deposits, while much less frequent on flat areas, which are associated with sedimentary bottom. At CA (Figures 7G–L) high canopy was scarce and scattered with very few localities where it was somehow continuous (present in the number of subsequent pixels). Dark shades of the relief indicated shallow water, getting lighter with increasing depth. In both sets of panels, the coast is located on the top left side of the panel and open water is on the bottom right side. At WA structures extending from the bottom (rock deposits, boulders etc.) are covered with high continuous canopy in most cases (panels *a, b, d, f*). It is different from the cold scenario (panels *g, i, j, k*) — high canopy is limited to parts of the

TABLE 3 Comparison of visual and acoustic classification of bottom.

Visual classification	SBES classification	
	soft	hard
hard	1	9
mixed	23	2
soft	15	1

structure located deeper. It is clearly seen in *k* and *i* panels. Also, at CA high continuous canopy is more likely to be located in between some extending bottom features compared to areas without such protection (panel h).

3.4 Video inspection of chosen parts of the investigated areas

All observed individuals were assigned to 18 taxa, 8 of which represented distinct species, 4 represented higher taxonomic affiliation that could not be identified precisely, two included two species that could not be distinguished on visual basis and 4 artificial taxa pooling together species that could only be assigned to higher taxonomic rank than species. The lowest number of species was found at WA with 10 taxa in total, while at CA 15 taxa were observed (Table 4). Altogether, the presence of 13 species of algae were identified on collected video footage. Red algae were represented by 5 and Phaeophyta by 6 taxa (Table 4). Taxa which could not be identified solely on video basis were pooled together into higher taxon.

At the WA site presence of the main kelp grazer — sea urchins — was observed, while no individuals were spotted at the CA site. Sea urchins' presence was limited to the deeper areas at WA (Table 4).

3.4.1 Species composition

Canopies were dominated by species typical for Arctic and boreal high latitudes of the Atlantic Ocean. The exception was an endemic Arctic species, *Laminaria solidungula*, which was observed at both sites. The most frequently observed species of macroalgae were kelps: *Alaria esculenta*, *Laminaria digitata/hyperborea* and *Desmarestia aculeata*. Distinction between *L. digitata* and *L. hyperborea* solely on visual inspection of recorded material was not possible. For that reason we pooled those taxa into one entity.

At WA 8 brown algae and one red algae (*Lithothamnion* sp.) were identified, while at CA 7 taxa of brown algae and 5 of red algae were observed (Table 5).

4 Discussion

Species composition list recorded in this study is much shorter than the checklist reported by comprehensive floristic studies in the area. Here, we identified 18 out of 83 species found previously (Fredriksen and Kile, 2012) in waters of the west Spitsbergen in the supralitoral, eulittoral (intertidal) and subtidal zones combined. The lower number of species identified here was due to the different methods we used. We identified the species based on visual inspection of the underwater footage, thus, only abundant species larger than 10 cm in size could be accurately identified. Our conclusions are derived specifically from the patterns of algae distribution, not from their species richness. Therefore, our method allowed us to collect relevant data quicker and over a much larger area than traditional methods, such as bottom dredging and scuba diving.

The macroalgal community in the surveyed places consisted of the same dominant kelp species as ones observed in adjacent areas: in Hornsund located south of WA (where combined biomass of *Laminaria digitata*, *Saccharina latissima* and *Alaria esculenta* accounts for over 70% of the total macroalgal biomass) (Tatarek et al., 2012) and in Kongsfjorden (Bartsch et al., 2016; Kruss et al., 2017).

At WA kelp grazers were observed. In deep water areas many individuals of sea urchins were found, whose presence shaped the lower depth limit of the kelp forest. Sea urchins are known to be the only herbivores able to graze on kelps to the point that they control its distribution. In extreme cases, when the population of sea urchins exceeds a certain threshold (>500 ind. m^2), the grazing exceeds kelps' ability to recover and their population collapses leaving barren zones (Scheibling et al., 1999; Gagnon et al., 2004). The water dynamics and presence of predation excludes sea urchins from shallow waters, therefore, the effect of sea urchins on kelps is only present starting from a certain depth. Since differences between canopies in deeper areas

TABLE 4 Share of different canopy types (according to Table 1) in each studied area.

ID	Canopy type	WA (Warm Arctic)	CA (Cold Arctic)
1	No Canopy	58%	59%
2	Low canopy (Canopy thickness < 0.5 m)Patchy (Coverage < 50%)	6%	17%
3	Low canopy (Canopy thickness < 0.5 m)Continuous (Coverage > 50%)	26%	21%
4	High canopy (Canopy thickness > 0.5 m)Patchy (Coverage < 50%)	0	0
5	High canopy (Canopy thickness > 0.5 m)Continuous (Coverage > 50%)	10%	2%

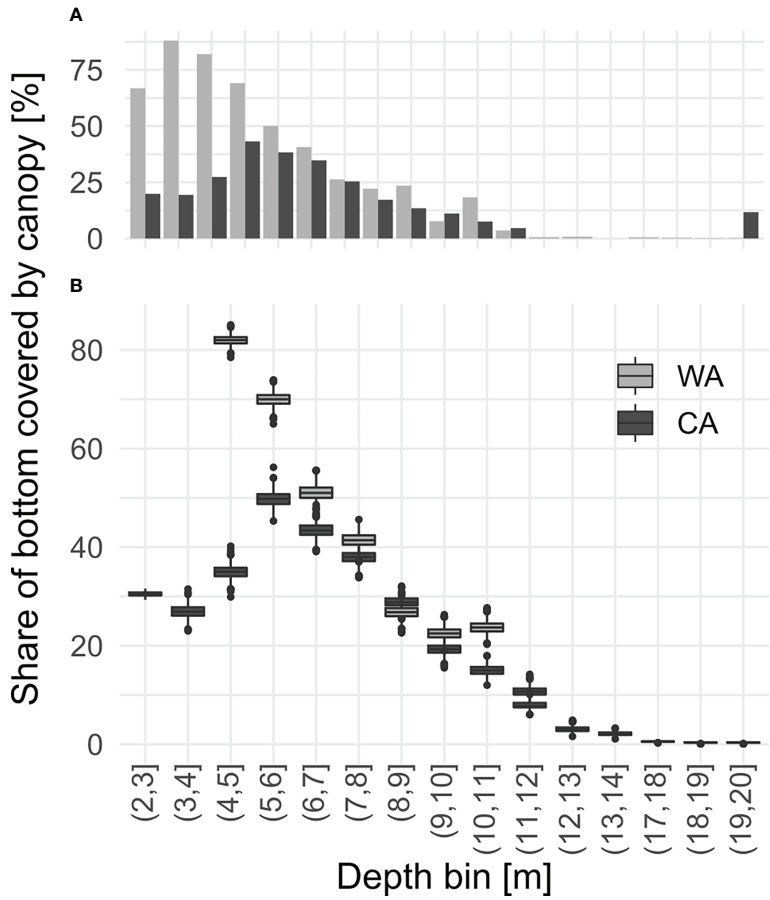

FIGURE 4
Algal coverages of inhabitable bottom averaged for distinct depth bins in sites Warm Arctic (WA) and Cold Arctic (CA): **(A)** based on all observations, **(B)** calculated from 1000 randomly selected samples within the given depth bin permuted 9999 times; boxplots represents distribution of values in all permutations.

were not very pronounced (especially when it comes to space utilization) we conclude that sea urchins have no significant top down control in considered areas.

Sea bottom is similar at both study sites. In shallow water areas (< 5 m) it is mostly hard with exposed bedrock and deposits of boulders and large stones, while deeper regions (>5 m) are covered with finer sediments like sand and mud. Bottom at WA is steeper compared to CA, which is generally very flat: average slope at WA is 2.06° (SD = 0.8), while at CA it is 0.05° (SD = 0.07). At greater slopes sediments are more likely to be transported into deeper water, which makes macroalgae less likely to be buried underneath (Duarte, 1996; Krause-Jensen and Duarte, 2016)

In both areas, less than a half of the surface identified as suitable for macroalgal canopy development was inhabited by algae and was nearly identical between two sites — 42% at WA and 41% at CA. Similar values were reported for nearby locations: 41% in Kongsfjorden (Tatarek et al., 2012; Kruss et al., 2017), 29% in Hornsund (Kruss, 2010).

We simplified the classification method compared with other studies that were specifically aimed to precisely describe bottom hardness and sediment types (LeBlanc et al., 1992; Kostylev et al., 2001; Kenny et al., 2003; Passlow et al., 2006; Longdill et al., 2007; Bartholomä et al., 2011; Haris et al., 2012; Diesing et al., 2014). Bottom hardness is the main factor influencing its ability to reflect acoustic waves, however this property is modified by a number of factors such as: layer of fine sediments covering hard bottom, stones covering fine substrate, vegetation, or orientation of the bottom surface. To decrease the effect of those modifiers, SBES readings were spatially aggregated. In our case, the distribution of aggregated reverberated signal strength was clearly bimodal, which corresponded to two bottom types present within studied areas: hard rocky bottom and soft sedimentary bottom. Indeed, by fitting the data with different runs of k-means, we achieved the best fit with the model with two classes (chosen by the mean silhouette width criterion). It resulted in a conservative split where only bedrock, boulders and dense stone beds were recognized as hard substrate, while mixed types like stones on sand and fine

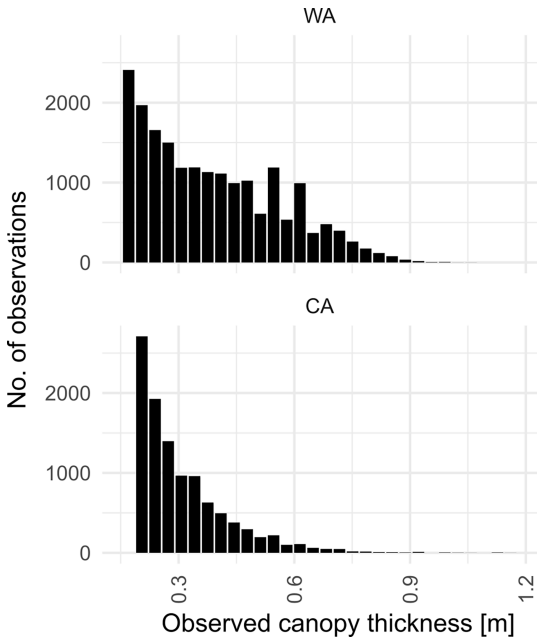

FIGURE 5
Histograms of canopy thickness observed at studied sites.

gravels were classified as soft substrate. While some algae were observed on bottom of mixed type, they did not form dense canopies. Therefore, we concluded that excluding those places from the analysis did not change the overall conclusions.

Continuous and high macrophyte canopy was more frequent at WA with 10% coverage of habitable surface, compared to only 2% coverage of suitable substrate at CA. Thicker (>0.5 m) canopies were only observed in areas where coverage reached more than 5%

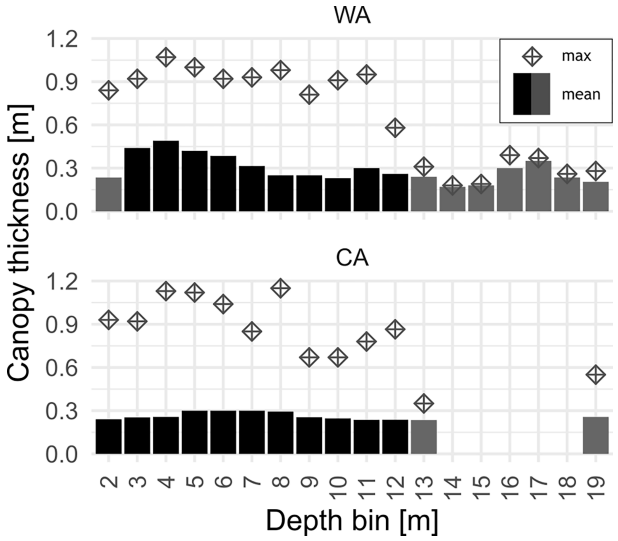

FIGURE 6
Canopy thickness in depth bins at each station: bars represents mean values, error bar — median canopy thickness and diamond point shows maximal value recorded in each bin. Bins with less than 100 observations were indicated by grey fill.

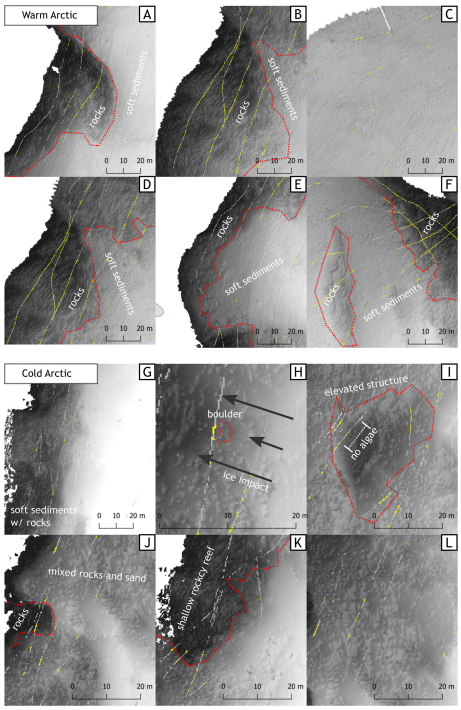

FIGURE 7
Selected close ups of algae presence along the observation routes indicated by yellow pixels (absence of algae showed in light grey) overlaid on bottom relief. Red lines indicate margins of the bed rock; arrows indicate direction of ice impact (for further explanations see text).

TABLE 5 List of taxa observed on video records.

			Cold Arctic (Agardhbukta)		Warm Arctic (Bohemanesset)	
			Depth of observation		Depth of observation	
	Taxon\depth		min [m]	max [m]	min [m]	max [m]
Brown algae	*Alaria esculenta*		3.50	11.70	4.60	15.30
	Laminaria digitata/hyperborea		3.50	11.70	4.70	7.60
	L. solidungula		8.60	8.80	6.10	7.50
	L. cf. solidungula		3.80	10.90		
	Saccharina latissima		3.80	11.80	4.50	12.30
	Chorda filum/tomentosa				5.79	10.75
	Desmarestia aculeata				5.68	13.81
	Dictyosiphon/Stictyosiphon sp.		6.32	11.82	5.81	12.08
	Laminaria sp.		3.47	3.94		
Red algae	*Lithothamnion* sp.		3.96	8.80	4.62	19.66
	Odonthalia dentata		3.70	11.77		
	Palmaria palmata		6.63			
	Phycodrys rubens		8.54	11.64		
	Ptilota plumosa		6.32	6.51		
Aggregative	Phaeophyta juveniles (blade)				6.26	8.28
	Rhodophyta indet. (filamentous)		3.55	8.53		
	Phaeophyta indet. (filamentous)		5.95	6.23	5.96	7.29
	Unidentified filamentous	3.45	11.78			
Herbivores	Sea urchins				7.72	20.79

of suitable habitat. Such high meadows can only be formed at undisturbed bottom (no scouring) by fully developed kelps growing close to each other. Solitary kelps lay flat on the bottom, rather than extend upright toward the surface (species that in the study area lack features facilitating buoyancy), thus its apparent height (measured with SBES as canopy thickness) would not be much more than the height of its strip. Individuals growing in dense canopy, in turn, support each other and thus form a thicker canopy.

Canopy at WA was better developed than the one observed at CA. Fronds at WA were big, regularly shaped, without any apparent damage (Supplementary Figure S4). Kelps covered most of the bottom where the substrate was made of bedrock or large boulders. Often, numerous blades were extending from rhizoids clustered together. On very few occasions we observed species of different kelps present in the same place – individuals of given species were grouped with each other, but such patches did not display any kind of zonation. Hardly ever *Desmarestia aculeata* occurred when kelps were present, while this species was very common there substrate contained stones and/or gravel too small to support kelps to keep their fronds in place.

The canopy thickness reached maximum value at depths between 3 m and 5 m. In the case of WA it is possible that more data from shallow water could potentially shift the distribution towards shallow water making the discrepancy between study sites more apparent. At WA shallow bottom is utilized to much higher degree than at CA which is most probably caused by the ice-scouring damaging older fronds. Below 6 m depth there is no difference in share of occupied space in both places, which suggests that this was the maximum depth of ice disturbance. A fully developed seaweed forest was observed at WA mainly in shallow water (less than 6 m), thus in the range of the observed depth of interaction with the ice at CA. This may explain the fact that there are few areas where a dense seaweed forest has been observed.

Interestingly, a similar pattern of the kelp distribution shifting towards shallower waters was observed in Kongsfjorden (Svalbard) where the biomass of kelp peaked around 5 m in 1988 and shifted to 2.5 m recently as a result of warming of the environment, namely: decreased ice-scouring and longer photic season allowing algae to occupy shallower areas, and increased turbidity limiting the amount of radiation available in deeper areas (Bartsch et al., 2016; Bischof et al., 2019b).

In heavy ice-scoured areas of the Canadian Arctic (Heine, 1989), where ice impact was observed down to 12 m, perennial algae presence was limited to crevasses and sloping bottoms, while macrophytes were nearly completely removed from exposed surfaces shallower than that. Algal community present there was different to one observed in this study, but it also consisted of *Laminaria* and *Alaria* species of similar body type, so they are expected to respond in the same way to the similar environmental pressures.

Destructive events in exposed areas of the sea bottom limit biomass of kelp species, which in turn limits new production in such areas (Filbee-Dexter et al., 2021). Those empty spaces can be utilized by ephemeral algae that are normally outcompeted by perennial species which results in higher species diversity of such a disturbed area (Dial and Roughgarden, 1998). We believe that the high number of observed species at CA can be explained by environmental restrictions on perennial species due to sea ice scouring

Along with the ongoing changes in the climatic system more Arctic coasts will experience sea ice loss. It will result in an increase of areas covered with continuous macroalgal canopy. As disturbance events (ice-scouring in this case) become less frequent, the ephemeral algae will have fewer opportunities to find suitable space, therefore their abundances will most likely decrease and overall we expect a lower macroalgae richness as a consequence of climate warming. Without ice-scouring, algae form much denser meadows — multilayered structures of many individuals intermixed with each other creating safe spaces for associated fauna to live in, protected from water dynamics and predators. By growing in close proximity, kelps give each other support dissipating environmental stresses among many individuals.

Obtained results are preliminary – we have studied one site in each region. We have made an effort to select the most representative sites, however living organisms experience conditions that are the result of complex interplay of many factors, some of which are hard to predict, and to control. It is possible that, despite expectations, areas we have selected to investigate were under conditions that deviate from typical.

The biggest change is expected to occur in shallow waters. Ice-scoured areas shallower than 5 m are strongly underutilized, so macrophytes released from ice pressure will increase their standing stocks to a greater extent. The sea bottom at low depth is affected by waves much stronger than bottom at greater depth. Waves rubbing macrophytes' thalli against the bottom causes fronds fragmentation which is released to the water column allowing for transfer of organic carbon produced by macroalgae into the pelagic system. This might lead to increased primary production of kelp forests, as declining ice would allow them to use previously underutilized space where a higher amount of energy is available. Interaction with water dynamics would release a lot of this new production into adjacent systems. On the other hand, kelps compete for nutrients with planktonic primary producers and, living at the bottom, where the resuspension occurs, do it in a very efficient way (Jiang et al., 2020). Inhabiting shallower water would make them more exposed to extreme events that would facilitate the process of their export into the deep water areas, where they are deposited as blue carbon, acting as a carbon pump, or onto the land, where they are built into terrestrial food chains.

5 Conclusions

1. There is a difference between macroalgal canopies present in the warm and cold study sites both in qualitative and quantitative terms.

2. In warm scenarios, exposed areas are more likely to be covered by a high, continuous vegetation than in cold areas.
3. Ice-scouring is a prominent source of damage to the frond, manifested in the cold areas.
4. Higher environmental pressure at the CA site leads to higher species diversity with turf algae utilizing barren spaces in between kelps fronds. Stable conditions at the WA site lead to more uniform kelp coverage and to segregation between dominant species.
5. As there is less ice cover in the cold regions of Svalbard kelp forests most probably will broaden its extent towards shallower waters and utilize more available surface increasing overall density of kelp forest.

Data availability statement

The raw data supporting the conclusions of this article will be made available by the authors, without undue reservation.

Author contributions

JMWjr. was responsible for method design, data collection, data analysis, and writing a manuscript. JMW and JS applied for money, organized an expedition, collected data and supervised works on manuscript. AT collected data and analyzed video footage. AK was responsible for all hydroacoustics data and RS analyzed MODIS data. All authors contributed to the article and approved the submitted version.

Funding

This research was funded through the 2017-2018 Belmont Forum and BiodivERsA joint call for research proposals, under the BiodivScen ERA-Net COFUND programme, and with the funding organisations Research Council of Norway (project nr. 296836 and National Science Centre Poland (project nr. UMO-2015/17/B/NZ8/02473).

Acknowledgement

We would like to thank Jakub Wiktor, Michał Strach and Bożena Skrzydlińska for reading and commenting on the manuscript. We would like to thank reviewers for taking the time and effort necessary to review the manuscript. We sincerely appreciate all valuable comments and suggestions, which helped us to improve the quality of the manuscript. We would like to acknowledge NASA OB.DAAC for providing satellite (MODIS-Aqua) data and NASA OBPG for developing and maintaining SeaDAS. PAR, cloud cover and ice concentrations were obtained and aggregated with the Giovanni online data system, developed and maintained by the NASA GES DISC. We also acknowledge the MODIS mission scientists and associated NASA personnel for the production of the data used in this research effort. Norbit Subsea and QPS made this study possible by sharing multibeam equipment and processing software.

Conflict of interest

Author AK is employed by NORBIT.

The remaining authors declare that the research was conducted in the absence of any commercial or financial relationships that could be construed as a potential conflict of interest.

Publisher's note

All claims expressed in this article are solely those of the authors and do not necessarily represent those of their affiliated organizations, or those of the publisher, the editors and the reviewers. Any product that may be evaluated in this article, or claim that may be made by its manufacturer, is not guaranteed or endorsed by the publisher.

Supplementary material

The Supplementary Material for this article can be found online at: https://www.frontiersin.org/articles/10.3389/fmars.2022.1021675/full#supplementary-material

SUPPLEMENTARY FIGURE 1
Example of rasterization results. Square mesh is 25 cm x 25 cm aligned with a bathymetry grid (here visualised with hillshade procedure to highlight bottom features) on different scales. Each pixel has a value when there is at least one SBES ping (red dots on panel c) within its limits. In this example, the canopy type category is presented. **(A)** aggregation results on a scale of study area (here: part of WA site), **(B)** conceptual diagram of procedure and **(C)** the real-life analogous case.

SUPPLEMENTARY FIGURE 2
Histogram of bottom mSv values at both areas. Readings are split into ones without canopy and ones with one. Over-representation of values close to zero (hence with higher ability to reflect acoustic waves) is due to our focus on canopy, which is linked to hard substrate.

SUPPLEMENTARY FIGURE 3
Optimal number of clusters for k-means procedure on rolling median averaged mean signal level reflected on sediments.

SUPPLEMENTARY FIGURE 4
Example snapshots (for more information see text).

References

Andersen, G. S., Pedersen, M. F., and Nielsen, S. L. (2013). Temperature acclimation and heat tolerance of photosynthesis in Norwegian saccharina latissima (Laminariales, phaeophyceae). *J. Phycol.* 49, 689–700. doi: 10.1111/jpy.12077

Anderson, J. T., Van Holliday, D., Kloser, R., Reid, D. G., and Simard, Y. (2008). Acoustic seabed classification: current practice and future directions. *ICES J. Mar. Sci.* 65, 1004–1011. doi: 10.1093/icesjms/fsn061

Baith, K., Lindsay, R., Fu, G., and McClain, C. R. (2001). Data analysis system developed for ocean color satellite sensors. *Eos* 82, 202–202. doi: 10.1029/01eo00109

Bartholomä, A., Holler, P., Schrottke, K., and Kubicki, A. (2011). Acoustic habitat mapping in the German wadden Sea–comparison of hydro-acoustic devices. *J. Coast. Res* 1–5. https://www.jstor.org/stable/26482121

Bartsch, I., Paar, M., Fredriksen, S., Schwanitz, M., Daniel, C., Hop, H., et al. (2016). Changes in kelp forest biomass and depth distribution in kongsfjorden, Svalbard, between 1996–1998 and 2012–2014 reflect Arctic warming. *Polar Biol.* 39, 2021–2036. doi: 10.1007/s00300-015-1870-1

Beaudoing, H., Rodell, M.NASA/GSFC/HSL (2020) *GLDAS Noah land surface model L4 monthly 0.25 x 0.25 degree V2.1* (Greenbelt, Maryland, USA: Goddard Earth Sciences Data and Information Services Center (GES DISC) (Accessed 06-07-2022).

Bekkby, T., Rinde, E., Gundersen, H., Norderhaug, K. M., and Christie, H. (2014). Length, strength and water flow: Relative importance of wave and current exposure on morphology in kelp laminaria hyperborea. *Mar. Ecol. Prog. Ser.* 506, 61–70. doi: 10.3354/meps10778

Bischof, K., Buschbaum, C., Fredriksen, S., Gordillo, F. J. L., Heinrich, S., Jiménez, C., et al. (2019a). "Kelps and environmental changes in kongsfjorden: Stress perception and responses," in *The ecosystem of kongsfjorden, Svalbard*. Eds. H. Hop and C. Wiencke (Cham: Advances in Polar Ecology Springer), 373–422. doi: 10.1007/978-3-319-46425-1_10

Bischof, K., Convey, P., Duarte, P., and Gattuso, J. P. (2019b). "Kongsfjorden as harbinger of the future Arctic: Knowns, unknowns and research priorities," in *The ecosystem of kongsfjorden, Svalbard*. (Cham: Advances in Polar Ecology Springer) doi: 10.1007/978-3-319-46425-1_14

Blondel, P., and Murton, B. (1997) *Handbook of seafloor sonar imagery*. Available at: https://www.semanticscholar.org/paper/e91bafb2dc2cf694fa542b8659ac9d0becb9d7cb (Accessed December 1, 2021).

Boertmann, D., Mosbech, A., Schiedek, D., and Dünweber, M. (2013) *Disko west. a strategic environmental impact assessment of hydrocarbon activities*. Available at: https://www.forskningsdatabasen.dk/en/catalog/2389318069.

Bonsell, C., and Dunton, K. H. (2018). Long-term patterns of benthic irradiance and kelp production in the central Beaufort sea reveal implications of warming for Arctic inner shelves. *Prog. Oceanography* 162, 160–170. doi: 10.1016/j.pocean.2018.02.016

Brown, C. J., Smith, S. J., Lawton, P., and Anderson, J. T. (2011). Benthic habitat mapping: A review of progress towards improved understanding of the spatial ecology of the seafloor using acoustic techniques. *Estuar. Coast. Shelf Sci.* 92, 502–520. doi: 10.1016/j.ecss.2011.02.007

Buchholz, C. M., and Wiencke, C. (2016). Working on a baseline for the kongsfjorden food web: production and properties of macroalgal particulate organic matter (POM). *Polar Biol.* 39, 2053–2064. doi: 10.1007/s00300-015-1828-3

Byrnes, J. E., Reed, D. C., Cardinale, B. J., Cavanaugh, K. C., Holbrook, S. J., and Schmitt, R. J. (2011). Climate-driven increases in storm frequency simplify kelp forest food webs. *Glob. Change Biol.* 17, 2513–2524. doi: 10.1111/j.1365-2486.2011.02409.x

Carbó, R., and Molero, A. C. (1997). Scattering strength of a gelidium biomass bottom. *Appl. Acoust.* 51, 343–351. doi: 10.1016/S0003-682X(97)00012-1

Castellani, G., Veyssière, G., Karcher, M., Stroeve, J., Banas, S. N., Bouman, A. H., et al. (2022). Shine a light: Under-ice light and its ecological implications in a changing Arctic ocean. *Ambio* 51, 307–317. doi: 10.1007/s13280-021-01662-3

Dial, R., and Roughgarden, J. (1998). Theory of marine communities: The intermediate disturbance hypothesis. *Ecology* 79, 1412–1424. doi: 10.1890/0012-9658(1998)079[1412:tomcti]2.0.co;2

Diesing, M., Green, S. L., Stephens, D., Lark, R. M., Stewart, H. A., and Dove, D. (2014). Mapping seabed sediments: Comparison of manual, geostatistical, object-based image analysis and machine learning approaches. *Cont. Shelf Res.* 84, 107–119. doi: 10.1016/j.csr.2014.05.004

Duarte, C. M. (1996) *The fate of marine autotrophic production*. Available at: https://play.google.com/store/books/details?id=y1RkuAAACAAJ.

Filbee-Dexter, K., MacGregor, K. A., Lavoie, C., Garrido, I., Goldsmit, J., de la Guardia, L. C., et al. (2021) *Sea Ice and substratum shape extensive kelp forests in the Canadian Arctic*. Available at: https://ecoevorxiv.org/t82cf/.

Filbee-Dexter, K., Wernberg, T., Norderhaug, K. M., Ramirez-Llodra, E., and Pedersen, M. F. (2018). Movement of pulsed resource subsidies from kelp forests to deep fjords. *Oecologia* 187, 291–304. doi: 10.1007/s00442-018-4121-7

Fortes, M. D., and Lüning, K. (1980). Growth rates of north Sea macroalgae in relation to temperature, irradiance and photoperiod. *Helgoländer Meeresuntersuchungen* 34, 15–29. doi: 10.1007/BF01983538

Fredriksen, S., and Kile, M. R. (2012). The algal vegetation in the outer part of isfjorden, spitsbergen: revisiting per svendsen's sites 50 years later. *Polar Res.* 31, 17538. doi: 10.3402/polar.v31i0.17538

Gagnon, P., Himmelman, J. H., and Johnson, L. E. (2004). Temporal variation in community interfaces: kelp-bed boundary dynamics adjacent to persistent urchin barrens. *Mar. Biol.* 144, 1191–1203. doi: 10.1007/s00227-003-1270-x

Global Modeling and Assimilation Office (GMAO) (2015) *MERRA-2 tavgM_2d_flx_Nx: 2d,Monthly mean,Time-Averaged,Single-Level,Assimilation, Surface flux diagnostics V5.12.4* (Greenbelt, MD, USA: Goddard Earth Sciences Data and Information Services Center (GES DISC) (Accessed 06-07-2022).

Haris, K., Chakraborty, B., Ingole, B., Menezes, A., and Srivastava, R. (2012). Seabed habitat mapping employing single and multi-beam backscatter data: A case study from the western continental shelf of India. *Cont. Shelf Res.* 48, 40–49. doi: 10.1016/j.csr.2012.08.010

Heine, J. N. (1989). Effects of ice scour on the structure of sublittoral marine algal assemblages of st. Lawrence and st. Matthew islands, Alaska. *Mar. Ecol. Prog. series.* 52, 253–260. Oldendorf. doi: 10.3354/meps052253

Hijmans, R. J., and van Etten, J. (2016). Raster: Geographic data analysis and modeling to pakiet R. *Package version 2*. Available at: https://cran.r-project.org/web/packages/raster/raster.pdf

Jackson, D. R., and Richardson, M. D. (2007). *High-frequency seafloor acoustics* (New York: Springer). doi: 10.1007/978-0-387-36945-7

Jiang, Z., Liu, J., Li, S., Chen, Y., Du, P., Zhu, Y., et al. (2020). Kelp cultivation effectively improves water quality and regulates phytoplankton community in a turbid, highly eutrophic bay. *Sci. Total Environ.* 707, 135561. doi: 10.1016/j.scitotenv.2019.135561

Kenny, A. J., Cato, I., Desprez, M., Fader, G., Schüttenhelm, R. T. E., and Side, J. (2003). An overview of seabed-mapping technologies in the context of marine habitat classification☆. *ICES J. Mar. Sci.* 60, 411–418. doi: 10.1016/s1054-3139(03)00006-7

Kostylev, V. E., Todd, B. J., Fader, G. B. J., Courtney, R. C., Cameron, G. D. M., and Pickrill, R. A. (2001). Benthic habitat mapping on the scotian shelf based on multibeam bathymetry, surficial geology and sea floor photographs. *Mar. Ecol. Prog. Ser.* 219, 121–137. doi: 10.3354/meps219121

Krause-Jensen, D., and Duarte, C. M. (2016). Substantial role of macroalgae in marine carbon sequestration. *Nat. Geosci.* 9, 737–742. doi: 10.1038/ngeo2790

Krause-Jensen, D., Marbà, N., Olesen, B., Sejr, M. K., Christensen, P. B., Rodrigues, J., et al. (2012). Seasonal sea ice cover as principal driver of spatial and temporal variation in depth extension and annual production of kelp in Greenland. *Glob. Change Biol.* 18, 2981–2994. doi: 10.1111/j.1365-2486.2012.02765.x

Krumhansl, K. A., Okamoto, D. K., Rassweiler, A., Novak, M., Bolton, J. J., Cavanaugh, K. C., et al. (2016). Global patterns of kelp forest change over the past half-century. *Proc. Natl. Acad. Sci. U. S. A.* 113, 13785–13790. doi: 10.1073/pnas.1606102113

Kruss, A. (2010). Akustyczna identyfikacja habitatów bentosowych Arktyki. 38 (2):205–229

Kruss, A., Blondel, P., Tegowski, J., Wiktor, J., and Tatarek, A. (2008). Estimation of macrophytes using single-beam and multibeam echosounding for environmental monitoring of Arctic fjords (Kongsfjord, West Svalbard island). *J. Acoust. Soc Am.* 123, 3213–3213. doi: 10.1121/1.2933397

Kruss, A., Tęgowski, J., Tatarek, A., Wiktor, J., and Blondel, P. (2017). Spatial distribution of macroalgae along the shores of kongsfjorden (West spitsbergen) using acoustic imaging. *Pol. Polar Res* 38, 205–229. doi: 10.1515/popore-2017-0009

Kruss, A., Wiktor, J. Jr, Wiktor, J., and Tatarek, A. (2019). "Acoustic detection of macroalgae in a dynamic Arctic environment (Isfjorden, West spitsbergen) using multibeam echosounder," in *2019 IEEE Underwater Technology (UT)*. (New York: IEEE), 1–7. doi: 10.1109/UT.2019.8734323

LeBlanc, L. R., Mayer, L., Rufino, M., Schock, S. G., and King, J. (1992). Marine sediment classification using the chirp sonar. *J. Acoust. Soc Am.* 91, 107–115. doi: 10.1121/1.402758

Longdill, P. C., Healy, T. R., Black, K. P., and Mead, S. T. (2007). Integrated sediment habitat mapping for aquaculture zoning. *J. Coast. Res.* 50, 173–179. Available at: https://www.jstor.org/stable/26481578

Lurton, X. (2002). *An introduction to underwater acoustics: Principles and applications* (UK and New York, NY, USA: Springer Science & Business Media). Available at: https://play.google.com/store/books/details?id=VTNRh3pyCyMC.

Markager, S., and Sand-Jensen, K. (1992). Light requirements and depth zonation of marine macroalgae. *Mar. Ecology-Progress Ser.* 88, 83–83. doi: 10.3354/meps088083

Michaels, W. L. (2007). Review of acoustic seabed classification systems. *ICES Coop. Res. Rep.* 286, 101–126.

Miller, R. J., Reed, D. C., and Brzezinski, M. A. (2011). Partitioning of primary production among giant kelp (Macrocystis pyrifera), understory macroalgae, and phytoplankton on a temperate reef. *Limnol. Oceanogr.* 56, 119–132. doi: 10.4319/lo.2011.56.1.0119

Minchinton, T. E., Scheibling, R. E., and Hunt, H. L. (1997). Recovery of an intertidal assemblage following a rare occurrence of scouring by Sea ice in Nova Scotia, Canada. *Botanica Marina* 40, 139–148. doi: 10.1515/botm.1997.40.1-6.139

NASA Goddard Space Flight Center, Ocean Ecology Laboratory and Ocean Biology Processing Group (2018) *Moderate-resolution imaging spectroradiometer (MODIS) aqua photosynthetically available radiation data; 2018 reprocessing* (Greenbelt, MD, USA) (Accessed 06-07-2022). NASA OB.DAAC.

Nechad, B., Ruddick, K. G., and Park, Y. (2010). Calibration and validation of a generic multisensor algorithm for mapping of total suspended matter in turbid waters. *Remote Sens. Environ.* 114, 854–866. doi: 10.1016/j.rse.2009.11.022

Passlow, V., O'Hara, T., Daniell, J., Beaman, R. J., and Twyford, L. M. (2006). *Sediments and biota of bass strait: an approach to benthic habitat mapping.* Geoscience Australia, Record 2004/23, pp. 1–93.

Pedersen, M. F., Filbee-Dexter, K., Norderhaug, K. M., Fredriksen, S., Frisk, N. L., Fagerli, C. W., et al. (2020). Detrital carbon production and export in high latitude kelp forests. *Oecologia* 192, 227–239. doi: 10.1007/s00442-019-04573-z

Perovich, D. K., Cota, G. F., Maykut, G. A., and Grenfell, T. C. (1993). Bio-optical observations of first-year Arctic sea ice. *Geophys. Res. Lett.* 20, 1059–1062. doi: 10.1029/93GL01316

Pörtner, H.-O., Roberts, D. C., Adams, H., Adler, C., Aldunce, P., Ali, E., et al. (2022). Climate change 2022: Impacts, adaptation and vulnerability. *Contribution of working group II to the sixth assessment report of the intergovernmental panel on climate change* H.-O. Pörtner, D.C. Roberts, M. Tignor, E.S. Poloczanska, K. Mintenbeck, A. Alegría, et al. (eds.)]. (Cambridge, UK and New York, NY, USA: Cambridge University Press), 3056 pp. doi: 10.1017/9781009325844

Renaud, P. E., Løkken, T. S., Jørgensen, L. L., Berge, J., and Johnson, B. J. (2015). Macroalgal detritus and food-web subsidies along an Arctic fjord depth-gradient. *Front. Mar. Sci.* 2. doi: 10.3389/fmars.2015.00031

Ronowicz, M., Legeżyńska, J., Kukliński, P., and Włodarska-Kowalczuk, M. (2013). Kelp forest as a habitat for mobile epifauna: case study ofCaprella septentrionalisKröyer 1838 (Amphipoda, caprellidae) in an Arctic glacial fjord. *Polar Res.* 32, 21037. doi: 10.3402/polar.v32i0.21037

Sabol, B. M., Eddie Melton, R., Chamberlain, R., Doering, P., and Haunert, K. (2002). Evaluation of a digital echo sounder system for detection of submersed aquatic vegetation. *Estuaries* 25, 133–141. doi: 10.1007/BF02696057

Scheibling, R. E., Hennigar, A. W., and Balch, T. (1999). Destructive grazing, epiphytism, and disease: the dynamics of sea urchin - kelp interactions in Nova Scotia. *Can. J. Fish. Aquat. Sci.* 56, 2300–2314. doi: 10.1139/f99-163

Shenderov, E. L. (1998). Some physical models for estimating scattering of underwater sound by algae. *J. Acoust. Soc Am.* 104, 791–800. doi: 10.1121/1.423353

Singh, R. K., Shanmugam, P., He, X., and Schroeder, T. (2019). UV-NIR approach with non-zero water-leaving radiance approximation for atmospheric correction of satellite imagery in inland and coastal zones. *Opt. Express* 27, A1118–A1145. doi: 10.1364/OE.27.0A1118

Skogseth, R., Haugan, P. M., and Jakobsson, M. (2005). Watermass transformations in storfjorden. *Cont. Shelf Res.* 25, 667–695. doi: 10.1016/j.csr.2004.10.005

Skogseth, R., Olivier, L. L. A., Nilsen, F., Falck, E., Fraser, N., Tverberg, V., et al. (2020). Variability and decadal trends in the isfjorden (Svalbard) ocean climate and circulation – an indicator for climate change in the European Arctic. *Prog. Oceanography* 187, 102394. doi: 10.1016/j.pocean.2020.102394

Smale, D. A., Burrows, M. T., Moore, P., O'Connor, N., and Hawkins, S. J. (2013). Threats and knowledge gaps for ecosystem services provided by kelp forests: a northeast Atlantic perspective. *Ecol. Evol.* 3, 4016–4038. doi: 10.1002/ece3.774

Stroeve, J., Holland, M. M., Meier, W., Scambos, T., and Serreze, M. (2007). Arctic Sea ice decline: Faster than forecast. *Geophys. Res. Lett.* 34, L09501. doi: 10.1029/2007gl029703

Tatarek, A., Wiktor, J., and Kendall, M. A. (2012). The sublittoral macroflora of hornsund. *Polar Res.* 31, 18900. doi: 10.3402/polar.v31i0.18900

Tom Dieck (Bartsch), I. (1992). North pacific and north Atlantic digitate laminaria species (Phaeophyta): hybridization experiments and temperature responses. *Phycologia* 31, 147–163. doi: 10.2216/i0031-8884-31-2-147.1

van Walree, P. A., Tęgowski, J., Laban, C., and Simons, D. G. (2005). Acoustic seafloor discrimination with echo shape parameters: A comparison with the ground truth. *Cont. Shelf Res.* 25, 2273–2293. doi: 10.1016/j.csr.2005.09.002

van Winden, E. M. (2016) *Quantification and consequences of glacier volume loss on meltwater fluxes and organic matter since 1971, edgeøya, Svalbard*. Available at: https://dspace.library.uu.nl/handle/1874/327686 (Accessed April 2, 2021).

von Biela, V. R., Newsome, S. D., Bodkin, J. L., Kruse, G. H., and Zimmerman, C. E. (2016). Widespread kelp-derived carbon in pelagic and benthic nearshore fishes suggested by stable isotope analysis. *Estuar. Coast. Shelf Sci.* 181, 364–374. doi: 10.1016/j.ecss.2016.08.039

Wiencke, C., Clayton, M. N., Gómez, I., Iken, K., Lüder, U. H., Amsler, C. D., et al. (2007). Life strategy, ecophysiology and ecology of seaweeds in polar waters. *Rev. Environ. Sci. Technol.* 6, 95–126. doi: 10.1007/s11157-006-9106-z

Wiencke, C., and Tom Dieck, I. (1990). Temperature requirements for growth and survival of macroalgae from Antarctica and southern Chile. *Mar. Ecol. Prog. Ser.* 59, 157–170. doi: 10.3354/meps059157

Włodarska-Kowalczuk, M., Kukliński, P., Ronowicz, M., Legeżyńska, J., and Gromisz, S. (2009). Assessing species richness of macrofauna associated with macroalgae in Arctic kelp forests (Hornsund, Svalbard). *Polar Biol.* 32, 897–905. doi: 10.1007/s00300-009-0590-9

frontiers | Frontiers in Marine Science

TYPE Original Research
PUBLISHED 09 December 2022
DOI 10.3389/fmars.2022.1063007

Check for updates

OPEN ACCESS

EDITED BY
Monica Montefalcone,
University of Genoa, Italy

REVIEWED BY
Edoardo Casoli,
Sapienza University of Rome, Italy
Andrew M. Fischer,
University of Tasmania, Australia

*CORRESPONDENCE
Rodolfo Silva
RSilvaC@iingen.unam.mx

SPECIALTY SECTION
This article was submitted to Marine Ecosystem Ecology, a section of the journal Frontiers in Marine Science

RECEIVED 06 October 2022
ACCEPTED 22 November 2022
PUBLISHED 09 December 2022

CITATION
de Almeida LR, Ávila-Mosqueda SV, Silva R, Mendoza E and van Tussenbroek BI (2022) Mapping the structure of mixed seagrass meadows in the Mexican Caribbean. *Front. Mar. Sci.* 9:1063007. doi: 10.3389/fmars.2022.1063007

COPYRIGHT
© 2022 de Almeida, Ávila-Mosqueda, Silva, Mendoza and van Tussenbroek. This is an open-access article distributed under the terms of the Creative Commons Attribution License (CC BY). The use, distribution or reproduction in other forums is permitted, provided the original author(s) and the copyright owner(s) are credited and that the original publication in this journal is cited, in accordance with accepted academic practice. No use, distribution or reproduction is permitted which does not comply with these terms.

Mapping the structure of mixed seagrass meadows in the Mexican Caribbean

Laura R. de Almeida[1], S. Valery Ávila-Mosqueda[2], Rodolfo Silva[1]*, Edgar Mendoza[1] and Brigitta I. van Tussenbroek[2]

[1]Instituto de Ingeniería, Universidad Nacional Autónoma de México, Mexico City, Mexico, [2]Unidad Académica de Sistemas Arrecifales, Instituto de Ciencias del Mar y Limnología, Universidad Nacional Autónoma de México, Puerto Morelos, Mexico

The physical and ecological importance of seagrass meadows in coastal processes is widely recognized, and the development of tools facilitating characterization of their structure and distribution is important for improving our understanding of these processes. Mixed (multi-specific) meadows in a Mexican Caribbean reef lagoon were mapped employing a multiparameter approach, using PlanetScope remote sensing images, and supervised classification based on parameters related to the structure of the seagrasses meadows, including the cover percentages of seagrass/algae/sediment, algae thalli and seagrass shoot densities, canopy heights and estimated leaf area index (LAI). The cover, seagrass and algae densities, and seagrass canopy heights were obtained using ground truth sampling, while the LAI was estimated using data obtained from long-term monitoring programs. The maps do not show the differentiation of seagrass species, but ground truthing contemplated characterization of the density of *Thalassia testudinum, Syringodium filiforme* and *Halodule wrightii* and their respective LAIs. *S. filiforme* was the dominant species in terms of shoot density, and *T. testudinum* was dominant in terms of LAI. In the multiparameter-based map four classes were defined, based on the cover and structural characteristics, and its overall accuracy was very high (~90%). Maps based on sediment cover and LAI alone also had 4 classes, but they were less accurate than the multiparameter-based map (~70% and ~80%, respectively). The multiparameter-based seagrass map provided spatially-explicit data on the abundance and structure of seagrasses, useful for future monitoring of the changes in the meadows, and also for studies of that require data of large-scale meadow structure, such as inventories of associated biota, blue carbon storage, or modelling of the local hydrodynamics.

KEYWORDS

seagrass mapping, LAI estimation, multiparameter classification, PlanetScope satellite image, reef lagoon

1 Introduction

Seagrass meadows provide a wide range of ecosystem services. These include the provision of habitat and refuge for many species, the improvement of water quality, coastal protection, erosion control, carbon sequestration, and services related to tourism, education and recreation (Barbier et al., 2011). Seagrass canopies attenuate the energy of waves and currents, contributing to sedimentation, and their root and rhizome systems trap and stabilize sediments (Madsen et al., 2001; Chen et al., 2007; Koch et al., 2009). In tropical reef lagoons, the seagrass meadows are interconnected with other coastal ecosystems, such as coral reefs and beach/dune systems. The reefs provide a suitable environment for the colonization and development of seagrass in the reef lagoons, while the seagrasses assimilate nutrients, entrap sediment and particles, thus improving the quality of coastal waters and favoring the growth of the coral reefs. Both coral reefs and seagrass meadows dampen wave and current energy, stabilizing the coast, and shaping the morphology of the beach/dune systems (Moberg and Rönnbäck, 2003; de Almeida et al., 2022). Spatially explicit information on the distribution of the seagrasses and their characteristics can provide a useful tool for understanding the dynamics of the meadows themselves, their impact on local hydro- and sediments dynamics, as well as interactions with other neighboring systems.

Spatially explicit information obtained by mapping the distribution of seagrasses in shallow waters using satellite images (especially those with high spatial resolution, i.e.<10 m pixel size) and field data, provide a quantitative and cost effective alternative for intensive *in situ* monitoring programs (Baumstark et al., 2013). Criteria used for seagrass maps are typically presence/absence (e.g. Hossain et al., 2015), the percentage of seagrass/sediment cover (e.g. Roelfsema et al., 2009) or spatial distribution of seagrass meadows (e.g. Kovacs et al., 2018). Such maps can be improved with the addition of information regarding the seagrass landscape, such as the density of the seagrasses and algae, seagrass canopy heights and their foliar area, which could then allow a better evaluation of ecosystem interactions and the services offered by the meadows.

For example, the propagation/dissipation of waves and currents, and consequent sediment dynamics, are determined by the extension and structure of the meadows in relation to the direction of wave propagation (Chen et al., 2007), the density of the plants (Gambi et al., 1990), the seagrass species, and the height of the canopy, and its ratio to the relative water submergence (Fonseca and Cahalan, 1992). Maps that reflect these parameters (multiparameter classes) can also be useful for the determination of blue carbon budgets and studies of infauna communities. Such maps could also be used as input for numerical models (e.g. Silva et al., 2020), incorporating mechanical traits (Soissons et al., 2018), friction, or damping coefficients, obtained from laboratory experiments (Stratigaki et al., 2011; Koftis et al., 2013; Schaefer and Nepf, 2022). Such experimentally determined coefficients are vital in the calibration and validation of hydrodynamic numerical models (e.g. Paquier et al., 2021). However, without information on the distribution and structure of the seagrass meadows, numerical models may be inaccurate in reproducing the actual coastal processes, as explained by Escudero et al. (2021).

The main aim of this study was to see whether it is possible to map seagrasses beyond mere cover, and to incorporate data on specific composition and structure to provide spatially explicit information that may be useful in studies that require such information. A map was created as a function of seagrass density, algae density, canopy height, seagrass the leaf area index (LAI) and percentage of seabed coverage (multiparameter map), for a shallow reef lagoon with clear waters in the Mexican Caribbean. Maps with classes defined only by LAI and sediment cover were also created to compare with the multiparameter class map. The advantages and disadvantages of each mapping method were evaluated.

2 Materials and methods

2.1 Study area

The study site is part of a reef lagoon in the north of the Marine Protected Area of Puerto Morelos, (20° 57' - 21° 00' N; 86° 47' - 86° 49'W), in front of the Moon Palace Resort, in the Mexican Caribbean, with a surface of 12.5 km^2 (Figure 1).

The fringing reefs, part of the Mesoamerican Reef System, are 1.7 – 3.1 km from the coast in the study area. The reef lagoon is relatively shallow, with an average depth of 3-4 m and maximum depth of 8 m (data measured in this study). The lagoon floor is usually composed of calcareous sand, and seagrass meadows are interspersed with underwater dunes consisting of loose calcareous sands devoid of vegetation. The dominant seagrass species is *Thalassia testudinum*, which is considered the climax species in the Caribbean, along with *Syringodium filiforme*, *Halodule wrightii* and rhizophytic algae (van Tussenbroek, 2011; Hedley et al., 2021).

The climate at Puerto Morelos is tropical. Mean surface-water temperatures vary from 25.1°C, in mid-winter, and 29.9°C, in late summer (Rodríguez-Martínez et al., 2010). Average annual rainfall is 1000 - 1400 mm, with a tendency of heavier rain in summer (June-October) (Martínez et al., 2014). The coast has a microtidal regime with semidiurnal spring and neap tidal ranges of 0.32 and 0.07 m, respectively (Coronado et al., 2007). The wave climate is characterized by calm conditions most of the time: significant wave heights (Hs) of 1-1.5 m and short wave periods (Tm) of 4-7 s. Swell waves are rare, occurring from November to April, associated with northerly cold fronts; Hs ~ 2-3 m, Tm ~ 6-8 s, or in the hurricane season, May to October; Hs ~ 6-15 m, Tm ~ 8-12 s (Escudero-Castillo et al., 2018; Rioja-

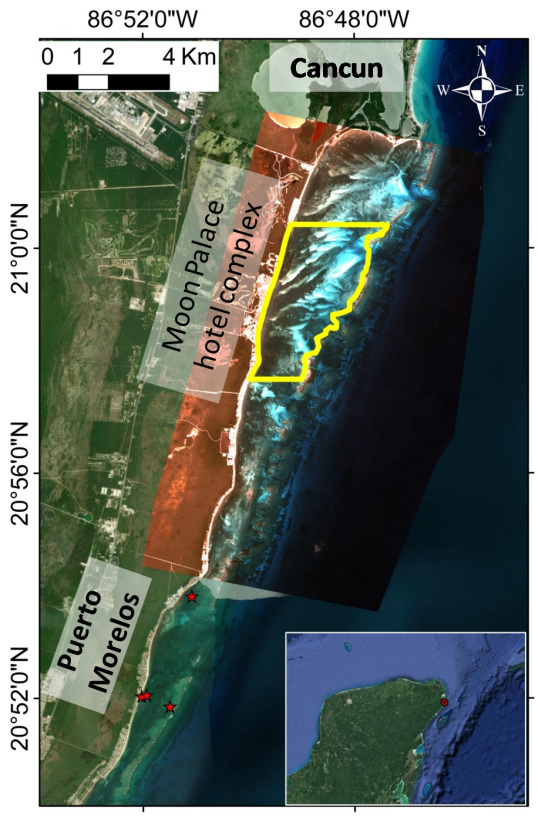

FIGURE 1
Study area (yellow outline) and long-term seagrass monitoring stations (red stars, acquired during the Caribbean Coral Reef Productivity Program (CARICOMP), from 1993 to 2016.

Nieto et al., 2018). However, the coral reef in the study area can reduce the incident wave height by up to 85% (Ruiz de Alegria-Arzaburu et al., 2013).

Surface rivers are absent (Ortíz Pérez and de la Lanza Espino, 2006) and precipitation flows to the sea through underground rivers that discharge into the sea through submarine springs (Kachadourian-Marras et al., 2020), meaning that the seawater tends to be clear, facilitating the use of satellite images for mapping the bottom of the reef lagoon.

2.2 Satellite image processing

PlanetScope satellite images from 23/01/2021, with 0% cloud cover and without sun glint, were used. These images are Ortho Scene Product, orthorectified and radiometrically-, sensor-, and geometrically corrected. Atmospheric effects were corrected using the 6SV2.1 radiative transfer code. AOD, water vapor and ozone inputs were retrieved from MODIS near-real-time data (MOD09CMA, MOD09CMG and MOD08-D3). The data of the pixels is expressed in reflectance units, with a spatial resolution of 3x3 m, radiometric resolution of 16 bits and 4 bands (PS2 sensor; B1-Blue: 455 - 515 nm; B2-Green: 500 - 590 nm; B3-Red: 590 - 670 nm; B4-Near Infra Red: 780 - 860 nm) (Planet Labs Inc, 2022).

The software SNAP from the European Space Agency (ESA) was used to preprocess and run the supervised classifications of the images. Although the images had an atmospheric correction, a dark object subtraction method was applied to each image before the construction of the mosaic, following the indications of Frazier and Hemingway (2021). A mask was applied to select a smaller area than the satellite image, of water only, from the shoreline towards the open sea. Using the Sen2Coral toolbox (Serco Italia SPA, 2019) on ESA's SNAP software, Cloud and White Cap Mask Algorithm was applied. Polygons were drawn manually over the areas to be excluded, including boat trails, structures (e.g. an anti-sargasso barrier) and other elements that the previous mask did not detect. Depth Invariant Indices (DI, also included in Sen2Coral) were calculated for water column correction, using the DI result for each pair of bands (B1+B2; B1+B3; B2+B3) as input for the supervised classifications together with B1, B2 and B3 bands. Finally, a mask was applied to select the study area only for the classifications.

2.3 Field data collection

2.3.1 Ground truth data sampling

A total of 105 points were defined, chosen based on visual assessment of the existing imagery, unsupervised classifications in combination with expert knowledge of the system, to provide an adequate representation of the variety of seagrass meadow throughout the area (Figure 2). In the field these points were located, using a GPS (Garmin, GPSMAP 65s) and they were slightly offset if necessary, to ensure that the bottom features were homogeneous within a radius of a least 10m, to consider descriptors as homogeneous within each 3x3m pixel. The survey was carried out between April 3rd and June 2nd, 2021, to define bottom and phytobenthos features used in a classification map (seed pixels). In the time between the seed pixels survey and satellite image no significant event occurred that would have affected the seagrass meadows. At each point, two photos were taken for the analysis. The first, from a 100 x 100cm quadrat to estimate the benthos coverage and the second, from a 25 x 25 cm quadrat to corroborate the phytobenthos characteristics.

Using the 25 x 25 cm quadrat, density was verified *in situ* by counting the foliar shoots for each seagrass species, and the thalli for algae (without species differentiation). The canopy height of the meadow was measured *in situ* from the sea bottom to the upper limit of the seagrass canopy with a ruler (1 mm resolution), regardless of the species. The depth of each sample point was measured using a Garmin STRIKER VIVID 5CV echo sounder. The photographs of the 100 x 100 cm quadrats were analyzed using a MATLAB coded routine to compute the percentage of sand cover, converting the images to binary following the method of Otsu (1979) (Yamamuro et al., 2002). To estimate the

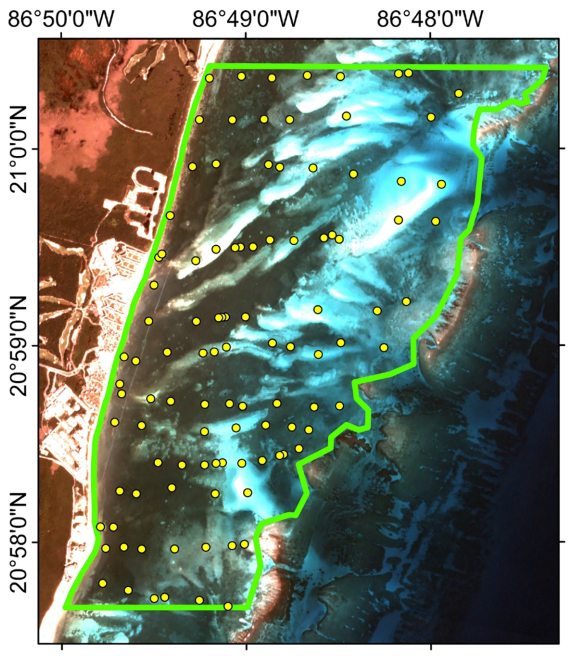

FIGURE 2
Location of the 105 points sampled to obtain ground truth data (between April 3rd and June 2nd, 2021) to be used as seed pixels in supervised classification.

abundance and percentage cover of macroalgae and seagrass, the Braun-Banquet scale was applied (Molina-Hernández and Van Tussenbroek, 2014).

2.3.2 Long-term monitoring survey

Seagrass data from four stations of the Caribbean Coral Reef Productivity Program (CARICOMP) in Puerto Morelos (1993-2016; CARICOMP, 2001; Rodríguez-Martínez et al., 2010; van Tussenbroek et al., 2014; Cortés et al., 2019) (Figure 1) were used to obtain data on the structure of the meadow, particularly to complement the data to estimate the Leaf Area Index (LAI) of the seed pixel points.

For the climax seagrass *Thalassia testudinum*, data from two periods were used, 1997 to 2000 (twice a year) and 2014 to 2016 (once a year). Six samples were taken at each of the monitored stations for each date. Foliar shoots were sampled in 10 x 20 cm quadrats to obtain the following parameters: shoot density/m^2, foliar dry weight (above-ground biomass) per m^2, the number of leaves per shoot, and the length and width of each leaf. The mean length of the 2nd youngest leaf per shoot per sample was considered to be equivalent to the height of the canopy, as this is a fully grown leaf on a shoot.

For the seagrass *Syringodium filiforme*, data from 1993 to 2000 (twice a year) and 2014 to 2016 (once a year) were used, and 3 core samples (20 cm diameter) were taken at each station to obtain leaf density per m^2 and foliar dry weight (above-ground biomass) per m^2. The lengths and diameters of the longest 10 leaves in a sample were measured. The mean length of these leaves was considered equivalent to canopy height.

Since the CARICOMP project did not monitor the pioneer seagrass *Halodule wrightii*, data on this species were obtained from Molina-Hernández and Van Tussenbroek (2014) and unpublished data from the same reef lagoon, surveyed between 2011 and 2015 (once a year) with a 11.2 cm diameter core. The data obtained were: shoot density/m^2, leaf density per m^2 and foliar dry weight (above-ground biomass) per m^2. In each foliar shoot evaluated, the length and width of the 2nd youngest leaf were recorded and the mean length in each sample was considered to be equivalent to the height of the canopy.

2.4 Leaf area index

The data obtained in the study area (points of seed pixels) were canopy height (in meters) and shoot density (shoots/m^2). As data on leaf width/diameter (W_m and D_m) and number of leaves per shoot were needed for the calculation of LAI, median data from long-term monitoring were used to obtain these parameters. For *T. testudinum* and *H. wrightii* tape-like leaves were considered, and the equation (1) was applied:

$$LAI_{estim} = Canopy\ \ height \star W_m \star Shoot\ \ Density \star \left(n^{\circ} \frac{leaves}{shoot} \right) \quad (1)$$

As *S. filiforme* leaves are cylindrical, the leaf area index was calculated as canopy height multiplied by the area of half a cylinder obtained by the median leaf diameter (D_m) (equation (2)). It was considered that each shoot contains only 1 leaf equivalent to the height of the canopy.

$$LAI_{estim} = Canopy\ \ height \star \left(\frac{\pi \star\ D_m}{2} \right) \star Shoot\ \ Density \quad (2)$$

LAI gives the total leaf area per seabed area (m^2/m^2) and is usually reported as unitless, a convention used throughout the manuscript.

To test LAI estimates, using median data of width/diameter and number of leaves per shoot, the same equations were applied to the long-term monitoring data. This estimated LAI was correlated with the leaf biomass data (for the 3 species), since the LAI must reflect the leaf biomass (Lebrasse et al., 2022). The coefficient of determination R^2 was used to verify the goodness of fit. In the case of *T. testudinum*, long-term monitoring data allow the calculation of real LAI, which is the sum of the total leaf area (total length (L) multiplied by the total width (W)) in a sample with n leaves (equation (3)).

$$LAI_{real} = \sum_{i=1}^{n} L_i \star W_i \quad (3)$$

2.5 Classification of the seed pixels

The first step in separating the seed pixels into classes was to analyze the proportional cover of sediment, algae and seagrass. Data were analyzed with Rstudio software. No normalization was applied to the data, since they are percentages. A cluster analysis using Bray-Curtis distance was performed to group the sites with similar cover characteristics. Then the seed pixels were explored, including the other parameters (seagrass density, algae density, canopy height, sediment cover and LAI). A detailed analysis was carried out for each sample point in order to establish the final class according to previous analyses, called multiparameter classes. For each point, a polygon was generated, encompassing 4-6 pixels, to classify and validate the map.

Based on the different ranges defined in the multiparameter classes, LAI and sediment cover classes were defined, to allow maps using multiparameter seeds to be compared with maps using only one parameter (such as the LAI or the percentage of sediment coverage).

2.6 Supervised classification

Two algorithms were used to produce the maps of the different classes defined, based on pixel classification. Both algorithms were used to classify the benthic communities, such as seagrasses (Lyons et al., 2011; Effrosynidis et al., 2018; Pham et al., 2019; Rende et al., 2020). The first, Maximum Likelihood (ML), classifies the data assuming a normal distribution of the pixels, and calculates the likelihood of them belonging to one class or another. The second algorithm, K-nearest neighbors (KNN), is a non-parametric method that assumes similar things exist in proximity and compares nearest neighbors to assign a pixel to a class. Within each class, 70% of the seed pixels were randomly defined for supervised classification. To verify the accuracy of the maps, the remaining 30% of the seed pixels were used as ground-truth ROIs module in ENVI 5.3 software, to generate a confusion matrix. In addition to the assessment of User's and Producer Accuracy for individual classes, this analysis estimates indicators of classification accuracy, overall accuracy and Kappa coefficient.

3 Results

3.1 Estimations using long-term monitoring data

3.1.1 *Thalassia testudinum*

The median leaf width of all CARICOMP samples (W_m) was 0.94 cm ($IC_{95\%}$ 0.02 cm) and the median number of leaves per shoot was 1.89 ($IC_{95\%}$ 0.04). The linear regression between the real LAI values and the above ground biomass (Figure 3A) showed a high correlation (R^2 = 0.95).

The linear regression between the real LAI and the estimated LAI (determined from mean shoot density and canopy height) showed a strong correlation (R^2 = 0.71) (Figure 3B). Although the estimated LAI is slightly underestimated, it was considered sufficiently precise to estimate the LAI of seed samples.

3.1.2 *Syringodium filiforme*

The median leaf diameter (D_m) of all CARICOMP samples was 1.3 mm ($IC_{95\%}$ 0.02 mm). Using these data, the LAI was estimated applying the equation (2). Unfortunately, there were not enough data to calculate the real LAI for this species and compare it with the estimated LAI. Nevertheless, correlation of the linear regression between the estimated LAI and above ground biomass was very strong (Figure 3C, R^2 = 0.91) showing that the estimate of the LAI closely represents above ground biomass.

3.1.3 *Halodule wrightii*

The median leaf width of all samples (W_m) was 0.87 mm ($IC_{95\%}$ 0.05 mm) and the median number of leaves per shoot was 2.0 ($IC_{95\%}$ 0.1). The estimated LAI, using equation (1), was compared with above ground biomass by a linear regression (Figure 3D).

3.2 General characterization of the seed pixels

The species of seagrasses analyzed were those commonly found in the Mexican Caribbean, *T. testudinum*, *S. filiforme* and *H. wrightti*. The general characteristics of depth, seagrass shoot density, canopy height, seagrass estimated LAI, algae density and sediment cover percentage, for all the points sampled, are shown in Supplementary Figure 1.

The depth of the sample points varied between 0.9 and 7.8 m. The highest shoot densities were found in an *H. wrightii* monospecific meadow near the coast (6528 shoots/m^2), and in *S. filiforme*-dominated meadows (over 3000 shoots/m^2). The highest density of *T. testudinum* was found in a monospecific meadow near the coast (1920 shoots/m^2). Canopy height showed great variation (4 - 50 cm). In some points quite high densities of algae were seen (more than 1000 thalli/m^2).

In terms of shoot density, *S. filiforme* dominated (in ~70% of the samples with seagrass, Figure 4A). However, in terms of estimated LAI, *T. testudinum* dominates in ~ 74% of the samples with seagrass (Figure 4B). Nevertheless, the contribution of *S. filiforme* in the total LAI is important, dominating in 16% of the samples (15 of the 93 points with seagrass had over 50% LAI) and contributing to over 15% of the LAI in an additional 45% of the samples (42 of the 93 points with seagrass).

A good correlation between LAI and sediment cover was found (logarithmic, R^2 = 0.79, Figure 5).

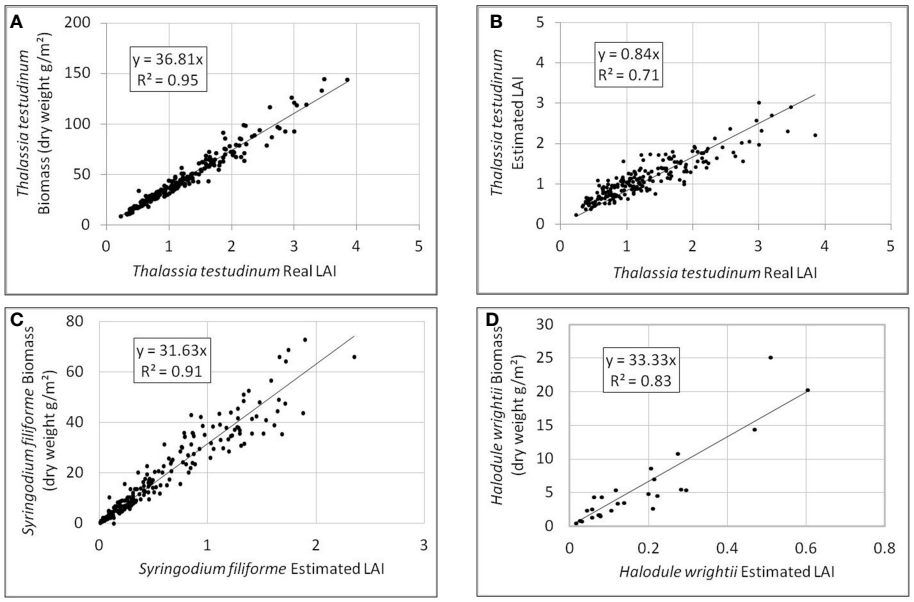

FIGURE 3
Relationships to verify the estimation of LAI. For *Thalassia testudinum* data (*n* data = 206) **(A)** real LAI vs above-ground biomass; **(B)** real LAI vs estimated LAI (using fixed values of leaf width (0.94 cm) and number of leaves/shoot (1.89). For the other species, relationship between estimated LAI and above-ground biomass for: **(C)** *Syringodium filiforme* (*n* data = 215); **(D)** *Halodule wrightii* (*n* data = 26).

3.3 Characterization of classes

For the study area, four multiparameter classes of bottom cover were defined through the cluster analysis (Supplementary Figure 2). Taking into consideration the density of seagrass and algae (green, brown, red and cyanophytes), canopy height and estimated LAI, 8.6% of the seeds (9 seeds) changed to another, more accurate, class cluster. The separation of species in the class definition process was not feasible, mainly because the seagrass meadows of this study area were usually mixed albeit with differing specific dominance, and in addition species had similar spectral signatures (Thorhaug et al., 2007; Hedley et al., 2017).

The classes and their characteristics (Figures 6, 7) were:

i. C1 (Dense seagrasses) seagrass beds, mainly *T. testudinum* and *S. filiforme*, with high density (average 2598 shoots/m^2) and relatively higher canopy height (between 12 and 50 cm; average 27 cm), with none or few algae (average density of 292 thalli/m^2). The mean estimated LAI was 3.4 ± 0.4 (95% CI). Average sediment coverage was 10%.
ii. C2 (Dense mixed vegetation) seagrass density was slightly lower than class C1 (mean 1716 shoots/m^2), as was canopy height (between 9 and 23 cm; mean 15 cm), with slightly higher density of algae with an average of 578 thalli/m^2. Mean sediment coverage was 24%, and mean estimated LAI of seagrasses was 1.5 ± 0.3.
iii. C3 (Low density seagrasses and algae) with measured seagrass density of 804 shoots/m^2 and algae density of 331 thalli/m^2. The canopy height between 7 and 17 cm (average 12 cm) and the estimated LAI was 0.8 ± 0.2. The sediment was more exposed, with an average coverage of 50%.
iv. C4 (Sediment) bottoms with very low seagrass or algae coverage, average sediment coverage of 96%. Occasionally, vegetation was present, usually *H. wrightii* with a mean LAI (± 95% CI) of 0.05 ± 0.06.

To compare the different seed class criteria, the classes using LAI and sediment cover data were defined based on the value ranges of each parameter (Table 1) verified in multiparameter classes, for the upper and lower quartiles (Figure 6).

3.4 Supervised classification

The classified maps obtained with the multiparameter criteria are presented in Figure 8, and visually, the differences obtained by the two different classification algorithms were minimal (Table 2). The accuracy of both maps is very high (~90%), although the K-nearest neighbors (KNN) algorithm is more accurate than Maximum likelihood (ML), since KNN gave

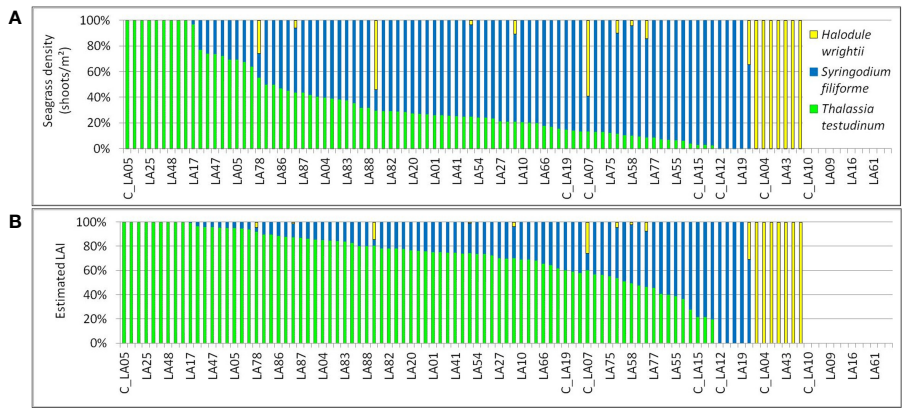

FIGURE 4
Percentages of seagrass species found in the study area, based on: **(A)** recorded density; and **(B)** estimated LAI.

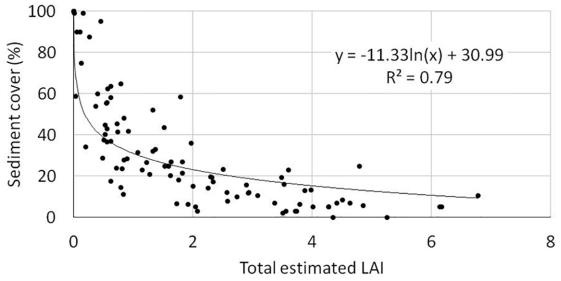

FIGURE 5
Relationship between total estimated LAI and bottom sediment cover (n=105).

higher values of overall accuracy (91.05%), Kappa (0.88) and user accuracy (77-97%).

When evaluating the confusion matrix, class C2 presented the lowest probability that a pixel belonged to this class (user's accuracy =77% and 69% respectively for KNN and ML), erroneously including pixels that corresponded to class C1 or C3. Algorithms misclassified class C3 as C2 for most pixels (producer accuracy =79% and 64% respectively for C3 for KNN and ML).

When the classification was carried out using the seeds only with sediment cover or LAI data, the overall accuracy of the maps was lower (~70% and ~80%, respectively) than using multiparameter seeds. The algorithms were not able to correctly classify the intermediate classes (C2.1; C3.1; C2.2 and C3.2), as indicated by less than 45% of producer accuracy (Table 3 for KNN algorithm and Supplementary Table 1 for ML algorithm). The accuracy of each class in the maps, indicated by the user accuracy, also had lower values than the multiparameter map. The classification, using seeds determined by the percentage of sediment, seems to overestimate class C4.2, classifying mainly C3.2 as C4.2 (e.g. user accuracy = 82% for C4.2, KNN algorithm, Table 3). Figure 9 shows the comparison between the map obtained with multiparameter seeds, LAI seeds and sediment cover seeds, using the most accurate KNN algorithm and the classes were better defined with the multiparameter seeds. Classification maps for sediment and LAI seeds, using the ML algorithm, are presented in Supplementary Figure 3.

3.5 Foliar biomass

Approximate foliar biomass was calculated, as LAI map application example. Foliar biomass was derived from linear fit equations of dry biomass as a function of LAI, per species (Figures 3A, C, D) at each of the seed points (Supplementary Figure 1). From the classification map, based on LAI data (Figure 9 and Supplementary Figure 3), the total area of each class was obtained and the mean value of biomass for each class was applied to estimate the leaf biomass of the study area (Table 4). The results indicate that there are approximately 670-710 tons (dry weight) of seagrass biomass above ground in the study area (12.5 km^2).

4 Discussion and conclusions

The spatial information obtained from mapping seagrass characteristics, using satellite images, is useful in coastal management and in decision making. Several scientific articles have published maps of seagrass cover obtained using satellite images (e.g. Roelfsema et al., 2009; Baumstark et al., 2013; Hossain et al., 2015; Coffer et al., 2020; Fauzan et al., 2021). In

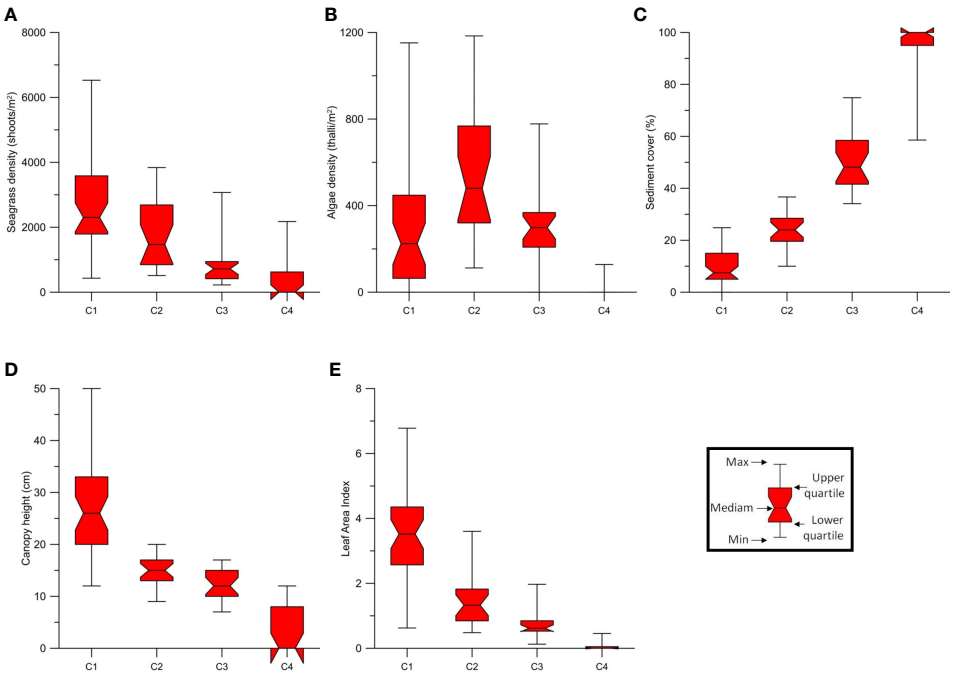

FIGURE 6
Characteristics of each multiparameter classes C1 (Dense seagrasses), C2 (Dense mixed vegetation), C3 (Low density seagrasses and algae) and C4 (Sediment) relative to: **(A)** seagrass density; **(B)** Algae density; **(C)** Sediment cover; **(D)** Seagrass canopy height; **(E)** Estimated Leaf Area Index (LAI).

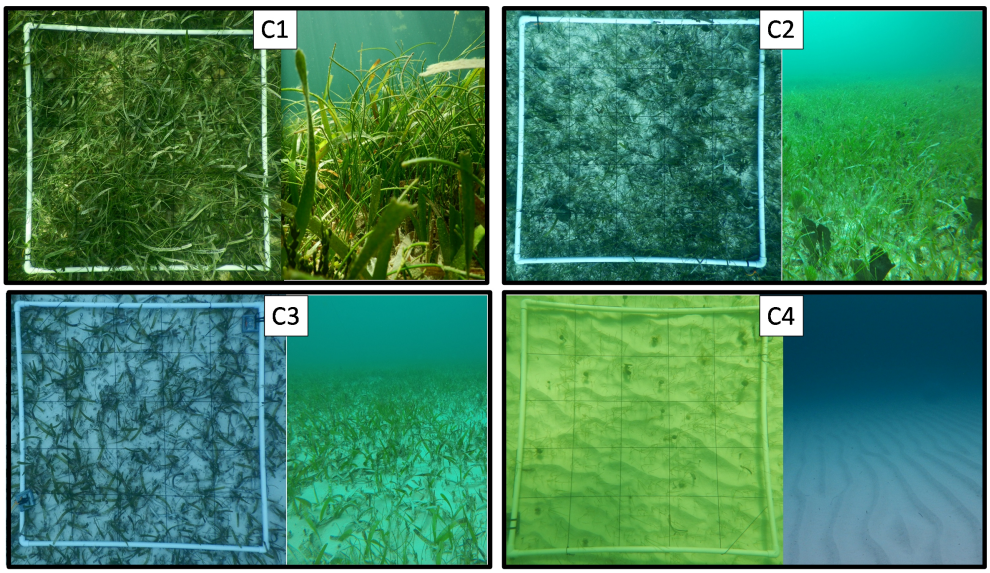

FIGURE 7
Examples of each multiparameter classes: C1 (Dense seagrasses), C2 (Dense mixed vegetation), C3 (Low density seagrasses and algae) and C4 (Sediment).

TABLE 1 Value range of LAI and sediment cover to define the classes.

LAI classes		Sediment cover classes	
Class code	**LAI range**	**Class code**	**Sediment cover range**
C1.1	≥ 2.1	C1.2	≤ 15%
C2.1	2 – 0.9	C2.2	15.1 – 30%
C3.1	0.8 – 0.5	C3.2	30.1 – 60%
C4.1	≤ 0.4	C4.2	≥ 60.1%

marine ecosystems, the use of PlanetScope satellite imagens has become a powerful tool for obtaining information about landscape characteristics and spatio temporal changes (Kim et al., 2015; Purnamasari et al., 2021). This is the first time that PlanetScope images were used to obtain maps of the mixed seagrass meadows in the Caribbean. These images have high spatial (3x3 m) and temporal resolution (daily) which is an advantage in detecting the spatio-temporal variability of coastal ecosystems, such as seagrass meadows (Wicaksono and Hafizt, 2013; Wicaksono and Lazuardi, 2018; Schill et al., 2021). Nevertheless, it is important to perform a detailed pre-selection of the scenes before analyzing the images (segmentation, classifications, indexes, etc.) and pre-processing, to overcome deficiencies in the products, for example, variation in radiometric and geometric quality (Frazier and Hemingway, 2021; Wicaksono et al., 2022). In this study, with PlanetScope images it was possible to classify four different types of bottoms covered with seagrass meadows. Seagrass meadows are often classified in only one or two categories; i.e. absent/present, as obtaining high-resolution images is difficult, or because the studies focus on mapping the coral reef system (Goodman et al., 2013; Wicaksono and Hafizt, 2013; Schill et al., 2021). This means that the complexity and variability of these ecosystems are lost and therefore, so too, the possibility of understanding more complex biophysical functions on seagrass meadows.

There are few articles that have included more complex parameters in mapping, such as LAI biomass or composition (Phinn et al., 2008; Dierssen et al., 2010; Wicaksono and Hafizt, 2013). No scientific publications on seagrass mapping using multiparameter-defined classes have been found. The multiparameter approach for the mixed, multi-specific meadow described here, allowed a more precise mapping of the meadow characteristics (such as shoot density and canopy height), important for further understanding of the seagrass landscapes, as well as the influence of extensive seagrass meadows on local biogeochemical, such as diurnal pH and O_2 fluctuations (Berg et al., 2019; James et al., 2020) or organic carbon storage (López-Mendoza et al., 2020). This map also should provide data sets to support studies for understanding the influence of different seagrass/bottom classes in the local hydrodynamics, since these parameters can influence the friction and drag force exerted by seagrasses on the propagation of waves and currents and on sediment transport (Fonseca and Cahalan, 1992; Mendez and Losada, 2004; Chen et al., 2007; Paul et al., 2012). In the study area, it was possible to define four bottom classes with different characteristics (Figures 6, 7). These classes

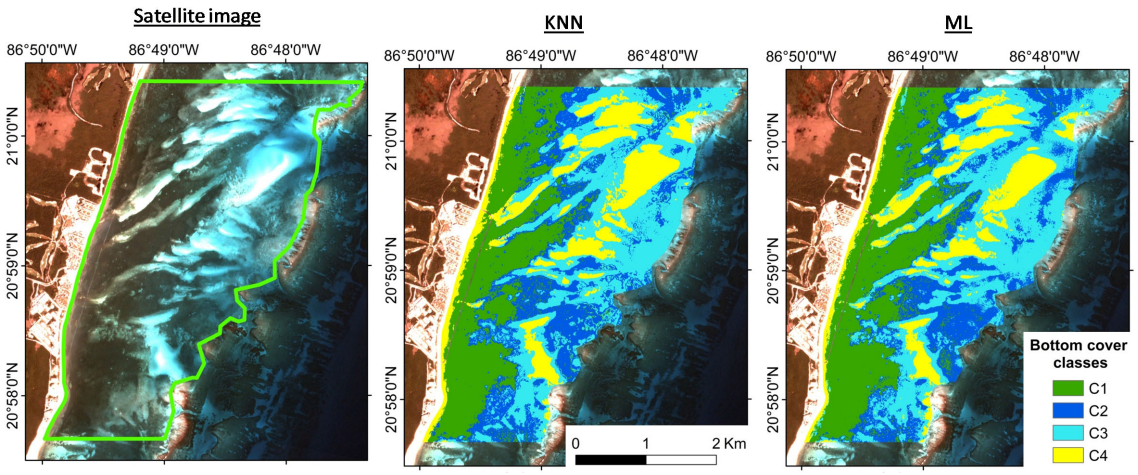

FIGURE 8
Supervised classification results obtained with multiparameter seeds, using K-nearest neighbors (KNN) and Maximum likelihood (ML) algorithms.

TABLE 2 Confusion matrix obtained as result of supervised classification using multiparameter seeds applying K-nearest neighbors and Maximum likelihood algorithms.

K-nearest neighbors

	Reference class					
Map class	C1	C2	C3	C4	total	User's accuracy (%)
C1	105	5	4	0	114	92
C2	9	65	10	0	84	77
C3	0	2	**52**	0	54	96
C4	4	0	0	124	128	97
total	118	72	66	124	380	
Producer accuracy (%)	89	90	79	100		
Overall Accuracy (%)	91.05					
Kappa	0.88					

Maximum likelihood

	Reference class					
Map class	C1	C2	C3	C4	total	User's accuracy (%)
C1	113	1	0	0	114	99
C2	3	59	24	0	86	69
C3	0	12	42	7	61	69
C4	2	0	0	117	119	98
total	118	72	66	124	380	
Producer accuracy (%)	96	82	64	94		
Overall Accuracy (%)	87.11					
Kappa	0.82					

were defined based on seagrass, algae and sediment cover data mainly, but also on the density of seagrasses and algae, canopy height and the LAI at each point. This definition, to a certain extent, depended on the local characteristics of the seagrasses, and has to be determined separately for meadows in different settings or environments, but the accuracy of the maps was high, and the map provided spatially explicit data on general meadow structure, in addition to cover.

The determination of real LAI and foliar biomass requires destructive sampling. Median values of leaf width/diameter, number of leaves per shoot, and the relationship between LAI and foliar biomass, obtained from long-term monitoring data, can be used for a reasonably reliable estimate of LAI and leaf biomass based only on shoot density per species and canopy height, which can be obtained in a non-destructive manner. The estimated LAI of *Thalassia testudinum*, from median data of leaves width, median number of leaves per m^2, shoot density and canopy height, compared well to the actual LAI (Figure 3B). However, such detailed verification was not possible for *Syringodium filiforme* and *Halodule wrightii*, but the good relationship between dry foliar biomass and estimated LAI (Figures 3C, D) indicated that the estimation is likely a good one, as LAI and biomass are usually closely related (Lebrasse et al., 2022). Dierssen et al. (2010) found a strong correlation between LAI and seagrass shoot density for meadows in the Bahama Banks (with R^2 0.83). To prove the influence of seagrass density in the variability of real LAI, this was examined for CARICOMP data (for *T. testudinum*, Supplementary Figure 4), but their relationship were weak. The lengths of the leaves greatly influence LAI and this must be taken into account, especially when the lengths vary greatly in the target area, as is the case in this study (van Tussenbroek, 1995). Another important point to consider is that *S. filiforme* was present at almost all seed pixel stations and, despite its high density, its LAI is lower than that of *T. testudinum*. In other words, in a mixed meadow, the canopy height, shoot density and estimation must be considered for each species, separately, to obtain a reliable estimation of LAI. It is worth emphasizing that a good inverse relationship (logarithm) has been found between LAI and the percentage of sediment cover. Using this relationship would help to estimate the LAI at the community level, similar to the work done by Wicaksono and Hafizt (2013). However, the percentage of sediment cover can also be influenced by the cover of algae or organic matter on the bottom, and may not reflect the LAI of seagrass alone.

In the study area, *T. testudium* dominated when considering LAI (and foliar biomass), but *S. filiforme* had the highest shoot density (Figure 4). *T. testudinum* has the greatest resistance to

TABLE 3 Confusion matrix obtained with KNN supervised classification, for different seed criteria.

LAI seeds

	Reference class					
Map class	C1.1	C2.1	C3.1	C4.1	total	User's accuracy (%)
C1.1	96	16	21	0	133	72
C2.1	19	29	21	0	69	42
C3.1	5	29	38	1	73	52
C4.1	4	0	22	317	343	92
total	124	74	102	318	618	
Producer accuracy (%)	77	39	37	100		
Overall Accuracy (%)	77.67					
Kappa	0.65					

Sediment cover seeds

	Reference class					
Map class	C1.2	C2.2	C3.2	C4.2	total	User's accuracy (%)
C1.2	87	40	8	0	135	64
C2.2	20	23	8	0	51	45
C3.2	1	21	46	18	86	53
C4.2	13	0	41	240	294	
total	121	84	103	248	566	
Producer accuracy (%)	72	27	45	93		
Overall Accuracy (%)	69.96					
Kappa	0.55					

hurricane events, and it is most effective in providing services such as coastal stabilization, due to its deep root structure and large biomass above, and below ground (van Tussenbroek, 2011; van Tussenbroek et al., 2014). However, the relative importance of this species is decreasing in many areas, including the study area, due to ongoing eutrophication or increasing turbidity (van Tussenbroek, 2011; van Tussenbroek et al., 2014). In the study area, groundwater discharges through submarine springs (Carruthers et al., 2005; Hernández-Terrones et al., 2011) and the massive sargasso influxes (van Tussenbroek et al., 2017) are of special concern. The maps obtained in this study provide baseline information on the seagrass meadows, to document possible changes in the meadow due to environmental pressures. This type of monitoring is important, as such changes can bring serious local consequences, such as lower resilience to hurricanes and major storms, as well as changes in the associated biota. Increasing dominance of less robust species, such as *S. filiforme* (with possible consequences for system structure, functioning and resilience), cannot be determined by remote sensing alone. The study by Hedley et al. (2021) carried out in the same system supposed a *T. testudinum* dominated vegetation, which is still correct, but may be changing in the future due to continuing pressures on this system. This only exemplifies the need for continuous ground truthing, as already proposed by Neckles et al. (2012).

The multiparameter maps obtained through the supervised classification method showed that class C1 (Dense seagrasses) was closer to the coast, interrupted by bare areas of submarine dunes (class C4). As they migrate inland, these submarine dunes bury the seagrass meadows. Some areas of these submarine dunes, as well as their edges, were covered with vegetation of class 3 (low density seagrasses and algae). Class C3 vegetation was also found in the shallow (up to 4 m) back reef area, with *T. testudinum* dominating, though with reduced canopies, due to the environmental conditions, such as higher hydrodynamic forcing and lower nutrient contents of the sediments (van Tussenbroek, 1995). A narrow strip of unvegetated seabed (C4 class), was found closest to the shore, landward of the dense seagrass (C1 class). This abrupt change from bare soil to highly productive seagrass beds at the shore was observed in the study area by Enríquez et al. (2019) and is thought to be a consequence of sargasso brown tides (van Tussenbroek et al., 2017). The loss of dense nearshore meadows probably means further destabilization of the coast (James et al., 2019). Class C2 was found in the transition zones between class C1 and C3 areas, or near the barrier reef at greater depths (average 6m), where dense seagrasses and algae occurred. Macroalgae were mostly ignored in the classifications, due to the difficulty of distinguishing them with remote sensing techniques (Wicaksono and Lazuardi, 2018). Nevertheless, using the multiparameter method and a detailed analysis of the seed pixels, it was possible to obtain a

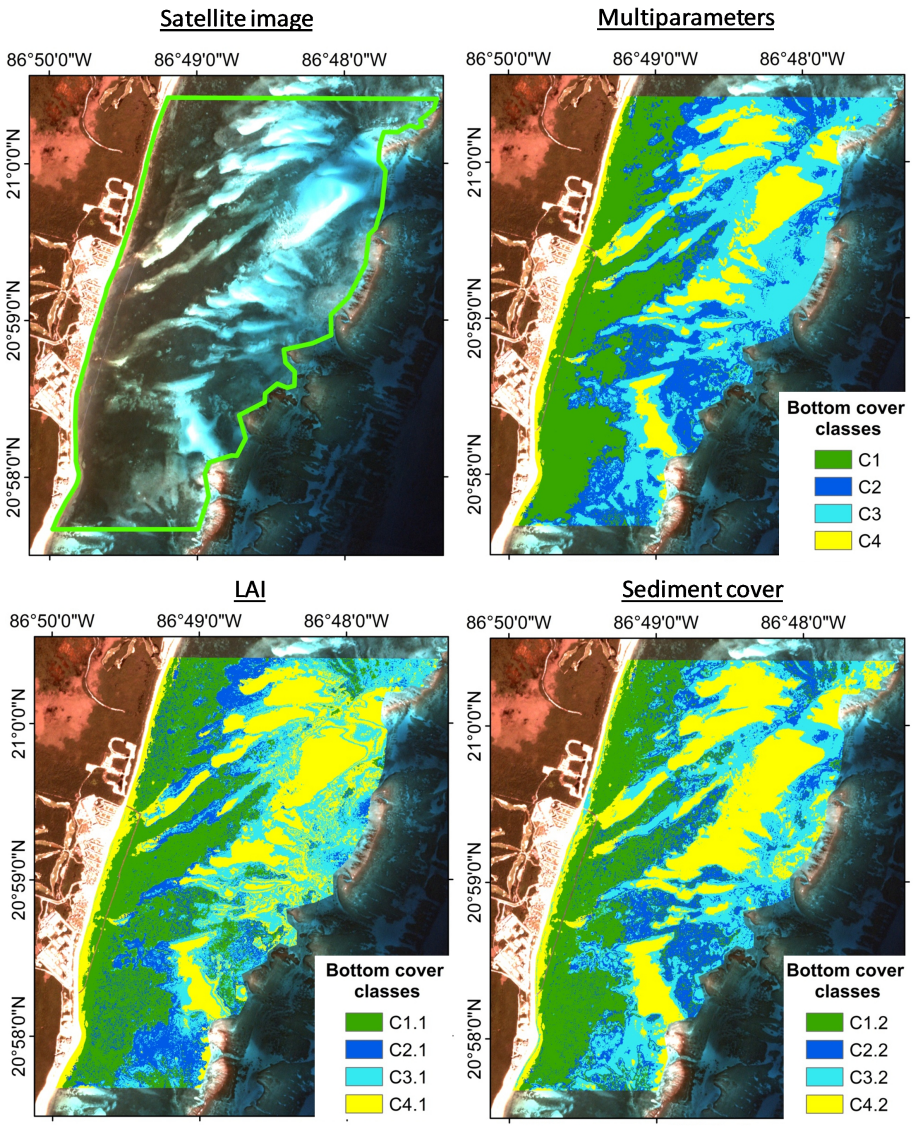

FIGURE 9
Comparison of supervised classification results obtained with multiparameter seeds, LAI seeds, and sediment cover seed, using the KNN algorithm.

good classification with low class confusion (Table 2). Further incorporation of macroalgae in classification may be useful in future monitoring, as changes in macroalgae cover could indicate disturbances in this community (van Tussenbroek, 2011; van Tussenbroek et al., 2017), with consequences on the stabilization of sediments and coastal protection from hurricanes (Cruz-Palacios and van Tussenbroek, 2005).

Classification maps that use only sediment cover, or LAI values, proved to be less accurate than the multiparameter-based map, but their accuracy was still acceptable. They have the advantage of using ranges to define classes, making them less subjective, but the algorithms do not make clear the class separations with these ranges, mainly for intermediate classes (2 and 3), which presented low values of producer accuracy (< 50%). These maps can be useful for monitoring seagrasses, and in helping to define suitable areas for restoration projects. An example of its use is the foliar biomass estimation did for the study area, based on the LAI class map and the relationships of LAI with biomass (Table 4). An above ground biomass of 700 tons implies 245 tons of organic carbon stock in the leaves alone, using the conversion factor (from dry weight to organic carbon) of 0.35 proposed by Fourqurean et al. (2012). As they comprise on average only 11.1% of total biomass in the area (CARICOMP data), the total estimated organic carbon stock in live seagrass tissue was in total 6300 tons in the study area (12.5 km^2), without considering the likely larger organic carbon stock in the

TABLE 4 Estimation of seagrass foliar biomass in the study area.

LAI classes	Mean biomass value (dry weight g/m^2)	Area (m^2) (KNN map)	Total foliar biomass(kg) estimated in the KNN map	Area (m^2) (ML map)	Total foliar biomass(kg) estimated in ML map
C1.1	131.15	3,810,114	499,696,451	3,422,142	448,813,923
C2.1	53.77	2,119,428	113,961,644	2,078,091	111,738,953
C3.1	22.97	3,249,054	74,630,770	3,760,587	86,380,683
C4.1	5.94	3,308,310	19,651,361	3,226,086	19,162,951
Total			707,940,226		666,096,511

sediments (López-Mendoza et al., 2020), showing that higher precision maps, can aid in obtaining better estimates of organic carbon stocks in seagrass meadows.

The presented tool in this study, to determine seagrass meadows structure (cover percentages of seagrass/algae/sediment, seagrass shoot densities, canopy heights and LAI) and its distribution along the coast, based on satellite images, has immediate application in understanding the hydrodynamics associated with seagrass meadows. Further information on the role of seagrass in controlling wave energy, when coupled with specific local data on its distribution allows field measurements of waves and currents to be better planned. Similarly, hydrodynamic numerical modelling may be more realistic and accurate if the proper drag and damping coefficient maps reproduce accurately the seagrass distribution. If a time series of satellite images exist, then the maps can also be updated in time using long-term numerical runs. The tool is also useful for coastal management, as coastal protection strategies depend on knowledge of the submerged ecosystems. Nature-based solutions, often involving seagrass restoration, as well as ecosystem conservation, will benefit from spatial explicit information, for proper planning as well as monitoring of effectiveness of implemented measures.

Data availability statement

The raw data supporting the conclusions of this article will be made available by the authors, without undue reservation.

Author contributions

LA, RS, EM and BT contributed to conception of the study. LA and SVA-M performed the field work and data analysis. BT provided historical data from long-term monitoring of seagrasses. LA wrote the first draft of the manuscript. All authors contributed to the article and approved the submitted version.

Funding

The study received financial support of DGAPA (Dirección General de Asuntos del Personal Académico, UNAM, Project No. PAPIIT AG100321), the "Newton Fund Impact Scheme CONACYT-British Council 2019" - Project 318671 "Technology development towards sustainable marine current energy harvesting for coastal communities in Mexico" and CEMIE-Océano (CONACYT -SENER-Fondo de Sustentabilidad Energética project: FSE-2014-06-249795). The first author received a Postdoctoral Grant of DGAPA-UNAM.

Acknowledgments

Thanks to the Academic Service for Meteorological and Oceanographic Monitoring (SAMMO) of UNAM, especially to Edgar Escalante and Miguel Gómez Reali, and Guadalupe Barba-Santos for technical support. Thank you also to Moon Palace Resort for facilitating this investigation.

Conflict of interest

The authors declare that the research was conducted in the absence of any commercial or financial relationships that could be construed as a potential conflict of interest.

Publisher's note

All claims expressed in this article are solely those of the authors and do not necessarily represent those of their affiliated organizations, or those of the publisher, the editors and the reviewers. Any product that may be evaluated in this article, or claim that may be made by its manufacturer, is not guaranteed or endorsed by the publisher.

Supplementary material

The Supplementary Material for this article can be found online at: https://www.frontiersin.org/articles/10.3389/fmars.2022.1063007/full#supplementary-material

References

Barbier, E. B., Hacker, S. D., Kennedy, C., Koch, E. W., Stier, A. C., and Silliman, B. R. (2011). The value of estuarine and coastal ecosystem services. *Ecol. Monogr.* 81, 169–193. doi: 10.1890/10-1510.1

Baumstark, R., Dixon, B., Carlson, P., Palandro, D., and Kolasa, K. (2013). Alternative spatially enhanced integrative techniques for mapping seagrass in florida's marine ecosystem. *Int. J. Remote Sens.* 34, 1248–1264. doi: 10.1080/01431161.2012.721941

Berg, P., Delgard, M. L., Polsenaere, P., McGlathery, K. J., Doney, S. C., and Berger, A. C. (2019). Dynamics of benthic metabolism, O2, and pCO2 in a temperate seagrass meadow. *Limnol. Oceanogr.* 64, 2586–2604. doi: 10.1002/lno.11236

CARICOMP (2001). *CARICOMP methods manual, levels 1 and 2* (St. Petersburg Florida, U.S.A: CARICOMP Data Management Center: Centre for Marine Sciences, University of the West Indies, Mona, Kingston, Jamaica, and Florida Institute of Oceanography, University of South Florida).

Carruthers, T. J. B., Van Tussenbroek, B. I., and Dennison, W. C. (2005). Influence of submarine springs and wastewater on nutrient dynamics of Caribbean seagrass meadows. *Estuar. Coast. Shelf. Sci.* 64, 191–199. doi: 10.1016/j.ecss.2005.01.015

Chen, S. N., Sanford, L. P., Koch, E. W., Shi, F., and North, E. W. (2007). A nearshore model to investigate the effects of seagrass bed geometry on wave attenuation and suspended sediment transport. *Estuaries. Coasts.* 30, 296–310. doi: 10.1007/BF02700172

Coffer, M. M., Schaeffer, B. A., Zimmerman, R. C., Hill, V., Li, J., Islam, K. A., et al. (2020). Performance across WorldView-2 and RapidEye for reproducible seagrass mapping. *Remote Sens. Environ.* 250, 11203. doi: 10.1016/j.rse.2020.112036

Coronado, C., Candela, J., Iglesias-Prieto, R., Sheinbaum, J., López, M., and Ocampo-Torres, F. J. (2007). On the circulation in the Puerto morelos fringing reef lagoon. *Coral. Reefs.* 26, 149–163. doi: 10.1007/s00338-006-0175-9

Cortés, J., Oxenford, H. A., van Tussenbroek, B. I., Jordán-Dahlgren, E., Cróquer, A., Bastidas, C., et al. (2019). The CARICOMP network of caribbean marine laboratories (1985-2007): History, key findings, and lessons learned. *Front. Mar. Sci.* 5, 1–18. doi: 10.3389/fmars.2018.00519

Cruz-Palacios, V., and van Tussenbroek, B. I. (2005). Simulation of hurricane-like disturbances on a Caribbean seagrass bed. *J. Exp. Mar. Bio. Ecol.* 324, 44–60. doi: 10.1016/j.jembe.2005.04.002

de Almeida, L. R., Silva, R., and Martínez, M. L. (2022). The relationships between environmental conditions and parallel ecosystems on the coastal dunes of the Mexican Caribbean. *Geomorphology* 397, 108006. doi: 10.1016/j.geomorph.2021.108006

Dierssen, H. M., Zimmerman, R. C., Drake, L. A., and Burdige, D. (2010). Benthic ecology from space: Optics and net primary production in seagrass and benthic algae across the great bahama bank. *Mar. Ecol. Prog. Ser.* 411, 1–15. doi: 10.3354/meps08665

Effrosynidis, D., Arampatzis, A., and Sylaios, G. (2018). Seagrass detection in the mediterranean: A supervised learning approach. *Ecol. Inform.* 48, 158–170. doi: 10.1016/j.ecoinf.2018.09.004

Enríquez, S., Olivé, I., Cayabyab, N., and Hedley, J. D. (2019). Structural complexity governs seagrass acclimatization to depth with relevant consequences for meadow production, macrophyte diversity and habitat carbon storage capacity. *Sci. Rep.* 9, 1–14. doi: 10.1038/s41598-019-51248-z

Escudero-Castillo, M., Felix-Delgado, A., Silva, R., Mariño-Tapia, I., and Mendoza, E. (2018). Beach erosion and loss of protection environmental services in cancun, Mexico. *Ocean. Coast. Manage.* 156, 183–197. doi: 10.1016/j.ocecoaman.2017.06.015

Escudero, M., Reguero, B. G., Mendoza, E., Secaira, F., and Silva, R. (2021). Coral reef geometry and hydrodynamics in beach erosion control in north quintana roo, Mexico. *Front. Mar. Sci.* 8. doi: 10.3389/fmars.2021.684732

Fauzan, M. A., Wicaksono, P., and Hartono, (2021). Characterizing derawan seagrass cover change with time-series sentinel-2 images. *Reg. Stud. Mar. Sci.* 48, 102048. doi: 10.1016/j.rsma.2021.102048

Fonseca, M. S., and Cahalan, J. A. (1992). A preliminary evaluation of wave attenuation by four species of seagrass. *Estuar. Coast. Shelf. Sci.* 35, 565–576. doi: 10.1016/S0272-7714(05)80039-3

Fourqurean, J. W., Duarte, C. M., Kennedy, H., Marbà, N., Holmer, M., Mateo, M. A., et al. (2012). Seagrass ecosystems as a globally significant carbon stock. *Nat. Geosci.* 5, 505–509. doi: 10.1038/ngeo1477

Frazier, A. E., and Hemingway, B. L. (2021). A technical review of planet smallsat data: Practical considerations for processing and using PlanetScope imagery. *Remote Sens.* 13, 3930. doi: 10.3390/rs13193930

Gambi, M., Nowell, A., and Jumars, P. (1990). Flume observations on flow dynamics in zostera marina (eelgrass) beds. *Mar. Ecol. Prog. Ser.* 61, 159–169. doi: 10.3354/meps061159

Goodman, J. A., Purkis, S. J., and Phinn, S. R. (2013). *Coral reef remote sensing.* Eds. J. A. Goodman, S. J. Purkis and S. R. Phinn (Dordrecht: Springer Netherlands). doi: 10.1007/978-90-481-9292-2

Hedley, J. D., Russell, B. J., Randolph, K., Pérez-Castro, M., Vásquez-Elizondo, R. M., Enríquez, S., et al. (2017). Remote sensing of seagrass leaf area index and species: The capability of a model inversion method assessed by sensitivity analysis and hyperspectral data of Florida bay. *Front. Mar. Sci.* 4. doi: 10.3389/fmars.2017.00362

Hedley, J. D., Velázquez-Ochoa, R., and Enríquez, S. (2021). Seagrass depth distribution mirrors coastal development in the Mexican Caribbean – an automated analysis of 800 satellite images. *Front. Mar. Sci.* 8. doi: 10.3389/fmars.2021.733169

Hernández-Terrones, L., Rebolledo-Vieyra, M., Merino-Ibarra, M., Soto, M., Le-Cossec, A., and Monroy-Ríos, E. (2011). Groundwater pollution in a karstic region (NE yucatan): Baseline nutrient content and flux to coastal ecosystems. *Water. Air. Soil pollut.* 218, 517–528. doi: 10.1007/s11270-010-0664-x

Hossain, M. S., Bujang, J. S., Zakaria, M. H., and Hashim, M. (2015). Application of landsat images to seagrass areal cover change analysis for lawas, terengganu and kelantan of Malaysia. *Cont. Shelf. Res.* 110, 124–148. doi: 10.1016/j.csr.2015.10.009

James, R. K., Silva, R., Van Tussenbroek, B. I., Escudero-Castillo, M., Mariño-Tapia, I., Dijkstra, H. A., et al. (2019). Maintaining tropical beaches with seagrass and algae: A promising alternative to engineering solutions. *Bioscience* 69, 136–142. doi: 10.1093/biosci/biy154

James, R. K., van Katwijk, M. M., van Tussenbroek, B. I., van der Heide, T., Dijkstra, H. A., van Westen, R. M., et al. (2020). Water motion and vegetation control the pH dynamics in seagrass-dominated bays. *Limnol. Oceanogr.* 65, 349–362. doi: 10.1002/lno.11303

Kachadourian-Marras, A., Alconada-Magliano, M. M., Carrillo-Rivera, J. J., Mendoza, E., Herrerías-Azcue, F., and Silva, R. (2020). Characterization of surface evidence of groundwater flow systems in continental Mexico. *Water* 12, 2459. doi: 10.3390/w12092459

Kim, K., Choi, J.-K., Ryu, J.-H., Jeong, H. J., Lee, K., Park, M. G., et al. (2015). Observation of typhoon-induced seagrass die-off using remote sensing. *Estuar. Coast. Shelf. Sci.* 154, 111–121. doi: 10.1016/j.ecss.2014.12.036

Koch, E. W., Barbier, E. B., Silliman, B. R., Reed, D. J., Perillo, G. M. E., Hacker, S. D., et al. (2009). Non-linearity in ecosystem services: Temporal and spatial variability in coastal protection. *Front. Ecol. Environ.* 7, 29–37. doi: 10.1890/080126

Koftis, T., Prinos, P., and Stratigaki, V. (2013). Wave damping over artificial posidonia oceanica meadow: A large-scale experimental study. *Coast. Eng.* 73, 71–83. doi: 10.1016/j.coastaleng.2012.10.007

Kovacs, E., Roelfsema, C., Lyons, M., Zhao, S., and Phinn, S. (2018). Seagrass habitat mapping: How do landsat 8 OLI, sentinel-2, ZY-3A, and worldview-3 perform? *Remote Sens. Lett.* 9, 686–695. doi: 10.1080/2150704X.2018.1468101

Lebrasse, M. C., Schaeffer, B. A., Coffer, M. M., Whitman, P. J., Zimmerman, R. C., Hill, V. J., et al. (2022). Temporal stability of seagrass extent, leaf area, and carbon storage in st. Joseph bay, Florida: A semi-automated remote sensing analysis. *Estuaries. Coasts* 45, 2082–2101. doi: 10.1007/s12237-022-01050-4

López-Mendoza, P. G., Ruiz-Fernández, A. C., Sanchez-Cabeza, J. A., van Tussenbroek, B. I., Cuellar-Martinez, T., and Pérez-Bernal, L. H. (2020). Temporal trends of organic carbon accumulation in seagrass meadows from the northern Mexican Caribbean. *CATENA* 194, 104645. doi: 10.1016/j.catena.2020.104645

Lyons, M., Phinn, S., and Roelfsema, C. (2011). Integrating quickbird multi-spectral satellite and field data: Mapping bathymetry, seagrass cover, seagrass species and change in moreton bay, Australia in 2004 and 2007. *Remote Sens.* 3, 42–64. doi: 10.3390/rs3010042

Madsen, J. D., Chambers, P. A., James, W. F., Koch, E. W., and Westlake, D. F. (2001). The interaction between water movement, sediment dynamics and submersed macrophytes. *Hydrobiologia* 444, 71–84. doi: 10.1023/A:1017520800568

Martínez, M. L., Moreno-Casasola, P., Espejel, I., Oroci, O. J., Mata, D. I., Revelo, N. R., et al. (2014). *Diagnóstico general de las dunas costeras de méxico* (Ciudad de México: SEMARNAT).

Mendez, F. J., and Losada, I. J. (2004). An empirical model to estimate the propagation of random breaking and nonbreaking waves over vegetation fields. *Coast. Eng.* 51, 103–118. doi: 10.1016/j.coastaleng.2003.11.003

Moberg, F., and Rönnbäck, P. (2003). Ecosystem services of the tropical seascape: Interactions, substitutions and restoration. *Ocean. Coast. Manage.* 46, 27–46. doi: 10.1016/S0964-5691(02)00119-9

Molina-Hernández, A. L., and Van Tussenbroek, B. I. (2014). Patch dynamics and species shifts in seagrass communities under moderate and high grazing pressure by green sea turtles. *Mar. Ecol. Prog. Ser.* 517, 143–157. doi: 10.3354/meps11068

Neckles, H. A., Kopp, B. S., Peterson, B. J., and Pooler, P. S. (2012). Integrating scales of seagrass monitoring to meet conservation needs. *Estuaries. Coasts.* 35, 23–46. doi: 10.1007/s12237-011-9410-x

Ortíz Pérez, M. A., and de la Lanza Espino, G. (2006). *Diferenciación del espacio costero de méxico: un inventario regional* (México: Instituto de Geografia UNAM).

Otsu, N. (1979). A tlreshold selection method from Gray-level histograms. *IEEE Trans. Syst. Man. Cybern.* 9, 62–66. doi: 10.1109/TSMC.1979.4310076

Paquier, A. E., Oudart, T., Le Bouteiller, C., Meulé, S., Larroudé, P., and Dalrymple, R. A. (2021). 3D numerical simulation of seagrass movement under waves and currents with GPUSPH. *Int. J. Sediment. Res.* 36, 711–722. doi: 10.1016/j.ijsrc.2020.08.003

Paul, M., Bouma, T. J., and Amos, C. L. (2012). Wave attenuation by submerged vegetation: Combining the effect of organism traits and tidal current. *Mar. Ecol. Prog. Ser.* 444, 31–41. doi: 10.3354/meps09489

Pham, T. D., Xia, J., Ha, N. T., Bui, D. T., Le, N. N., and Tekeuchi, W. (2019). A review of remote sensing approaches for monitoring blue carbon ecosystems: Mangroves, seagrasses and salt marshes during 2010–2018. *Sensors* 19, 1933. doi: 10.3390/s19081933

Phinn, S., Roelfsema, C., Dekker, A., Brando, V., and Anstee, J. (2008). Mapping seagrass species, cover and biomass in shallow waters: An assessment of satellite multi-spectral and airborne hyper-spectral imaging systems in moreton bay (Australia). *Remote Sens. Environ.* 112, 3413–3425. doi: 10.1016/j.rse.2007.09.017

Planet Labs Inc (2022) *Planet imagery products specifications*. Available at: https://assets.planet.com/docs/Planet_Combined_Imagery_Product_Specs_letter_screen.pdf (Accessed June 01, 2022).

Purnamasari, E., Kamal, M., and Wicaksono, P. (2021). Comparison of vegetation indices for estimating above-ground mangrove carbon stocks using PlanetScope image. *Reg. Stud. Mar. Sci.* 44, 101730. doi: 10.1016/j.rsma.2021.101730

Rende, S. F., Bosman, A., Di Mento, R., Bruno, F., Lagudi, A., Irving, A. D., et al. (2020). Ultra-High-Resolution mapping of *posidonia oceanica* (L.) delile meadows through acoustic, optical data and object-based image classification. *J. Mar. Sci. Eng.* 8, 647. doi: 10.3390/jmse8090647

Rioja-Nieto, R., Garza-Pérez, R., Álvarez-Filip, L., Mariño-Tapia, I., and Enríquez, C. (2018). "The Mexican Caribbean: From xcalak to holbox," in *World seas: An environmental evaluation volume I: Europe, the americas and West Africa*. Ed. C. Sheppard (London: Elsevier), 637–653. doi: 10.1016/B978-0-12-805068-2.00033-4

Rodríguez-Martínez, R. E., Ruíz-Rentería, F., van Tussenbroek, B., Barba-Santos, G., Escalante-Mancera, E., Jordán-Garza, G., et al. (2010). Environmental state and tendencies of the Puerto morelos CARICOMP site, Mexico. *Rev. Biol. Trop.* 58, 23–43. doi: 10.15517/rbt.v58i0.20039

Roelfsema, C. M., Phinn, S. R., Udy, N., and Maxwell, P. (2009). An integrated field and remote sensing approach for mapping seagrass cover, moreton bay, Australia. *J. Spat. Sci.* 54, 45–62. doi: 10.1080/14498596.2009.9635166

Ruiz de Alegria-Arzaburu, A., Mariño-Tapia, I., Enriquez, C., Silva, R., and González-Leija, M. (2013). The role of fringing coral reefs on beach morphodynamics. *Geomorphology* 198, 69–83. doi: 10.1016/j.geomorph.2013.05.013

Schaefer, R. B., and Nepf, H. (2022). Wave damping by seagrass meadows in combined wave-current conditions. *Limnol. Oceanogr.* 67, 1554–1565. doi: 10.1002/lno.12102

Schill, S. R., McNulty, V. P., Pollock, F. J., Lüthje, F., Li, J., Knapp, D. E., et al. (2021). Regional high-resolution benthic habitat data from planet dove imagery for conservation decision-making and marine planning. *Remote Sens.* 13, 4215. doi: 10.3390/rs13214215

Serco Italia SPA (2019) *Sen2Coral toolbox for coral reef monitoring, great barrier reef (version 1.1)*. Available at: https://rus-copernicus.eu/portal/wp-content/uploads/library/education/training/OCEA05_Sen2Coral_GBR_Tutorial.pdf (Accessed March 13, 2021).

Silva, R., Martínez, M. L., van Tussenbroek, B. I., Guzmán-rodríguez, L. O., Mendoza, E., and López-portillo, J. (2020). A framework to manage coastal squeeze. *Sustain* 12, 1–21. doi: 10.3390/su122410610

Soissons, L. M., van Katwijk, M. M., Peralta, G., Brun, F. G., Cardoso, P. G., Grilo, T. F., et al. (2018). Seasonal and latitudinal variation in seagrass mechanical traits across Europe: The influence of local nutrient status and morphometric plasticity. *Limnol. Oceanogr.* 63, 37–46. doi: 10.1002/lno.10611

Stratigaki, V., Manca, E., Prinos, P., Losada, I. J., Lara, J. L., Sclavo, M., et al. (2011). Large-Scale experiments on wave propagation over posidonia oceanica. *J. Hydraul. Res.* 49, 31–43. doi: 10.1080/00221686.2011.583388

Thorhaug, A., Richardson, A. D., and Berlyn, G. P. (2007). Spectral reflectance of the seagrasses: Thalassia testudinum, halodule wrightii, syringodium filiforme and five marine algae. *Int. J. Remote Sens.* 28, 1487–1501. doi: 10.1080/01431160600954662

van Tussenbroek, B. I. (1995). Thalassia testudinum leaf dynamics in a Mexican Caribbean coral reef lagoon. *Mar. Biol.* 122, 33–40. doi: 10.1007/BF00349275

van Tussenbroek, B. (2011). Dynamics of seagrasses and associated algae in coral reef lagoons dinámica de los pastos marinos y macroalgas asociadas en lagunas arrecifales. *Hidrobiológica* 21, 293–310.

van Tussenbroek, B. I., Cortés, J., Collin, R., Fonseca, A. C., Gayle, P. M. H., Guzmán, H. M., et al. (2014). Caribbean-Wide, long-term study of seagrass beds reveals local variations, shifts in community structure and occasional collapse. *PloS One* 9, e90600. doi: 10.1371/journal.pone.0090600

van Tussenbroek, B. I., Hernández Arana, H. A., Rodríguez-Martínez, R. E., Espinoza-Avalos, J., Canizales-Flores, H. M., González-Godoy, C. E., et al. (2017). Severe impacts of brown tides caused by sargassum spp. on near-shore Caribbean seagrass communities. *Mar. Pollut. Bull.* 122, 272–281. doi: 10.1016/j.marpolbul.2017.06.057

Wicaksono, P., and Hafizt, M. (2013). Mapping seagrass from space: Addressing the complexity of seagrass LAI mapping. *Eur. J. Remote Sens.* 46, 18–39. doi: 10.5721/EuJRS20134602

Wicaksono, P., and Lazuardi, W. (2018). Assessment of PlanetScope images for benthic habitat and seagrass species mapping in a complex optically shallow water environment. *Int. J. Remote Sens.* 39, 5739–5765. doi: 10.1080/01431161.2018.1506951

Wicaksono, P., Maishella, A., Lazuardi, W., and Muhammad, F. H. (2022). Consistency assessment of multi-date PlanetScope imagery for seagrass percent cover mapping in different seagrass meadows. *Geocarto. Int.* 0, 1–26. doi: 10.1080/10106049.2022.2096122

Yamamuro, M., Nishimura, K., Kishimoto, K., Nozaki, K., Kato, K., Negishi, A., et al. (2002). "Mapping tropical seagrass beds with an underwater remotely operated vehicle (ROV)" in: *Recent Advances in Marine Science and Technology*, ed. N. Saxena. (Yokosuka: Japan International Marine Science and Technology Federation).

frontiers | Frontiers in Marine Science

TYPE Original Research
PUBLISHED 13 January 2023
DOI 10.3389/fmars.2022.1096594

Check for updates

OPEN ACCESS

EDITED BY
Monica Montefalcone,
University of Genoa, Italy

REVIEWED BY
Luca Fallati,
University of Milano-Bicocca, Italy
Thanos Dailianis,
Hellenic Centre for Marine Research, Greece

*CORRESPONDENCE
Daniele Ventura
daniele.ventura@uniroma1.it

SPECIALTY SECTION
This article was submitted to Marine Ecosystem Ecology, a section of the journal Frontiers in Marine Science

RECEIVED 12 November 2022
ACCEPTED 30 December 2022
PUBLISHED 13 January 2023

CITATION
Ventura D, Grosso L, Pensa D, Casoli E, Mancini G, Valente T, Scardi M and Rakaj A (2023) Coastal benthic habitat mapping and monitoring by integrating aerial and water surface low-cost drones. *Front. Mar. Sci.* 9:1096594. doi: 10.3389/fmars.2022.1096594

COPYRIGHT
© 2023 Ventura, Grosso, Pensa, Casoli, Mancini, Valente, Scardi and Rakaj. This is an open-access article distributed under the terms of the Creative Commons Attribution License (CC BY). The use, distribution or reproduction in other forums is permitted, provided the original author(s) and the copyright owner(s) are credited and that the original publication in this journal is cited, in accordance with accepted academic practice. No use, distribution or reproduction is permitted which does not comply with these terms.

Coastal benthic habitat mapping and monitoring by integrating aerial and water surface low-cost drones

Daniele Ventura[1]*, Luca Grosso[2], Davide Pensa[2], Edoardo Casoli[1], Gianluca Mancini[1], Tommaso Valente[1], Michele Scardi[2,3] and Arnold Rakaj[2,3]

[1]Department of Environmental Biology, University of Rome "la Sapienza"-V. le dell'Università 32, Rome, Italy, [2]Experimental Ecology and Aquaculture Laboratory, Department of Biology, University of Rome Tor Vergata, Rome, Italy, [3]National Inter-University Consortium for Marine Sciences-CoNISMa, Rome, Italy

Accurate data on community structure is a priority issue in studying coastal habitats facing human pressures. The recent development of remote sensing tools has offered a ground-breaking way to collect ecological information at a very fine scale, especially using low-cost aerial photogrammetry. Although coastal mapping is carried out using Unmanned Aerial Vehicles (UAVs or drones), they can provide limited information regarding underwater benthic habitats. To achieve a precise characterisation of underwater habitat types and species assemblages, new imagery acquisition instruments become necessary to support accurate mapping programmes. Therefore, this study aims to evaluate an integrated approach based on Structure from Motion (SfM) photogrammetric acquisition using low-cost Unmanned Aerial (UAV) and Surface (USV) Vehicles to finely map shallow benthic communities, which determine the high complexity of coastal environments. The photogrammetric outputs, including both UAV-based high (sub-meter) and USV-based ultra-high (sub-centimetre) raster products such as orthophoto mosaics and Digital Surface Models (DSMs), were classified using Object-Based Image Analysis (OBIA) approach. The application of a supervised learning method based on Support Vector Machines (SVM) classification resulted in good overall classification accuracies > 70%, proving to be a practical and feasible tool for analysing both aerial and underwater ultra-high spatial resolution imagery. The detected seabed cover classes included above and below-water key coastal features of ecological interest such as seagrass beds, "banquettes" deposits and hard bottoms. Using USV-based imagery can considerably improve the identification of specific organisms with a critical role in benthic communities, such as photophilous macroalgal beds. We conclude that the integrated use of low-cost unmanned aerial and surface vehicles and GIS processing is an effective strategy for allowing fully remote detailed data on shallow water benthic communities.

KEYWORDS

SfM photogrammetry, seagrass, algal assemblages, cartography, GIS, OBIA, unmanned aerial vehicles (UAV), unmanned surface vehicles (USV)

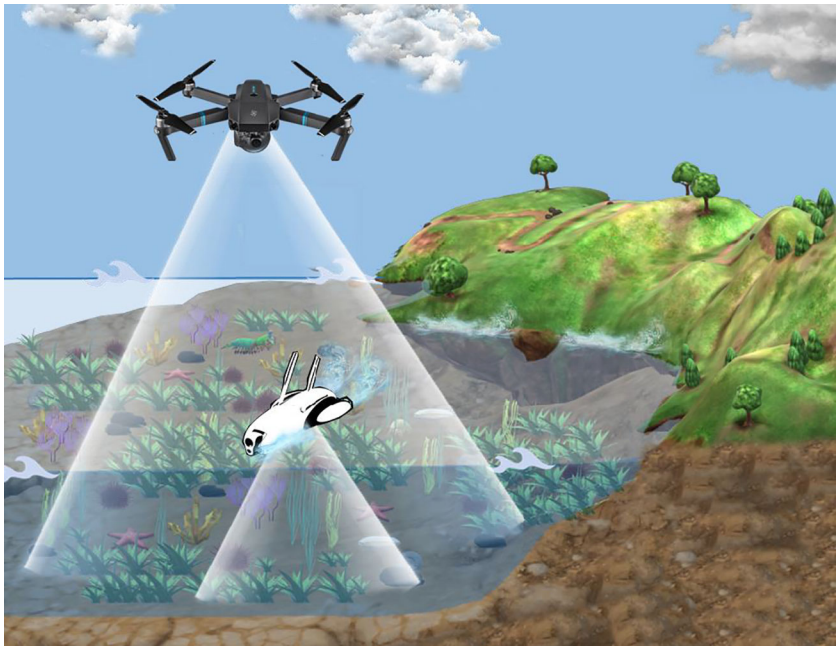

GRAPHICAL ABSTRACT

1 Introduction

Coastal areas are vital for human activities and biological processes, constituting a critical interface between land and sea (Lakshmi and Rajagopalan, 2000). Although coastal areas cover only 10% of the earth's surface area, they host over 60% of the world's population and drive the growth of fisheries, infrastructure development and tourism, resulting in additional pressure on natural coastal ecosystems (Parravicini et al., 2012). Over half of the world's coastal ecosystems can be considered under "moderate" or "high" threat from human development, implying an increased risk for benthic communities and associated species (Bryant et al., 1995; Dauvin et al., 2012; Morroni et al., 2020; Rakaj et al., 2021). Coastal areas are often composed of habitat mosaics, including terrestrial (above water) and marine (below water) features that play a key role in ecosystem functioning. For instance, in tropical environments, mangroves, coral, rocky reefs, and seagrasses usually form a continuum of shallow water habitats in which organisms spend parts of their early lifestages being nursery grounds for marine biota (Nagelkerken et al., 2015). Similarly, in temperate waters, coastal areas, including transitional waters (estuaries and lagoons), intertidal zone as well as shallow marine underwater habitats, are the result of the dynamic interactions between land and sea, resulting in very high level of productivity (Courrat et al., 2009). Shallow Mediterranean benthic habitats are generally dominated by seagrass meadows, macroalgal beds, sandy, and rocky substrates that form complex landscapes. This complexity influences the distribution of living organisms that are dispersed neither uniformly nor randomly but display various gradients or other types of spatial patterns due to microhabitat availability and resource utilisation (Letourneur et al., 2003). Considering such very highly localised and patchy diversity, how these organisms distribute spatially and temporally across habitats is thus relevant for understanding species ecology and for conservation purposes (Tait et al., 2021). Habitat availability and spatio-temporal segregation are often important underlying factors that explain the distribution of animal and vegetal assemblages along coastal environments (Harmelin-Vivien et al., 1995; Seytre and Francour, 2014; Ventura et al., 2015; Cheminée et al., 2017; Cheminée et al., 2021). One necessary step to comprehend these spatio-temporal dynamics in marine organism distribution consists in the characterization at appropriate spatial scales of the seascapes (Castellanos-Galindo et al., 2019). Furthermore, some species of seagrasses and macroalgae are among the most important marine ecosystem engineers, forming extended carpets and canopies which provide a wide range of ecological services such as primary production, carbon sequestration, nutrient recycling, dissipation of wave energy, and nursery habitats for many juvenile species (Heck et al., 2003; Sales et al., 2012; Cheminée et al., 2013; Cheminée et al., 2017; Morris et al., 2020). The increase of human activities such as coastal development, fisheries and marine traffics exacerbates the anthropogenic pressure on coastal ecosystems through pollution, alteration of sedimentary processes and habitat fragmentation, that together with climate change, strongly affect the distribution of seagrass meadows (Boudouresque et al., 2009) and macroalgal forests (Duarte et al., 2018), impacting, in turn, ecosystem functionig (Claudet and Fraschetti, 2010; Coll et al., 2012; Chand and Bollard, 2021). This dynamic scenario demands baseline information and adequate monitoring to understand the processes driving the ongoing ecological shifts. In this framework, solid spatial knowledge of habitat and species distribution over fine spatial and temporal scales is critical to support all stages of marine spatial planning, to provide scientific knowledge for decision-makers and

guidance for the sustainable exploitation of marine resources (Levin et al., 2014; Martin et al., 2014; Fabbrizzi et al., 2020). Different technologies and methods based on remote sensing such as aerial imagery has been used for decades, and earth-observation satellites are now a staple of ecological monitoring globally (Tait et al., 2021). Spatial mapping of shallow-water benthic habitats using satellite data has been widely performed in temperate (Mumby and Edwards, 2002; Borfecchia et al., 2019) and tropical environments (Roelfsema and Phinn, 2010). New proprietary satellite systems (QuickBird, GeoEye-1, Ikonos, Worldview-4) offer up to 31 cm spatial resolution for panchromatic imagery (Alkan, 2018) and commercial aerial photography capable to reachup to 6 cm pixel area (Zhang and Hu, 2012). However, their use for ultra-fine scale ecological studies is still hindered by considerable limitations such as high costs per scene, revisit time, spatial resolution, and cloud cover which may negatively affect many applications for mapping shallow-water benthic environments (Anderson and Gaston, 2013). In this scenario, unmanned aerial vehicles (UAVs) represent a valuable tool for local scale monitoring thanks to their relatively low cost and high customizability, which allow fast and automatic data acquisition over difficult or dangerous areas to access (Hardin and Hardin, 2010). UAVs equipped with Inertial Measurement Units (IMU), GPS and RGB cameras can deliver georeferenced imagery that can be processed by a plethora of Structure from Motion (SfM) photogrammetry software, opening new possibilities for the development of effective algorithms capable of producing ultra-high spatial resolution orthophoto mosaic and digital elevation models (DEMs). In fact, UAVs and SfM processing have been successfully applied for natural resource assessment and environmental monitoring of the coastal areas (Burns et al., 2015; Nikolakopoulos et al., 2017; Ventura et al., 2018; Burns et al., 2019; Taddia et al., 2019; Kabiri, 2020; Ventura et al., 2022). These products, other than playing a key role in assessing 3D habitat complexity and health conditions of specific biotopes such as biogenic reefs in tropical (Raoult et al., 2017; Burns et al., 2019; Fallati et al., 2020; Nieuwenhuis et al., 2022) and temperate (Zapata-Ramírez et al., 2013; Marre et al., 2019; Prado et al., 2020; Ventura et al., 2020) environnements, can also provide valuable information for fine-scale assessment and monitoring of seagrass and macroalgal beds limits, level of fragmentation, and restoration activities (Marre et al., 2020; Rende et al., 2020; Ventura et al., 2022). Moreover, UAVs provide a means to map the distribution and behaviour of many organisms in shallow aquatic environments that typically have high contrast against the substrate (Raoult and Gaston, 2018; Raoult et al., 2018; Williamson et al., 2021). Despite the recent extensive adoption of drones for marine research, this methodology still presents some constraints in providing a detailed analysis of the benthic community in terms of species assemblages. Underwater operator surveys must combine and integrate this form of remote-sensed imagery with biological data. For that purpose, Unmanned Surface Vehicles (USVs) can provide accurate information on habitat distribution in shallow waters, potentially overcoming underwater operator survey constraints through remote imagery acquisition.

This study aimed to employ two types of low-cost unmanned vehicles (UAVs and USVs) as integrated aerial and underwater acquisition tools for shallow coastal habitat mapping, combining SfM-based outputs consisting of aerial and underwater imagery of benthic assemblages. To analyse high and ultra-high spatial resolution maps, taxonomic identification by experts and supervised image classification to identify and provide information on the structure of distinct benthic habitats were employed within the same study area, according to the various levels of detail. Subsequently, we evaluated the accuracy of image classifications based on the Support Vector Machine (SVM) supervised learning algorithm to map shallow benthic habitats using both UAV and USV-based imagery. Finally, in this study we propose some general guidelines to encourage the adoption of this integrated methodological strategy in the mapping of local coastal habitats and associated biotopes and future applications for monitoring proposes.

2 Material and methods

2.1 Study area

The study area (3 Ha) is located north of Civitavecchia in the central Tyrrhenian Sea, Italy (11°44'2.233"E; 42°9'43.043"N). This is an important ecological area within a marine Site of Community Importance (SCI), "Fondali tra Punta S. Agostino e Punta Mattonara" and the natural monument "La Frasca" on the coastal side (Figure 1). This area included in a small bay, encompassing shallow sandy and rocky shorelines with gentle slope, is characterised by a rocky coast, halophilous vegetation and a healthy pinewood. The shallow infralittoral rocky bottoms are characterised at depths from 0.1 m up to 3 m by complex communities constituted by seagrass patches of *Posidonia oceanica* (L.) Delile, brown (Phaeophyta), red (Rhodophyta), and green (Chlorophyta) photophilous algal assemblages that host a large number of endemic species (Gravina et al., 2020). Considering this complex landscape, the shallow water and the high heterogeneity of benthic habitats, this area was selected to apply this integrated methodological approach encompassing aerial and underwater imagery acquisition using an unmanned aerial vehicle (UAV) and an unmanned surface vehicle (USV), respectively. Therefore, for a fine-scale characterisation inside the total mapped area, we identified two additional subplots to improve the image classification routine and detect specific cover classes characterizing the submerged benthic habitats. More specifically, for the UAV fine scale classification we chose an area with very high heterogeneity (microhabitat availability) and complex topographic characteristics (outcropping rocks) which allowed the presence of indicator species such as seagrasses, brown (Fucales) and green (Ulvales and Cladophorales) algae. For ultra-fine scale mapping and classification using USV a representative area of the deeper seabed displaying *Posidonia oceanica* patches and hard rocky substrata with photophilic algae was chosen (Figure 1).

2.2 Imagery acquisition with UAV

High-resolution optical aerial images were acquired using a modified DJI Mavic 2 Pro quadcopter (Figure 2) in May 2022. This consumer-grade UAV is a lightweight (0.9 kg) and easy-to-carry drone equipped with a fully stabilised 3-axis gimbal Hasselblad L1D-20c camera with a 1-inch CMOS RGB sensor with a resolution

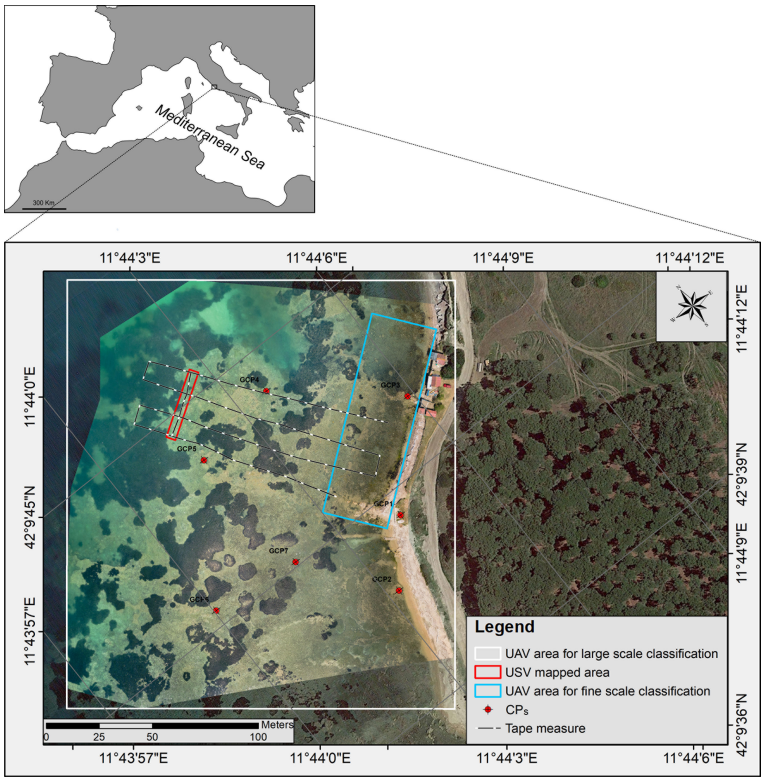

FIGURE 1
The study area along the central Latium coast where shallow benthic habitats were mapped using low-cost unmanned aerial (UAV) and water surface vehicles (USV). The white and blue polygons represent the areas mapped for large and fine-scale classification using UAV-based imagery, whereas the red polygon identifies the area mapped by the USV for ultra-fine classification of benthic communities. The positions of checkpoints (CPs) and tape measure used for accuracy assessments are reported.

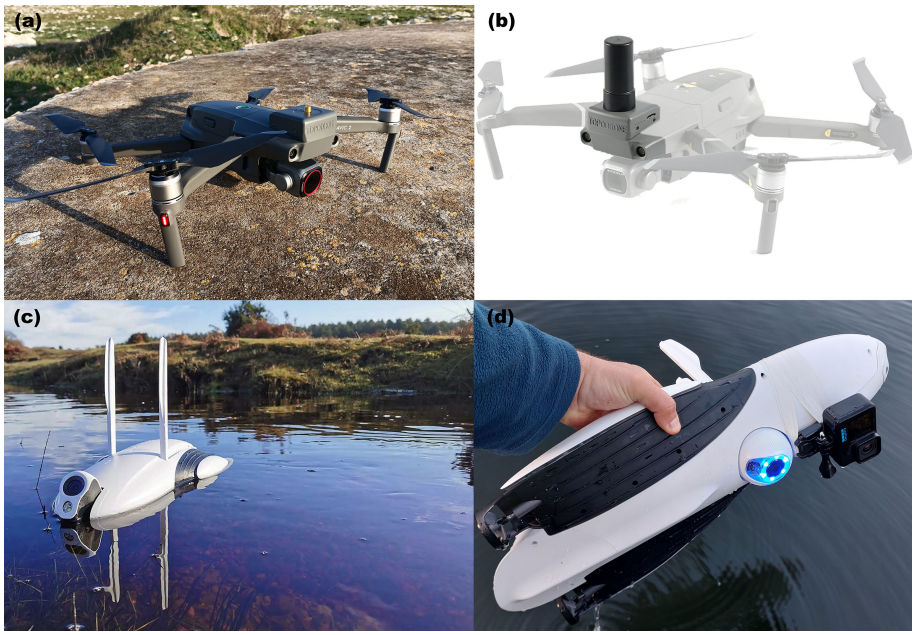

FIGURE 2
The two unmanned vehicles used in this research for mapping above and below water coastal habitats. **(A, B)** Mavic 2 pro (UAV) equipped with additional GNSS antenna for PPK and **(C, D)** Power Dolphin (USV) equipped with Gopro Hero 10 action camera.

capability of 5472 x 3648 (20 MP). Considering a GPS flight speed of 5 m/s and a flight height of 40 above mean sea level (AMSL), to maintain a sufficient overlap (>70%) between images, we took photos every 2 s by using the time-lapse mode with auto white balance and shutter priority (1/400 sec) to avoid motion blur in the acquired imagery. A circular polarizer (CPL) filter was used to minimise the effect of sun-glint. Even though the drone was equipped with a built-in GPS/GLONASS receiver, we mounted an additional GNSS antenna with Post Processing Kinematics (PPK) capabilities. With PPK, the acquired images can be georeferenced at centimetre-scale resolution and do not require a real-time connection between the base station and the rover. As the base station, we used Rinex 3.03 files downloaded from the nearby Continuously Operating Reference Station (CORS) of Civitavecchia of the Latium Permanent GNSS Network. GNSS Rinex files from the UAV (rover unit) and the base station (CORS) were post-processed with the Toposetter 2.0 app to obtain an accurate positioning of the images along the track of the pre-established autonomous flight path defined with the DJI Pilot app (https://www.dji.com/it/downloads/djiapp/dji-pilot) running on a mobile device connected to the remote controller *via* Android debug bridge (ADB). Finally, the image coordinates were inspected spatially using RTKPLOT of RTKLib software to check the accuracy of post-processed coordinates (Takasu and Yasuda, 2009).

2.3 Imagery acquisition with USV

Immediately after the UAV fight, high-resolution underwater images were acquired using the Power Dolphin (PowerVision Inc., Beijing, China) (Figure 2). This aquatic Unmanned Surface Vehicle (USV) was chosen based on its low-price range comparable to other consumer-level USVs. This device was operated by remote control and mobile device with the Vision+2 app, communicating through a built-in Wi-Fi signal. The Power Dolphin is a device that floats on the water surface and is propelled by two horizontal rear propellers. The built-in camera is mounted on the front of the USV with a user-adjustable tilt mechanism that can be oriented up and down in real-time using a remote control, independently of the direction of the USV (Diefenbacher, 2022). This device is also equipped with a GPS and depth echosounder, allowing to continuously collect depth data and reference coordinates. However, considering the low resolution of the built-in camera (1/2.3-inch CMOS 12 MP sensor), we decided to improve the acquisition of underwater imagery by adding a GoPro Hero 10 action camera with a 23 MP sensor. The camera was attached under Power Dolphin's hull, pointing 90° downwards and acquiring photos every 1 sec. No protective housing was used, as this device is waterproof up to 10 m. The underwater imagery collected was then georeferenced using the onboard GPS and scaled during the photogrammetric processing using images representing the tape measure as a reference. The main features of the two systems used for imagery acquisition are reported in Table 1 in the supplementary material section.

2.4 Image processing and classification

The UAV- and USV-based imagery were processed using Agisoft Metashape v 1.8.1. With this low-cost SfM software package, 3D models and 2D raster products can be generated in a fully automated five-step process, comprising: (i) alignment of the photographs, (ii) calculation of a sparse point cloud, (iii) calculation of a dense 3D, (iv) polygonal mesh model generation and texture mapping, (v) generation of Digital Surface Models (DSMs) and orthorectification of the imagery (De Reu et al., 2013). Firstly, we performed the alignment of images with the parameter accuracy set to 'high'. After the photoalignment, this initial bundle adjustment created sparse point clouds from overlapping digital images. The sparse point clouds included the position and orientation of each camera position and the 3D coordinates of all image features. The internal camera geometry was modelled by self-calibration during the bundle adjustment (Price et al., 2019). Subsequently, dense point clouds were built based on multi-view stereopsis (MVS) algorithms with high-quality and mild depth filtering. After filtering the dense point clouds according to points confidence (points with values less than three were removed), these were used for producing polygonal meshes and DSMs using an Inverse Distance Weighting (IDW) interpolation. Finally, the DSMs generated ortho-rectified RGB photomosaics of emerged and submerged habitats.

Orthophoto mosaics and DSMs generated in Metashape were exported as raster images (GeoTIFF format, in the reference system WGS84/UTM zone 33 N, EPSG:32633) and transferred to a

TABLE 1 Residuals of the bundle adjustment transformation on seven checkpoints (CPs) and the total RMSE (cm).

UTM coordinates UTM 32 N				Individual residuals after bundle adjustment transformation (cm)				
Label	Easting	Northing	Elevation		Easting	Northing	Elevation	3D
CP 1	725897.1	4671334	1.56	CP 1	-5.523	4.803	-6.130	9.547
CP 2	725875.3	4671306	0.416	CP 2	-4.072	-0.002	-14.729	15.281
CP 3	725933.4	4671377	-0.173	CP 3	-2.185	-7.520	-16.005	17.818
CP 4	725881.4	4671419	-0.729	CP 4	4.025	-2.183	4.837	6.660
CP 5	725838.3	4671411	-0.607	CP 5	7.392	-1.001	-1.228	7.560
CP 6	725800.5	4671350	-0.774	CP 6	5.388	0.484	7.447	9.204
CP 7	725844.3	4671346	-0.217	CP 7	1.284	-0.725	-6.590	6.753
				Total RMSE	**4.681**	**3.508**	**9.520**	**11.174**

geographical information system (GIS) using ArcMap 10.6 software (Esri, 2011) for subsequent Object-Based Image Classification (OBIA) processing. At this stage, classification methods based only on pixel information are time-consuming and limited due to the spectral similarities. Therefore, we reduced the pixel complexity by segmenting the orthophotos into more meaningful objects to speed up the aerial and underwater imagery classification. A means-shift (MS) algorithm was applied using the segment means-shift function in ArcMap. The MS is a non-parametric segmentation/clustering algorithm that uses the number of pixels and the Euclidean distance defined within a spectral space to segment an image (Lee et al., 2009). In our case, the spectral details, spatial details, and minimum segment size parameters were set to 20, 15 and 600, respectively. The spectral detail setting was used to discriminate between objects based on spectral signatures. In contrast, spatial detail was used to discriminate between objects based on the shape of the features to produce sharper segments (Gaw et al., 2019). A minimum mapping unit of 500 pixels (approximately 5 cm^2) was chosen. After the segmentation process, we manually selected a set of image objects as training samples to train the Support vector machine (SVM) algorithm, which is a supervised machine learning classifier well adapted to solving non-linear, high dimensional space classifications that have become increasingly popular in remote sensing classification (Heumann, 2011; Pipaud and Lehmkuhl, 2017). Spectral reflectance signature files for both segmented UAV- and USV-based orthomosaics were generated after collecting training samples in the Training Sample Manager Toolbar. We manually selected a set of image objects as training samples to train the SVM algorithm. The SVM model uses each band's mean and standard deviation to classify the image objects in the whole dataset.

For comparison purposes, a subset of 0.3 Ha of the UAV-based orthophoto mosaics was classified using SVM without running MS segmentation to avoid spectral smoothing and detect specific cover classes.

To optimise the results, we then performed a post-classification routine (Droppova, 2011) on all the classification outputs by removing some misclassified regions of pixels and small isolated objects. This task was carried out using the Spatial Analyst extension in ArcMap, which provides a set of generalisation tools for the post-classification processing task involving three main steps: a) filtering the classified output using the 'Majority Filter' tool; b) smoothing the ragged class boundaries and clumping the classes using the 'Boundary Clean' tool and, c) generalising classified output by reclassifying small, isolated regions of pixels to the nearest classes with the 'Region group', 'Set Null' and 'Nibble' tools).

2.5 Accuracy assessment of cartographic outputs

We used GNSS coordinates of seven checkpoints (CPs) to assess the horizontal (x and y) and vertical (z) positional accuracy of UAV-based SfM products. For checkpoint (CPs) coordinates' acquisition, an Emlid Reach RS+, a low-cost single-frequency (L1 - 1575.42 MHz) GNSS receiver, was employed. We used both small reflective target and natural features such as rocks that were easily detectable in the UAV imagery. The quality of the photogrammetric models based on the CPs residuals was computed as the difference between the position estimated through PPK and the coordinates of the manually surveyed CPs. We computed the Root Mean Square Error (RMSE) for each mapped area in the E, N, and U directions and 3D. Small values of the Root Mean Square Error (RMSE) indicate good image alignment processes and block adjustments resulting in accurate 3D point clouds, digital elevation models (DEMs), and orthophoto mosaics.

Before starting imagery acquisition, four metric tape measures were positioned on the seabed from 0.1 up to 2.5 m depth to have a constant reference distance during field operation and for scaling and estimating the accuracy of the underwater 3D models acquired with the USV. Snorkelers followed the tape measure during underwater video acquisition for ground truth data collection (Figure 1).

To assess the proportional accuracy of the underwater USV-based model, we compared the known dimensions of objects (lengths measured along the metric tape measures) to their estimated dimensions in the model. The measurement accuracy for each linear distance estimated from the 3D models was expressed as a percentage of difference (Young et al., 2017).

A confusion matrix for each mapped area (from large-scale UAV-based to ultra-fine scale USV-based imagery) was calculated to evaluate the accuracy of the final classifications, including (i) producer's accuracy, (ii) user's accuracy; (iii) overall accuracy (OA); and (iv) the Kappa Index of Agreement (KIA). The confusion matrices were built using GNSS-based ground truth data points collected by snorkelers along the tape measure and randomly placed accuracy assessment points (distinct from the training sample areas). An expert classified each point manually by visually inspecting the original true colour orthophotos. Due to the ultra-high spatial resolution, visual photo interpretation could be considered very reliable for assessing the accuracy of thematic maps (Lechner et al., 2012).

3 Results

3.1 UAV-based large/fine-scale mapping and classification

The whole study area (3 Ha) was mapped after a flight time of 25'35" from a height of 40 m, leading to the acquisition of 339 aerial images (Supplementary Material Figure 2). After PPK, all the UAV GPS antenna positions showed a high ambiguity-fixed solutions percentage (Q1 = 100%, Supplementary Material Figure 1), resulting in a planimetric precision estimated after bundle adjustment at each CPs of 5.8 cm. In contrast, the altimetric precision was 11.1 cm (Table 1). The orthophoto mosaics and DSM showed a spatial resolution of 1.3 cm/pix and 1.6 cm/pix, respectively (Figures 3A, B). The 3D mesh model of the mapped with the UAV area is available at the following link: https://skfb.ly/oBEEL

The high-resolution imagery allowed for a fine-scale characterisation of the site after MS segmentation and SVM classification (Figure 4). In fact, eleven cover classes encompassing both above and below the sea surface features are identified with an OA and KIA accuracy value of 0.77 and 0.75%, respectively (Supplementary Material Table 1). Among these, five major seabed cover classes representing broad benthic community-level categories

10.3389/fmars.2022.1096594

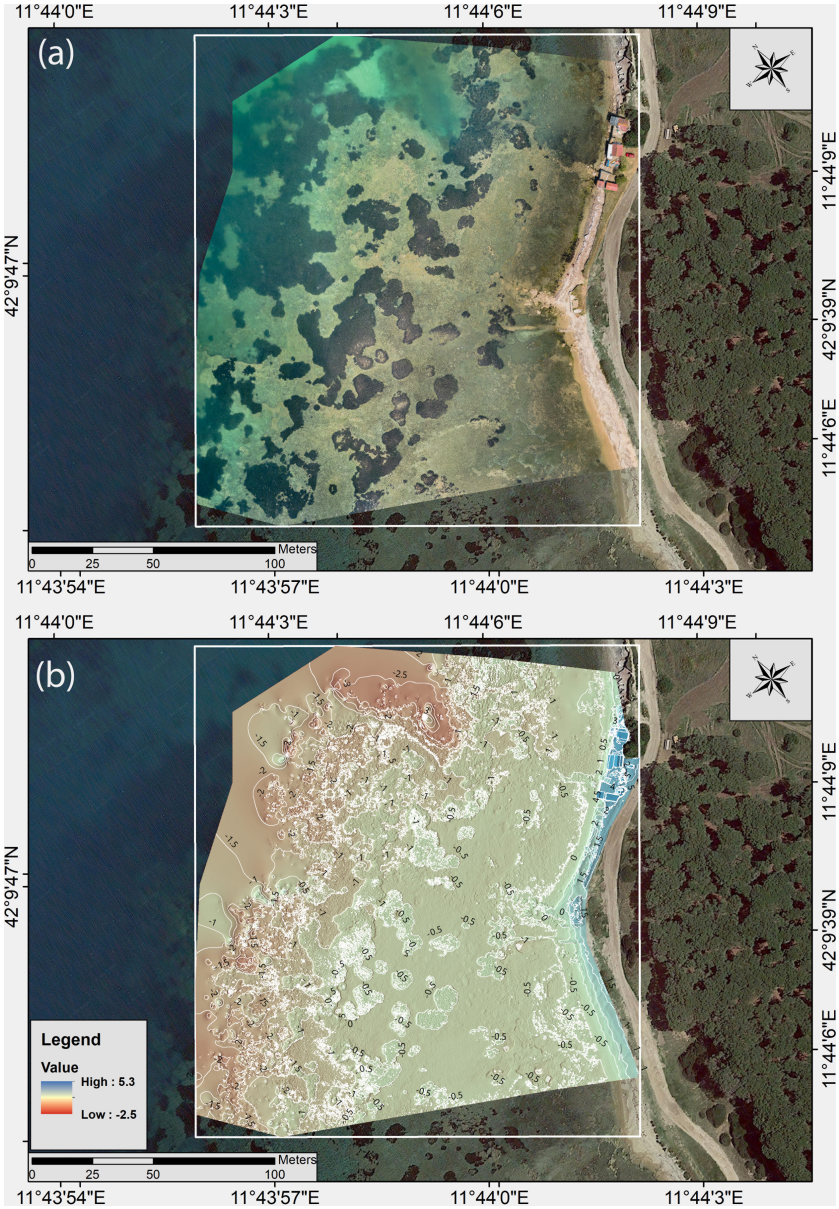

FIGURE 3
(A) High spatial resolution UAV-based RGB orthophoto mosaic and **(B)** Digital surface models (DSM) with depth contour interval at 50 cm.

were identified: *Posidonia oceanica* patches, soft bottoms with *Cymodocea nodosa*, hard bottoms with photophilic algae, hard bottoms with photophilic algae mixed with seagrass detritus (dead leaves and rhizomes), and sand. Significant seabed cover misclassification errors involved spectral confusion among classes with very similar spectral signatures, such as 'beach' class constituted by fine and wet sand (with a total of 35.6% of samples interpreted as coarse sand and banquette), hard bottoms with photophilic algae (with a total of 27.3% of samples interpreted as hard bottoms with photophilic algae with detritus and sand). *Posidonia oceanica* was classified with more than 90% user and producer accuracy, while *Cymodocea nodosa* reported only a 60% user accuracy value.

Inside the selected subarea of 0.3 ha, the SVM classification was performed on the raw RGB orthomosaics without applying MS segmentation. This choice implied a longer computation time (+3h 20') to train SVM, classify, and generalise classified raster outputs. However, working at pixel levels, without smoothing spectral signatures during segmentation, allowed a more detailed classification of the benthic habitats by splitting the two classes ('hard bottoms with photophilic algae' and 'hard bottoms with photophilic algae and seagrass detritus') into four additional cover classes with high ecological interest (Figures 5, 6). In fact, hard bottoms with photophilic algae can be distinguished by water depth (0-50 cm and > 50 cm) and according to the presence of algal assemblages dominated by Fucales brown algae of the genus *Cystoseira* spp., or green algae (Cladophorales and Ulvales). Seagrass cover classes represented by *Posidonia oceanica* and *Cymodocea* showed higher user and producer accuracy values than the large-scale classification carried out after MS segmentation. The other benthic cover classes displayed comparable values of percentage cover, with only slightly lower OA and KIA values (0.75 and 0.71, respectively) due to the misclassification of rocks covered by

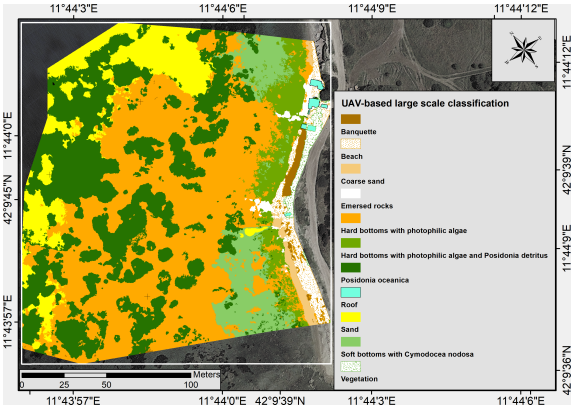

FIGURE 4
Thematic map showing the eleven cover classes identified after MS segmentation and SVM classification of the UAV-based high spatial resolution orthophoto mosaic.

Cystoseira spp. As shallow rocks with other photophilic algae (represented by the 'hard bottoms with photophilic algae (0- 50 cm)' class) (Supplementary Material Table 2).

3.2 USV-based ultra-fine scale mapping and classification

Images were acquired from the surface using the PowerDolphin USV to map an area of 150 m^2. The dimensions of the underwater objects (tape measure) rendered in the mesh model of the seabed matched strongly with their actual dimensions with a mean procedural accuracy for the length of 98.08% ± 0.02, resulting in a total error of 0.017 m. The generated orthomosaics (Figure 7A) and DSM showed an ultra-high spatial resolution of 1.3 and 2.2 mm/pixel, respectively. Through hill-shade map, a fine terrain representation based on topographic shielding factors for improving seabed morphology visualisation was generated using elevation data (Figure 7B). The 3D mesh model of the mapped area with the USV is available at the following link: https://skfb.ly/oBEHt

The SVM classification allowed the identification of five cover classes that implied a more detailed definition of the benthic habitat variability compared to the UAV-based classification. The benthic cover was mainly represented by hard calcareous bottoms covered by a carpet of photophilic red (52%) and brown algae (33%) (Figures 8, 9). Inside the broad cover class 'hard bottom with photophilic algae' previously identified also by UAV-based imagery, we mapped at the species level

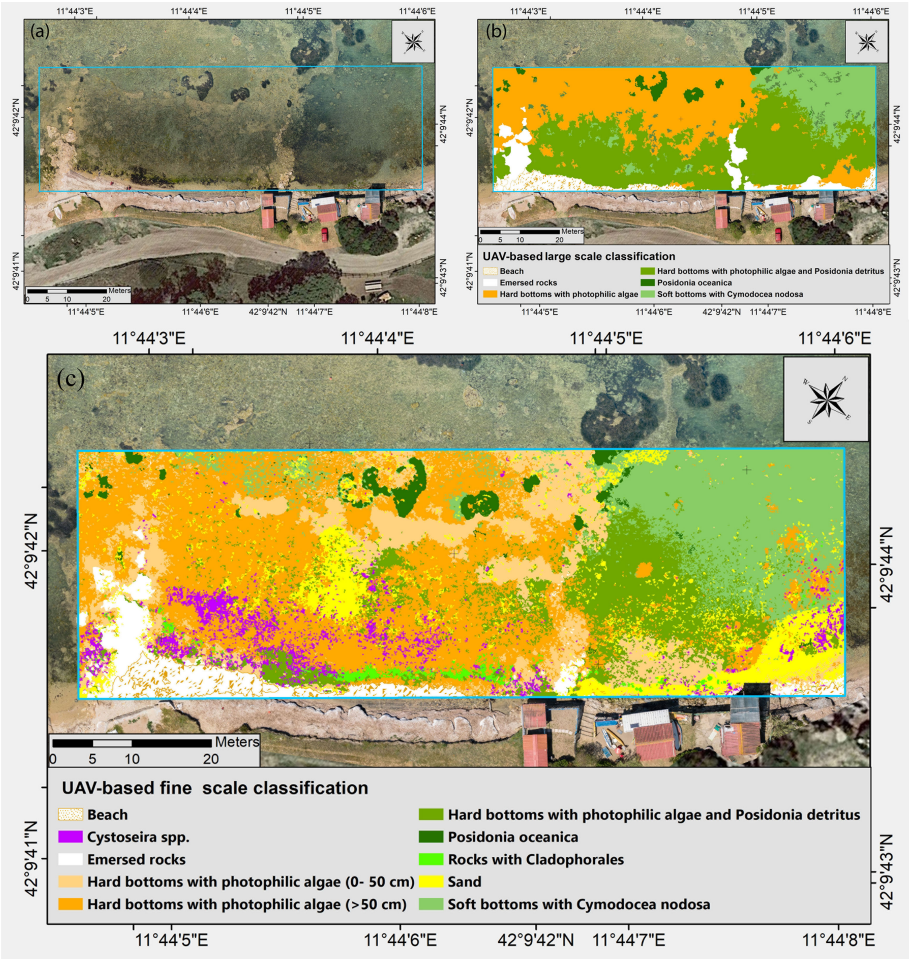

FIGURE 5
Comparison between large and fine scale UAV-based thematic maps. **(A)** UAV-based orthomosaics; **(B)** UAV-based large scale classification results after MS segmentation and SVM classification; **(C)** UAV-based fine scale classification results after SVM classification carried out without MS segmentation.

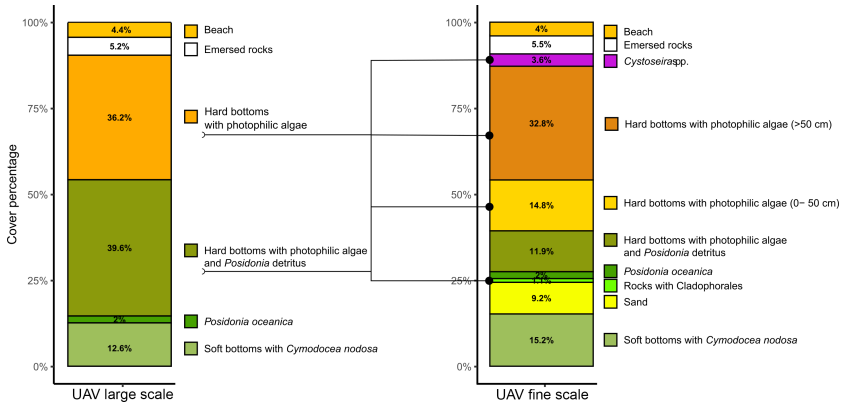

FIGURE 6
Bar plots reporting the percentage cover of each benthic cover class of UAV-based fine scale classification reported in Figure 4C.

the arborescent algal cover (Figure 10), mainly represented by red algae (*Jania rubens*, Corallinales) and brown algae (*Padina pavonica*, *Halopteris scoparia* and *Dictyota dichotoma*). After MS segmentation, we reported lower per-class accuracies than other classifications, resulting in OA and KIA values of 73.4% and 0.61, respectively (Supplementary Material Table 2). Significant seabed cover misclassification errors involved spectral confusion among small sandy patches (with 53.6% of samples interpreted as brown and red algae) and brown algae (with a total of 53% of samples classified as red algae). In addition, the tape measure was classified as brown algae (*Padina pavonica*) due to its white colour. Similarly, to other classification method, *Posidonia oceanica* is identified in most cases with both user and producer accuracy values of > 80%.

4 Discussion

This study demonstrated that integrating consumer-grade unmanned aerial and surface vehicles (UAV and USV) is an effective tool for the characterization and mapping of shallow benthic habitats at fine and ultra-fine scales. Coastal benthic habitats, such as shallow rocky bottoms and seagrass beds, are among the most heavily anthropogenically-impacted marine ecosystems and are also among the most productive in terms of ecosystem functioning implying rigorous monitoring programs (O'Connor, 2013). Seagrass and seaweed are sensitive to changes in the ecosystem, making them valuable indicators of ecosystem health (Dokulil, 2003). The type, distribution, and condition of algal assemblages can drive water quality (pH, dissolved oxygen, suspended sediment) and local benthic and fish assemblages health (food resources, habitat), making the quantification of these species very useful in identifying mechanisms responsible for changes at both community and ecosystem-level (Airoldi et al., 1995; Benedetti-Cecchi and Cinelli, 1995; Kislik et al., 2020). In this context, the identification and fine mapping of canopy-forming species is a critical point in monitoring actions among coastal areas, which often exhibit significant habitat heterogeneity, even on a small scale, and are subject to various anthropogenic stressors (agricultural run-off and discharge of sewage, sedimentary alteration). Although numerous studies have already focused on the dynamics of seagrasses under the impact of human activities and have defined seagrass distribution and temporal trends on a large scale (Duarte, 2002; Telesca et al., 2015; Chefaoui et al., 2018), only a few have associated spatial, temporal and structural local data to these changes (Leriche et al., 2006; Pergent-Martini et al., 2022). To answer this question, UAV platforms can provide high spatial resolution at a frequency greater than traditional methods such as satellites, piloted aircraft, and LiDAR. We reported how some algal taxa could be detected directly as a good proxy for monitoring environmental quality changes (*Cystoeira* spp. Cladophorales and Ulvales) after refining the classification approach used for UAV imagery. We could detect, using the

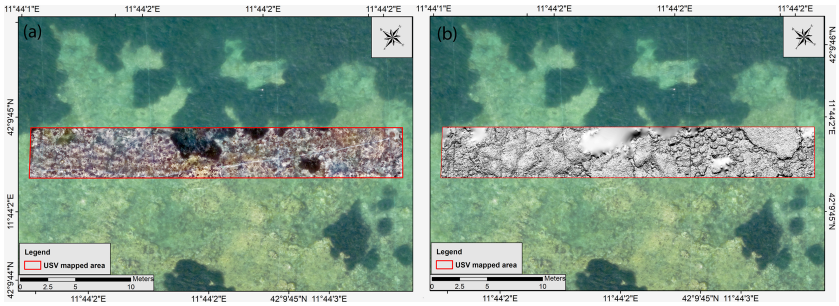

FIGURE 7
(A) The orthophoto mosaic derived from USV-based underwater imagery and **(B)** seabed morphology visualised through the hill shading map. The areas covered by *Posidonia* patches are missing due to significant errors during the DSM generation.

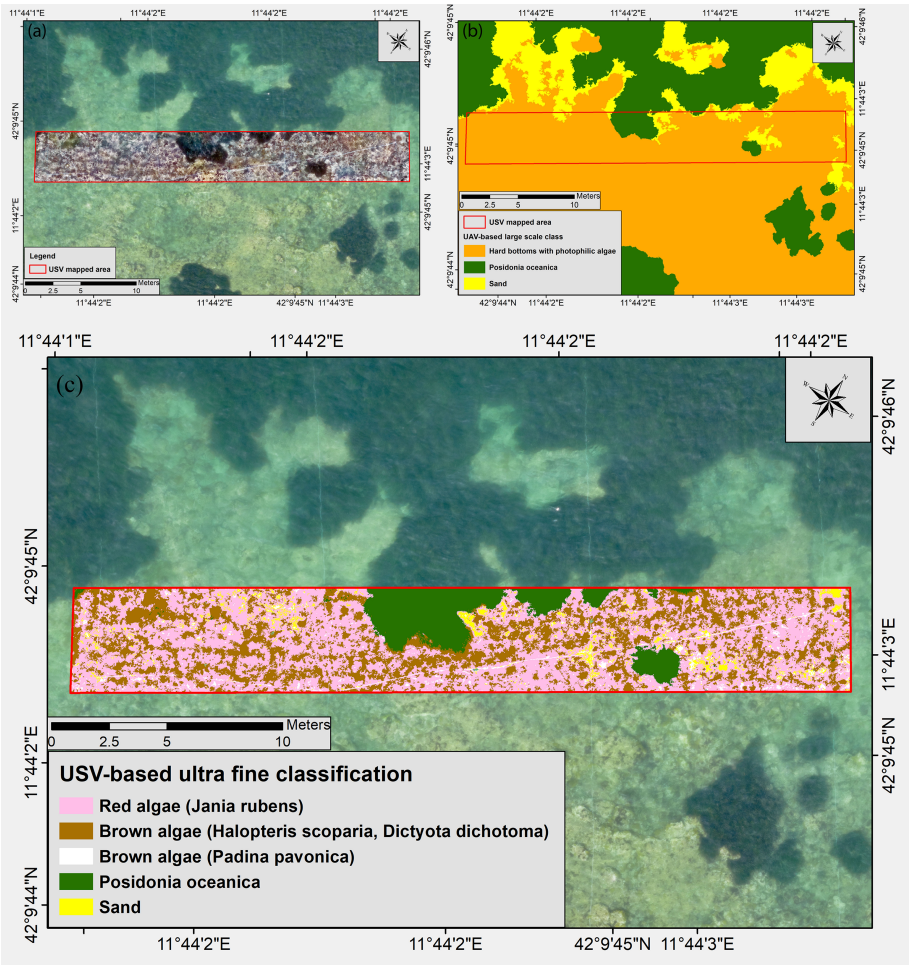

FIGURE 8
Comparison between large scale UAV-based and ultra-fine scale USV-based thematic maps. **(A)** USV-based underwater orthomosaics over imposed on the UAV-based aerial orthomosaics; **(B)** UAV-based large scale classification results after MS segmentation and SVM classification; **(C)** USV-based ultra-fine classification results after SVM classification and MS segmentation.

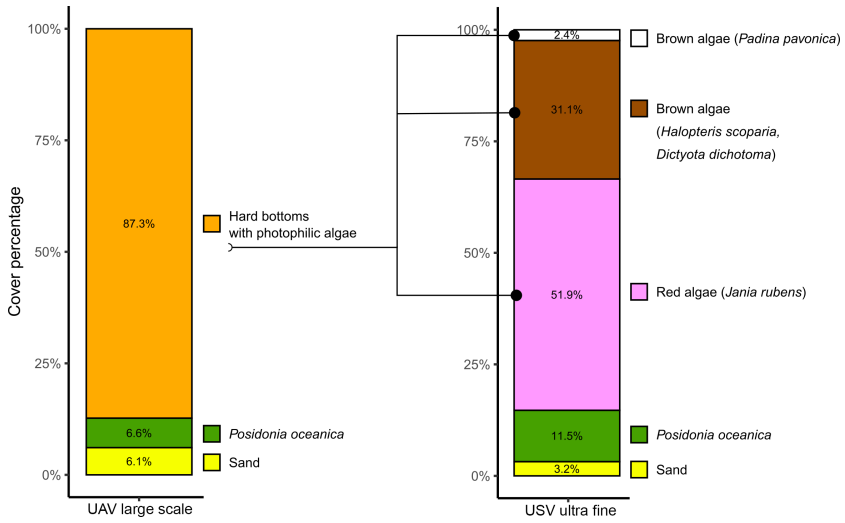

FIGURE 9
Bar plots reporting the percentage cover of each benthic cover class of USV-based ultra-fine classification reported in Figure 7C.

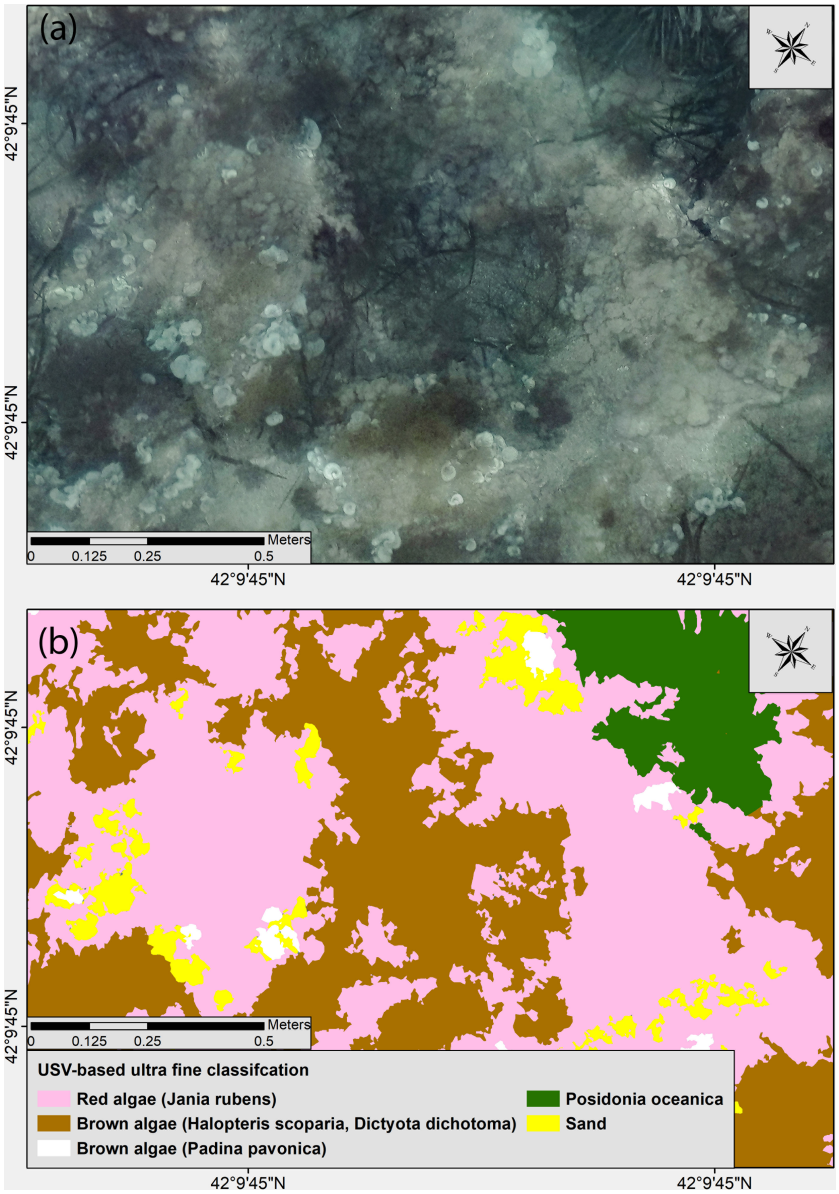

FIGURE 10
(A) Detailed view of the USV-based underwater orthophoto mosaic in which the shrubby algal assemblage is visible and **(B)** the results after MS segmentation and SVM classification.

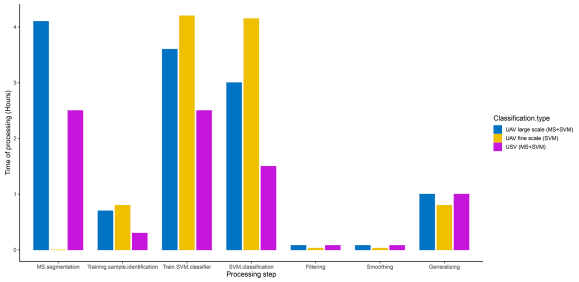

FIGURE 11
Processing times (in hours) of the main steps used in this work to classify high (UAV-based) and ultra-high (USV-based) imagery.

complete information available at the pixel level, the most critical algal assemblages among a limited shallow area with a relatively good level of accuracy. These sensing instruments may even provide quasi-continuous temporal coverage that results in a detailed description of the ecological dynamics that characterise most coastal species with fast development and short life cycles (e.g., algal blooms). We demonstrated that low-altitude UAV imagery is powerful in detecting and quantifying submerged vegetation over shallow areas characterised by fair water clarity and can be integrated into monitoring programs where recurrent sampling and mapping are needed. Therefore, as reported in other studies (Duffy et al., 2018; Yang et al., 2020), UAV-based imagery is a flexible, low-cost, and time-effective technique for monitoring intertidal and shallow water

marine vegetation. Nevertheless, the acquisition methods carried out with a single instrument (e.g., UAV) show resolution limits that cannot be exceeded (e.g., species recognition and organism counting). Therefore, to achieve a precise characterization of the benthic assemblages, an integrated use of several acquisition instruments is necessary. Therefore, the integration of USV with consumer-grade UAV for photogrammetric acquisition makes it possible to characterise complex benthic communities at a broader resolution scale (from large to ultra-fine). The use of the USV for benthic habitat mapping can be considered an emerging tool to be implemented in monitoring plans since classification accuracy decreases with water depth, particularly in water deeper than 3 m (Shintani and Fonstad, 2017), limiting the use of UAV-based optical data to a narrow stretch of coast. Aerial images cannot capture the taxonomic detail with the same accuracy as *in-situ* surveys, whereas USV-based data can provide comparable results regarding species identification. This has the advantage of adding accurate spatial information that can help address other research questions and monitoring goals.

However, without using an image segmentation approach, there are several technical challenges that scholars need to be fully aware of, including extensive processing time to train the classifiers and define the training sample, as well as the long and complex post-processing routine linked to more 'salt-and-pepper' artefacts due to spurious pixel classifications (Figure 11). Therefore, for extensive scale assessment where broad classification is needed, it is advisable to reduce the amount of computer memory available per processing unit by smoothing the spectral complexity of UAV imagery, before training the classifier. This step becomes mandatory for the imagery acquired using the USV due to their ultra-high spatial resolution. Even though after MS segmentation of USV-based imagery, small spectral difference among similar classes are too smoothed, making impossible to distinguish species with similar colours (e.g., Dictyotales from Sphacelariales), we performed a very detailed habitat characterisation of the deeper rocky bottoms by identifying the patchy algal assemblages. The OBIA processing applied in ArcMap can be substituted with other approaches available in the eCognition software (Trimble Geospatial Imaging, Munich, Germany), which has a powerful multi-resolution algorithm for image segmentation capable of reducing computational complexity and processing times compared to MS segmentation (Fu et al., 2013). Moreover, the lengthy trial-and-error processing time required to configure the suitable parameters for image segmentation can be reduced by enabling a more statistically-based solution for selecting scale parameters (Drăguţ et al., 2014).

Another primary aspect to investigate during monitoring campaigns is the presence of organisms with a key role in benthic communities. Research on target species, such as herbivorous, deposit-feeders or filter-feeders, is critical for the development of conservation and management measures of coastal areas since they play a vital role in the sea floor dynamics (Boncagni et al., 2019; Morroni et al., 2020; Grosso et al., 2022; Pensa et al., 2022). When the research is focused on benthic organisms living in shallow rocky-bottom areas, data collection through SCUBA diving and snorkelling has traditionally been the most widely chosen method. However, among recent benthic sampling techniques, remote photographic recording methods offer a variety of advantages by reducing the time spent by divers underwater and logistics costs (Piazza et al., 2019). More specifically, photogrammetric outputs such as 2D plots or transects cropped from large orthophotos can be usable in software specifically dedicated to the elaboration of benthic images (e.g., PhotoQuad, Seascape, CPC, ImageJ), enabling the analysis and comparison of defined seabed areas to investigate changes in the benthic communities over time (Piazza et al., 2019). In this context, the adoption of the integrated approach with UAV and USV to evaluate any modification due to small-scale habitat variability, registering the position of sessile specimens (e.g., algae, bryozoans, sponges, bivalves) and determining the abundance, the distribution, and the aggregation patterns of vagile fauna (e.g., sea urchins, sea cucumbers, sea stars and epimegabenthos assemblages in general), is unprecedented and fulfils the main aim of fine-scale monitoring programmes.

4.1 Methodology constraints

Although our approach can provide a fast, low-cost, and accurate method for fine-scale mapping of shallow benthic underwater habitats and other above-water coastal features of ecological interest, several drawbacks should be considered when field operations are carried out in sub-optimal conditions. In fact, we performed UAV imagery acquisition with calm sea conditions with wind speed < 1 knot (Beaufort scale = 0) and in very shallow waters where moderate water turbidity have a limited effect on light penetration (mean measured value of Secchi disk transparency = 4.2 ± 0.3 m). However, along the deeper edges of the mapped area, at depths > 3 m, the imagery was more affected by transparency, resulting in a less sharp identification of seagrassmeadows patches which also involved image alignment issues during photogrammetric processing. Sea conditions and weather are also key factors to be carefully evaluated during USV operation. This tool is highly promising in shallow lagoons and back-reef monitoring, although in open coastal areas are necessary low hydrodynamic conditions for optimal imagery acquisition, due to limited stability and manoeuvrability. However, the distance from the seafloor of the camera sensor mounted on USV can be an important limitation in obtaining reliable models in very shallow waters (< 1 m).

Seasonality can also play a crucial role in achieving reliable maps for thematic cartography because macroalgae assemblages can considerably vary over seasons (e.g., summer vegetative phase versus wintry quiescence period of Cystoseira spp. that may lead to the impossibility of thalli detection). Significant accumulation of phanerogamic detritus (dead *P. oceanica* leaves) can affect the mapping of both above-water features (covered by thick banquettes layers) and below-water substrata (by depositing in sandy patches and holes inside rocky reef) in winter. Regarding aerial and surface platforms configuration most limiting factors for using such tools over large areas are primarily due to the LiPo battery that implies short-medium (< 30 min) flight times. This aspect is less evident for USV platforms which are capable of slow navigation over a longer time (> 2 hours).

5 Conclusions

Understanding heterogeneity within benthic habitats is a primary step for the environmental monitoring of perturbed and pristine

coastal ecosystems. Drones open the possibility to capture data that is useful to finely depict hard bottoms assemblages, seagrass and other above-water features (e.g., banquette, artificial structures), which can play a crucial role in coastal dynamics. Traditional boundary mapping has often been conducted using satellite and airborne imagery. Still, it can be considerably improved with UAV-based imagery, highlighting the need to investigate the fragmentation within meadows, which can provide researchers, stakeholders and ecosystem managers with data on whether a meadow is potentially deteriorating or recovering (Duffy et al., 2018). The combination of aerial and underwater imagery provides high-quality and cost-effective data that can be stored for assessment over time, offering valuable information that can be used in the case of retrospective analyses.

Potential improvements to the methods described here are extensive, including using fixed-wing platforms for increased flight efficiency and spatial coverage, enhanced imaging acquisition (multispectral sensors), and positioning (direct imagery georeferencing with RTK systems) techniques. Finally, applying powerful algorithms for image segmentation and classification capable of processing large datasets will be highly informative in aquatic system management and decision-making, showing great promise in applying UAV and USV high spatial resolution imagery for shallow benthic habitats conservation and monitoring.

Data availability statement

The raw data supporting the conclusions of this article will be made available by the authors, without undue reservation.

Author contributions

DV: conceptualization, methodology, field investigation, data analysis, writing original draft. LG, DP: field investigation, writing—review and editing. EC, GM, TV, MS: writing—review and editing. AR: conceptualization, methodology, field investigation, writing—review and editing, project administration. All authors contributed to the article and approved the submitted version.

Acknowledgments

We thank Antonio d'Argenio, Enrico Iuliano from Strumenti Topografici (GEC Software company) and Aleksandr Levchik from Topodrone team for their support during UAV configuration and PPK processing.

Conflict of interest

The authors declare that the research was conducted in the absence of any commercial or financial relationships that could be construed as a potential conflict of interest.

Publisher's note

All claims expressed in this article are solely those of the authors and do not necessarily represent those of their affiliated organizations, or those of the publisher, the editors and the reviewers. Any product that may be evaluated in this article, or claim that may be made by its manufacturer, is not guaranteed or endorsed by the publisher.

Supplementary material

The Supplementary Material for this article can be found online at: https://www.frontiersin.org/articles/10.3389/fmars.2022.1096594/full#supplementary-material

References

Airoldi, L., Rindi, F., and Cinelli, F. (1995). Structure, seasonal dynamics and reproductive phenology of a filamentous turf assemblage on a sediment influenced, rocky subtidal shore. *Botanica Marina* 38, 227–237. doi: 10.1515/botm.1995.38.1-6.227

Alkan, M. (2018). Information content analysis from very high resolution optical space imagery for updating spatial database. *Int. Arch. Photogramm. Remote Sens. Spat. Inf. Sci.* 42, 4. doi: 10.5194/isprs-archives-XLII-4-25-2018

Anderson, K., and Gaston, K. J. (2013). Lightweight unmanned aerial vehicles will revolutionize spatial ecology. *Front. Ecol. Environ.* 11, 138–146. doi: 10.1890/120150

Benedetti-Cecchi, L., and Cinelli, F. (1995). Habitat heterogeneity, sea urchin grazing and the distribution of algae in littoral rock pools on the west coast of Italy (western Mediterranean). *Mar. Ecol. Prog. Ser.* 126, 203–212. doi: 10.3354/meps126203

Boncagni, P., Rakaj, A., Fianchini, A., and Vizzini, S. (2019). Preferential assimilation of seagrass detritus by two coexisting Mediterranean sea cucumbers: Holothuria polii and holothuria tubulosa. *Estuar. Coast. Shelf Sci.* 231, 106464. doi: 10.1016/j.ecss.2019.106464

Borfecchia, F., Consalvi, N., Micheli, C., Carli, F. M., Cognetti De Martiis, S., Gnisci, V., et al. (2019). Landsat 8 OLI satellite data for mapping of the posidonia oceanica and benthic habitats of coastal ecosystems. *Int. J. Remote Sens.* 40, 1548–1575. doi: 10.1080/01431161.2018.1528020

Boudouresque, C. F., Bernard, G., Pergent, G., Shili, A., and Verlaque, M. (2009). Regression of Mediterranean seagrasses caused by natural processes and anthropogenic disturbances and stress: A critical review. *Bot. Mar.* 52, 395–418. doi: 10.1515/BOT.2009.057

Bryant, D., Rodenburg, E., Cox, T., and Nielsen, D. (1995). Coastlines at risk: An index of potential development-related threats to coastal ecosystems. *World Resour. Institute.* 8.

Burns, J. H. R. R., Delparte, D., Gates, R. D., and Takabayashi, M. (2015). Integrating structure-from-motion photogrammetry with geospatial software as a novel technique for quantifying 3D ecological characteristics of coral reefs. *PeerJ* 3, e1077. doi: 10.7717/peerj.1077

Burns, J. H. R., Fukunaga, A., Pascoe, K. H., Runyan, A., Craig, B. K., Talbot, J., et al. (2019). 3D habitat complexity of coral reefs in the northwestern Hawaiian islands is driven by coral assemblage structure. *Int. Arch. Photogramm. Remote Sens. Spatial Inf. Sci.* XLII-2/W10, 61–67. doi: 10.5194/isprs-archives-XLII-2-W10-61-2019

Castellanos-Galindo, G. A., Casella, E., Mejía-Rentería, J. C., and Rovere, A. (2019). Habitat mapping of remote coasts: Evaluating the usefulness of lightweight unmanned aerial vehicles for conservation and monitoring. *Biol. Conserv.* 239, 108282. doi: 10.1016/j.biocon.2019.108282

Chand, S., and Bollard, B. (2021). Detecting the spatial variability of seagrass meadows and their consequences on associated macrofauna benthic activity using novel drone technology. *Remote Sens.* 14, 160. doi: 10.3390/rs14010160

Chefaoui, R. M., Duarte, C. M., and Serrão, E. A. (2018). Dramatic loss of seagrass habitat under projected climate change in the Mediterranean Sea. *Glob. Change Biol.* 24, 4919–4928. doi: 10.1111/gcb.14401

Cheminée, A., Le Direach, L., Rouanet, E., Astruch, P., Goujard, A., Blanfuné, A., et al. (2021). All shallow coastal habitats matter as nurseries for Mediterranean juvenile fish. *Sci. Rep.* 11, 14631. https://doi.org/10.1038/s41598-021-93557-2ù

Cheminée, A., Pastor, J., Bianchimani, O., Thiriet, P., Sala, E., Cottalorda, J. M., et al. (2017). Juvenile fish assemblages in temperate rocky reefs are shaped by the presence of macro-algae canopy and its three-dimensional structure. *Sci. Rep.* 7, 14638. doi: 10.1038/s41598-017-15291-y

Cheminée, A., Sala, E., Pastor, J., Bodilis, P., Thiriet, P., Mangialajo, L., et al. (2013). Nursery value of cystoseira forests for Mediterranean rocky reef fishes. *J. Exp. Mar. Bio. Ecol.* 442, 70–79. doi: 10.1016/j.jembe.2013.02.003

Claudet, J., and Fraschetti, S. (2010). Human-driven impacts on marine habitats: A regional meta-analysis in the Mediterranean Sea AN - prod.academic_MSTAR_814234566; 13249761. *Biol. Conserv.* 143, 2195–2206. doi: 10.1016/j.biocon.2010.06.004

Coll, M., Piroddi, C., Albouy, C., Ben Rais Lasram, F., Cheung, W. W. L., Christensen, V., et al. (2012). The Mediterranean Sea under siege: Spatial overlap between marine biodiversity, cumulative threats and marine reserves. *Glob. Ecol. Biogeogr.* 21, 465–480. doi: 10.1111/j.1466-8238.2011.00697.x

Courrat, A., Lobry, J., Nicolas, D., Laffargue, P., Amara, R., Lepage, M., et al. (2009). Anthropogenic disturbance on nursery function of estuarine areas for marine species. *Estuar. Coast. Shelf Sci.* 81, 179–190. doi: 10.1016/j.ecss.2008.10.017

Dauvin, J.-C., Alizier, S., Rolet, C., Bakalem, A., Bellan, G., Gesteira, J. L. G., et al. (2012). Response of different benthic indices to diverse human pressures. *Ecol. Indic.* 12, 143–153. doi: 10.1016/j.ecolind.2011.03.019

De Reu, J., Plets, G., Verhoeven, G., De Smedt, P., Bats, M., Cherretté, B., et al. (2013). Towards a three-dimensional cost-effective registration of the archaeological heritage. *J. Archaeol. Sci.* 40, 1108–1121. doi: 10.1016/j.jas.2012.08.040

Diefenbacher, E. (2022). Notes on the operation of two types of aquatic remotely operated vehicles used during a mock turtle survey. *J. North Am. Herpetol.* 2022. 1, 20–23.

Dokulil, M. T. (2003). "Algae as ecological bio-indicators,". *Trace metals other contaminants Environ. (Elsevier)* 285–327. doi: 10.1016/S0927-5215(03)80139-X

Drăguţ, L., Csillik, O., Eisank, C., and Tiede, D. (2014). Automated parameterisation for multi-scale image segmentation on multiple layers. *ISPRS J. Photogramm. Remote Sens.* 88, 119–127. doi: 10.1016/j.isprsjprs.2013.11.018

Droppova, V. (2011). The tools of automated generalization and building generalization in an ArcGIS environment. *Slovak J. Civ. Eng.* 19, 1. doi: 10.2478/v10189-011-0001-4

Duarte, C. M. (2002). The future of seagrass meadows. *Environ. Conserv.* 29, 192–206. doi: 10.1017/S0376892902000127

Duarte, B., Martins, I., Rosa, R., Matos, A. R., Roleda, M. Y., Reusch, T. B. H., et al. (2018). Climate change impacts on seagrass meadows and macroalgal forests: an integrative perspective on acclimation and adaptation potential. *Front. Mar. Sci.* 5, 190. doi: 10.3389/fmars.2018.00190

Duffy, J. P., Pratt, L., Anderson, K., Land, P. E., and Shutler, J. D. (2018). Spatial assessment of intertidal seagrass meadows using optical imaging systems and a lightweight drone. *Estuar. Coast. Shelf Sci.* 200, 169–180. doi: 10.1016/j.ecss.2017.11.001

Esri, R. (2011). ArcGIS desktop: release 10. *Environ. Syst. Res. Institute CA*.

Fabbrizzi, E., Scardi, M., Ballesteros, E., Benedetti-Cecchi, L., Cebrian, E., Ceccherelli, G., et al. (2020). Modeling macroalgal forest distribution at Mediterranean scale: Present status, drivers of changes and insights for conservation and management. *Front. Mar. Sci.* 7, 20. doi: 10.3389/fmars.2020.00020

Fallati, L., Saponari, L., Savini, A., Marchese, F., Corselli, C. , and Galli, P. (2020). Multi-temporal UAV data and object-based image analysis (OBIA) for estimation of substrate changes in a post-bleaching scenario on a maldivian reef. *Remote Sens.* 12, 2093. doi: 10.3390/rs12132093

Fu, G., Zhao, H., Li, C., and Shi, L. (2013). Segmentation for high-resolution optical remote sensing imagery using improved quadtree and region adjacency graph technique. *Remote Sens.* 5, 3259–3279. doi: 10.3390/rs5073259

Gaw, L. Y.-F., Yee, A. T. K., and Richards, D. R. (2019). A high-resolution map of singapore's terrestrial ecosystems. *Data* 4, 116. https://doi.org/10.3390/data4030116

Gravina, M. F. M. F., Bonifazi, A., Del Pasqua, M., Giampaoletti, J., Lezzi, M., Ventura, D., et al. (2020). Perception of changes in marine benthic habitats: The relevance of taxonomic and ecological memory. *Diversity* 12, 480. doi: 10.3390/d12120480

Grosso, L., Rakaj, A., Fianchini, A., Tancioni, L., Vizzini, S., Boudouresque, C., et al. (2022). Trophic requirements of the Sea urchin paracentrotus lividus varies at different life stages: Comprehension of species ecology and implications for effective feeding formulations. *Front. Mar. Sci.* 9, 865450. doi: 10.3389/fmars.2022.865450

Hardin, P. J., and Hardin, T. J. (2010). Small-scale remotely piloted vehicles in environmental research. *Geogr. Compass* 4, 1297–1311. doi: 10.1111/j.1749-8198.2010.00381.x

Harmelin-Vivien, M. L., Harmelin, J. G., and Leboulleux, V. (1995). Microhabitat requirements for settlement of juvenile sparid fishes on Mediterranean rocky shores. *Hydrobiologia*, 300, 309–320. doi: 10.1007/BF00024471

Heck, K. L.Jr., Hays, G., Orth, R. J., Heck, K. L., Hays, G., and Orth, R. J. (2003). Critical evaluation of the nursery role hypothesis for seagrass meadows. *Mar. Ecol. Prog. Ser.* 253, 123–136. doi: 10.3354/meps253123

Heumann, B. W. (2011). An object-based classification of mangroves using a hybrid decision tree–support vector machine approach. *Remote Sens.* 3, 2440–2460. doi: 10.3390/rs3112440

Kabiri, K. (2020). Mapping coastal ecosystems and features using a low-cost standard drone: case study, nayband bay, Persian gulf, Iran. *J. Coast. Conserv.* 24, 1–8. doi: 10.1007/s11852-020-00780-6

Kislik, C., Genzoli, L., Lyons, A., and Kelly, M. (2020). Application of UAV imagery to detect and quantify submerged filamentous algae and rooted macrophytes in a non-wadeable river. *Remote Sens.* 12, 1–24. doi: 10.3390/rs12203332

Lakshmi, A., and Rajagopalan, R. (2000). Socio-economic implications of coastal zone degradation and their mitigation: a case study from coastal villages in India. *Ocean Coast. Manage.* 43, 749–762. doi: 10.1016/S0964-5691(00)00057-0

Lechner, A. M., Fletcher, A., Johansen, K., and Erskine, P. (2012). Characterising upland swamps using object-based classification methods and hyper-spatial resolution imagery derived from an unmanned aerial vehicle. *ISPRS Ann. Photogramm. Remote Sens. Spat. Inf. Sci.*, I–4, 101–106. doi: 10.5194/isprsannals-I-4-101-2012

Lee, I.-C., Wu, B., and Li, R. (2009). Shoreline extraction from the integration of lidar point cloud data and aerial orthophotos using mean-shift segmentation. in. *Proc. ASPRS Annu. Conf*, 2, 3033–3040.

Leriche, A., Pasqualini, V., Boudouresque, C.-F., Bernard, G., Bonhomme, P., Clabaut, P., et al. (2006). Spatial, temporal and structural variations of a posidonia oceanica seagrass meadow facing human activities. *Aquat. Bot.* 84, 287–293. doi: 10.1016/j.aquabot.2005.10.001

Letourneur, Y., Ruitton, S., and Sartoretto, S. (2003). Environmental and benthic habitat factors structuring the spatial distribution of a summer infralittoral fish assemblage in the north-western Mediterranean Sea. *J. Mar. Biol. Assoc. United Kingdom* 83, 193–204. doi: 10.1017/S0025315403006970h

Levin, P. S., Kelble, C. R., Shuford, R. L., Ainsworth, C., deReynier, Y., Dunsmore, R., et al. (2014). Guidance for implementation of integrated ecosystem assessments: a US perspective. *ICES J. Mar. Sci.* 71, 1198–1204. doi: 10.1093/icesjms/fst112

Marre, G., Deter, J., Holon, F., Boissery, P., and Luque, S. (2020). Fine-scale automatic mapping of living posidonia oceanica seagrass beds with underwater photogrammetry. *Mar. Ecol. Prog. Ser.* 643, 63–74. doi: 10.3354/meps13338

Marre, G., Holon, F., Luque, S., Boissery, P., and Deter, J. (2019). Monitoring marine habitats with photogrammetry: A cost-effective, accurate, precise and high-resolution reconstruction method. *Front. Mar. Sci.* 6. doi: 10.3389/fmars.2019.00276

Martin, C. S., Giannoulaki, M., De Leo, F., Scardi, M., Salomidi, M., Knitweiss, L., et al. (2014). Coralligenous and maërl habitats: predictive modelling to identify their spatial distributions across the Mediterranean Sea. *Sci. Rep.* 4, 1–8. doi: 10.1038/srep05073

Morris, R. L., Graham, T. D. J., Kelvin, J., Ghisalberti, M., and Swearer, S. E. (2020). Kelp beds as coastal protection: wave attenuation of ecklonia radiata in a shallow coastal bay. *Ann. Bot.* 125, 235–246. https://doi.org/10.1093/aob/mcz127

Morroni, L., Rakaj, A., Grosso, L., Fianchini, A., Pellegrini, D., and Regoli, F. (2020). Sea Cucumber holothuria polii (Delle chiaj) as new model for embryo bioassays in ecotoxicological studies. *Chemosphere* 240, 124819. doi: 10.1016/j.chemosphere.2019.124819

Mumby, P. J., and Edwards, A. J. (2002). Mapping marine environments with IKONOS imagery: enhanced spatial resolution can deliver greater thematic accuracy. *Remote Sens. Environ.* 82, 248–257. doi: 10.1016/S0034-4257(02)00041-X

Nagelkerken, I., Sheaves, M., Baker, R., and Connolly, R. M. (2015). The seascape nursery: a novel spatial approach to identify and manage nurseries for coastal marine fauna. *Fish Fish.* 16, 362–371. doi: 10.1111/faf.12057

Nieuwenhuis, B. O., Marchese, F., Casartelli, M., Sabino, A., van der Meij, S. E. T., and Benzoni, F. (2022). Integrating a UAV-derived DEM in object-based image analysis increases habitat classification accuracy on coral reefs. *Remote Sens.* 14, 5017. doi: 10.3390/rs14195017

Nikolakopoulos, K. G., Kozarski, D., and Kogkas, S. (2017). Coastal areas mapping using UAV photogrammetry. *Earth Resour. Environ. Remote Sensing/GIS Appl. VIII (SPIE)* 10428, 104280O. doi: 10.1117/12.2278121

O'Connor, N. E. (2013). Impacts of sewage outfalls on rocky shores: Incorporating scale, biotic assemblage structure and variability into monitoring tools. *Ecol. Indic.* 29, 501–509. doi: 10.1016/j.ecolind.2013.01.020

Parravicini, V., Rovere, A., Vassallo, P., Micheli, F., Montefalcone, M., Morri, C., et al. (2012). Understanding relationships between conflicting human uses and coastal ecosystems status: a geospatial modeling approach. *Ecol. Indic.* 19, 253–263. doi: 10.1016/j.ecolind.2011.07.027

Pensa, D., Fianchini, A., Grosso, L., Ventura, D., Scardi, M., and Rakaj, A. (2022). Tracking population status and structure of Mediterranean pen shell pinna nobilis after a mass mortality outbreak. *npj biodivers* 1, 3. doi: 10.21203/rs.3.rs-1425249/v1

Pergent-Martini, C., Monnier, B., Lehmann, L., Barralon, E., and Pergent, G. (2022). Major regression of posidonia oceanica meadows in relation with recreational boat anchoring: A case study from Sant'Amanza bay. *J. Sea Res.* 188, 102258. doi: 10.1016/j.seares.2022.102258

Piazza, P., Cummings, V., Guzzi, A., Hawes, I., Lohrer, A., Marini, S., et al. (2019). Underwater photogrammetry in Antarctica: Long-term observations in benthic ecosystems and legacy data rescue. *Polar Biol.* 42, 1061–1079. doi: 10.1007/s00300-019-02480-w

Pipaud, I., and Lehmkuhl, F. (2017). Object-based delineation and classification of alluvial fans by application of mean-shift segmentation and support vector machines. *Geomorphology* 293, 178–200. doi: 10.1016/j.geomorph.2017.05.013

Prado, E., Rodríguez-Basalo, A., Cobo, A., Ríos, P., and Sánchez, F. (2020). 3D fine-scale terrain variables from underwater photogrammetry: A new approach to benthic microhabitat modeling in a circalittoral rocky shelf. *Remote Sens.* 12, 2466. doi: 10.3390/rs12152466

Price, D. M., Robert, K., Callaway, A., Lo Iacono, C., Hall, R. A., and Huvenne, V. A. I. (2019). Using 3D photogrammetry from ROV video to quantify cold-water coral reef

structural complexity and investigate its influence on biodiversity and community assemblage. *Coral Reefs* 38, 1007–1021. doi: 10.1007/s00338-019-01827-3

Rakaj, A., Morroni, L., Grosso, L., Fianchini, A., Pensa, D., Pellegrini, D., et al. (2021). Towards sea cucumbers as a new model in embryo-larval bioassays: Holothuria tubulosa as test species for the assessment of marine pollution. *Sci. Total Environ.* 787, 147593. doi: 10.1016/j.scitotenv.2021.147593

Raoult, V., and Gaston, T. F. (2018). Rapid biomass and size-frequency estimates of edible jellyfish populations using drones. *Fish. Res.* 207, 160–164. doi: 10.1016/j.fishres.2018.06.010

Raoult, V., Reid-Anderson, S., Ferri, A., and Williamson, J. (2017). How reliable is structure from motion (SfM) over time and between observers? a case study using coral reef bommies. *Remote Sens.* 9, 740. doi: 10.3390/rs9070740

Raoult, V., Tosetto, L., and Williamson, J. E. (2018). Drone-based high-resolution tracking of aquatic vertebrates. *Drones* 2, 37. doi: 10.3390/drones2040037

Rende, S. F., Bosman, A., Di Mento, R., Bruno, F., Lagudi, A., Irving, A. D., et al. (2020). Ultra-High-Resolution mapping of posidonia oceanica (L.) delile meadows through acoustic, optical data and object-based image classification. *J. Mar. Sci. Eng.* 8, 647. https://doi.org/10.3390/jmse8090647

Roelfsema, C. M., and Phinn, S. R. (2010). Integrating field data with high spatial resolution multispectral satellite imagery for calibration and validation of coral reef benthic community maps. *J. Appl. Remote Sens.* 4, 43527. doi: 10.1117/1.3430107

Sales, M., Ballesteros, E., Anderson, M. J., Iveša, L., and Cardona, E. (2012). Biogeographical patterns of algal communities in the Mediterranean Sea: Cystoseira crinita-dominated assemblages as a case study. *J. Biogeogr.* 39, 140–152. doi: 10.1111/j.1365-2699.2011.02564.x

Seytre, C., and Francour, P. (2014). A long-term survey of posidonia oceanica fish assemblages in a Mediterranean marine protected area: emphasis on stability and no-take area effectiveness. *Mar. Freshw. Res.* 65, 244–254. doi: 10.1071/MF13080

Shintani, C., and Fonstad, M. A. (2017). Comparing remote-sensing techniques collecting bathymetric data from a gravel-bed river. *Int. J. Remote Sens.* 38, 2883–2902. doi: 10.1080/01431161.2017.1280636

Taddia, Y., Stecchi, F., and Pellegrinelli, A. (2019). Using DJI phantom 4 RTK drone for topographic mapping of coastal areas. *Int. Arch. Photogramm. Remote Sens. Spat. Inf. Sci.* 42, 625–630. https://doi.org/10.5194/isprs-archives-XLII-2-W13-625-2019

Tait, L. W., Orchard, S., and Schiel, D. R. (2021). Missing the forest and the trees: Utility, limits and caveats for drone imaging of coastal marine ecosystems. *Remote Sens.* 13, 3136. doi: 10.3390/rs13163136

Takasu, T., and Yasuda, A. (2009). "Development of the low-cost RTK-GPS receiver with an open source program package RTKLIB," in *International symposium on GPS/GNSS* (Jeju Korea: International Convention Center).

Telesca, L., Belluscio, A., Criscoli, A., Ardizzone, G., Apostolaki, E. T., Fraschetti, S., et al. (2015). Seagrass meadows (Posidonia oceanica) distribution and trajectories of change. *Sci. Rep.* 5, 1–14. doi: 10.1038/srep12505

Ventura, D., Bonifazi, A., Gravina, M. F., Belluscio, A., and Ardizzone, G. (2018). Mapping and classification of ecologically sensitive marine habitats using unmanned aerial vehicle (UAV) imagery and object-based image analysis (OBIA). *Remote Sens.* 10, 1331. doi: 10.3390/rs10091331

Ventura, D., Dubois, S. F. S. F., Bonifazi, A., Jona Lasinio, G., Seminara, M., Gravina, M. F. M. F. M. F., et al. (2020). Integration of close-range underwater photogrammetry with inspection and mesh processing software: a novel approach for quantifying ecological dynamics of temperate biogenic reefs. *Remote Sens. Ecol. Conserv.* 7, 169–186. doi: 10.1002/rse2.178

Ventura, D., Jona Lasinio, G., and Ardizzone, G. (2015). Temporal partitioning of microhabitat use among four juvenile fish species of the genus diplodus (Pisces: Perciformes, sparidae). *Mar. Ecol.* 36, 1013–1032. doi: 10.1111/maec.12198

Ventura, D., Mancini, G., Casoli, E., Pace, D. S. D. S., Lasinio, G. J. G. J., Belluscio, A., et al. (2022). Seagrass restoration monitoring and shallow-water benthic habitat mapping through a photogrammetry-based protocol. *J. Environ. Manage.* 304, 114262. doi: 10.1016/j.jenvman.2021.114262

Williamson, J. E., Duce, S., Joyce, K. E., and Raoult, V. (2021). Putting sea cucumbers on the map: projected holothurian bioturbation rates on a coral reef scale. *Coral Reefs* 40, 559–569. doi: 10.1007/s00338-021-02057-2

Yang, B., Hawthorne, T. L., Hessing-Lewis, M., Duffy, E. J., Reshitnyk, L. Y., Feinman, M., et al. (2020). Developing an introductory UAV/drone mapping training program for seagrass monitoring and research. *Drones* 4, 70. doi: 10.3390/drones4040070

Young, G. C., Dey, S., Rogers, A. D., and Exton, D. (2017). Cost and time-effective method for multiscale measures of rugosity, fractal dimension, and vector dispersion from coral reef 3D models. *PloS One* 12, 1–18. doi: 10.1371/journal.pone.0175341

Zapata-Ramírez, P., Scaradozzi, D., Sorbi, L., Palma, M., Pantaleo, U., Ponti, M., et al. (2013). Innovative study methods for the Mediterranean coralligenous habitats. *Adv. Oceanogr. Limnol.* 4, 102–119. doi: 10.1080/19475721.2013.849758

Zhang, K., and Hu, B. (2012). Individual urban tree species classification using very high spatial resolution airborne multi-spectral imagery using longitudinal profiles. *Remote Sens.* 4, 1741–1757. doi: 10.3390/rs4061741

frontiers | Frontiers in Marine Science

TYPE Original Research
PUBLISHED 20 March 2023
DOI 10.3389/fmars.2023.1111592

Check for updates

OPEN ACCESS

EDITED BY
Elena Maggi,
University of Pisa, Italy

REVIEWED BY
José Lino Vieira De Oliveira Costa,
University of Lisbon, Portugal
Marco C. Brustolin,
Norwegian Institute of Marine Research (IMR), Norway

*CORRESPONDENCE
Alice Oprandi
alice.oprandi@edu.unige.it

SPECIALTY SECTION
This article was submitted to Marine Ecosystem Ecology, a section of the journal Frontiers in Marine Science

RECEIVED 29 November 2022
ACCEPTED 06 March 2023
PUBLISHED 20 March 2023

CITATION
Oprandi A, Atzori F, Azzola A, Bianchi CN, Cadoni N, Carosso L, Desiderà E, Frau F, Garcia Gutiérrez ML, Guidetti P, Morri C, Piazzi L, Poli F and Montefalcone M (2023) Multiple indices on different habitats and descriptors provide consistent assessments of environmental quality in a marine protected area.
Front. Mar. Sci. 10:1111592.
doi: 10.3389/fmars.2023.1111592

COPYRIGHT
© 2023 Oprandi, Atzori, Azzola, Bianchi, Cadoni, Carosso, Desiderà, Frau, Garcia Gutiérrez, Guidetti, Morri, Piazzi, Poli and Montefalcone. This is an open-access article distributed under the terms of the Creative Commons Attribution License (CC BY). The use, distribution or reproduction in other forums is permitted, provided the original author(s) and the copyright owner(s) are credited and that the original publication in this journal is cited, in accordance with accepted academic practice. No use, distribution or reproduction is permitted which does not comply with these terms.

Multiple indices on different habitats and descriptors provide consistent assessments of environmental quality in a marine protected area

Alice Oprandi [1*], Fabrizio Atzori [2], Annalisa Azzola [1], Carlo Nike Bianchi [1,3], Nicoletta Cadoni [2], Lara Carosso [2], Elena Desiderà [3], Francesca Frau [2], Maria Leonor Garcia Gutiérrez [2], Paolo Guidetti [3,4], Carla Morri [1,3], Luigi Piazzi [5], Federica Poli [3] and Monica Montefalcone [1,6]

[1]Seascape Ecology Laboratory (SEL), Distav, Department of Earth, Environmental and Life Sciences, University of Genoa, Genova, Italy, [2]Capo Carbonara Marine Protected Area, Cagliari, Italy, [3]Department of Integrative Marine Ecology (EMI), Genoa Marine Centre (GMC), Stazione Zoologica Anton Dohrn–National Institute of Marine Biology, Ecology and Biotechnology, Genoa, Italy, [4]National Research Council, Institute for the Study of Anthropic Impact and Sustainability in the Marine Environment (CNR-IAS), Genoa, Italy, [5]Department of Chemical, Physical, Mathematical and Natural Sciences, University of Sassari, Sassari, Italy, [6]National Biodiversity Future Center (NBFC), Palermo, Italy

In the last decades, climate change and human pressures have increasingly and dramatically impacted the ocean worldwide, calling for urgent actions to safeguard coastal marine ecosystems. The European Commission, in particular, has set ambitious targets for member states with two major directives, the Water Framework Directive (WFD) and the Marine Strategy Framework Directive (MSFD), both designed to protect the marine environment in EU waters. Diverse biotic indices have accordingly been developed to assess water and habitat quality. The WFD adopts four Biological Quality Elements (BQEs), whereas the MSFD recommends a set of eleven qualitative descriptors. The borderline between water quality and habitat quality is hard to trace and so far most assessments have involved the use of a few indices and were mainly related to a single BQE or qualitative descriptor. In this study, thanks to the availability of a large dataset encompassing a wide array of descriptors, we compared the performance of 11 biotic indices relative to three habitats/biotic components (reefs, seagrass, and fish) of the Marine Protected Area (MPA) of Capo Carbonara (SE Sardinia, Italy). The aim was to assess whether the indices were consistent in defining the environmental status in the MPA investigated. We used the graphical approach RESQUE (REsilience and QUality of Ecosystem), which enabled us to obtain a single and comprehensive measure of the status of the environment by integrating several metrics. This approach was applied here to different habitats for the first time. All indices were consistent with each other in confirming the good status of Capo Carbonara MPA. The use of RESQUE provided insights to interpret the differences between water quality, defined according to the WFD, and habitat

quality, defined according to the MSFD. Differences between the two EU directives, in terms of either requirements or goals, have long been discussed but the present study highlights for the first time that they are congruent in their assessment of the environmental status of marine ecosystems.

KEYWORDS

water quality, habitat quality, marine biotic indices, water framework directive, Marine Strategy Framework Directive , Mediterranean Sea

1 Introduction

Over the last decades, the need for assessment of the state of the natural environment has become a primary concern. Marine habitats, under increasing human pressure, are declining at an accelerating rate (Claudet and Fraschetti, 2010). Change is now affecting so many compartments and levels of the ecosystems that, while easily perceived, the phenomenon is challenging to quantify (Sala et al., 2000). To address this need, diverse biotic indices have been developed based on different target organisms or habitats deemed particularly sensitive to alterations of the surrounding environment (Birk et al., 2012). In addition, there is a growing trend to develop novel indices that consider the resources required to make an ecosystem function (Rigo et al., 2020, 2021), the ecological complexity (Paoli et al., 2016) or the environmental DNA (Pawlowski et al., 2018). Indices typically provide measures of the structure, function or some particular characteristics of marine communities that show a predictable response to anthropogenic disturbances. Regardless of the wide range of indices available, there is to date no rule for the proper selection of an index or a combination of indices that should be used in the assessment of the environmental quality (Borja et al., 2015).

Across the European seas, the use of biotic indices to define the ecological quality of the marine environment has been strongly supported by two consecutive EU directives: the Water Framework Directive (WFD, Directive 2000/60/EC) and the Marine Strategy Framework Directive (MSFD, Directive 2008/56/EC). The WFD suggests the use of four Biological Quality Elements (BQEs) (i.e., phytoplankton, aquatic flora, benthic invertebrates, and fish) through which a measure of water quality can be obtained and ranked, on the basis of their abundance, diversity, biomass, distribution and/or cover. The MSFD describes the quality of the habitat on the basis of 11 qualitative descriptors (Annex 1) (Borja et al., 2013). The overlapping of the two European directives has generated some confusion in the distinction between 'water quality' and 'habitat quality': the two compartments might not be equivalent, as water naturally has a more rapid turnover with respect to the whole habitat. In practice, however, the borderline between water quality and habitat quality is hard to trace and indices initially created for the WFD in 2000 were then adopted for the MSFD in 2008 and are still widely used today. All the indices considered in the present paper may be taken as responsive to the requirements of both directives. In both the MSFD and WFD, the good status of the environment may correspond to the so-called reference condition from which the change is measured, in the absence of pre-disturbance historic data or data referring to analogous pristine areas (Smit et al., 2021).

Marine Protected Areas (MPAs), where the goal of marine conservation dovetails with the regulated use of marine resources (i.e., fishing) (Grorud-Colvert et al., 2021), have gained further relevance in this context as they are often taken as a reference point, and improved environmental conditions are expected to be found there (Bianchi et al., 2022; Fraschetti et al., 2022). Most of the priority habitats and valuable species with conservation priority considered in the EU directives and typically included in MPAs, are concentrated in coastal areas (Vassallo et al., 2020), where they are also exposed to multiple pressures (Azzola et al., 2023). The alteration of the natural environment due to anthropogenic and natural disturbances may be more evident if the flora and fauna are investigated together (Smit et al., 2021). The quality of the marine environment is often assessed on the basis of a single index and/or the status of a single indicator, which can be an oversimplification. The combination of several metrics has been proved to be more accurate than the use of single metrics in habitat assessment (Pinto et al., 2009; Ruitton et al., 2014; Rastorgueff et al., 2015; Sartoretto et al., 2017; Thibaut et al., 2017; Enrichetti et al., 2019; Astruch et al., 2022). The challenge is to understand the complexity of coastal systems by considering all their components without trying to oversimplify them (Paoli et al., 2016).

The present study aims to compare 11 biotic indices with reference to three habitats/biotic components (*i.e.*, reefs, seagrass, and fish) of the Marine Protected Area (MPA) of Capo Carbonara (SE Sardinia, Italy). Although data have been collected in the frame of distinct projects with different specific objectives focused on single descriptors each time, the resulting large dataset offers a unique opportunity to compare the performance of a variety of indices. We used the graphical approach RESQUE (REsilience and QUality of Ecosystem), which provides a single and comprehensive measure of the status of the environment by integrating several metrics (Oprandi et al., 2021), here applied to different habitats for the first time.

2 Material and methods

2.1 Study area

The Capo Carbonara MPA has been in existence since 1998, and it is recognized as a Specially Protected Area of Mediterranean

Importance (SPAMI) due to its ecologically significant habitats and the presence of rare, threatened, and/or endemic species. It is located around the south-eastern tip of Sardinia Island (Italy) (39° 5.626'N; 9° 31.462'E), where it covers a surface area of 14,360 ha and comprises about 31 km of coastline, including two minor islets: Cavoli and Serpentara (Figure 1). A complete description and map of the benthic habitats of the area can be found in Andromède (2017): seagrass meadows, formed by *Posidonia oceanica*, are located between about 5 m and 35 m, in three large patches; shallow reefs, where macroalgal communities thrive, are located all around the main coast and the islets; deeper reefs, including coralligenous reefs down to about 45 m depth, are mostly found in relation with the islets and rocky shoals.

2.2 Data collection and sampling activities

All data were collected independently during two consecutive summers, in 2020 and 2021, within the Capo Carbonara MPA. As the specific target habitats (fish, seagrass and reefs) were not necessarily present in the same territorial units within the investigated MPA, sampling sites did not always overlap for the different targets assessed in this study. Fish assemblages were studied in 2021, seagrass and reefs in 2020 (shallow reefs and deep reefs surveyed separately at distinct sites). Data were collected following a sampling design stratified per habitat, with survey sites randomly placed within each habitat type. We collated *a posteriori* all the data available to calculate 11 indices (Table 1). Each index provided information on the status of a specific ecosystem or biotic component (reef, seagrass or fish), and matched at least one of the three, out of four, Biological Quality Elements (BQEs) for coastal and transitional waters advocated by the WFD (i.e., aquatic flora; benthic invertebrates; fish) and one of the five, out of eleven, qualitative descriptors set out by the MSFD (i.e., biodiversity; non-indigenous species; exploited fish; food web; seafloor integrity).

2.2.1 Indices describing the 'fish' component

Data on fish assemblages were collected at 5 sites all characterized by rocky reefs (Figure 1), as the inherent complexity of these habitats is known to support fish diversity (Lingo and Szedlmayer, 2006). Fish assemblages were assessed by scuba diving in a depth range of 5–18 m through underwater visual census along non-overlapping random transects of 25 m × 5 m (Harmelin-Vivien et al., 1985). A total of 16 transects were surveyed per site. Sampling was repeated at two random times through the study year, for a total of 160 visual census transects. Abundance and size (total length) of all fishes encountered along each transect were recorded by trained diving scientists. Fish biomass was estimated from size data by means of length–weight relationships (Froese and Pauly, 2018), then the total biomass of fish per transect (expressed in g m^{-2}) was used to calculate the indices (Morey et al., 2003; Guidetti et al., 2014).

- *Fish H'*. Diversity of the fish community was estimated using the Shannon–Wiener diversity index, performed on the data matrix of fish biomass by means of the free software PaSt (Hammer et al., 2001).
- *Exploited Fish*. The total biomass of exploited fish per site was calculated considering only the 23 species targeted by commercial and recreational fisheries listed by Di Franco et al. (2009).
- *High Level Predators*. The abundance of top carnivores has been suggested as an indicator of the integrity of the marine

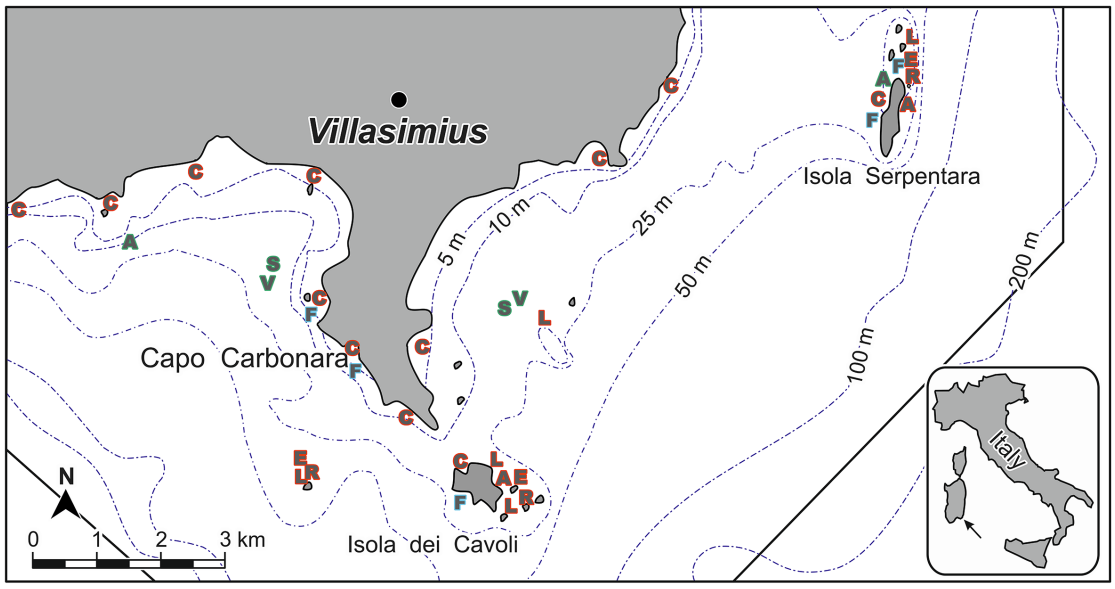

FIGURE 1
Survey sites within the study area. Colors refer to the different habitat/biotic components (blue: fish; red: reef; green: seagrass) for which indices provide information. Capital letters indicate the measured index: A (ALEX); C (CARLIT); E (ESCA); F (all three fish indices); L (LIMA); R (COARSE); S (SI); V (CI).

TABLE 1 List of the indices adopted in the present study and their corresponding Biological Quality Elements (BQEs) and qualitative descriptors according to the European directives.

Index	Habitat/ Biotic component	Biological Quality Elements (WFD)	Qualitative descriptors (MSFD)	Recovery time
Fish H'	Fish	Fish fauna	1 Biodiversity	fast
CARLIT	Reef	Aquatic flora	1 Biodiversity	fast
ESCA	Reef	Aquatic flora and benthic invertebrates	1 Biodiversity	medium
$ALEX_S$	Seagrass	Aquatic flora	2 NIS	medium (or not evaluable)
$ALEX_R$	Reef	Aquatic flora	2 NIS	medium (or not evaluable)
SI	Seagrass	Aquatic flora	2 NIS	medium
Exploited Fish	Fish	Fish fauna	3 Exploited fish	fast
Fish (High Level Predators)	Fish	Fish fauna	4 Food web	fast
LIMA	Reef	Aquatic flora and benthic invertebrates	6 Seafloor integrity	slow
COARSE	Reef	Aquatic flora and benthic invertebrates	6 Seafloor integrity	slow
CI	Seagrass	Aquatic flora	6 Seafloor integrity	slow

food web structure (Bianchi and Morri, 1985; Heithaus et al., 2008). Fishes belonging to the category of High Level Predators (HLP) were selected on the basis of the Trophic Level, using the information on diet from previous Mediterranean studies (Stergiou and Karpouzi, 2002; Froese and Pauly, 2011; Sala et al., 2012). Based on the literature and according to our expert judgement, we set the threshold of 3.65 as the minimum trophic level value for a species to be included in the category, and then the total biomass of HLP per site was estimated.

2.2.2 Indices describing the 'reef' habitat

Surveys were carried out from the surface down to about 40 m depth, at different sites within the MPA depending on the index considered.

- *CARLIT*. Shallow benthic communities of rocky substrate dominated by macroalgae were visually investigated through the CARLIT (Cartography of Littoral and upper-sublittoral rocky-shore communities) method (Ballesteros et al., 2007). Observations were done from the boat, considering only macroalgal communities between 20 cm above and 50 cm below the surface. The sampling unit was 50 linear meters, at 12 sites randomly dispersed along the 31 km of the MPA coastline, including the two islets of Serpentara and Cavoli.
- *ESCA*. Circalittoral benthic communities, including macroalgal assemblages and sessile invertebrates typical of coralligenous reefs, were assessed using the ESCA (Ecological Status of Coralligenous Assemblages) index (Cecchi et al., 2014; Piazzi et al., 2017a). Vertical rocky walls at three sites within the MPA were investigated at about 35 m depth by means of photographic sampling. At each site, a total of 30 photographic samples of 0.2 m^2 were collected across three areas 10 m apart from each other.
- *$ALEX_R$*. Non-indigenous macroalgal species (no information on the invertebrate fauna was available, while non-indigenous fish species were not recorded) detected within the sessile assemblages of hard bottom habitats have been quantified through the application of ALEX (ALien Biotic IndEX) (Çinar and Bakir, 2014; Piazzi et al., 2015), here renamed $ALEX_R$ to indicate that it was applied to reefs. Two sites were selected, then the sampling was carried out on shallow and deep rocky bottoms, respectively at 5 and 30 m depth, in three replicates of 400 cm^2 (within which area all macroalgae were collected by scraping). A total substrate area of 2400 cm^2 was sampled per site.
- *LIMA*. The environmental quality of rocky reefs and the seascape complexity were assessed through the implementation of the LIMA index (Gobert et al., 2014), with some adjustments. Data were collected along depth transects from a depth of about 40 m to the surface at five sites. Compared to the original formulation of LIMA, we considered as negative the scores attributed to the typology 'dead matte' and 'sandy-muddy' in the topographical description, as their occurrence is deemed to reduce the submerged seascape value; similarly, the biological indicator 'invasive species' was subtracted, instead of added, in the biological description formula, as aliens are universally perceived as harmful for the native communities (Morri et al., 2019). With these adjustments, the final index increases as the quality of the site increases.
- *COARSE*. The three-dimensional structure of coralligenous reefs, together with their biotic cover and conspicuous species richness, were assessed using the COARSE

(COralligenous Assessment by Reef Scape Estimation) index (Gatti et al., 2015). Three sites within the MPA were investigated at about 35 m depth through the RVA (Rapid Visual Assessment) method proposed by Gatti et al. (2012), replicated three times at each site.

2.2.3 Indices describing the 'seagrass' habitat

Four sites within *Posidonia oceanica* meadows were investigated by scuba diving. Field activities included visual surveys of the seafloor at random isolated stations and collection of samples depending on the index considered.

- *ALEX*$_S$. Non-indigenous species (NIS) of macroalgae (no data were available for the fauna) detected within the *P. oceanica* seagrass meadows were quantified using ALEX (Piazzi et al., 2015, 2021a), here renamed ALEX$_S$ to indicate that it was applied to seagrass meadows. Two sites were selected to sample shallow and deep areas of bare 'matte' (tangle of seagrass rhizomes and roots with trapped sediment, without living shoots) at the edge of the meadows, in three replicates of 400 cm^2 (area within which all macroalgae were manually sampled) for a total of 2400 cm^2 of bottom area sampled per site.
- *CI*. Loss of *P. oceanica* meadow areas, mostly due to human induced disturbances, was assessed by means of the Conservation Index (CI) (Moreno et al., 2001; Montefalcone, 2009). Percent cover data of the seabed by dead matte and living *P. oceanica* were visually estimated at the lower limit, at the upper limit and in the central sector of two *P. oceanica* meadows for a total of 18 visual surveys per site.
- *SI*. The extent of colonization by less structuring species than *P. oceanica*, such as the other Mediterranean seagrass *Cymodocea nodosa* and the green algae of the genus *Caulerpa*, was assessed through the Substitution Index (SI) (Montefalcone, 2009). Data on percent cover of the bottom by substitute species were visually estimated at the lower limit, at the upper limit and in the central sector of two *P. oceanica* meadows for a total of 18 visual surveys per site.

2.3 Implementation of RESQUE approach

In order to test whether the different indices were consistent in defining the environmental status of the MPA and to highlight either concordant or discordant responses, data were normalized to obtain comparable values within the range between 0 and 1. To this end, the Ecological Quality Ratio (EQR) was estimated for each index by dividing the measured values for a reference value and then its mean value was graphically depicted on a radar chart. In the absence of known references for the territorial unit under investigation, reference values were calculated as the average of the three highest values of the considered metric after having discarded the maximum, following the protocol established by Gobert et al. (2009). However, expert advice has been elicited to set references whenever necessary (e.g., in case of conditions with little variability and low environmental quality); all experts are included among the authors of the present paper. The complement to unit (1-EQR) of SI was calculated to make the index increase with the quality of the habitat and to allow comparison with the other indices.

Following the RESQUE approach, the total area of the polygon resulting from the radar chart was considered as a measure of the overall environmental quality. The consistency among indices was expressed by the circularity of the polygon perimeter and has been interpreted as a measure of resilience (Oprandi et al., 2021). Area (in pixels) and circularity of polygons were computed using the software Adobe Photoshop® CC.

3 Results

3.1 Indices values

Biodiversity

The quality and occurrence of habitats, and the distribution and abundance of species were described by three out of eleven measured indices: Fish H', CARLIT (shallow water macroalgae) and ESCA (macroalgae and sessile invertebrates). Fish H' ranged between 1.59 and 1.72 across the five sites investigated with an average of 1.64 ± 0.05. CARLIT ranged between 0.738 (good status) and 0.989 (high status) showing an average value of 0.829 ± 0.07, which revealed an overall high status of shallow water macroalgal communities. ESCA showed very little variation between sites, displaying an average value of 0.847 ± 0.05 that revealed again a high status of coralligenous benthic assemblages.

Non-indigenous Species

The evidence that the presence of NIS was at levels that did not adversely alter the ecosystems was provided by three of the indices measured: ALEX$_R$, ALEX$_S$ and SI. ALEX$_R$ exhibited values ranging from moderate (0.632) to high (1), while ALEX$_S$ ranged from good (0.716) to high (0.983). Overall, ALEX$_R$ showed a high status (0.901 ±0.13), while ALEX$_S$ only had a good status (0.851± 0.07). SI showed a moderate status (0.30) at only one of the sites investigated, while no substitute species was detected in the other *P. oceanica* meadows. The average SI value was 0.05±0.12, corresponding to a high status.

Exploited fish

The biomass of the target species ranged from 32.7 g m^{-2} to 68.7 g m^{-2}, with an average value of 53.8 ± 15.3 g m^{-2}.

Food web

The biomass of High Level Predators was taken into account in the assessment of the food web status. Biomass of HLP ranged from a minimum of 11.42 g m^{-2} to a maximum of 33.9 g m^{-2}, with an average of 24.4 ± 9.5 g m^{-2}.

Seafloor integrity

Information about the structure and functions of the benthic ecosystems was obtained through the indices LIMA, COARSE and CI. LIMA varied widely between the five sites surveyed, from poor (0.38) to good (0.78) status, overall showing a moderate status (0.59), possibly due to the complexity of the MPA seascapes. COARSE showed little variation between the three sites, exhibiting an overall high status (2.48± 0.29) of coralligenous reefs. CI ranged from 0.50 (moderate status) to 0.83 (good status) showing an average value of 0.63 ± 0.14, which ultimately revealed a moderate conservation status of the meadows.

3.2 Comparison through the RESQUE approach

Overall, the eleven indices analyzed through the RESQUE approach showed consistent responses, as confirmed by the quite rounded shape of the irregular hendecagon and the resulting high value of circularity (0.848) (Figure 2). Polygon area (132060 pixels) corresponded to 73% of the area of an ideal regular hendecagon (180258 pixels) where all EQR values are equal to 1 (circularity: 0.877) (Figure 2). In particular, the indices describing *Biodiversity* and *NIS* showed the highest values of EQR (on average 0.91 ± 0.06 and 0.91± 0.04, respectively) and were followed by the *Seafloor integrity* indices with a mean EQR of 0.83 ± 0.09, the *Exploited fish* index with an EQR value of 0.78 ± 0.11, and lastly by the *Food webs* index with an EQR of 0.72 ± 0.16 (Figure 3).

When indices were grouped according to the BQEs indicated by the WFD, their EQR values showed virtually no differences. *Benthic invertebrates*' indices (i.e., ESCA, LIMA and COARSE) showed the higher mean EQR value corresponding to 0.88 ± 0.09, followed by the *Aquatic flora* indices (i.e., CARLIT, $ALEX_R$, $ALEX_S$, 1-SI, CI) with a mean EQR of 0.86 ± 0.07 and the *Fish* fauna indices (H', Exploited fish and HLP) with an EQR equal to 0.82 ± 0.12 (Figure 3).

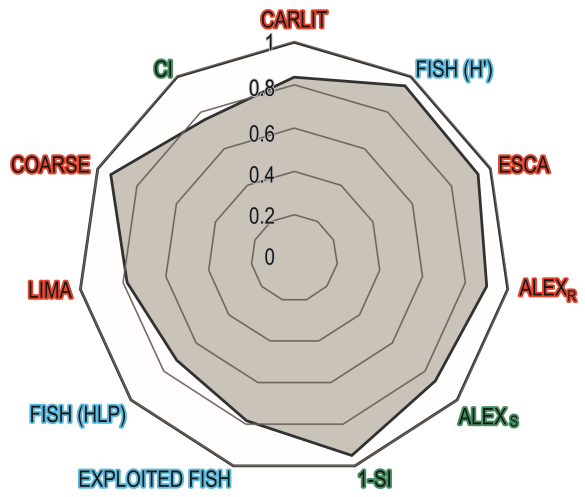

FIGURE 2
Polygon resulting from the EQR scores of all the indices (grey shape). An ideal hendecagon (white polygon) is shown below as a reference. Colors refer to the different habitat/biotic components (blue: fish; red: reef; green: seagrass) for which indices provide information.

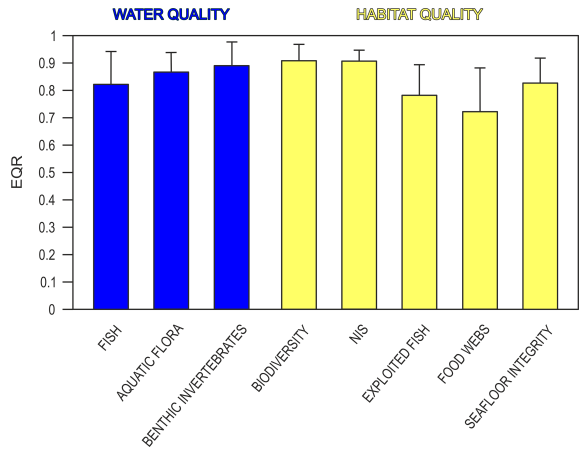

FIGURE 3
Mean EQR scores according to the indices of Water quality (blue) and Habitat quality (yellow).

4 Discussion

To reliably assess the state of the marine environment, considering as many habitats and biotic components as possible, is desirable, as single indicators/indices may provide only partial answers (Rombouts et al., 2013; Smit et al., 2021). The dataset collated for the present study has enabled us to consider three out of the four BQEs mentioned in the WFD and five out of the 11 qualitative descriptors listed in the MSFD. Being based on a significant proportion of the biological indicators suggested by the abovementioned EU directives, the analysis we carried out can be considered a useful alternative when more specific assessments with purposely planned sampling designs cannot be applied.

Indices are indeed suitable and easy to use tools for management purposes (Gatti et al., 2012), but when possible analytical approaches such as BACI and beyond BACI (Underwood, 1994; Smith, 2002; Christie et al., 2019) should be preferred to get a solid assessment of environmental status or of the impacts occurred in a certain area. These approaches, however, require data collected specifically according to dedicated protocols, which was not the case for the present study.

We utilized data collected for different purposes, with specific and distinct sampling designs, which certainly represents one of the limitations of our study. Of course, some important habitats/biotic components (e.g., soft bottom) were not taken into account, but the main aim of our work was not to explore all the marine habitats included within the MPA, nor to verify the efficacy of the protection regime, but rather to see whether a number of components of the marine environment that are customarily considered by environmental agencies and administrations were in agreement in terms of state of the environment. Even with a dedicated study, sampling all the habitats/biotic components of the MPA would have required a huge effort in terms of funds, time, and people, and

therefore be virtually impossible to implement. The monitoring activities that are carried out more or less regularly in the MPA enabled us to dispose of a large dataset covering most of the environmental features of the study area.

The problem is not only the availability of data but also how to assess the whole to achieve an unequivocal measure of the ecosystem status, avoiding loss of information. The risk, when considering many different or conflicting responses together, is to fail to interpret them and thus simplify the final result (Gatti et al., 2012; Gatti et al., 2015; Thibaut et al., 2017; Mancini et al., 2020). The RESQUE approach had already revealed its potential in comparing different metrics related to the same ecosystem (seagrass meadows), whether it changed over time or space (Oprandi et al., 2021, 2022). Here, it also proved to be effective in the comparison of indices relating to different habitats and biological components, clearly showing that all the indices were highly congruent. In contrast, previous Mediterranean studies comparing different indices in soft bottom habitats provided results that were not conclusive or were even contradictory (Occhipinti Ambrogi et al., 2009; Reizopoulou et al., 2014; Sánchez-Moyano et al., 2017; Magni et al., 2023). Peleg et al. (2023) found only "some consistent patterns" when using nine health indicators to assess the status of rocky reefs in New Zealand.

The available reference classifications of indices are often inadequate when the geographical context is different from the one in which they were originally created (Pinto et al., 2009). The method we used does not actually require the use of reference classifications, but is based on the calculation of EQRs, and thus on the identification of a reference value for each index, which represents the best obtainable value for that index in the investigated area (Oprandi et al., 2021). Having a large available dataset is a key asset in order to identify reference values consistent with local scale patterns (Smit et al., 2021). In the case of Capo Carbonara MPA, it was possible to successfully apply the RESQUE approach thanks to the availability of a considerable amount of data which, being collected in independent studies, were designed to maximize information in the study area.

For simplicity, in the present work, we have referred to the method of Gobert et al. (2009) for the identification of the reference values, which is widely used by the Italian environmental agencies in their monitoring plans. This approach, however, implies that particularly low EQR values can only be observed when there is great variability in the data. Thus, values close to 1 could also be observed in the case of conditions with little variability but low environmental quality. This was never the case for Capo Carbonara MPA: all indices, taken individually, presented ecological status between good and high, and the data used to calculate them showed high variability.

The choice of reference is a hotly-debated issue that has no univocal answers (Muxika et al., 2007; Borja et al., 2012). Standardizing (i.e., bring all values in the range 0-1) remains the correct thing to do (Legendre and Legendre, 2012). However, a better definition of the references and related EQR calculation would certainly be desirable; to this end, expert judgement is a key tool to include. Future studies may explore further this issue to find more effective ways of providing a reference for the EQR.

We assumed that an ideal hendecagon, which is obtained when all indices values reach their maximum (i.e., are equal to 1), was the benchmark describing the best conditions for the Capo Carbonara MPA, corresponding to a high environmental status. Area and circularity values of the polygon obtained from RESQUE analysis corresponded to 73% and 97%, respectively, of those of the ideal hendecagon: thus, all the indices considered not only provided strong suggestive evidence that support the good status of Capo Carbonara MPA, but also – and even more importantly – that they are fully consistent.

NIS and Biodiversity are, by far, the descriptors that contributed the most to the overall good status of the MPA. Paradoxically, NIS also represents the only descriptor that should not be directly affected by the protection. There is evidence, however, that habitat maintenance contributes, to some extent, to limiting NIS establishment (Bernardeau-Esteller et al., 2020; Houngnandan et al., 2022). The general healthy status of the benthic communities within the MPA possibly manages to keep allochthonous species at a rather low level (Piazzi et al., 2021a). This is particularly true with regard to *Posidonia oceanica* meadows, as NIS substitutes are known to settle mostly on dead matte areas rather than within dense canopies of living shoots (Oprandi et al., 2014; Montefalcone et al., 2015; Piazzi et al., 2016). In Capo Carbonara MPA, the values of the Conservation Index, which measures meadow degradation (by comparing the cover of dead matte with that of living *P. oceanica*), indicated a reduced state of conservation in some areas inside the meadow, which likely facilitated the establishment of NIS. In fact, the mean value of $ALEX_S$ was slightly lower than $ALEX_R$. The reduced abundance of macroalgal NIS could be the result of successive colonization stages that led to the achievement of a balance between native and NIS assemblages (Boudouresque and Verlaque, 2012). It is likely that the general healthy status of the benthic communities manages to limit the expansion of NIS in the study area (Piazzi et al., 2021a).

According to CARLIT, more than 50% of the rocky coastline of the Capo Carbonara AMP is characterized by species with a medium to medium-high level of sensitivity (Ballesteros et al., 2007; Atzori et al., 2020), thus indicating good water quality. Similarly, the ESCA index, which is known to be sensitive to human disturbances (Piazzi et al., 2021b), displayed high values. These outcomes underline how proper management can positively affect both shallow macroalgal communities and circalittoral coralligenous assemblages.

The benefits of protection on fish biomass and abundance are well known (Guidetti et al., 2014), and can be perceived over a time span of 5 to 20 years (Edgar et al., 2009; Babcock et al., 2010), while the reserve effect on fish diversity is still debated, as it may depend on the time since the enforcement of the protection and other factors not yet fully elucidated. A recent study showed that a stabilizing effect on fish biodiversity is apparent within 4 years since the establishment of an MPA (Pettersen et al., 2022): Capo Carbonara MPA was established about 20 years ago.

COARSE was created in the frame of the MSFD, for the specific purpose of providing information on seafloor integrity (Gatti et al., 2015). The index consists of three distinct parts concerning bioconstruction, biodiversity, and the three-dimensional structure

of the coralligenous habitat. These are able to detect alterations in the environmental quality that are not only related to human pressure. In particular, the diversity of the intermediate layer and the conditions of the upper layer seem to be sentinels of climate change (Piazzi et al., 2017b). Recent comparative studies reported significant changes in the deep reef communities of Capo Carbonara MPA over the last 20 years (Azzola et al., 2022), including a local mass mortality event of gorgonians following summer heatwaves (Piazzi et al., 2021b). Boundaries of MPAs do not constitute a physical barrier against sea warming. However, the high COARSE value we found, may indicate high resilience of the coralligenous reefs of Capo Carbonara MPA.

CI and LIMA indices, adopted to assess seafloor integrity, reported comparatively lower values. However, both indices consider benthic associations that have a wider distribution and bathymetric range than coralligenous reefs and are, therefore, potentially exposed to greater risk of impact and a greater natural variability. CI in particular may have been affected by leisure boating, as signs of anchoring were reported during routine monitoring activities on *P. oceanica* meadows (Montefalcone and Oprandi, 2020). With regard to LIMA, it should be emphasized that the formulation of this index takes the topography of the seabed into account when assessing habitat complexity. This can be to the detriment of the biological part at those sites where, notwithstanding equal presence of species, bottom rugosity is lower.

Indices of exploited fish and food webs (Exploited fish and HLP) showed similar trends as they focus mostly on the same species: approximately 75% of high-level predators are actually commercially exploited. The average biomasses of exploited fish and HLP we estimated in Capo Carbonara MPA are comparable to those found in other regional-scale studies where the MPA management was deemed sufficient to obtain measurable effects on fish (Di Franco et al., 2009; Guidetti et al., 2014; Guidetti et al., 2019; Rojo et al., 2021).

Besides the comparison of different indices, the use of RESQUE provided some valuable insights into the way of interpreting the differences between water quality, defined according to the WFD, and habitat quality, defined according to the MSFD. This type of analysis strengthened our results, because apparently both Good Ecological Status and Good Environmental Status were achieved in the Capo Carbonara MPA. The differences, in terms of requirements and goals, between the two European directives have long been discussed (Borja et al., 2010), but the present study evidences for the first time that they are congruent in their assessments of the status of marine ecosystems.

The necessity of using a combination of several indicators to define the quality of the marine environment has been emphasized more than once. To date, there is no risk of failing to achieve this objective given the number of existing indices. The question is no longer just how (structural approach vs. functional approach) to assess what (water quality or habitat quality), but more importantly, with which metrics/indices and how many (Borja et al., 2015).

Although our study has been carried out at a local scale, the approach used here offers a starting point for further work in the near future, as biological indicators are being implemented at broader scales (Fraschetti et al., 2022). We consider that our approach may represent an example to be followed in other areas where monitoring data are available, in comparative studies involving both protected and unprotected environments.

Data availability statement

The raw data supporting the conclusions of this article will be made available by the authors, without undue reservation.

Author contributions

AO: conceptualization, investigation, data analysis, and writing original draft – review & editing. FA: writing – review & editing. AA: investigation and data analysis. CNB: conceptualization, data analysis, and writing – review & editing. NC: investigation and data analysis. LC: data analysis. ED: investigation and writing – review & editing. FF: investigation and data analysis. MG: investigation. PG: investigation and writing – review & editing. CM: data analysis and writing – review & editing. LP: investigation, data analysis, and writing – review & editing. FP: data analysis and writing – review & editing. MM: investigation, supervision, and project administration. All authors contributed to the article and approved the submitted version.

Acknowledgments

Work carried out in the frame of the agreement between Capo Carbonara MPA and SEL (University of Genoa). Thanks are especially due to Luca Marci for his support during field activities.

Conflict of interest

The authors declare that the research was conducted in the absence of any commercial or financial relationships that could be construed as a potential conflict of interest.

Publisher's note

All claims expressed in this article are solely those of the authors and do not necessarily represent those of their affiliated organizations, or those of the publisher, the editors and the reviewers. Any product that may be evaluated in this article, or claim that may be made by its manufacturer, is not guaranteed or endorsed by the publisher.

References

Andromède, (2017). *Inventaire et cartographie des biocénoses marines de l'Aire Marine Protégée Capo Carbonara – Sardaigne (Italie)* (France: Contrat Andromède Océanologie / Agence de l'Eau RMC / Area Marina Protetta Capo Carbonara).

Astruch, P., Orts, A., Schohn, T., Belloni, B., Ballesteros, E., Bianchi, C. N., et al. (2022). "Towards an ecosystem-based index to assess the ecological status of Mediterranean coastal detrital bottoms," in *Proceedings of the 4th Mediterranean symposium on the conservation of coralligenous & other calcareous bio-concretions*. Eds. C. Bouafif and A. Ouerghi (Tunis, TN: SPA/RAC Publications), 137–138.

Atzori, F., Cadoni, N., Carosso, L., Frau, F., and Garcìa Gutiérrez, M. L. (2020). *Monitoraggio dello stato ecologico delle acque costiere dell'area marina protetta "Capo carbonara" secondo la metodologia CARLIT* (Villasimius (IT: Area Marina Protetta Capo Carbonara).

Azzola, A., Atzori, F., Bianchi, C. N., Cadoni, N., Frau, F., Mora, F., et al. (2022). Variability between observers does not hamper detecting change over time in a temperate reef. *Mar. Environ. Res.* 177, 105617. doi: 10.1016/j.marenvres.2022.105617

Azzola, A., Picchio, V., Asnaghi, V., Bianchi, C. N., Morri, C., Oprandi, A., et al. (2023). Troubles never come alone: outcome of multiple pressures on a temperate rocky reef. *Water* 15 (4), 825. doi: 10.3390/w15040825

Babcock, R. C., Shears, N. T., Alcala, A. C., Barrett, N. S., Edgar, G. J., Lafferty, K. D., et al. (2010). Decadal trends in marine reserves reveal differential rates of change in direct and indirect effects. *Proc. Natl. Acad. Sci. U.S.A.* 107, 18256–18261. doi: 10.1073/pnas.0908012107

Ballesteros, E., Torras, X., Pinedo, S., Garcìa, M., Mangialajo, L., and De Torres, M. (2007). A new methodology based on littoral community cartography for the implementation of the European water framework directive. *Mar. pollut. Bull.* 55, 172–180. doi: 10.1016/j.marpolbul.2006.08.038

Bernardeau-Esteller, J., Marín-Guirao, L., Sandoval-Gil, J. M., García-Muñoz, R., Ramos-Segura, A., and Ruiz, J. M. (2020). Evidence for the long-term resistance of *Posidonia oceanica* meadows to *Caulerpa cylindracea* invasion. *Aquat. Bot.* 160, 103167. doi: 10.1016/j.aquabot.2019.103167

Bianchi, C. N., Azzola, A., Cocito, S., Morri, C., Oprandi, A., Peirano, A., et al. (2022). Biodiversity monitoring in Mediterranean marine protected areas: Scientific and methodological challenges. *Diversity* 14 (1), 43. doi: 10.3390/d14010043

Bianchi, C. N., and Morri, C. (1985). Polychaetes as descriptors of the trophic structure of benthic marine ecosystems. *Oebalia* 11, 203214.

Birk, S., Bonne, W., Borja, A., Brucet, S., Courrat, A., Poikane, S., et al. (2012). Three hundred ways to assess europe's surface waters: an almost complete overview of biological methods to implement the water framework directive. *Ecol. Indic.* 18, 31–41. doi: 10.1016/j.ecolind.2011.10.009

Borja, Á., Dauer, D. M., and Grémare, A. (2012). The importance of setting targets and reference conditions in assessing marine ecosystem quality. *Ecol. Indic.* 12 (1), 1–7. doi: 10.1016/j.ecolind.2011.06.018

Borja, Á., Elliott, M., Andersen, J. H., Cardoso, A. C., Carstensen, J., Ferreira, J. G., et al. (2013). Good environmental status of marine ecosystems: what is it and how do we know when we have attained it? *Mar. pollut. Bull.* 76 (1-2), 16–27. doi: 10.1016/j.marpolbul.2013.08.042

Borja, Á., Elliott, M., Carstensen, J., Heiskanen, A. S., and van de Bund, W. (2010). Marine management–towards an integrated implementation of the European marine strategy framework and the water framework directives. *Mar. pollut. Bull.* 60 (12), 2175–2186. doi: 10.1016/j.marpolbul.2010.09.026

Borja, Á., Marín, S. L., Muxika, I., Pino, L., and Rodríguez, J. G. (2015). Is there a possibility of ranking benthic quality assessment indices to select the most responsive to different human pressures? *Mar. pollut. Bull.* 97 (1-2), 85–94. doi: 10.1016/j.marpolbul.2015.06.030

Boudouresque, C. F., and Verlaque, M. (2012). An overview of species introduction and invasion processes in marine and coastal lagoon habitats. *Cah. Biol. Mar.* 53, 309–317.

Cecchi, E., Gennaro, P., Piazzi, L., Ricevuto, E., and Serena, F. (2014). Development of a new biotic index for ecological status assessment of Italian coastal waters based on coralligenous macroalgal assemblages. *Eur. J. Phycol.* 49, 298–312. doi: 10.1080/09670262.2014.918657

Christie, A. P., Amano, T., Martin, P. A., Shackelford, G. E., Simmons, B. I., and Sutherland, W. J. (2019). Simple study designs in ecology produce inaccurate estimates of biodiversity responses. *J. Appl. Ecol.* 56 (12), 2742–2754. doi: 10.1111/1365-2664.13499

Çinar, M. E., and Bakir, K. (2014). ALien biotic IndEX (ALEX) – a new index for assessing impacts of alien species on benthic communities. *Mar. pollut. Bull.* 87, 171–179. doi: 10.1016/j.marpolbul.2014.07.061

Claudet, J., and Fraschetti, S. (2010). Human-driven impacts on marine habitats: a regional meta-analysis in the Mediterranean Sea. *Biol. Conserv.* 143 (9), 2195–2206. doi: 10.1016/j.biocon.2010.06.004

Di Franco, A., Bussotti, S., Navone, A., Panzalis, P., and Guidetti, P. (2009). Evaluating effects of total and partial restrictions to fishing on Mediterranean rocky-reef fish assemblages. *Mar. Ecol. Prog. Ser.* 387, 275–285. doi: 10.3354/meps08051

Edgar, G. J., Barrett, N. S., and Stuart-Smith, R. D. (2009). Exploited reefs protected from fishing transform over decades into conservation features otherwise absent from seascapes. *Ecol. Appl.* 19, 1967–1974. doi: 10.1890/09-0610.1

Enrichetti, F., Bo, M., Morri, C., Montefalcone, M., Toma, M., Bavestrello, G., et al. (2019). Assessing the environmental status of temperate mesophotic reefs: a new, integrated methodological approach. *Ecol. Indic.* 102, 218–229. doi: 10.1016/j.ecolind.2019.02.028

Fraschetti, S., Fabbrizzi, E., Tamburello, L., Uyarra, M. C., Micheli, F., Sala, E., et al. (2022). An integrated assessment of the good environmental status of Mediterranean marine protected areas. *J. Environ. Manage.* 305, 114370. doi: 10.1016/j.jenvman.2021.114370

Froese, R., and Pauly, D. (2011). *FishBase* Vol. 2011 (World wide web electronic publication).

Froese, R., and Pauly, D. (2018) *FishBase, version (06/2018)*. Available at: www.fishbase.org.

Gatti, G., Bianchi, C. N., Morri, C., Montefalcone, M., and Sartoretto, S. (2015). Coralligenous reefs state along anthropized coasts: Application and validation of the COARSE index, based on a rapid visual assessment (RVA) approach. *Ecol. Indic.* 52, 567–576. doi: 10.1016/j.ecolind.2014.12.026

Gatti, G., Montefalcone, M., Rovere, A., Parravicini, V., Morri, C., Albertelli, G., et al. (2012). Sea-Floor integrity down the harbor waterfront: the coralligenous shoals off vado ligure (NW Mediterranean). *Adv. Oceanol. Limnol.* 3 (1), 51–67. doi: 10.1080/19475721.2012.671190

Gobert, S., Chéry, A., Volpon, A., Pelaprat, C., and Lejeune, P. (2014). "The seascape as an indicator of environmental interest and quality of the Mediterranean benthos: the in situ development of a description index: the LIMA," in *Underwater seascapes* (Cham: Springer), 277–291. doi: 10.1007/978-3-319-03440-9_18

Gobert, S., Sartoretto, S., Rico-Raimondino, V., Andral, B., Chery, A., Lejeune, P., et al. (2009). Assessment of the ecological status of Mediterranean French coastal waters as required by the water framework directive using the *Posidonia oceanica* rapid easy index: PREI. *Mar. pollut. Bull.* 58 (11), 1727–1733. doi: 10.1016/j.marpolbul.2009.06.012

Grorud-Colvert, K., Sullivan-Stack, J., Roberts, C., Constant, V., Horta e Costa, B., Pike, E. P., et al. (2021). The MPA guide: A framework to achieve global goals for the ocean. *Science* 373 (6560), eabf0861. doi: 10.1126/science.abf0861

Guidetti, P., Addis, P., Atzori, F., Bussotti, S., Calò, A., Cau, A., et al. (2019). Assessing the potential of marine natura 2000 sites to produce ecosystem-wide effects in rocky reefs: A case study from Sardinia island (Italy). *Aquat. Conserv. Mar. Freshw. Ecosyst.* 29 (4), 537–545. doi: 10.1002/aqc.3026

Guidetti, P., Baiata, P., Ballesteros, E., Di Franco, A., Hereu, B., Macpherson, E., et al. (2014). Large-Scale assessment of Mediterranean marine protected areas effects on fish assemblages. *PloS One* 9 (4), e91841. doi: 10.1371/journal.pone.0091841

Hammer, Ø., Harper, D. A. T., and Ryan, P. D. (2001). PaSt: Paleontological statistics software package for education and data analysis. *Palaeontol. Electron* 4, 4.

Harmelin-Vivien, M. L., Harmelin, J. G., Chauvet, C., Duval, C., Galzin, R., Lejeune, P., et al. (1985). Evaluation visuelle des peuplements et populations de poissons méthodes et problèmes. *Rev. d'Ecologie Terre Vie* 40 (4), 467–539. doi: 10.3406/revec.1985.5297

Heithaus, M. R., Frid, A., Wirsing, A. J., and Worm, B. (2008). Predicting ecological consequences of marine top predator declines. *Trends Ecol. Evol.* 23 (4), 202–210. doi: 10.1016/j.tree.2008.01.003

Houngnandan, F., Kefi, S., Bockel, T., and Deter, J. (2022). The joint influence of environmental and anthropogenic factors on the invasion of two alien caulerpae in northwestern Mediterranean. *Biol. Invasions* 24 (2), 449–462. doi: 10.1007/s10530-021-02654-w

Legendre, P., and Legendre, L. (2012). *Numerical ecology* (Netherlands: Elsevier Amsterdam).

Lingo, M. E., and Szedlmayer, S. T. (2006). The influence of habitat complexity on reef fish communities in the northeastern gulf of Mexico. *Environ. Biol. Fishes* 76, 71–80. doi: 10.1016/j.marpolbul.2009.06.012

Magni, P., Vesal, S. E., Giampaoletti, J., Como, S., and Gravina, M. F. (2023). Joint use of biological traits, diversity and biotic indices to assess the ecological quality status of a Mediterranean transitional system. *Ecol. Indic.* 147, 109939. doi: 10.1016/j.ecolind.2023.109939

Mancini, I., Rigo, I., Oprandi, A., Montefalcone, M., Morri, C., Peirano,, et al. (2020). What biotic indices tell us about ecosystem change: Lessons from the seagrass *Posidonia oceanica*. *Vie Milieu/Life Environ.* 70 (3-4), 55–56.

Montefalcone, M. (2009). Ecosystem health assessment using the Mediterranean seagrass *Posidonia oceanica*: a review. *Ecol. Indic.* 9 (4), 595–604. doi: 10.1016/j.ecolind.2008.09.013

Montefalcone, M., and Oprandi, A. (2020). *Definizione della qualità ecologica dell'habitat marino prioritario praterie di Posidonia oceanica nell'Area Marina protetta Capo Carbonara (Villasimius)* (Genoa (IT: University of Genoa).

Montefalcone, M., Vassallo, P., Gatti, G., Parravicini, V., Paoli, C., Morri, C., et al. (2015). The exergy of a phase shift: ecosystem functioning loss in seagrass meadows of the Mediterranean Sea. *Estuar. Coast. Shelf Sci.* 156, 186–194. doi: 10.1016/j.ecss.2014.12.001

Moreno, D., Aguilera, P. A., and Castro, H. (2001). Assessment of the conservation status of seagrass (*Posidonia oceanica*) meadows: implications for monitoring strategy and the decision-making process. *Biol. Conserv.* 102 (3), 325–332. doi: 10.1016/S0006-3207(01)00080-5

Morey, G., Moranta, J., Massuti, E., Grau, A., Linde, M., Riera, F., et al. (2003). Weight-length relationships of littoral to lower slope fishes from the Western Mediterranean. *Fish Res.* 62, 89–96. doi: 10.1016/S0165-7836(02)00250-3

Morri, C., Montefalcone, M., Gatti, G., Vassallo, P., Paoli, C., and Bianchi, C. N. (2019). An alien invader is the cause of homogenization in the recipient ecosystem: a simulation-like approach. *Diversity* 11, 146. doi: 10.3390/d11090146

Muxika, I., Borja, Á., and Bald, J. (2007). Using historical data, expert judgement and multivariate analysis in assessing reference conditions and benthic ecological status, according to the European water framework directive. *Mar. Poll. Bull.* 55, 16–29. doi: 10.1016/j.marpolbul.2006.05.025

Occhipinti Ambrogi, A., Forni, G., and Silvestri, C. (2009). The Mediterranean intercalibration exercise on soft-bottom benthic invertebrates with special emphasis on the Italian situation. *Mar. Ecol.* 30 (4), 495–504. doi: 10.1111/j.1439-0485.2009.00317.x

Oprandi, A., Bianchi, C. N., Karayali, O., Morri, C., Rigo, I., and Montefalcone, M. (2021). RESQUE: A novel comprehensive approach to compare the performance of different indices in evaluating seagrass health. *Ecol. Indic.* 131, 108118. doi: 10.1016/j.ecolind.2021.108118

Oprandi, A., Mancini, I., Bianchi, C. N., Morri, C., Azzola, A., and Montefalcone, M. (2022). "Indices from the past: relevance in the status assessment of posidonia oceanica meadows," in *Proceedings of the 7th Mediterranean symposium on marine vegetation*. Eds. C. Bouafif and A. Ouerghi (Tunis, TN: SPA/RAC Publications), 71–77.

Oprandi, A., Montefalcone, M., Vacchi, M., Coppo, S., Diviacco, G., Morri, C., et al. (2014). "Combining modelling and historical data to define the status of posidonia oceanica meadows," in *Proceedings of the 5th Mediterranean symposium on marine vegetation*. Eds. H. Langar, C. Bouafif and A. Ouerghi (Tunis, TN: RAC/SPA Publications), 119–124.

Paoli, C., Morten, A., Bianchi, C. N., Morri, C., Fabiano, M., and Vassallo, P. (2016). Capturing ecological complexity: OCI, a novel combination of ecological indices as applied to benthic marine habitats. *Ecol. Indic.* 66, 86–102. doi: 10.1016/j.ecolind.2016.01.029

Pawlowski, J., Kelly-Quinn, M., Altermatt, F., Apothéloz-Perret-Gentil, L., Beja, P., Boggero, A., et al. (2018). The future of biotic indices in the ecogenomic era: Integrating (e) DNA metabarcoding in biological assessment of aquatic ecosystems. *Sci. Total Environ.* 637, 1295–1310. doi: 10.1016/j.scitotenv.2018.05.002

Peleg, O., Blain, C., and Shears, N. (2023). Multi-indicator 'state space'approach to assessing changes in shallow urban reef ecosystem health. *Mar. Environ. Res.* 186, 105895. doi: 10.1016/j.marenvres.2023.105895

Pettersen, A. K., Marzinelli, E. M., Steinberg, P. D., and Coleman, M. A. (2022). Impact of marine protected areas on temporal stability of fish species diversity. *Conserv. Biol.* 36 (2), e13815. doi: 10.1111/cobi.13815

Piazzi, L., Atzori, F., Cadoni, N., Cinti, M. F., Frau, F., and Ceccherelli, G. (2021a). Monitoring non-indigenous macroalgae in a Mediterranean MPA: Lessons from a short-temporal variability of pristine habitats invasion. *Ocean Coast. Manage.* 207, 105608. doi: 10.1016/j.ocecoaman.2021.105608

Piazzi, L., Atzori, F., Cadoni, N., Cinti, M. F., Frau, F., Pansini, A., et al. (2021b). Animal forest mortality: Following the consequences of a gorgonian coral loss on a Mediterranean coralligenous assemblage. *Diversity* 13 (3), 133. doi: 10.3390/d13030133

Piazzi, L., Balata, D., Bulleri, F., Gennaro, P., and Ceccherelli, G. (2016). The invasion of *Caulerpa cylindracea* in the Mediterranean: the known, the unknown and the knowable. *Mar. Biol.* 163, 161. doi: 10.1007/s00227-016-2937-4

Piazzi, L., Bianchi, C. N., Cecchi, E., Gatti, G., Guala, I., Morri, C., et al. (2017b). What's in an index? comparing the ecological information provided by two indices to assess the status of coralligenous reefs in the NW Mediterranean Sea. *Aquat. Conserv.: Mar. Freshw. Ecosyst.* 27 (6), 1091–1100. doi: 10.1002/aqc.2773

Piazzi, L., Gennaro, P., and Ceccherelli, G. (2015). Suitability of the alien biotic index (ALEX) for assessing invasion of macroalgae across different Mediterranean habitats. *Mar. Pollut. Bull.* 97, 234–240. doi: 10.1016/j.marpolbul.2015.06.011

Piazzi, L., Gennaro, P., Cecchi, E., Serena, F., Bianchi, C. N., Morri,, et al. (2017a). Integration of ESCA index through the use of sessile invertebrates. *Sci. Mar.* 81, 1–8. doi: 10.3989/scimar.04565.01B

Pinto, R., Patrício, J., Baeta, A., Fath, B. D., Neto, J. M., and Marques, J. C. (2009). Review and evaluation of estuarine biotic indices to assess benthic condition. *Ecol. Indic.* 9 (1), 1–25. doi: 10.1016/j.ecolind.2008.01.005

Rastorgueff, P. A., Bellan-Santini, D., Bianchi, C. N., Bussotti, S., Chevaldonné, P., Guidetti, P., et al. (2015). An ecosystem-based approach to evaluate the ecological quality of Mediterranean undersea caves. *Ecol. Indic.* 54, 137–152. doi: 10.1016/j.ecolind.2015.02.014

Reizopoulou, S., Simboura, N., Sigala, K., Barbone, E., Aleffi, F., Kaisakis, G., et al. (2014). Assessing the ecological status of Mediterranean coastal lagoons using macroinvertebrates. comparison of the most commonly used methods. *Medit. Mar. Sci.* 15 (3), 602–612. doi: 10.12681/mms.606

Rigo, I., Dapueto, G., Paoli, C., Massa, F., Oprandi, A., Venturini, S., et al. (2020). Changes in the ecological status and natural capital of *Posidonia oceanica* meadows due to human pressure and extreme events. *Vie Milieu/Life Environ.* 70, 137–148.

Rigo, I., Paoli, C., Dapueto, G., Pergent-Martini, C., Pergent, G., Oprandi, A., et al. (2021). The natural capital value of the seagrass *Posidonia oceanica* in the north-Western Mediterranean. *Diversity* 13, 499. doi: 10.3390/d13100499

Rojo, I., Anadón, J. D., and García-Charton, J. A. (2021). Exceptionally high but still growing predatory reef fish biomass after 23 years of protection in a marine protected area. *PloS One* 16 (2), e0246335. doi: 10.1371/journal.pone.0246335

Rombouts, I., Beaugrand, G., Artigas, L. F., Dauvin, J. C., Gevaert, F., Goberville, E., et al. (2013). Evaluating marine ecosystem health: case studies of indicators using direct observations and modelling methods. *Ecol. Ind.* 24, 353–365. doi: 10.1016/j.ecolind.2012.07.001

Ruitton, S., Personnic, S., Ballesteros, E., Bellan-Santini, D., Boudouresque, C. F., Chevaldonné, P., et al. (2014). "An ecosystem-based approach to assess the status of the Mediterranean coralligenous habitat," in *Proceedings of the 2nd Mediterranean symposium on the conservation of coralligenous and other calcareous bio-concretions*. Eds. C. Bouafif, H. Langar and A. Ouerghi (Tunis, TN: SPA/RAC Publications), 153–158.

Sala, E., Ballesteros, E., Dendrinos, P., Di Franco, A., Ferretti, F., Foley, D., et al. (2012). The structure of Mediterranean rocky reef ecosystems across environmental and human gradients, and conservation implications. *PloS One* 7 (2), e32742. doi: 10.1371/journal.pone.0032742

Sala, O. E., Stuart Chapin, F., Armesto, J. J., Berlow, E., Bloomfield, J., Dirzo, R., et al. (2000). Global biodiversity scenarios for the year 2100. *Science* 287 (5459), 1770–1774. doi: 10.1126/science.287.5459.1770

Sánchez-Moyano, J. E., García-Asencio, I., Donázar-Aramendía, I., Miró, J. M., Megina, C., and García-Gómez, J. C. (2017). BENFES, a new biotic index for assessing ecological status of soft-bottom communities. towards a lower taxonomic complexity, greater reliability and less effort. *Mar. Environ. Res.* 132, 41–50. doi: 10.1016/j.marenvres.2017.10.014

Sartoretto, S., Schohn, T., Bianchi, C. N., Morri, C., Garrabou, J., Ballesteros, E., et al. (2017). An integrated method to evaluate and monitor the conservation state of coralligenous habitats: the INDEX-COR approach. *Mar. pollut. Bull.* 120, 222–231. doi: 10.1016/j.marpolbul.2017.05.020

Smit, K. P., Bernard, A. T., Lombard, A. T., and Sink, K. J. (2021). Assessing marine ecosystem condition: A review to support indicator choice and framework development. *Ecol. Indic.* 121, 107148. doi: 10.1016/j.ecolind.2020.107148

Smith, E. P. (2002). "BACI design," in *Encyclopedia of environmetrics*. Eds. A. H. El-Shaarawi and W. W. Piegorsch (Chichester: John Wiley and Sons Ltd), 141–148.

Stergiou, K.I., and Karpouzi, V.S. (2002). Feeding habits and trophic levels of Mediterranean fish. *Rev. Fish Biol. Fisheries* 11, 217-254. doi: 10.1023/A:1020556722822

Thibaut, T., Blanfuné, A., Boudouresque, C. F., Personnic, S., Ruitton, S., Ballesteros, E., et al. (2017). An ecosystem-based approach to assess the status of Mediterranean algae-dominated shallow rocky reefs. *Mar. Pollut. Bull.* 117, 311–329. doi: 10.1016/j.marpolbul.2017.01.029

Underwood, A. J. (1994). On beyond BACI: sampling designs that might reliably detect environmental disturbances. *Ecol. Appl.* 4 (1), 3–15. doi: 10.2307/1942110

Vassallo, P., Paoli, C., Aliani, S., Cocito, S., Morri, C., and Bianchi, C. N. (2020). Benthic diversity patterns and predictors: a study case with inferences for conservation. *Mar. Pollut. Bull.* 150, 110748. doi: 10.1016/j.marpolbul.2019.110748

frontiers | Frontiers in Marine Science

TYPE Original Research
PUBLISHED 27 March 2023
DOI 10.3389/fmars.2023.1130540

Check for updates

OPEN ACCESS

EDITED BY
Chiara Piroddi,
Joint Research Centre, Italy

REVIEWED BY
Lucia Fanini,
University of Salento, Italy
Roberto Carlucci,
University of Bari Aldo Moro, Italy

*CORRESPONDENCE
Patrick Astruch
patrick.astruch@univ-amu.fr

†Deceased

SPECIALTY SECTION
This article was submitted to Marine Ecosystem Ecology, a section of the journal Frontiers in Marine Science

RECEIVED 23 December 2022
ACCEPTED 06 March 2023
PUBLISHED 27 March 2023

CITATION
Astruch P, Orts A, Schohn T, Belloni B, Ballesteros E, Bănaru D, Bianchi CN, Boudouresque C-F, Changeux T, Chevaldonné P, Harmelin J-G, Michez N, Monnier B, Morri C, Thibaut T, Verlaque M and Daniel B (2023) Ecosystem-based assessment of a widespread Mediterranean marine habitat: The Coastal Detrital Bottoms, with a special focus on epibenthic assemblages.
Front. Mar. Sci. 10:1130540.
doi: 10.3389/fmars.2023.1130540

COPYRIGHT
© 2023 Astruch, Orts, Schohn, Belloni, Ballesteros, Bănaru, Bianchi, Boudouresque, Changeux, Chevaldonné, Harmelin, Michez, Monnier, Morri, Thibaut, Verlaque and Daniel. This is an open-access article distributed under the terms of the Creative Commons Attribution License (CC BY). The use, distribution or reproduction in other forums is permitted, provided the original author(s) and the copyright owner(s) are credited and that the original publication in this journal is cited, in accordance with accepted academic practice. No use, distribution or reproduction is permitted which does not comply with these terms.

Ecosystem-based assessment of a widespread Mediterranean marine habitat: The Coastal Detrital Bottoms, with a special focus on epibenthic assemblages

Patrick Astruch[1]*, Ameline Orts[1], Thomas Schohn[1], Bruno Belloni[1], Enric Ballesteros[2], Daniela Bănaru[3], Carlo Nike Bianchi[4,5], Charles-François Boudouresque[3], Thomas Changeux[3], Pierre Chevaldonné[6], Jean-Georges Harmelin[1], Noëmie Michez[7,8], Briac Monnier[9], Carla Morri[4,5], Thierry Thibaut[3], Marc Verlaque[3] and Boris Daniel[8†]

[1]Groupement d'Intérêt Scientifique (GIS) Posidonie, Observatoire des Sciences de l'Univers (OSU) Pythéas, Marseille, France, [2]Center for Advenced Studies of Blanes, Spanish National Research Council (CSIC) Blanes, Girona, Spain, [3]Aix Marseille University, Université de Toulon, Centre National de la Recherche Scientifique (CNRS), Institut de Recherche pour le Développement (IRD), Mediterranean Institute of Oceanography (MIO) Marseille, France, [4]Seascape Ecology Laboratory, Department of Earth, Environment and Life Sciences (DiSTAV), University of Genoa, Genova, Italy, [5]Department of Integrative Marine Ecology (EMI), Stazione Zoologica Anton Dohrn–National Institute of Marine Biology, Ecology and Biotechnology, Genoa Marine Centre (GMC), Genova, Italy, [6]Institut Méditerranéen de Biodiversité et d'Ecologie Marine et Continentale (IMBE), Centre National de la Recherche Scientifique (CNRS), Institut de Recherche pour le Développement (IRD), Aix-Marseille University, Avignon University, Station Marine d'Endoume, Marseille, France, [7]Natural Marine Park of the Gulf of Lion, Argelès-sur-mer, France, [8]French Office for Biodiversity, Vincennes, France, [9]Université de Corse Pasquale Paoli, Centre National de la Recherche Scientifique (CNRS), Unité Mixte de Recherche (UMR) 6134 Science pour l'Environnement (SPE), Corte, France

Introduction: Coastal detrital bottoms (CDB) are one of the most extensive habitats of the continental shelf worldwide, in the upper levels of the circalittoral zone. Hosting a diverse community structured by sediment grain size, trophic interactions and calcified organisms, CDB exhibit important ecological functions. In the Mediterranean Sea, CDB are constituted by recent elements partly provided by adjacent infralittoral and circalittoral ecosystems. Since the 2010s, the offshore extension of many Marine Protected Areas (MPAs) has resulted in the incorporation of vast areas of CDB, raising the issue of their management. The Marine Strategy Framework Directive (MSFD) has embraced the concept of an ecosystem-based approach involving taking into account the functioning of marine habitats and their related ecosystem services. The purpose of this paper is to propose an ecosystem-based quality index (EBQI) tested on CDB from the north-western Mediterranean Sea, focusing mainly on epibenthic assemblages.

Methods: The first step has been to define a conceptual model of the CDB functioning, including the main trophic compartments and their relative weighting, then to identify appropriate assessment methods and potential descriptors. Twenty-nine sites were sampled along the coast of Provence and

French Riviera (Southern France). Study sites were chosen with a view to encompassing a wide range of hydrological conditions and human pressures.

Results: Very well-preserved sites were found in Provence in areas without trawling and terrigenous inputs, while impacted and low-ES sites were located in the vicinity of urbanized areas. The cover of rhodoliths characterizes the seascape and might be an indicator of the good ES of CDB and reduced human pressure. However, the absence of rhodoliths may also be induced by natural phenomena.

Discussion: The EBQI designed for CDB proved representative and useful for a functional assessment based on epibenthic assemblages. However, some descriptors have shown their limitations and should be further explored. We highlight here the priority of establishing an index corresponding to a societal demand (e.g., European Directives, Barcelona convention) as a basis for a broad and large-scale assessment, for practical reasons. We stress the need to better apprehend the role of the macro-infauna and to extend this index over a wider geographical scale.

KEYWORDS

coastal detrital bottoms, ecosystem-based approach (EBA), quality assessment, marine habitat, rhodolith beds, epibenthic assemblages

1 Introduction

Coastal detrital bottoms (CDB), sometimes also referred to as coastal (bio-)detritic bottoms in the literature, are sea bottoms composed of mineral and biogenic particles, characterized by a distinct structural complexity hosting sedimentary infauna together with epifauna and epiflora settled or not on coarser granules (Rees, 1999). They are considered as a distinctive biotope in the circalittoral zone of the continental shelf worldwide (Pérès, 1982; Konar et al., 2006; Amado-Filho and Pereira-Filho, 2012; La Rivière et al., 2021).

In the Mediterranean Sea, CDB are one of the most widespread ecosystems between 30 and 100 m depth, corresponding to the upper part of the circalittoral zone (Pérès and Picard, 1964; Pérès, 1967), and house a high alpha species diversity (Stamouli et al., 2022). Besides a mineral component (typically coarse sand with a variable proportion of finer particles), these bottoms contain significant quantities of recent organogenic and bioclastic sediments (remains from hard bottoms, shell debris, bryozoans or calcified macro-algae), either autogenous or imported from adjacent ecosystems (e.g., coralligenous reefs, photophilic rocky reefs, seagrass meadows). The structure and composition of CDB can therefore differ depending on adjacent ecosystems, light availability and hydrodynamic conditions (Pérès and Picard, 1964; Joher et al., 2015; Agnesi et al., 2020). The pelitic proportion (sediment grain< 63 µm) of the sediment is usually very low, but muddy CDB can be found (Bellan-Santini et al., 1994). Located within the same depth range as CDB, Muddy Detrital Bottoms (MDB) are characterized by a high sedimentation rate influenced by the terrigenous input from coastal rivers. MDB can be constituted by a compact mud including bioclastic shells, muddy sand, or sandy mud (Carpine, 1964; Pérès and Picard, 1964; Picard, 1965; Bellan-Santini et al., 1994; Michez et al., 2014; La Rivière et al., 2021). Deep Detrital Bottoms (DDB), generally between 80 and 250 m depth, correspond to fossilized detrital sediments from terrigenous (fluviatile) and bioclastic inputs corresponding to earlier environmental conditions and a lower sea level (Pérès and Picard, 1964; Bellan-Santini et al., 1994), covering the deepest part of the continental shelf. The sediment is a mix of pebbles, sand and mud but with a mud proportion significantly higher than in the CDB. Coarser sediment is made of calcareous remains from thanatocenoses of the Pleistocene ice ages (Laborel et al., 1961; Pérès and Picard, 1964; Bourcier and Zibrowius, 1973; Michez et al., 2011; Michez et al., 2014). Distinguishing the boundary between CDB and muddy or deep detrital ecosystems is sometime challenging.

Pérès and Picard (1964) based their description of CDB on the infauna, which contain the most characteristic species; however, the same authors and others (Costa, 1960; Joher et al., 2015; La Rivière et al., 2021) identified a number of CDB facies on the basis of epibenthic species, especially macroalgae, either erect or encrusting. The former include perennial and seasonal species, such as *Cystoseira* spp. C.Agardh, *Ericaria* spp. Stackhouse, *Gongolaria* spp. Boehmer, *Osmundaria volubilis* (L.) R.E.Norris, etc.; the latter are represented by the Corallinales *Lithophyllum racemus* (Lamarck) Foslie, *Lithothamnion corallioides* (P.Crouan & H.Crouan) P.Crouan & H.Crouan, *L. crispatum* Hauck, *L. minervae* Basso, *L. valens* Foslie, *Neogoniolithon hauckii*

(Rothpletz) R.A.Townsend & Huisman, *Spongites fruticulosa* Kützing, the Peyssonneliales *Peyssonnelia crispata* Boudouresque & Denizot, *P. heteromorpha* (Zanardini) Athanasiadis, *P. rosa-marina* Boudouresque & Denizot, *P. rubra* (Greville) J.Agardh, *P. squamaria* (S.G.Gmelin) Decaisne ex J.Agardh, and the Sporolithales *Sporolithon mediterraneum* Heydrich, among others (Huvé, 1954; Huvé, 1956; Carpine, 1958; Jacquotte, 1962; Boudouresque and Denizot, 1973; Ballesteros, 1994). Free-living calcified macroalgae forming nodules of varied morphology, referred to as 'rhodoliths' (or more specifically 'maerl' in the case of branched growth forms), gave rise to a great interest among benthic ecologists (Sciberras et al., 2009; Basso et al., 2017; Deidun et al., 2022). Their conservation value is recognized under EU rules and international conventions (Barbera et al., 2003; Salomidi et al., 2012). Marion (1883); Meinesz et al. (1983); Holon and Harmelin (2014) and La Rivière et al. (2021) described a CDB facies with large calcified bryozoans, such as *Pentapora fascialis* (Pallas, 1766), *Smittina cervicornis* (Pallas, 1766), *Turbicellepora avicularis* (Hincks, 1860), *Hornera* spp. Lamouroux, 1821, etc., but the highest diversity of bryozoans on CDB is found among small species (Harmelin, 2017). By analogy with calcareous rhodophytes, free bryozoan nodules are called bryoliths (James et al., 2006; Lombardi et al., 2014). This bryozoan facies is classified as a priority habitat according to the Barcelona Convention (Bianchi, 2009a). Recently, coralliths formed by the scleractinian coral *Cladocora caespitosa* (L., 1767), also considered of conservation interest (Morri et al., 2000; Bianchi, 2009b), have been described from coarse sandy bottoms in the Balearic Islands (Kersting et al., 2017a; Kersting et al., 2017b). Several octocoral species, such as *Eunicella singularis* (Esper, 1791), *E. verrucosa* (Pallas, 1766), *Leptogorgia sarmentosa* (Esper, 1791), *Alcyonium palmatum* Pallas, 1766, *Pennatula rubra* (Ellis, 1764), *Pteroeides griseum* (Bohadsch, 1761) and others, may also form epibenthic facies on detrital seabeds (Morri et al., 1991). Fauna and flora associated with all these epibenthic facies are sometimes very similar to coralligenous assemblages (Ballesteros, 2006; Pergent et al., 2015). The EUNIS typology defines as coralligenous platforms bioconstructed horizontal formations developing within sedimentary beds subject to currents, at down to at least 100 metres depth in clear waters (Davies et al., 2004; Bajjouk et al., 2015). These formations are not usually built on rock substrata but result from the active development of constructional organisms (e.g., calcified algae, hard-skeleton invertebrates) from scattered elements on loose beds, such as shells, stones, and gravel (Pérès and Picard, 1964).

Important ecological functions and ecosystem services, up to now poorly assessed, are provided by CDB (Ballesteros, 1994; Barbera et al., 2003): (i) primary production (Basso, 2012; Basso et al., 2012); (ii) key habitat and trophic resources for invertebrates and fish; (iii) breeding, spawning and nursery grounds for fish and crustaceans including species of fishery interest, sometimes close to the deep limit of the *Posidonia oceanica* (L.) Delile meadow (e.g., Mullidae, Sparidae, Scorpaenidae, *Palinurus elephas* (Fabricius, 1787)) (Harmelin and Harmelin-Vivien, 1976; Verlaque, 1990; Kamenos et al., 2004; Soykan et al., 2010); (iv) fishing ground for trawlers and artisanal fishers (Stamouli et al., 2022); (v) long term carbon sink (Basso, 2012; Basso et al., 2012; Savini et al., 2012; Burrows et al., 2014; Watanabe et al., 2020); (vi) recycling of necromass (e.g., rhizomes and dead *Posidonia oceanica* leaves and drift macroalgae) (Boudouresque et al., 2016); (vii) exportation and settlement of larvae towards or from adjacent ecosystems (source-sink hypothesis; Levin and Dayton, 2009). In addition, CDB host numerous protected species and other species of conservation interest (Astruch et al., 2012; Joher et al., 2015; Astruch et al., 2019): e.g., the fan shell *Pinna nobilis* L. 1758 (annexe II Berne convention and UICN Red list: critically endangered), the red coralline alga *Lithothamnion corallioides* (Annexe 5 of the HD: species of interest with regulation of its exploitation), and several Fucales (Annexe 2 of the Barcelona convention), among others. Management goals for maerl beds are different in the Mediterranean compared to the rest of the world, where extraction activities are carried out (Foster et al., 1997; Steller et al., 2003; Foster et al., 2013; Amado-Filho et al., 2017; Harvey et al., 2017).

Nowadays, like most coastal biocenoses, CDB are facing the impact of human activities and climate change. They are threatened by numerous pressures (Dutertre et al., 2015; Demestre et al., 2017) such as trawling (Bordehore et al., 2000; Bordehore et al., 2003; Fragkopoulou et al., 2021), artisanal or recreational fishing (Rendina et al., 2020), dredging (De Grave and Whitaker, 1999; Bermejo et al., 2018; Bernard et al., 2019), terrigenous input, dumping of sediment and waste (Aliani et al., 1994; Cocito et al., 1994), fish farming (Sanz-Lázaro et al., 2011; Aguado-Giménez and Ruiz-Fernández, 2012), consequences of coastal development, sea water warming, the spread of non-indigenous species (Klein and Verlaque, 2009; Katsanevakis et al., 2014; Martin and Hall-Spencer, 2017; Hall-Spencer and Harvey, 2019) and potentially acidification (Noisette et al., 2013).

Until recently, studies on CDB in the Mediterranean Sea were mainly focused on the description of infauna (e.g., Pérès and Picard, 1964; Picard, 1965; Somaschini et al., 1998), rhodolith beds and associated communities (e.g., Ledoyer, 1966; Ballesteros, 1994; Basso et al., 2017), and taxonomy (e.g., Boudouresque and Denizot, 1973; Souto et al., 2010), without any overview at ecosystem scale (e.g., Gautier and Picard, 1957; Jacquotte, 1962; Boudouresque and Denizot, 1973; Augier and Boudouresque, 1975; Laborel et al., 1976; Augier and Boudouresque, 1978; Harmelin, 1978; Bourcier, 1982; Bourcier, 1985; Bourcier, 1988; Fornos et al., 1988; Joher et al., 2012; Joher et al., 2015).

Despite the high ecological and heritage value of CDB and the many threats facing it, this ecosystem was not considered as a habitat of European interest (Bensettiti et al., 2004) by the Habitats Directive of the European Union (Natura 2000, 92/43/CEE) while some facies of CDB are described in EUNIS typology (Gayet et al., 2018) and are included in the Barcelona convention. Recently, the Habitats Directive has taken a step forward, considering rhodolith beds as a reef habitat (1170) if they host communities characteristic of hard substrates (De Bettignies et al., 2021). In France, the extension of the overall surface areas of Marine Protected Area (MPA) (national parks, Natura 2000 sites, etc.) (Petit, 2019), since the 2010s, has incorporated large expanses of seabed occupied by CDB. In accordance with these new management priorities, it has

become a challenge to better take into account this widespread ecosystem.

Even with the improving accuracy of technologies (e.g., side-scan sonar, multibeam, remotely operated vehicles, autonomous underwater vehicles, etc.) (Bianchi et al., 2004; Astruch et al., 2012; Valette-Sansevin et al., 2019) and prediction models (Martin et al., 2014; Vassallo et al., 2018), the mapping of CDB is still challenging. The assessment of coastal water body masses, marine habitats or ecosystems involves numerous indices with different purposes (Bianchi et al., 2022). None of these indices alone offers an adequate basis for solving all the issues: specific descriptors may assess the ecological status linked with water quality (WFD; e.g., Borja et al., 2000; Borja et al., 2003; Ballesteros et al., 2007; Gobert et al., 2009; Lopez y Royo et al., 2010; Blanfuné et al., 2017; Piazzi et al., 2021), ecosystem functioning (descriptor 1 of the MSFD; e.g., Personnic et al., 2014; Montefalcone et al., 2015a; Giakoumi et al., 2015), seafloor integrity (descriptor 6 of the MSFD; e.g., Montefalcone et al., 2007; Gatti et al., 2015; Enrichetti et al., 2019; Piazzi et al., 2019), the conservation status of natural habitats (HD; e.g., Maciejewski et al., 2016; Sartoretto et al., 2017), natural and anthropogenic stressors (Holon et al., 2015; La Rivière et al., 2017; Ruitton et al., 2020).

Obviously, the future of coastal zone management policies will not be based on a single integrative index (Bond, 2001), but an appropriate combination of the most relevant ones (Pikaver et al., 2004; Paoli et al., 2016; Borja et al., 2021; Oprandi et al., 2021). Indicators are currently used to underpin guidelines for managers and stakeholders. In this context, the ecosystem-based approach should be deployed (Laffoley et al., 2004; Boudouresque et al., 2020a), with the aim of achieving a better understanding of ecosystem functioning as a basis for more suitable management strategies. Ecosystem-Based Quality Indices (EBQIs) have been already defined for a number of coastal marine ecosystems, namely *Posidonia oceanica* seagrass meadows (Personnic et al., 2014), coralligenous reefs (Ruitton et al., 2014), undersea caves (Rastorgueff et al., 2015) and rocky reefs (Thibaut et al., 2017). The aim of the present work is to develop and apply a new EBQI expressly designed for CDB (Astruch et al., 2022a). Although CDB is traditionally identified mostly on the basis of the study of the infaunal component, which requires sampling with grabs or dredges operated from large vessels, the approach presented here will focus on the epibenthic component, which can be studied with a lighter and less costly approach, i.e., photographic, video and/or visual techniques - to be privileged in a conservation context (Bianchi et al., 2022). The effectiveness of this novel index was tested along the coasts of Provence and French Riviera (France, Mediterranean Sea) (Figure 1).

2 Material and methods

2.1 Conceptual model of coastal detrital bottom functioning

A workshop involving 15 experts in benthic ecology (mainly the authors of the present work) was held the 2nd of April 2019 **(i)** to propose and validate a conceptual model of the CDB functioning, **(ii)** to define the weight of each functional compartment (=box) corresponding to its importance in the ecosystem, and **(iii)** to develop a sampling protocol with suitable operational descriptors to assess the different compartments. A DELPHI approach was implemented (Rowe and Wright, 1999). The conceptual model thus defined schematizes the functioning of CDB (Figure 2). The compartments of the conceptual model are described in the following pages.

2.2 Sampling strategy

Twenty-nine sampling sites were investigated (Table 1, Figure 1). Sampling took place between June and July 2020 and

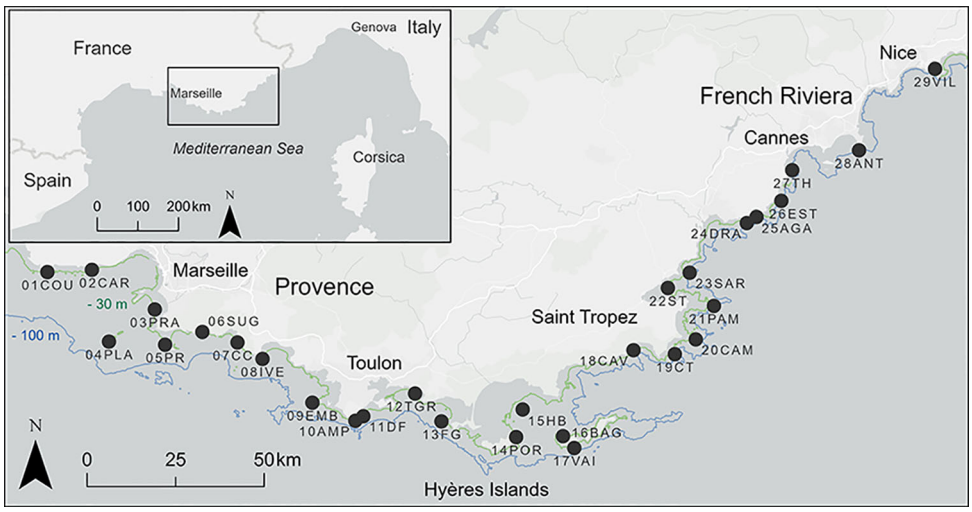

FIGURE 1
Study area along the French Mediterranean coast and location of the 29 sampling sites.

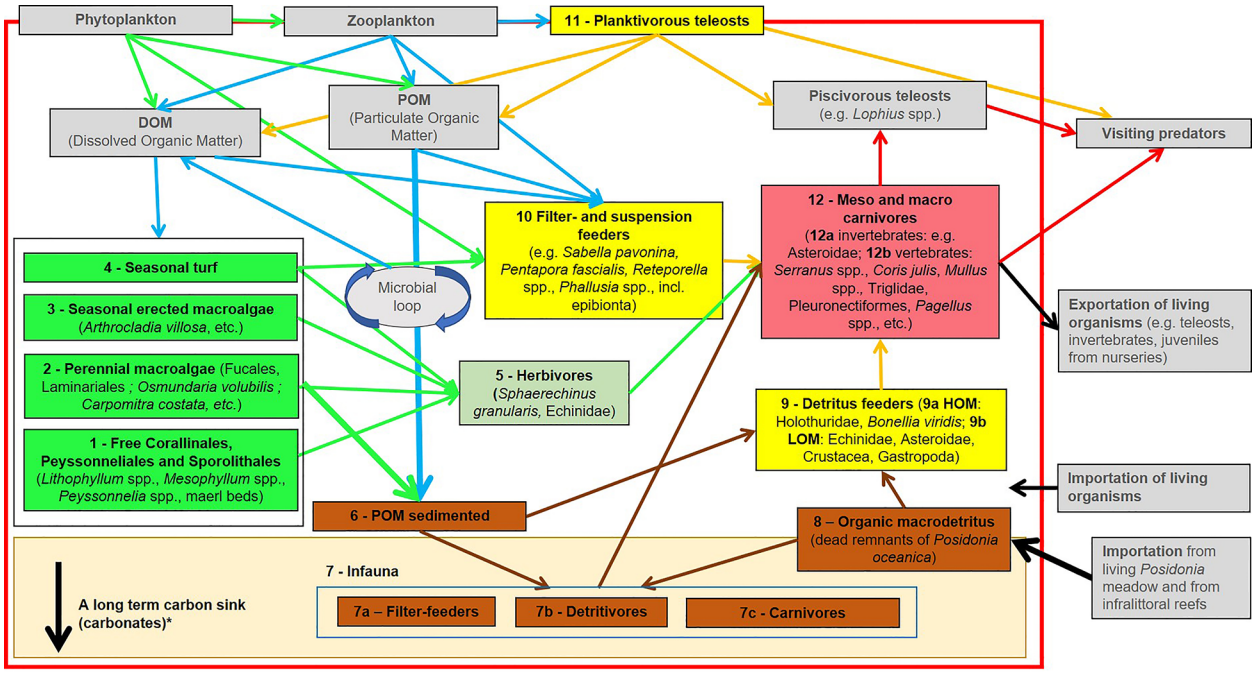

FIGURE 2
Conceptual functional model of the Coastal Detrital Bottom Ecosystem. Arrows correspond to a flux of organic matter between boxes. Light grey boxes are not assessed directly. *See corresponding paragraph for more details about Carbon sink.

2021 during the maximum development of the macroalgal communities (Piazzi et al., 2002). Site selection took into account different levels of pressures linked with human activities, from pristine-like to urbanized sites. The study area presents a gradient in hydrological conditions, involving the Rhône River to the west, the oligotrophic waters of eastern Provence and the run-offs in the urbanized French Riviera.

Two depth ranges were sampled at each site: the upper zone (between 28 and 43 m, according to the lower limit of the *P. oceanica* meadow), and the deep zone (between 48 and 79 m depth). Upper sites were selected far enough away from *P. oceanica* meadows to avoid the transitional zone and ensure a correct assessment of CDB compartments.

Sampling was carried out by SCUBA diving, photoquadrats and seascape video. In the upper zone, observations were carried out by scuba divers for inventory of *in situ* recognizable taxa and assessment of their abundance. Each dive corresponds to the observation of 2 divers during ~12 minutes. Assuming the movements of the divers at an average speed of ~10 m·min^{-1} (including stops) observing the bottom on a 2 m wide strip, each dive corresponds to an investigated surface area of ~500 m^2. Three cores of sediment were sampled per site to assess organic matter and sediment grain size. In both upper and deep zone, an original device, the 'Biocube' (Figure 3), was deployed to sample: (i) photoquadrats with an 80 cm × 80 cm sized frame using a compact camera with a 15 s time lapse. On-board video monitoring using a GoPro® Hero 3 was used to control the position of the quadrat during sampling. Each quadrat was randomly positioned according to the drift of the operating boat. (ii) Seascape videos were taken during the photoquadrat sampling. The aim of the diversity of sampling methods is to provide complementary observations at the scale of each sampling site for a standardized assessment.

2.3 Compartments assessed

2.3.1 Box 1: Rhodoliths: Free living corallinales, peyssonneliales, and sporolithales

This compartment is involved in the structuring of the ecosystem by increasing sediment grain size and providing a support for other compartments (see boxes 2, 3, 10 in Figure 2). Among Corallinales, several species can be found such as *Lithothamnion corallioides*. Peyssonneliales can be calcareous or not, several species occur in CDB, such as *Peyssonnelia rosa-marina* (Boudouresque and Denizot, 1973) or *P. squamaria*. The Sporolithale *Sporolithon mediterraneum* is a frequent rhodolith species of CDB. For some species, *in situ* identification is challenging or impossible and collection is needed. The cover naturally decreases according to depth and the corresponding reduction of light availability. In oligotrophic and clear waters, rhodolith beds can be found down to 80 m depth (Ballesteros, 1994). Aguilar et al. (2009) described rhodolith beds at 140-150 m depth around the Balearic Islands. Rhodoliths play an important role in the deep benthic fixing and sequestration of organic and inorganic carbon (Basso, 2012; Basso et al., 2016). The cover (mean percentage) of living rhodoliths appears to be the easiest descriptor to assess the structure of CDB, which conditions its functioning in both the upper and the deep zones (Bosellini and Ginsburg, 1971; Basso et al., 2016).

10.3389/fmars.2023.1130540

TABLE 1 Sampling sites position (DD: Decimal degrees), depth at upper and deep zones (m) and management level (MPA, Marine Protected Area; NTZ, No-take Zone; MUM, Multi-use Management).

Code	Sites	Upper zone			Deep zone			Management level
		Latitude DD	Longitude DD	Z (m)	Latitude DD	Longitude DD	Z (m)	
01COU	La Couronne	43.318006	5.068738	36	43.309006	5.069218	54	Natura 2000
02CAR	Carry	43.322321	5.181404	37	43.31703	5.185064	51	Natura 2000
03PRA	Baie du Prado	43.249276	5.341165	32	43.238208	5.311782	51	MPA-MUM
04PLA	Planier	43.189937	5.224995	33	43.187317	5.226625	58	MPA-NTZ
05PR	Passe de Riou	43.183998	5.367319	42	43.185715	5.355298	59	MPA-NTZ
06SUG	Sugiton	43.207808	5.461533	40	43.20354	5.461815	62	MPA-MUM
07CC	Cap Canaille	43.188278	5.550706	39	43.186743	5.547737	62	MPA-NTZ
08IVE	Île Verte	43.158016	5.614341	49	43.154661	5.608425	68	MPA-MUM
09EMB	Embiez	43.077151	5.740709	38	43.076248	5.733459	63	Natura 2000
10AMP	Amphitria	43.043668	5.84977	39	43.041536	5.850354	61	Natura 2000
11DF	Deux Frères	43.052152	5.869729	41	43.051563	5.875795	62	Natura 2000
12TGR	Toulon Grande Rade	43.094181	6.001158	37	43.075055	5.995539	64	No protection
13FG	Fourmigue de Giens	43.042368	6.067969	42	43.035908	6.068579	64	MPA-MUM
14POR	Porquerolles Est	43.013374	6.257428	38	43.03322	6.297224	49	MPA-MUM
15HB	Baie d'Hyères	43.064543	6.273882	40	43.054147	6.360791	63	MPA-MUM
16BAG	Passe de Bagaud	43.015193	6.376252	41	43.022061	6.383424	63	MPA-MUM
17VAI	Vaisseau	42.993327	6.404658	41	42.9905	6.404757	65	MPA-NTZ
18CAV	Cavalaire	43.173947	6.555193	39	43.16926	6.560022	58	Natura 2000
19CT	Cap Taillat	43.166685	6.659678	43	43.152653	6.669391	79	Natura 2000
20CAM	Cap Camarat	43.193892	6.712775	41	43.188749	6.718136	68	Natura 2000
21PAM	Pampelonne	43.255746	6.758933	42	43.255049	6.766981	66	No protection
22ST	Saint Tropez	43.288836	6.642193	35	43.292658	6.664679	51	No protection
23SAR	Sardinaux	43.31683	6.697555	44	43.318675	6.707096	60	No protection
24DRA	Dramont	43.408298	6.842286	43	43.406108	6.836703	60	Natura 2000
25AGA	Agay	43.41966	6.86717	41	43.417686	6.871251	61	Natura 2000
26EST	Esterel	43.4493	6.92991	39	43.449293	6.934245	61	MPA-NTZ
27TH	Théoule sur mer	43.50549	6.957715	28	43.506943	6.960811	50	MPA-MUM
28ANT	Cap Antibes	43.541966	7.127123	36	43.537103	7.126363	59	Natura 2000
29VIL	Villefranche sur mer	43.691278	7.319585	41	43.692724	7.314388	58	Natura 2000

2.3.2 Box 2: Perennial non-calcified macroalgae

The abundance of perennial non-calcified macroalgae can be linked to good ecological conditions and the absence of significant pressures (mechanical erosion, terrigenous inputs, diminution of light). Fucales (*Sargassum* spp., *Ericaria* spp., *Gongolaria* spp., *Cystoseira* spp.), Laminariales (*Laminaria rodriguezii* Bornet), *Osmundaria volubilis* and *Carpomitra costata* (Stackhouse) Batters are among the most representative taxa (Gautier and Picard, 1957; Joher et al., 2012; Thibaut et al., 2016; Aouissi et al., 2018; Bermejo et al., 2018; Bruno de Sousa et al., 2019; Jódar-Pérez et al., 2020; Reynes et al., 2021). These long-lived species provide a stand for seasonal macroalgae (boxes 3 and 4) and sessile fauna (box 10), a habitat (boxes 9 and 12) and a trophic resource (box 5). They contribute significantly to the primary production of the ecosystem (Ballesteros, 1990). *Codium bursa* (Olivi) C.Agardh, *C. vermilara* (Olivi) Delle Chiaje and *Sphaerococcus coronopifolius* Stackhouse, perennial species observed during the present work, were not considered. The abundance of these species known as tolerant can be linked to a stressor (Vidondo and Duarte, 1995; Ruitton et al., 2017). In addition, *C. fragile* (Suringar) Hariot is a non-indigenous species (Provan et al., 2005). The mean percentage cover in the upper zone is a suitable descriptor to assess this compartment.

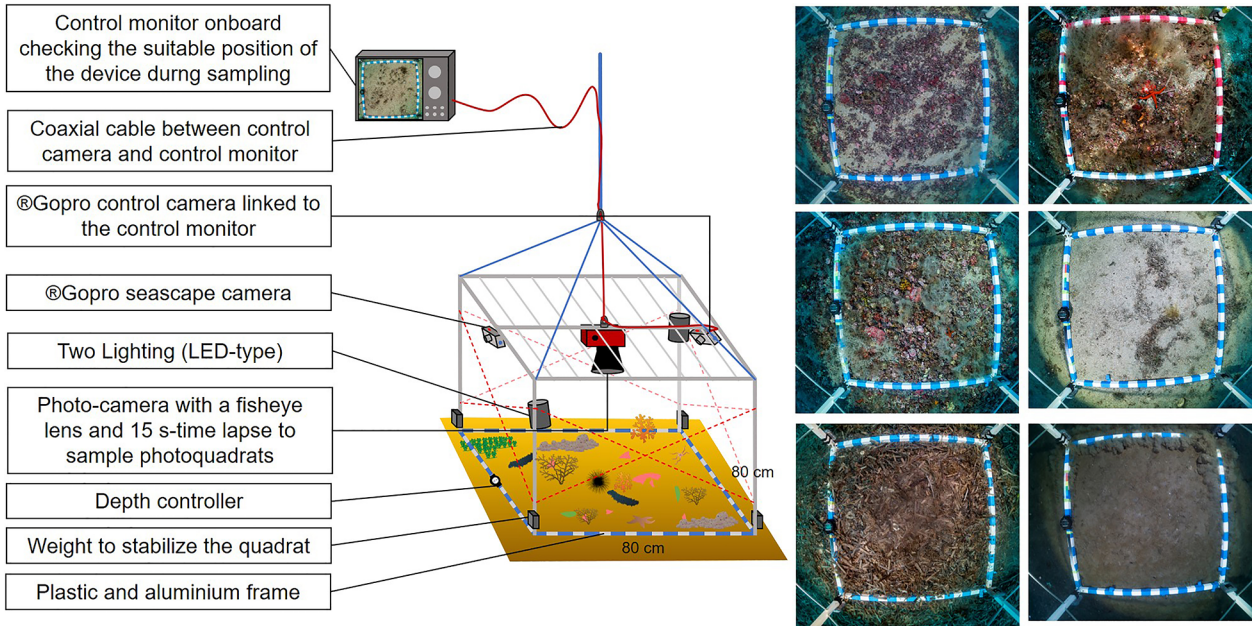

FIGURE 3
Diagram of the Biocube device. The pictures on the right show different types of CDB sampled on photoquadrats.

2.3.3 Box 3: Seasonal erect macroalgae

Macroalgal species from this compartment, characterized by fast growth rate and seasonal cycle, thrive mainly from spring to a maximum development during summer. Seasonal macroalgae also contribute significantly to primary production (Ballesteros, 1989). The most frequent and abundant taxa are the Phaeophyceae *Arthrocladia villosa* (Hudson) Duby and *Sporochnus pedunculatus* (Hudson) C.Agardh, widespread in the circalittoral both in Coralligenous reefs and CDB. Some species usually observed in the infralittoral can be found such as *Acetabularia acetabulum* (L.) P.C.Silva or *Padina pavonica* (Linnaeus) Thivy. *Umbraulva dangeardii* M.J.Wynne & G.Furnari is an Ulvophyceae that can be observed often associated with rhodolith beds. *Chrysymenia ventricosa* (J.V.Lamouroux) J.Agardh and *Sebdenia* spp. (J.Agardh) Berthold are among the main characteristic Florideophyceae. Identification at species level is impossible based on *in situ* observation or video and photograph analysis. The mean cover (percentage) of seasonal macroalgae appears to be a suitable descriptor. Non-indigenous and invasive species with a seasonal dynamic can thrive in the CDB: *Caulerpa cylindracea* Sonder (Klein and Verlaque, 2008), *C. taxifolia* (M.Vahl) C.Agardh (Meinesz et al., 2001; Montefalcone et al., 2015b), mucilage (several species including NIS: *Acinetospora crinita* (Carmichael) Sauvageau, *Chrysonephos lewisii* (W.R.Taylor) W.R.Taylor, *Nematochrysopsis marina* (J.Feldmann) C.Billard, *Zosterocarpus oedogonium* (Meneghini) Bornet) (Giuliani et al., 2005; Schiaparelli et al., 2007; Bianchi et al., 2019a). The latter taxa have been considered as stressors and are therefore not taken into account in the assessment of Compartment 3.

2.3.4 Box 4: Seasonal turf

Seasonal turf is defined as an algal community with a low height (a few centimetres at most). Worldwide, turf is more and more often observed replacing more structuring communities, influenced by stressors (Littler and Littler, 1980; Connell et al., 2014). Seasonal turfs include numerous species but very few can be identified *in situ* like the Ulvophyceae *Pseudochlorodesmis furcellata* (Zanardini) Børgesen and *Valonia macrophysa* Kützing. *Womersleyella setacea* (Hollenberg) R.E.Norris and *Acrothamnion preissii* (Sonder) E.M.Wollaston, two alien species (Boudouresque and Verlaque, 2002), can be present and are considered as stressors. These two species are often invasive in coralligenous reefs, *Posidonia oceanica* meadows, and infralittoral photophilic reefs (Piazzi and Cinelli, 2000; Piazzi et al., 2007; Bianchi et al., 2019b), and were found in CDB at Port-Cros National Park (Provence, France; Astruch et al., 2019). The distinction by visual assessment between seasonal turf and seasonal erect macroalgae is difficult. Considering that the two compartments progress with the same dynamics, it is relevant to consider their cumulative cover as the descriptor of their status in both upper and deep zones. The 'Compartments 3 and 4' are therefore named hereafter 'Compartment 3-4'.

2.3.5 Box 5: Herbivores

The high diversity of the macroalgal communities on CDB (boxes 1, 2, 3, 4) influences the abundance and the diversity of epibenthic herbivores. In the present work, the following taxa were considered as herbivores: echinids (*Sphaerechinus granularis* (Lamarck, 1816), *Stylocidaris affinis* (Philippi, 1845); occasionnaly *Centrostephanus longispinus* (Philippi, 1845), *Echinus melo*

Lamarck, 1816), and the gastropods *Cerithium* sp. Bruguière, 1789 and *Aplysia* spp. L., 1767. While *S. granularis* is strictly a herbivore (Weinberg, 1996; Wirtz and Debelius, 2003), *S. affinis*, *C. longispinus* and *E. melo* are omnivores. The latter two are not characteristic of CDB, even if they can be found in the vicinity of coralligenous beds. According to food availability and habitat (Wilkie et al., 1996), they are able to shift into herbivorous-dominant behaviour (De Ridder and Lawrence, 1982; Francour, 1989; Francour, 1991; Bergbauer and Humberg, 2000). *Sphaerechinus granularis* and *S. affinis* are known to be observed gathering on detrital bottoms (Harmelin and Duval, 1983). Vertebrate herbivores are mainly represented seasonally by the fish *Sarpa salpa* (L., 1758) during its breeding period (late summer) (Verlaque, 1990). Considering the short duration of the phenomenon, this species is not taken into account in this compartment. The alpha taxonomic richness (number of taxa per site) is a relevant descriptor to assess the herbivores compartment.

2.3.6 Box 6: Particulate organic matter (POM) of the sediment

Particulate organic matter (POM) of the sediment observed in abundance can be linked to natural eutrophic conditions or to a stressor (Sciberras et al., 2009). Based on our sampling strategy, the assessment of this compartment is feasible by considering the cover of muddy sediment on the bottom observed on the photoquadrats. This descriptor is already applied to assess the POM sedimented on coralligenous reefs (Ruitton et al., 2017). However, its assessment on CDB proved difficult. We therefore propose the percentage of pelitic fraction (<63 µm) as a proxy of the POM of the sediment. Organic matter accumulation is determined by environmental dynamics (currents, fine particles transfer to deep areas) (Orekhova and Ovsyany, 2020). A considerable percentage of pelitic fraction can also correspond to Muddy Detrital Bottoms (MDB).

2.3.7 Box 7: Infauna

Infauna constitutes a key compartment, influenced by sediment grain size and organic matter content (Pérès and Picard, 1964; Word, 1978; Cocito et al., 1990). Part of the Infauna can also be part of the Epifauna. We distinguished here three trophic groups within the infauna: (Box 7a) Filter and suspension-feeders: Represented by Phoronida, bivalves (ie. *Laevicardium oblongum* (Gmelin, 1791) or *Acanthocardia deshayesii* (Payraudeau, 1826)), Porifera (e.g., *Suberites domuncula* (Olivi, 1792)), Ophiuroidae and annelids such as Serpulidae; (Box 7b) Detritivores: Regroup surface and sub-surface deposit feeders such as annelids such as *Petta pusilla* Malmgren, 1866 (or Capitellidae, particularly in case of organic enrichment) and other different groups of worms (Echiura, Sipuncula, Nematoda), and molluscs such as *Turritellinella tricarinata* (Brocchi, 1814), *Moerella donacina* (L., 1758), *Abra nitida* (O. F. Müller, 1776) or *A. prismatica* (Montagu, 1808) (Zenetos, 1996); (Box 7c) Carnivores> (including scavengers): annelids such as Nephtyidae, Eunicidae or Polynoidae, molluscs gastropods such as Naticidae or Conidae, decapods and starfishes.

CDB, particularly in the upper circalittoral zone, are characterized by a relatively coarse grain size, decreasing with depth. It directly influences the trophic network in the sediment. Consequently, coarse sediment hosts a lower content in organic matter and a lower abundance of the infauna (Blanchard et al., 2009). According to Bellan et al. (1980), high organic matter content can be a stressor for infauna, by preventing the recycling of organic matter due to polluted water inputs. The organic matter content is often used as a descriptor of the trophic status of infauna (Cocito et al., 1990; Dell'Anno et al., 2002). However, the natural abundance of organic matter can be linked to the vicinity of seagrass meadows, (i) providing dead leaves that partly remain in the sediment, or (ii) with dead matte a few cm under the sediment surface (Boudouresque et al., 2019). In the present work, we assess the whole infauna compartment on the basis of the organic matter content in the sediment (percentage).

2.3.8 Box 8: Organic microdetritus

Posidonia oceanica seagrass meadows produce and export a huge number of dead leaves to adjacent ecosystems, including CDB (Boudouresque et al., 2016). Infralittoral photophilous reefs and coralligenous reefs also export macroalgae, which accumulate or move over circalittoral soft bottoms. Organic macrodetritus composition and biomass vary according to source ecosystems: dead leaves of *P. oceanica*, macroalgae or terrestrial plant remains. Before reaching greater depth, off the continental shelf, organic macrodetritus are used as a trophic resource by the detritivores of the CDB.

2.3.9 Box 9: Detritivores (epibenthic)

Detritivores play an important role, degrading litter and organic debris on the sediment. This compartment is composed of Echinodermata (Holothuroidea, Echinoidea and Asteroidea), Crustacea and Gastropoda. The abundance of some taxa can be favoured by eutrophic (i.e., HOM: High Organic Matter) or oligotrophic (LOM: Low Organic Matter) conditions. Two categories are distinguished: (9a) HOM Detritivores: Including *Holothuria* spp. L., 1767, *Bonellia viridis* Rolando, 1822 and Paguridea; (9b) LOM Detritivores: Represented by *Spatangus purpureus* O.F. Müller, 1776, *Chaetaster longipes* (Bruzelius, 1805), *Echinaster sepositus* (Retzius, 1783), Gastropoda and Crustacea (Mysidacea, Malacostraca). While a high abundance of HOM detritivores can be linked with a CDB that is potentially degraded (eutrophication), the abundance of LOM detritivores, more sensitive to eutrophication, indicates a good status of this compartment. Mean density (individuals per m^2 observed in the photoquadrats at both depths) is a relevant descriptor to assess detritivores 9a and 9b.

2.3.10 Box 10: Filter and suspension feeders (epibenthic)

Benthic filter and suspension feeders on CDB belong to various taxonomic groups: Annelida, Ascidiacea, Bryozoa, Cnidaria, Porifera) (Harmelin, 1978; Souto et al., 2010). On coralligenous reefs, the abundance of *Cliona viridis* (Schmidt, 1862) is considered

as a consequence of stressors (bioerosion in a eutrophic configuration) (Cerrano et al., 2001). However, the presence of *C. viridis* with a relatively low density on CDB, as observed in our case study, cannot be considered as an indicator of stress. Mean density of individuals or colonies per m² (observed in the photoquadrats at both depths) seems to be the most suitable descriptor for filter and suspension feeder assessment, unlike taxonomic richness, due to the difficulty of identification *in situ* or from videos or photographs.

2.3.11 Box 11: Planktivorous teleosts

This compartment includes planktivorous pelagic or demersal fish, with life traits significantly linked with the substrate. Strictly pelagic planktivorous teleosts with no interaction with the bottom (e.g., Clupeidae, Engraulidae) were not considered. The main species observed were *Spicara maena* (L., 1758), *S. smaris* (L., 1758), *Boops boops* (L., 1758), *Chromis chromis* (L., 1758) and *Anthias anthias* (L., 1758). The latter two indicate the vicinity of hard substrates. CDB play an important role for these species: a spawning ground for *Spicara* spp. (Harmelin and Harmelin-Vivien, 1976) and an essential habitat for *Boops boops* juveniles. Planktivorous species are also essential in the trophic network providing a food supply for high level predators (Bănaru et al., 2013; Cresson et al., 2020). The alpha specific richness (number of species per site, considering all methods) was measured to assess the planktivorous teleosts compartment.

2.3.12 Box 12: Carnivores

This box encompasses all carnivorous species, predators of crustaceans, annelids, fishes and other benthic invertebrates. This box is divided in two: Invertebrate carnivores (12a) and Vertebrate carnivores (12b). *(12a) Invertebrate carnivores*: This includes mainly motile species: crustaceans, echinids (Asteroidea, Ophiuroidea), Gastropoda, Nudibranchia, Cnidaria, etc. The alpha taxonomic richness of invertebrate carnivores (per site considering all methods) is a suitable descriptor for this compartment. *(12b) Vertebrate carnivores:* This includes teleost fish species (e.g., Pleuronectidae, Trachinidae, Sparidae, Gobiidae, Blenniidae, Mullidae, Labridae, Triglidae) and chondrichthyans (e.g., *Scyliorhinus* spp. Blainville, 1816, Rajidae). Carnivorous fish find an important trophic resource at the surface or inside the sediment of CDB. Some use CDB as a nursery habitat (e.g., *Serranus hepatus* (L., 1758), *Blennius ocellaris* L., 1758) or a breeding habitat (e.g., *Symphodus cinereus* (Bonnaterre, 1788), *Solea* spp. Quensel, 1806). The assessment of abundance or diversity of fish assemblages normally applied in other marine habitats, such as reefs or seagrass meadows (Harmelin-Vivien et al., 1985), proved of little applicability in CDB. The most suitable descriptor to assess the compartment 12b is the alpha taxonomic richness (number of species observed per site using all methods).

2.4 Compartments not assessed

In the frame of an ecosystem-based approach, it is necessary to considerer all the main functional compartments even if some are not assessed.

2.4.1 Phyto- and zooplankton

Together with POM, phytoplankton and zooplankton are the basis of planktivore diet (Khoury, 1987; Cresson et al., 2014; Chen et al., 2022). This compartment can vary very quickly, and its proper assessment would require too much time and resources relative to its weight in the ecosystem functioning (Table 1). In the framework of an index assessment, it is more suitable to assess it indirectly through its consumers, as is done for other ecosystems (see Personnic et al., 2014; Thibaut et al., 2017).

2.4.2 Pelagic dissolved and particulate organic matter (DOM and POM)

Dissolved organic matter (DOM) and particulate organic matter (POM), provided by phytoplankton exudation, grazing by zooplankton and terrestrial inputs, play a key-role in the marine microbial trophic network (Mostajir et al., 2012) and in some coastal food webs (Darnaude, 2005; Bănaru et al., 2007). As far as the CDB ecosystem is concerned, this compartment is considered as indirectly assessed by the filter feeders and suspension feeder compartment (Box 10) and therefore was not assessed directly.

2.4.3 Microbial loop

The microbial loop is driven by the DOM and the POM (Velimirov et al., 1984; Buffoni et al., 1990). DOM is an important substrate for bacterial production. The microbial loop is defined as a community including heterotrophic micro-organisms, namely Archaea, bacteria, flagellated eukaryotes and ciliates (Azam et al., 1983; Boudouresque, 2015). This compartment is not directly assessed in the present work but it is strictly linked with POM and DOM, plankton communities, filter and suspension feeders (Box 10), planktivores (Box 11) and carnivores (Box 12).

2.4.4 Piscivores

Piscivorous teleosts strictly linked with CDB are very few. High level predators that can be found are mostly casual visitors from adjacent ecosystems (see below). *Lophius* spp. L., 1758 and *Scorpaena scrofa* L., 1758, two nocturnal and benthic predators, more frequently occupy CDB. At the scale of a given sampling site, the occurrence of piscivores is very low.

2.4.5 Transiting live organisms

Many organisms transit through the CDB mainly from the infralittoral and circalittoral ecosystems to the bathyal and abyssal bottoms. Consequently, numerous species from coralligenous reefs, infralittoral reefs and *Posidonia oceanica* meadows can be found in CDB. The assessment of this transiting fauna was indirect through the main compartments of CDB assessed (Boxes 1, 2, 3-4, 5, 9, 10, 12).

Numerous high-level predators can visit CDB occasionally (see the compartment 'Visiting predators' in Figure 2), such as *Dentex dentex* (L., 1758), *Pagrus pagrus* (L., 1758), *Zeus faber* L., 1758, and feed on planktivorous or mesocarnivorous fish species. Because of a very low and occasional occurrence, this compartment was not taken into account.

2.4.6 Carbon sink

Rhodolith beds act as major carbon sinks through their high storage capacity of both organic (C_{org}) and inorganic carbon (C_{inorg}). The effectiveness of this role is strictly associated with the vitality of calcareous organisms living with these ecosystems (Martin et al., 2007; Basso, 2012; Burrows et al., 2014; Watanabe et al., 2020). While the C_{inorg} sequestration results mainly from the significant calcium carbonate contents of the rhodolith skeleton (Van der Heijden and Kamenos, 2015), the capture and the trapping of C_{org} within rhodolith beds come from autochthonous and allochthonous sources (Mao et al., 2020). The C_{org} production is mainly completed through the photosynthesis of rhodolith organisms (B1) and the occurrence of facies of calcareous invertebrates (e.g., Bryozoa, Echinidae, Gastropoda, Annelida, Bivalvia). Though the C_{org} fixation is well known for rhodolith beds (Watanabe et al., 2020), its long-term sequestration in the sediments is still to be specified. For *P. oceanica* meadows, the fixation and C_{org} sequestration capacity proved to be closely related with water depth and its state of conservation. Thus, healthy and shallow meadows are considered as carbon sinks whereas deeper and altered ones may act as carbon sources (Monnier, 2020; Monnier et al., 2021; Pergent-Martini et al., 2021; Monnier et al., 2022).

2.5 Descriptors selection

Fifteen descriptors were selected to assess the 12 boxes of CDB (Table 2). Boxes 3 and 4 were considered together as seasonal macroalgae, so that 11 boxes were actually considered. The weight of each box (W), first defined during the workshop, was successively adjusted according to the results of the test in the field. The compartments selected as providing the main contribution to the functioning of the ecosystem are: Box 1-rhodoliths (W=6), Box 5-infauna (W=5), box 10-filter and suspension feeders, Box 2-perennial and Box 3-4-seasonal macroalgae (W=4).

Descriptors for each compartment were selected among a wide range of available descriptors tested during the sampling. The

TABLE 2 Boxes, descriptors, weight (W) and status for the EBQI assessment (POM, Particulate Organic Matter; HOM, High Organic Matter; LOM, Low Organic Matter).

Box		Descriptors	W	Status				
				4	3	2	1	0
1	Rhodoliths	% cover (upper zone)	6	≥ 20%	20 > x ≥ 10%	10 > x ≥ 5%	5 > x > 0%	0%
		% cover (deep zone)		≥ 10%	10 > x ≥ 5%	5 > x ≥ 1%	1 > x > 0%	0%
2	Perennial macroalgae	% cover (upper zone)	4	≥ 2%	2 > x ≥ 1%	1 > x ≥ 0.2%	0.2 > x ≥ 0%	0%
3-4	Seasonal erected macroalgae	% cover (upper zone)	4	≥ 10%	10> x ≥ 5%	5 > x ≥ 1%	1 > x > 0%	0%
		% cover (deep zone)		≥ 5%	5 >x≥ 2%	2 > x ≥ 1%	1 > x > 0%	0%
5	Herbivores	Alpha taxonomic richness	2	≥ 2		1		0
6	Sedimented POM	% pelitic (< 63 µm) in the sediment	2	<0.02%	0.05 > x ≥ 0.02%	0.1 > x ≥ 0.05%	1 > x≥ 0.1%	≥ 1%
7	Infauna	% Organic Matter in the sediment (status +2 if matte or remains of *Posidonia oceanica* in the sample)	5	3 > x ≥ 2%	4 > x ≥ 3%	5 > x ≥ 4%	2 > x ≥ 0%	≥ 5%
8	Organic macrodetritus	% cover by litter	2	10 > x ≥ 5%	5 > x ≥ 1%	< 1%	25 > x ≥ 10%	≥ 25%
9a	Detritivores HOM	Mean density per m²	3	0	0.6 > x > 0	1> x ≥ 0.6	2>x≥1	≥ 2
9b	Detritivores LOM	Mean density per m²		≥ 2	2 > x ≥ 1	1 > x ≥ 0.6	0.6 > x > 0	0
10	Filter- and Suspension-feeders	Mean density per m²	4	≥ 30	30 > x ≥ 15	15 > x ≥ 10	10 > x ≥ 5	< 5
11	Planktivores	Alpha specific richness	1	≥ 2	–	1	–	0
12a	Carnivorous invertebrates	Alpha taxonomic richness	3	≥ 5	4	3	2	≤ 1
12b	Carnivorous vertebrates	Alpha taxonomic richness		≥ 5	4	3	2	≤ 1

10.3389/fmars.2023.1130540

criteria for descriptor selection were (i) its applicability, (ii) a wide enough range of values across the sampled sites, (iii) the absence of redundancy with the descriptors of other compartments in order to reduce the total number of descriptors.

The method to assess each descriptor is presented in Table 3. The monitoring of one sampling site can be carried out in less than one day with a small boat and 3 operators. It involves (i) one dive with two operators in the upper zone with 12 minutes of investigations (sampling of 3 sediment cores, photographs and videos), covering a mean surface of about 500 m², and (ii) the deployment of the Biocube at the two depths (upper and deep zones) to sample 30 photoquadrats per depth and seascape videos. (iii) Analysis of the cores involves measurement of grain size and percentage of organic matter.

2.6 EBQI calculation

The EBQI is then calculated using the following formula:

$$EBQI = [\sum_{i=1}^{11}(W_i \times S_i)/\sum_{i=1}^{11}(W_i \times S_{max})\ ] \times 10$$

W_i is the weight of the box, S_i the status of the box and S_{max} maximum status possible (4/4). A notation between 0 and 10 is obtained. An ecological status is defined according to the EBQI notation (Personnic et al., 2014; Table 4). The ecological status limits are similar to those defined for *Posidonia oceanica* seagrass meadow (Personnic et al., 2014), coralligenous reefs (Ruitton et al., 2014) and rocky reefs (Thibaut et al., 2017).

A confidence index (CI) was used to assess the quality of the data (suitable protocol, recent data, expert judgment) (see Personnic et al., 2014 for CI calculation) (Table 5). The CI allows assessment of the quality of the sampling according to the recommended methods. If a sampling does not combine all the suitable methods, it will still be possible to calculate an EBQI with a low CI (e.g., data available with other protocols, expert judgement).

TABLE 4 Ecological status according to EBQI notation.

Colour code	Ecological status	EBQI notation
	Very good	EBQI ≥ 7.5
	Good	7.5 > EBQI ≥ 6
	Intermediate	6 > EBQI ≥ 4.5
	Poor	4.5 > EBQI ≥ 3.5
	Bad	EBQI< 3.5

TABLE 3 Method for the assessment of the descriptors for each functional compartment.

Box		Descriptors	Method
1	Rhodoliths	% cover (upper zone)	Photoquadrats (80 cm × 80 cm) at upper zone
		% cover (deep zone)	Photoquadrats (80 cm × 80 cm) at intermediate zone
2	Perennial macroalgae	% cover (upper zone)	Photoquadrats (80 cm × 80 cm) at upper zone
3-4	Seasonal macroalgae	% cover (upper zone)	Photoquadrats (80 cm × 80 cm) at upper zone
		% cover (deep zone)	Photoquadrats (80 cm × 80 cm) at intermediate zone
5	Herbivores	Alpha taxonomic richness	SCUBA, photoquadrats and seascape videos
6	Sedimented POM	% pelitic (< 63 µm) in the sediment	3 sediment cores sampled per site. Grain size analysis (< 63 µm)
7	Infauna	% OM in the sediment (status +2 if matte or *Posidonia oceanica* remains in the sample)	3 sediment cores sampled per site. After drying the samples 48h at 60°C, burning it 4h at 400°C. The difference between the dry weight and the remains after burning is the dry mass of OM.
8	Organic macrodetritus	% cover by litter	Photoquadrats (80 cm × 80 cm) at the 2 depths
9a	Detritivores HOM	Mean density per m²	Photoquadrats (80 cm × 80 cm) at the 2 depths
9b	Detritivores LOM	Mean density per m²	Photoquadrats (80 cm × 80 cm) at the 2 depths
10	Filter- and Suspension-feeders	Mean density per m²	Photoquadrats (80 cm × 80 cm) at the 2 depths
11	Planktivores	Alpha specific richness	SCUBA, photoquadrats and seascape videos
12a	Carnivorous invertebrates	Alpha taxonomic richness	SCUBA, photoquadrats and seascape videos
12b	Carnivorous vertebrates	Alpha taxonomic richness	SCUBA, photoquadrats and seascape videos

10.3389/fmars.2023.1130540

TABLE 5 Confidence index (CI) related with data quality or expert judgement (Criteria from Personnic et al., 2014).

CI	Criteria
4	Field data available, recent, and suitable with the recommended methods
3	Field data recent, partially completed with expert judgement
2	No quantitative field data but recent expert judgement
1	No quantitative field data but ancient expert judgement
0	No quantitative field data and no suitable expert judgement

2.7 Statistical analysis

Correlation between descriptors notation has been tested by calculating Spearman rank-order correlation and assessing its significance with p-value. Principal Component Analysis (PCA) was used without standardization to show the relation between boxes and EBQI sites notations.

The robustness of the EBQI for CDB has been tested with regard to the ecological status per box and the weight per box. A robustness analysis involving 1000 simulations with 25, 50, 75 or 100% of probability of perturbation of ±1 or ±2 (of each ecological status per box and each weighting per box) has been tested. The analysis recalculates the EBQI notation considering the corresponding perturbation (± 1 or ±2) and the probability of perturbation (25, 50, 75 or 100%).

Box status has been plotted on radar charts and the uniformity of box status has been assessed through circularity of polygons representing those charts. Circularity is the ratio between the polygon area and the area of a circle having a circumference equal to the polygon perimeter (Oprandi et al., 2021). Perimeter and area have been calculated using ArcGIS Pro 3.0®.

The influence of the management level was tested on EBQI notations and circularity value using PERMANOVA analysis, using Euclidian distance and 999 permutations (Anderson, 2001). Following Thibaut et al. (2017), four management levels were defined: (i) sites without protection (hereafter named 'No protection'), (ii) Natura 2000 sites (EU Habitats Directives) with no effective protection (hereafter named 'Natura 2000), (iii) protected sites, including MPA with Multi-Use Management (hereafter named MPA-MUM) and (iv) highly protected, including MPA with No-Take Zone (hereafter named 'MPA-NTZ').

P-value threshold was set at 5% for all tests. Analyses were performed with R software (R core team, 2022).

3 Results

3.1 EBQI notation

EBQI notation ranged from 2.05 (27TH) to 8.06 (21PAM) (Table 6; Supplementary Figure 1). Eight sites out of 29 exhibited a Good or Very Good notations while 10 showed a Poor or Bad status. The Confidence CI was lower in Box 7 (infauna) for all sites because of the method used (organic matter assessment instead of macrofauna analysis). The CI was Very Good for all sites, ranging from 88 to 93%.

EBQI notation and box status attributed to each site are mainly explained by local specificities and the vicinity or not of human activities (i.e., urbanized areas). PCA showed a gradient along Axis 2 (16.8% of the total variance) from Poor to Very Good sites. Good and Very Good EBQI notations were mainly explained by the high status of Boxes 1, 2 and 3-4 (primary producers). Boxes 6 (sedimented POM), 7 (infauna), 8 (organic macrodetritus) and 12 (carnivores) were less discriminating (Figure 4).

Radar plot projection helps in assessing the heterogeneity of ecological status per box for each sampling site (Supplementary Figure 2). For example, 21PAM (Pampelonne), with the best notation (EBQI = 8.06), is defined by an ecological status ranging from 2 to 4 while 09EMB (Embiez), also with a good notation (EBQI = 6.98), is characterized by an ecological status between 0 and 4.

A Spearman rank correlation has been tested between the fifteen descriptors used for EBQI calculations (Figure 5). Positive correlations moderately to highly significant are observed between descriptors related to primary producers (Box 1 - rhodoliths, Box 2 - perennial macroalgae, and Box 3-4: seasonal macroalgae and turf). These same descriptors also show significant correlations with the mean density of LOM detritivores (Box 9b). The diversity of herbivores (Box 5) shows a significant negative correlation with the cover of organic macrodetritus (Box 8). The percentage of organic matter (Box 7) shows low but significant correlations (R^2< 0.34) with sedimented POM (Box 6). The percentage of pelitic fraction of the sediment (Box 6) shows a significant negative correlation with the cover of perennial macroalgae (Box 2), rhodoliths (Box 1-UZ) and seasonal macroalgae and turf (Box 3-4). HOM detritivores density (Box 9a) shows no correlations with any other descriptor.

3.2 Circularity analysis

The circularity of radar charts reflects the uniformity of box status. Values range from 0.25 (28ANT) to 0.73 (21PAM) and are independent of the EBQI notation (Spearman correlation: R=0.242 and p=0.206). According to the EBQI notation and circularity value, 4 different situations are identified (Figure 6): (i) CDB sites with moderate-good notation (EBQI≥5) and high homogeneity of box status (circularity≥0.5) such as 24DRA, 04PLA, 09EMB, 16BAG and 21PAM; (ii) CDB sites with moderate-good notation but low homogeneity of box status such as 13FG, 18CAV, 15HB, 20CAM, 26EST, 24PQR and 17 VAI; (iii) CDB sites with poor notation (EBQI<5) and high homogeneity of box status status like 22ST, 10AMP, 07 CC and 29VIL; (iv) CDB sites with poor overall notation and low homogeneity of quality status such as 27TH, 01COU, 06SUG, 11DF, 05PR, 25AGA, 03PRA, 02CAR, 12TGR, 28ANT, 23SAR and 19CT.

3.3 Influence of the management level

The management level at the 29 sampling sites is heterogeneous. Four sites have no protection, 12 sites are included in Natura 2000 sites, 5 sites are within MPA-MUMs, and 8 are within MPA-NTZs. Analysis of EBQI mean notation and Circularity mean value per management level shows no significant differences between management levels (Permanova: respectively p=0.866 and 0.737; Figure 7).

10.3389/fmars.2023.1130540

TABLE 6 EBQI notation, status per box, Confidence Index (CI in %) and Circularity value (Cir.) for the 29 sampling sites (see Figure 1 for location).

Code	Sites	1-UZ	1-DZ	2	3-4-UZ	3-4-DZ	5	6	7	8	9a	9b	10	11	12a	12b	EBQI	CI	Cir.
01COU	La Couronne	0	0	0	1	0	0	1	4	2	4	3	0	0	0	2	2.88	93	0.44
02CAR	Carry	1	0	1	1	0	4	2	4	3	3	0	1	4	0	4	4.55	93	0.27
03PRA	Baie du Prado	1	1	1	2	1	2	1	2	3	4	1	2	0	2	4	4.34	93	0.46
04PLA	Planier	1	2	1	3	2	0	3	4	4	4	2	2	2	2	4	5.9	93	0.56
05PR	Passe de Riou	2	1	1	2	1	0	1	2	2	3	0	1	0	3	3	3.65	93	0.45
06SUG	Sugiton	1	1	1	1	1	0	1	1	4	1	0	3	2	1	1	3.30	93	0.42
07CC	Cap Canaille	1	1	0	1	1	4	3	4	3	1	0	0	2	1	1	3.92	93	0.58
08IVE	Île Verte	3	1	2	4	2	2	4	4	1	1	3	4	0	3	4	6.84	93	0.46
09EMB	Embiez	4	2	2	3	2	4	4	3	2	2	3	4	0	1	3	6.98	93	0.63
10AMP	Amphitria	0	1	0	1	1	0	2	4	3	3	1	0	0	1	0	3.09	93	0.58
11DF	Deux Frères	1	0	0	1	0	2	1	4	3	3	1	1	0	2	0	3.47	93	0.48
12TGR	Toulon Grande Rade	1	1	0	2	3	2	1	4	3	1	0	4	0	1	0	4.65	93	0.29
13FG	Fourmigue de Giens	1	2	2	3	1	0	3	4	3	1	1	3	0	3	2	5.52	93	0.41
14POR	Porquerolles Est	3	4	4	2	4	2	1	4	2	1	3	1	0	3	2	6.70	93	0.48
15HB	Baie d'Hyères	4	2	2	4	4	4	2	0	2	4	3	1	0	4	3	5.76	93	0.48
16BAG	Passe de Bagaud	4	4	4	4	4	4	1	3	2	1	2	1	2	4	1	7.15	93	0.52
17VAI	Vaisseau	4	2	4	4	4	0	3	4	3	3	1	4	0	0	3	7.53	93	0.39
18CAV	Cavalaire	1	3	1	2	2	4	1	4	3	0	1	3	0	4	1	5.63	93	0.27
19CT	Cap Taillat	4	2	1	2	1	4	1	0	2	2	3	4	2	4	1	5.21	93	0.41
20CAM	Cap Camarat	4	3	1	3	2	4	1	4	2	3	4	1	0	1	1	6.01	93	0.40
21PAM	Pampelonne	4	4	2	4	4	4	4	4	2	4	3	2	2	2	3	8.06	93	0.73
22ST	Saint Tropez	0	0	0	1	0	0	1	4	3	1	0	0	2	2	2	2.74	93	0.51
23SAR	Sardinaux	4	0	1	4	1	2	1	3	2	0	0	3	4	0	4	5.07	93	0.33
24DRA	Dramont	4	1	2	3	1	2	1	1	3	0	3	4	4	2	4	5.66	88	0.54
25AGA	Agay	1	1	1	2	1	0	1	4	1	1	3	0	0	4	4	4.03	93	0.33
26EST	Esterel	3	4	2	2	2	4	1	3	2	3	4	2	0	2	4	6.49	93	0.49
27TH	Théoule sur mer	1	0	0	2	1	2	0	0	3	3	1	0	0	1	2	2.05	93	0.43
28ANT	Cap Antibes	1	2	1	2	1	4	0	2	0	3	1	3	0	4	4	4.65	93	0.25
29VIL	Villefranche sur mer	1	0	1	2	1	2	1	4	4	1	2	2	2	3	4	5.00	93	0.54

Red: Poor; Yellow: Bad; Green: Intermediate; Blue: Good; Dark Blue: Very Good. UZ, Upper zone; DZ, Deep zone.

3.4 Robustness analysis

3.4.1 Robustness regarding perturbation of the ecological status

The higher the perturbation and the probability of perturbation, the less similarity is observed in the iterations compared to the initial EBQI calculation (Figure 8; Supplementary Table 1). The percentage of similarity decreases with the probability of perturbation or the number of perturbations (± 1 or ±2). With perturbation of the ecological status per box, the mean similarity (all sites included) moves from 81.8% (25%) to 61.7% (100%) for a ±1 perturbation and from 68.8% (25%) to 38.8% (100%) for a ±2 perturbation. A high perturbation of the ecological status implies a lower stability of the EBQI.

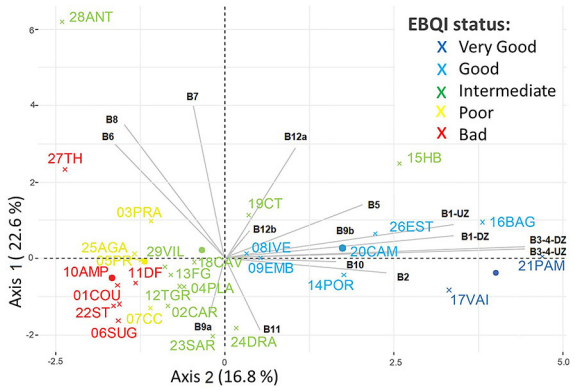

FIGURE 4
Principal Component Analysis. Sampling sites are coloured according to their EBQI notation. Boxes descriptors are projected in light grey. Red: Poor; Yellow: Bad; Green: Intermediate; Blue: Good; Dark Blue: Very Good.

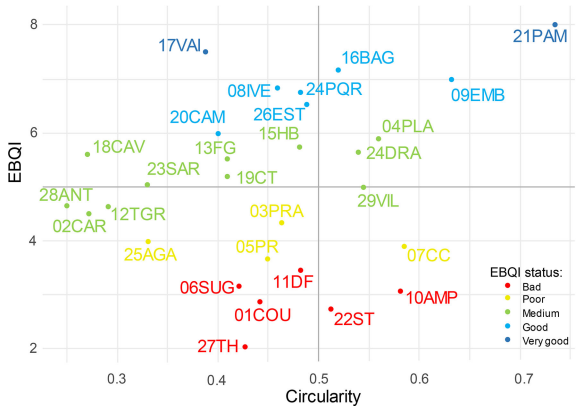

FIGURE 6
Scores of EBQI and Circularity for the 29 sites. Red: Poor; Yellow: Bad; Green: Intermediate; Blue: Good; Dark Blue: Very Good.

3.4.2 Robustness regarding perturbation of the weighting

When perturbing the weighting per box, the mean similarity is higher, moving from 91.5% (25%) to 84.5% (100%) for a ±1 perturbation and from 86.5% (25%) to 73.3% (100%) for a ±2 perturbation (Figure 9; Supplementary Table 1). The perturbation of the weighting does not affect the stability of the index as much as the perturbation of the ecological status per box.

The lower values of similarity for high levels of perturbation (± 2) of both the ecological status per box and the weighting confirm the fact that weighting the boxes is consistent and useful, as already shown by Personnic et al. (2014) for *Posidonia oceanica* seagrass meadows. It is worth noting that the sites with the lowest similarity are often the sites where the initial EBQI notation is close to a threshold between two statuses (e.g., 7.53 is a Very Good notation but very close to the Good status<7.50).

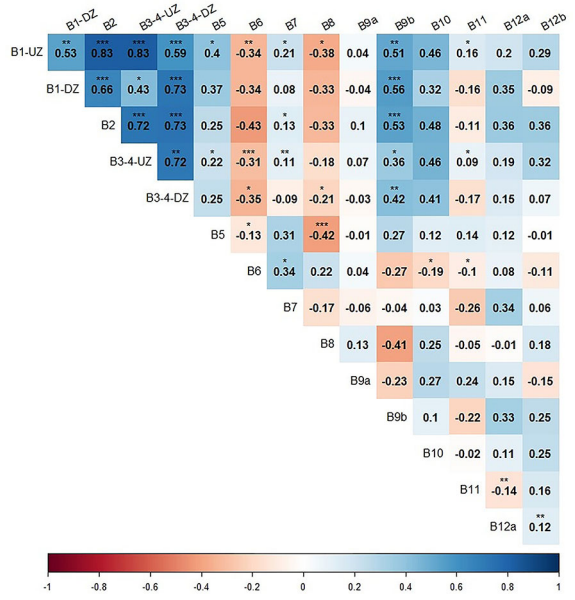

FIGURE 5
Spearman rank correlation between the fifteen descriptors related to ecosystem boxes of the coastal detrital bottoms. The number in bold is the correlation coefficient R. *: p< 0.05; **: p< 0.01; ***: p< 0.001. Blue, positive correlation; Red, negative correlation.

4 Discussion

4.1 An original Ecosystem-Based Quality Index for Coastal Detrital Bottoms

This paper proposes an original Ecosystem-Based Quality Index to assess the health status of the Coastal Detrital Bottoms in the North-Western Mediterranean context. The goal is to provide (i) a useful tool, embracing the concept of the ecosystem-based approach, for coastal managers (MPAs, local authorities), and (ii) arguments for a better consideration of this key habitat according to the MSFD and Barcelona Convention. To determine a relevant biological indicator, the main issue is finding the balance between

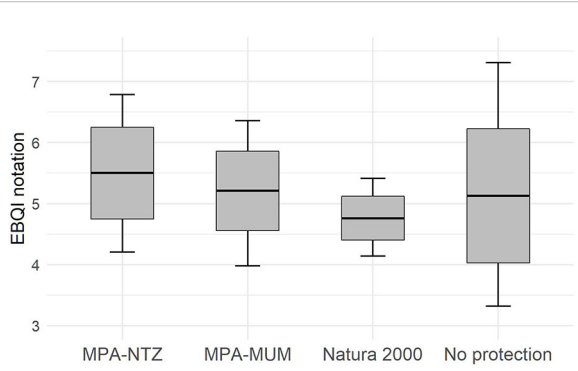

FIGURE 7
Box plots showing EBQI notation (left) and circularity value (right) according management level. The black crossbar corresponds to the mean EBQI notation, the grey rectangle corresponds to the standard error, the vertical bars correspond to the 95% confidence interval.

10.3389/fmars.2023.1130540

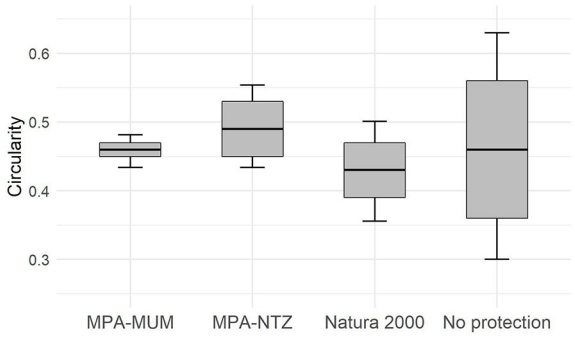

FIGURE 8
Robustness of the EBQI with regard to the Ecological status per box. Sampling sites (x-axis) are sorted in ascending order according to the EBQI notation from left to right. In order to test the effect of the status per box on the EBQI (robustness), status values have been randomly perturbed (above, ± 1; below, ± 2) 25% (left) and 100% (right) of probability; 1000 iterations were performed. The change of the EBQI notation (Bad through Very Good) of a site, for a given iteration, is shown by the colour of the new class in which it falls). Red: Poor; Yellow: Bad; Green: Intermediate; Blue: Good; Dark Blue: Very Good.

the most suitable descriptors versus the feasibility of methods of implementation according to available human and material resources. Unlike ecosystems of priority interest such as *Posidonia oceanica* meadows (Montefalcone, 2009; Lopez y Royo et al., 2010; Personnic et al., 2014; Oprandi et al., 2021), no indices or descriptors are available for the functional or ecosystem-based analysis of CDB.

The EBQI is a suitable tool to broadly assess the functioning of an ecosystem (Boudouresque et al., 2020a; Boudouresque et al., 2020b). It aims at providing a first integrated insight with a general notation and status per compartment, useful at the scale of a sampling site or in the frame of a monitoring network at larger scale. The CI for CDB, between 88 to 93%, is far higher than the mean CI assessed for sites used to defined other EBQI indices: 53% for *Posidonia oceanica* seagrass meadows (Personnic et al., 2014), 62% for undersea caves (Rastorgueff et al., 2015), and 74% for rocky reefs (Thibaut et al., 2017).

As expected, our analysis highlights the influence of both natural features and anthropogenic activities on the ecological status of CDB. Sites in areas without trawling or dredging activities, far from urbanized zones, show the best notation. The Provence and French Riviera coasts provide a wide range of anthropogenic pressure and local natural specificities. This heterogeneity was the key for defining an EBQI for CDB and testing the reliability of the descriptors of the functional compartments. A further analysis will have the benefit of new and detailed data to identify the causes of such a status: natural feature (hydrological context, geology, adjacent habitats) or pressures linked with human activities (trawling, terrigenous input, coastal development, etc.). As for all point measurement methods to assess the ecological quality, the EBQI requires a high number of replicates per site to give a better insight into the structure of the ecosystem assessed. The aim of this approach is to offer a broader view of the ecosystem functioning of a given ecosystem.

According to our results, the protocol proposed is accurate, using accessible methods involving SCUBA diving, photographs,

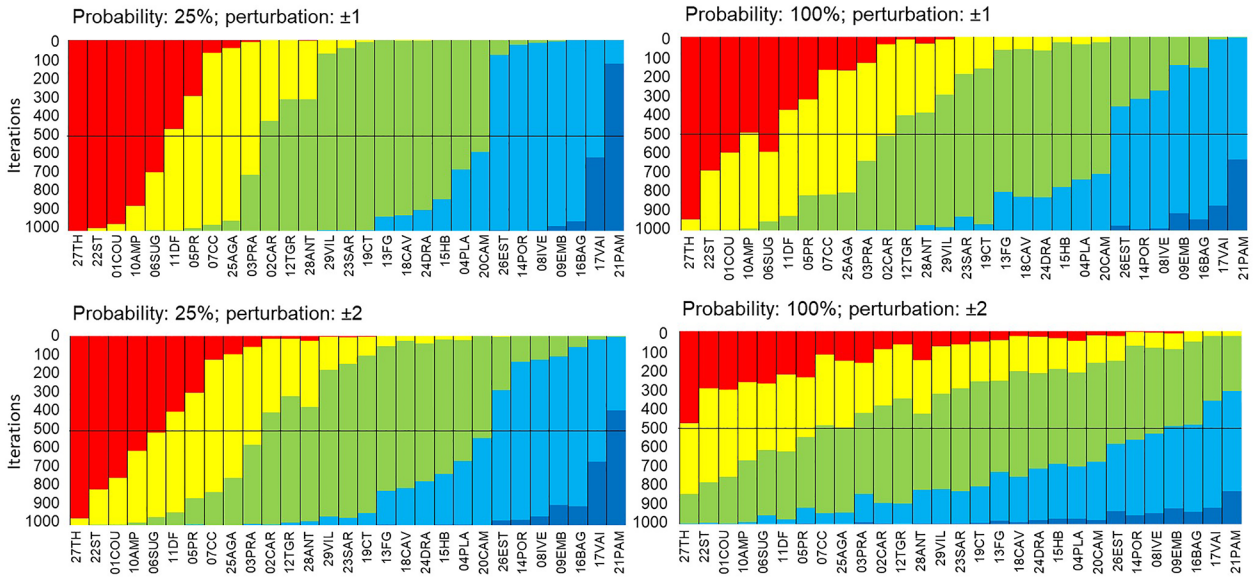

FIGURE 9
Robustness of the EBQI with regard to the weighting per box. Sampling sites (x-axis) are sorted in ascending order according to the EBQI notation from left to right. In order to test the effect of the weighting per box on the EBQI (robustness), status values have been randomly perturbed (above, ± 1; below, ± 2) 25% (left) and 100% (right) of probability; 1000 iterations were performed. The change of the EBQI notation (Bad through Very Good) of a site, for a given iteration, is shown by the colour of the new class within which it falls. Red: Poor; Yellow: Bad; Green: Intermediate; Blue: Good; Dark Blue: Very Good.

photoquadrats and videos. The robustness analysis showed an effect of a perturbation of the ecological status per box or weighting. Nevertheless, the percentage of similarity remained high for a relatively moderate perturbation. The probability of 25% was tested to simulate a theoretical application with one in four chances of being wrong, which is consistent and closer to the reality of field application. Keeping in mind that the EBQI aims at a broad assessment of ecosystem quality and functioning, the results confirmed the robustness of the approach.

4.2 Criticism and improvement perspectives

It would have been a much-improved method if the sediment macrofauna had been properly assessed instead of just measuring the organic matter (Box 7). The quality of the assessment would have been improved, at ecosystem scale, but this would have been very time-consuming during the sampling process. The AMBI index (the AZTI's Marine Biotic Index: Borja et al., 2000; Borja et al., 2003), and other indexes that have been developed, such as e.g., BENTIX (Simboura and Zenetos, 2002), the BQI (Benthic Quality Index; Rosenberg et al., 2004), the GPBI (General Purpose Biological Index; Labrune et al., 2021) and MEDOCC (specifically for Mediterranean assemblages; Pinedo et al., 2015), allow the assessment of the ecological quality of soft bottoms based on sediment macrofauna (see also Labrune et al., 2006). They consider the abundance in the sediment of species sensitive to stressors, tolerant and opportunistic. They can provide reliable information about infauna status to complete and improve the ecosystem-based assessment, but can be ineffective for detection of an impact of physical pressures (e.g., AMBI: see Labrune et al., 2006, but also Borja et al., 2015). The macrofauna of the sediment is of importance in terms of ecological functioning and trophic interactions with epibenthic and demersal communities (Austen et al., 2002), and obviously an assessment considering only the organic matter content is far from being entirely satisfactory (Cocito et al., 1990). It could also be argued that while the proper identification of CDB must be based on the infauna (Pérès and Picard, 1964), the index presented here focuses mostly on the epibenthos. However, characterization and assessment are two distinct steps of environmental diagnostics (Bianchi et al., 2012): assessment criteria can be applied only after the habitat in question has been characterized. We do believe that the health status of the CDB epibenthic facies is an acceptable proxy for the quality of the whole ecosystem; that is why we have decided to assign the highest weighting to Box 1 (Rhodoliths), which may require discussion. All the direct anthropogenic physical pressures mentioned in the previous pages obviously threaten the epibenthos first, rather than the infauna, which is known to be more resilient. Furthermore, as far as we are aware, the ongoing seawater warming in the Western Mediterranean region (Cerrano et al., 2000; Garrabou et al., 2009) is affecting epibenthic species more than the infauna. But it may be true that the degradation of the CDB epibenthic facies may not necessarily imply a bad status for the infauna, and further research is needed. An accurate assessment of the entire ecosystem should imply more than just a selection of functional compartments, as evoked by de Jonge et al. (2019).

Rhodolith beds in CDB can be considered both soft and hard substrata, according to the associated benthic communities (Jacquotte, 1962; Hall-Spencer, 1998; Basso et al., 2017). Rhodolith beds are also described as a step towards the edification of coralligenous banks, from a soft bottom towards a hard bottom, under specific environmental conditions (Basso et al., 2007). The pioneer zoologist André Fortuné Marion named as 'coralligenous gravels' the rhodolith beds of the Gulf of Marseille (Marion, 1883). The '*Coralligène de plateau*' described by Pérès and Picard (1951, 1964); Laborel (1961) and Bellan-Santini et al. (1994) is a coralligenous bank developing from the growth and coalescence of rhodoliths and calcified invertebrates. This highlights the key-role of calcareous macroalgae in inducing autogenic ecological succession (Laborel, 1961; Laubier, 1966; Odum, 1971; Begon et al., 1986; Basso et al., 2007). In some circumstances, the epibenthic associations of the CDB, particularly rhodolith beds, can be considered as being at the threshold between a circalittoral sandy bottom and an actual upcoming coralligenous bank. A CDB facies with small concretionary boulders has also been described by Meinesz et al. (1983). This does not mean that CDB are necessarily hard substrates. The slow evolution towards a coralligenous bank cannot be generalized to all CDB, even in presence of rhodolith beds.

Bryozoan facies, as described by Bianchi (2009a) and Harmelin (2017), have not been found at the 29 sampling sites considered in the present work. The patchiness of epibenthic associations and facies and the rarity of such a feature might explain our result. Yet facies of *Pentapora fascialis* and other branched bryozoans on CDB are known for example around Port-Cros Island (Laborel et al., 1976; Holon and Harmelin, 2014; Harmelin, 2017) but were not found during our investigations. Such rarity highlights the conservation issue and the importance of protecting and monitoring CDB. Bryozoans are known to contribute significantly to the bioclastic part of soft bottoms worldwide (Halfar et al., 2006).

The assessment of widespread and patchy habitat such as CDB requires a seascape approach. It is known that the seascape can directly influence the trophic network and the ecosystem functioning (Boström et al., 2011; Abadie et al., 2018; Santos et al., 2022). In the light of that, a seascape approach should be a potential suitable descriptor to assess the quality of an ecosystem (e.g., marine forests, habitat structure, etc.; Cheminée et al., 2014; Thiriet et al., 2014). We have proposed a combination of methods to provide as broad and as representative an assessment as possible, involving direct observation *via* SCUBA diving, photoquadrats and seascape videos, taking into account functional ecosystem compartments structuring the seascape. The compartments assessed exhibited structuring communities (filter and suspension feeders, rhodoliths) which contribute to the seascape. For example, Gobert et al. (2014) proposed the LIMA index, which is based on a topographical and a biological description and could be applied on all types of habitat from 0 to 40 m depth. Such an approach could be of interest for CDB hosting structuring facies and associations; in the case of CDB without such features, a relatively unstructured seascape cannot be interpreted as a low-functioning ecosystem,

considering the macrofauna of the sediment, a compartment of importance but with little or barely perceptible consequences for the seascape structure (bioturbation, calcified organisms providing bioclastic elements, etc.).

Our analysis showed strong and expected correlations between some of the descriptors. Defining an indicator implies the selection of suitable descriptors but that are not too numerous for an operational implementation. Our purpose was to assess the main compartments of the ecosystem, as defined in Figure 2, using as few descriptors as possible. The correlation observed between the final set of descriptors could lead us to reduce the number of descriptors and then simplify the assessment and avoid redundancy; at the same time, a combination of correlated descriptors assessing different ecological functions improves the robustness. As reported by Personnic et al. (2014), the removal of correlated boxes might result in a loss of accuracy of the method.

An ecosystem-based approach can be useful for Ecosystem Services assessment, providing quantitative data for the different ecosystem compartments (Seitz et al., 2014; Burgos et al., 2017). Such an approach has already been carried out for several ecosystems, including seagrass meadows and considering different bundles of ecosystem services according to different quality status (Kermagoret et al., 2019; Scémama et al., 2020).

4.3 A tool to support assessment of anthropogenic pressures

The next step should be the design of an anthropogenic pressure assessment tool to estimate the links between ecological status and cumulated anthropogenic pressures (Holon et al., 2015; Guarnieri et al., 2016; Quemmerais-Amice et al., 2020). Assessing anthropogenic pressures is challenging. Moreover, the assessment of human activities can be considered as a good proxy. In the present work, we did not identify visible evidence of trawling or dredging, the main physical pressures affecting CDB. Such evidence can be difficult to find, even in long-time trawled areas (Ordines et al., 2017). The main evidences of stress observed was the occurrence of macrowastes (e.g., glass, plastic, fishing gears) and invasive alien species (e.g., *Caulerpa cylindracea*) or the transition to Muddy detrital bottoms. A complementary approach is needed to better characterize human pressures. Our study sites are not located in areas with heavy impact of trawling activity, compared to e.g., the Gulf of Lion, the Catalan Coast or Balearic Islands (Farriols et al., 2017; Jac and Vaz, 2020). New data in different configurations with regard to anthropogenic pressures need to be sampled and assessed.

4.4 The need for an effective protection

The increase in the surface area of Marine Protected Areas driven by the European Union since the 2010s has led to the extension of MPAs over the continental shelf, including coastal detrital bottoms. The new borders of these MPAs do not automatically mean an effective protection and management, and it takes time for coastal managers to integrate these new areas in dashboards and management plans (Vassallo et al., 2020). As a result, the ecological status of CDB sites shows no correlation with the management level in contrast with the findings of Thibaut et al. (2017), who evidenced differences in sublittoral rocky reefs according to the level of management. In addition, we observed no statistical difference between Natura 2000 and unprotected sites, pointing some weaknesses already discussed by Gianni et al. (2022). These results highlight the need to enhance the conservation of widespread ecosystems of the continental shelf such as the CDB, requiring the implementation of effective marine protected areas (Sala et al., 2021).

The conservation or the restoration of CDB implies the reduction or at least the regulation of anthropogenic pressures to allow the natural resilience of communities identified as impacted by such activities. In that case, the role of effective MPAs is limited to the regulation or prohibition of certain human activities: e.g., trawling, dredging, artisanal fishing, mooring. The regulation of other pressures (e.g., terrigenous inputs, the spread of NIS, eutrophication, sedimentation) calls for larger scale policies.

4.5 EBQI implementation for CDB

As an indicator embracing the concept of the ecosystem-based approach, the aim of the EBQI defined for CDB is to provide relevant and useful data for both European Directives (MSFD, WFD, HD) and local management purposes. Compared to other indicators dedicated to soft bottoms (e.g., Borja et al., 2000; Labrune et al., 2006; Labrune et al., 2021), using the EBQI does not require a strong expertise in taxonomy even if more parameters are involved for its calculation. Fifteen descriptors are needed to assess the EBQI for CDB, 13 for *Posidonia oceanica* seagrass meadows (Personnic et al., 2014) and 10 for infralittoral rocky reefs (Thibaut et al., 2017). Data sampling can be carried out in less than one day per site, involving three operators, which is reasonable if planning a long-term monitoring network at regional (e.g., French Mediterranean coast) or local scale (e.g., MPA; Astruch et al., 2022b). The frame proposed by the EBQI can provide a standardized method for assessing the conservation status according to the Habitats Directive (e.g., assessment of the structure and the function of a given habitat), where diagnosis is usually based on expert judgement and broad data. Repeated applications over time would be welcome to assess the suitability of this index for describing change following management actions (Mancini et al., 2020; Oprandi et al., 2022).

The EBQI on CDB should be applied and tested in contexts with other biogeographical specificities and pressures: oligotrophic, warmer and impacted by non-indigenous species, where very little knowledge is available (e.g., Southern and Eastern Mediterranean Sea). The same approach could also be applied on subtidal rhodolith beds in other areas worldwide of high concern with regard to related human activities (e.g., Brittany). The strength of the EBQIs implemented from now in the Mediterranean Sea is the possibility to measure an ecological status even without all the

descriptors assessed with the appropriate method, using the Confidence Index (CI) (see Bevilacqua et al., 2020; Güreşen et al., 2020). This point could allow a preliminary evaluation of CDB in areas with limited human and material resources.

5 Conclusion

An original Ecosystem-Based Quality Index (EBQI) for the Coastal Detrital Bottoms (CDB) has been defined, inspired by already existing EBQIs for *Posidonia oceanica* seagrass meadows, coralligenous reefs, underwater marine caves, and infralittoral rocky reefs, all based mainly on the assessment of their epibenthic assemblages. Relatively easy to implement and robust, the CDB EBQI provides a fit-for-purpose tool to assess the quality of this widespread ecosystem in accordance with public policies at national and European levels. In the context of the increase in the surface areas of Marine Protected Areas, management goals should include CDB in upcoming plans to secure the conservation of a habitat of importance at Mediterranean scale. Our approach is mainly focused on epibenthic assemblages and improvement is needed in order to better take into account the assessment of the macrofauna of the sediment. We suggest applying and testing this approach in other areas within the Mediterranean Sea and beyond.

Data availability statement

The raw data supporting the conclusions of this article will be made available by the authors, without undue reservation.

Author contributions

All authors (excepting AO, NM, BM, and BD) participated in a workshop in Marseille in April 2019. PA, BB, TS, and AO carried out the field investigations and the data sampling in 2020 and 2021. All authors contributed to the content for their associated sections. TS and AO produced the statistical analysis. PA compiled content from all authors and prepared the final version. All authors contributed to the article and approved the submitted version.

Funding

The present work was funded by the French Biodiversity Office in the frame of the ACDSea project (Assessment of Coastal Detrital ecosystem conservation Status: an ecosystem-based approach).

Acknowledgments

This work was carried out in the frame of the ACDSea project (Assessment of Coastal Detrital ecosystem conservation Status: an ecosystem-based approach). We kindly thank the French Biodiversity Office (OFB) for financial support, the experts involved in the working out of the index, Michèle Perret-Boudouresque for documentation assistance, and Michael Paul for proof-reading of the text. This work is dedicated to the memory of our late colleague Boris Daniel, involved in the ACDSea project since the first steps.

Conflict of interest

The authors declare that the research was conducted in the absence of any commercial or financial relationships that could be construed as a potential conflict of interest.

Publisher's note

All claims expressed in this article are solely those of the authors and do not necessarily represent those of their affiliated organizations, or those of the publisher, the editors and the reviewers. Any product that may be evaluated in this article, or claim that may be made by its manufacturer, is not guaranteed or endorsed by the publisher.

Supplementary material

The Supplementary Material for this article can be found online at: https://www.frontiersin.org/articles/10.3389/fmars.2023.1130540/full#supplementary-material

References

Abadie, A., Pace, M., Gobert, S., and Borg, J. A. (2018). Seascape ecology in *Posidonia oceanica* seagrass meadows: Linking structure and ecological processes for management. *Ecol. Indic.* 87, 1–13. doi: 10.1016/j.ecolind.2017.12.029

Agnesi, S., Annunziatellis, A., Inghilesi, R., Mo, G., and Orasi, A. (2020). The contribution of wind-wave energy at sea bottom to the modelling of rhodolith beds distribution in an offshore continental shelf. *Mediterr. Mar. Sci.* 21 (2), 433–441. doi: 10.12681/mms.22462

Aguado-Giménez, F., and Ruiz-Fernández, J. M. (2012). Influence of an experimental fish farm on the spatio-temporal dynamic of a Mediterranean maerl algae community. *Mar. Environ. Res.* 74, 47–55. doi: 10.1016/j.marenvres.2011.12.003

Aguilar, R., Pastor, X., Torriente, A., and Garcia, S. (2009). "Deep-sea coralligenous beds observed with ROV on four seamounts in the western Mediterranean," in *UNEP–MAP–RAC/SPA proceedings of the 1st Mediterranean symposium on the conservation of the coralligenous and other calcareous bio-concretions*. Eds. C. Pergent-Martini and M. Brichet (Tabarka, Tunisia: RAC/SPA), 148–150.

Aliani, S., Bianchi, C. N., and De Biasi, A. M. (1994). Benthos changes in a dumping site. *Biol. Marina Mediterr.* 1 (1), 265–269.

Amado-Filho, G. M., Bahia, R. G., Pereira-Filho, G. H., and Longo, L. L. (2017). "South Atlantic rhodolith beds: latitudinal distribution, species composition, structure and ecosystem functions, threats and conservation status," in *Rhodolith/Maërl beds: A global perspective* (Cham.: Springer), 299–317. doi: 10.1007/978-3-319-29315-8_12

Amado-Filho, G. M., and Pereira-Filho, G. H. (2012). Rhodolith beds in Brazil: a new potential habitat for marine bioprospection. *Rev. Bras. Farmacognosia* 22, 782–788. doi: 10.1590/S0102-695X2012005000066

Anderson, M. J. (2001). A new method for non-parametric multivariate analysis of variance. *Austral Ecol.* 26, 32–46.

Aouissi, M., Sellam, L. N., Boudouresque, C. F., Blanfuné, A., Derbal, F., Frihi, H., et al. (2018). Insights into the species diversity of the genus *Sargassum* (Phaeophyceae) in the Mediterranean Sea, with a focus on a previously unnoticed taxon from Algeria. *Mediterr. Mar. Sci.* 19 (1), 48–57. doi: 10.12681/mms.14079

Astruch, P., Boudouresque, C. F., Bonhomme, D., Goujard, A., Antonioli, P. A., Bonhomme, P., et al. (2012). Mapping and state of conservation of benthic marine habitats and assemblages of port-cros national park (Provence, France, northwestern Mediterranean Sea). *Sci. Rep. Port-Cros Natl. Park* 26, 45–90.

Astruch, P., Goujard, A., Rouanet, E., Boudouresque, C. F., Verlaque, M., Berthier, L., et al. (2019). "Assessment of the conservation status of coastal detrital sandy bottoms in the Mediterranean Sea: An ecosystem-based approach in the framework of the ACDSea project," in *Proceedings of the 3rd Mediterranean Symposium on the conservation of coralligenous and other calcareous bio-concretions*, Antalya, Turquie, 15-16 january 2019 Eds. H. Langar and A. Ouerghi (Tunis: RAC/SPA Publ.) 23–29.

Astruch, P., Orts, A., Schohn, T., Belloni, B., Ballesteros, E., Bianchi, C. N., et al. (2022a). "Towards an ecosystem-based index to assess the ecological status of Mediterranean coastal detrital bottoms," in *Proceedings of the 4th Mediterranean symposium on the conservation of coralligenous & other calcareous bio-concretions*. Eds. C. Bouafif and A. Ouerghi (Tunis: SPA/RAC), 137–138.

Astruch, P., Schohn, T., Belloni, B., Cassetti, O., Cabral, M., Ruitton, S., et al. (2022b). "Involving managers in the ecosystem-based assessment of marine habitats: A case study in French Catalonia," in *Proceedings of the 7th Mediterranean symposium on marine vegetation Mediterranean symposia on marine vegetation*. Eds. C. Bouafif and A. Ouerghi (Tunis: SPA/RAC).

Augier, H., and Boudouresque, C. F. (1975). Dix ans de recherches dans la zone marine du parc national de port- cros-troisième partie. *Annales la SSNATV* 27, 133–170.

Augier, H., and Boudouresque, C. F. (1978). Végétation marine de l'île de port-cros (Parc national) XVI: Contribution à l'étude de l'épiflore du détritique côtier. *Travaux Scientifiques du Parc Natl. Port-Cros* 4, 101–125.

Austen, M. C., Lambshead, P. J. D., Hutchings, P. A., Boucher, G., Snelgrove, P. V. R., Heip, C., et al. (2002). Biodiversity links above and below the marine sediment–water interface that may influence community stability. *Biodiversity Conserv.* 11 (1), 113–136. doi: 10.1023/A:1014098917535

Azam, F., Fenchel, T., Field, J. G., Gray, J. S., Meyer-Reil, L. A., and Thingstad, F. (1983). The ecological role of water-column microbes in the sea. *Mar. Ecol. Prog. Ser.* 10, 257–263. doi: 10.3354/meps010257

Bajjouk, T., Guillaumont, B., Michez, N., Thouin, B., Croguennec, C., Populus, J., et al. (2015). Classification EUNIS, système d'information européen sur la nature: Traduction française des habitats benthiques des régions atlantique et méditerranée. *Habitats subtidaux complexes d'habitats* 2, 237.

Ballesteros, E. (1989). Production of seaweeds in northwestern Mediterranean marine communities: its relation with environmental factors. *Scientia Marina* 53 (2-3), 357–364.

Ballesteros, E. (1990). Structure and dynamics of the community of *Cystoseira zosteroides* (Turner) c. agardh (Fucales, phaeophyceae) in the northwestern Mediterranean. *Scientia Marina* 54 (3), 217–229.

Ballesteros, E. (1994). The deep-water *Peyssonnelia* beds from the Balearic islands (Western Mediterranean). *Mar. Ecol.* 15 (3-4), 233–253. doi: 10.1111/j.1439-0485.1994.tb00055.x

Ballesteros, E. (2006). Mediterranean Coralligenous assemblages: A synthesis of present knowledge. *Oceanogr. Mar. Biol.* 44, 123–195. doi: 10.1201/9781420006391.ch4

Ballesteros, E., Torras, X., Pinedo, S., García, M., Mangialajo, L., and De Torres, M. (2007). A new methodology based on littoral community cartography dominated by macroalgae for the implementation of the European water framework directive. *Mar. Pollut. Bull.* 55 (1-6), 172–180. doi: 10.1016/j.marpolbul.2006.08.038

Bănaru, D., Harmelin-Vivien, M., Gomoiu, M. T., and Onciu, T. M. (2007). Influence of the Danube river inputs on c and n stable isotope ratios of the Romanian coastal waters and sediment (Black Sea). *Mar. Pollut. Bull.* 54, 1385–1384. doi: 10.1016/j.marpolbul.2007.05.022

Bănaru, D., Mellon-Duval, C., Roos, D., Bigot, J. L., Souplet, A., Jadaud, A., et al. (2013). Trophic interactions in the gulf of lions ecosystem (northwestern Mediterranean) and fishing impacts. *ICES J. Mar. Syst.* 111-112, 45–68. doi: 10.1016/j.jmarsys.2012.09.010

Barbera, C., Bordehore, C., Borg, J. A., Glémarec, M., Grall, J., Hall-Spencer, J. M., et al. (2003). Conservation and management of northeast Atlantic and Mediterranean maerl beds. *Aquat. Conservation: Mar. Freshw. Ecosyst.* 13 (S1), S65–S76. doi: 10.1002/aqc.569

Basso, D. (2012). Carbonate production by calcareous red algae and global change. *Geodiversitas* 34 (1), 13–33. doi: 10.5252/g2012n1a2

Basso, D., Babbini, L., Kaleb, S., Bracchi, V., and Falace, A. (2016). Monitoring deep Mediterranean rhodolith beds. *Aquat. Conservation: Mar. Freshw. Ecosystem* 26, 549–561. doi: 10.1002/aqc.2586

Basso, D., Babbini, L., Ramos-Esplá, A. A., and Salomidi, M. (2017). "Mediterranean Rhodolith beds," in *Rhodolith/Maerl beds: a global perspective* (Cham.: Springer), 281–298. doi: 10.1007/978-3-319-29315-8_11

Basso, D., Nalin, R., and Massari, F. (2007). Genesis and composition of the pleistocene coralligène de plateau of the cutro terrace (Calabria, southern Italy). *Neues Jahrbuch für Geol. und Paläontologie–Abhandlungen* 244 (2), 73–182. doi: 10.1127/0077-7749/2007/0244-0173

Basso, D., Quaranta, F., Vannucci, G., and Piazza, M. (2012). Quantification of the coralline carbonate from a serravallian rhodolith bed of the tertiary piedmont basin (Stazzano, alessandria, NW Italy). *Geodiversitas* 34 (1), 137–149. doi: 10.5252/g2012n1a8

Begon, M., Harper, J. L., and Townsend, C. R. (1986). *Ecology: Individuals, populations and communities* (Oxford: Blackwell Scientific Publications), 876.

Bellan, G., Bellan-Santini, D., and Picard, J. (1980). Mise en évidence de modèles écobiologique dans des zones soumises à perturbations par matières organiques. *Oceanol. Acta* 3 (3), 383–390.

Bellan-Santini, D., Lacaze, J. C., and Poizat, C. (1994). Les Biocénoses marines et littorales de méditerranée. synthèse, menaces et perspectives. *Collection Patrimoines naturels* 19, 246. Secrétariat de la faune et de la flore/MNHN, Paris.

Bensettiti, F., Bioret, F., Roland, J., and Lacoste, J. P. (2004). *Cahiers d'habitats natura 2000. connaissance et gestion des habitats et des espèces d'intérêt communautaire. tome 2 - habitats côtiers* (Paris: La Documentation française), 399. MEDD/MAAPAR/MNHN.

Bergbauer, M., and Humberg, B. (2000). "La vie sous-marine en méditerranée," in *Guide vigot* (p: Vigot), 318.

Bermejo, R., Chefaoui, R. M., Engelen, A. H., Buonomo, R., Neiva, J., Ferreira-Costa, J., et al. (2018). Marine forests of the Mediterranean-Atlantic *Cystoseira tamariscifolia* complex show a southern Iberian genetic hotspot and no reproductive isolation in parapatry. *Sci. Rep.* 8, 10427. doi: 10.1038/s41598-018-28811-1

Bernard, G., Romero-Ramirez, A., Tauran, A., Pantalos, M., Deflandre, B., Grall, J., et al. (2019). Declining maerl vitality and habitat complexity across a dredging gradient: Insights from *in situ* sediment profile imagery (SPI). *Sci. Rep.* 9 (1), 1–12. doi: 10.1038/s41598-019-52586-8

Bevilacqua, S., Katsanevakis, S., Micheli, F., Sala, E., Rilov, G., Sarà, G., et al. (2020). The status of coastal benthic ecosystems in the Mediterranean Sea: evidence from ecological indicators. *Front. Mar. Sci.* 7. doi: 10.3389/fmars.2020.00475

Bianchi, C. N. (2009a). Gli habitat prioritari del protocollo SPA/BIO (Convenzione di barcellona) presenti in italia. schede descrittive per l'identificazione. IV. 2. 2. 10. facies with large bryozoans. *Biol. Marina Mediterr.* 16 (Suppl. 1), 209–212.

Bianchi, C. N. (2009b). Gli habitat prioritari del protocollo SPA/BIO (Convenzione di barcellona) presenti in italia. schede descrittive per l'identificazione. III. 6. 1.14. facies with *Cladocora caespitosa*. *Biol. Marina Mediterr.* 16 (Suppl. 1), 163–166.

Bianchi, C. N., Ardizzone, D., Belluscio, A., Colantoni, P., Diviacco, G., Morri, C., et al. (2004). Benthic cartography. *Biol. Marina Mediterr.* 11 (suppl. 1), 347–370.

Bianchi, C. N., Azzola, A., Bertolino, M., Betti, F., Bo, M., Cattaneo-Vietti, R., et al. (2019a). Consequences of the marine climate and ecosystem shift of the 1980-90s on the ligurian Sea biodiversity (NW Mediterranean). *Eur. Zool. J.* 86 (1), 458–487. doi: 10.1080/24750263.2019.1687765

Bianchi, C. N., Azzola, A., Cocito, S., Morri, C., Oprandi, A., Peirano, A., et al. (2022). Biodiversity monitoring in Mediterranean marine protected areas: scientific and methodological challenges. *Diversity* 14, 43. doi: 10.3390/d14010043

Bianchi, C. N., Azzola, A., Parravicini, V., Peirano, A., Morri, C., and Montefalcone, M. (2019b). Abrupt change in a subtidal rocky reef community coincided with a rapid acceleration of sea water warming. *Diversity* 11, 215. doi: 10.3390/d11110215

Bianchi, C. N., Parravicini, V., Montefalcone, M., Rovere, A., and Morri, C. (2012). The challenge of managing marine biodiversity: a practical toolkit for a cartographic, territorial approach. *Diversity* 4, 419–452. doi: 10.3390/d4040419

Blanchard, J. L., Jennings, S., Law, R., Castle, M. D., McCloghrie, P., Rochet, M. J., et al. (2009). How does abundance scale with body size in coupled size-structured food webs? *J. Anim. Ecol.* 78 (1), 270–280. doi: 10.1111/j.1365-2656.2008.01466.x

Blanfuné, A., Thibaut, T., Boudouresque, C. F., Mačić, V., Markovic, L., Palomba, L., et al. (2017). The CARLIT method for the assessment of the ecological quality of European Mediterranean waters: Relevance, robustness and possible improvements. *Ecol. Indic.* 72, 249–259. doi: 10.1016/j.ecolind.2016.07.049

Bond, W. (2001). Keystone species–hunting the snark? *Science* 292, 63–64. doi: 10.1126/science.1060793

Bordehore, C., Borg, J. A., Lanfranco, E., Espla, A. A., Rizzo, M., and Schembri, P. J. (2000). "Trawling as a major threat to Mediterranean maerl beds," in *First Mediterranean Symposium on Marine Vegetation, Ajaccio*. (Tunis: RAC/SPA publ.) 105–109.

Bordehore, C., Ramos-Esplá, A. A., and Riosmena-Rodríguez, R. (2003). Comparative study of two maerl beds with different otter trawling history, southeast Iberian peninsula. *Aquat. Conservation: Mar. Freshw. Ecosyst.* 13 (S1), S43–S54. doi: 10.1002/aqc.567

Borja, A., Franco, J., and Pérez, V. (2000). A marine biotic index to establish the ecological quality of soft-bottom benthos within European estuarine and coastal environments. *Mar. Pollut. Bull.* 40, 1100–1114. doi: 10.1016/S0025-326X(00)00061-8

Borja, Á., Marín, S. L., Muxika, I., Pino, L., and Rodríguez, J. G. (2015). Is there a possibility of ranking benthic quality assessment indices to select the most responsive to different human pressures? *Mar. Pollut. Bull.* 97 (1-2), 85–94. doi: 10.1016/j.marpolbul.2015.06.030

Borja, A., Menchaca, I., Garmendia, J. M., Franco, J., Larreta, J., Sagarminaga, Y., et al. (2021). Big insights from a small country: The added value of integrated assessment in the marine environmental status evaluation of Malta. *Front. Mar. Sci.* 8, 375. doi: 10.3389/fmars.2021.638232

Borja, A., Muxika, I., and Franco, J. (2003). The application of a marine biotic index to different impact sources affecting soft-bottom benthic communities along European coasts. *Mar. Pollut. Bull.* 46, 835–845. doi: 10.1016/S0025-326X(03)00090-0

Bosellini, A., and Ginsburg, R. N. (1971). Form and internal structure of recent algal nodules (rhodolites) from Bermuda. *J. Geol.* 79 (6), 669–682. doi: 10.1086/627697

Boström, C., Pittman, S. J., Simenstad, C., and Kneib, R. T. (2011). Seascape ecology of coastal biogenic habitats: advances, gaps, and challenges. *Mar. Ecol. Prog. Ser.* 427, 191–217. doi: 10.3354/meps09051

Boudouresque, C. F. (2015). "Taxonomy and phylogeny of unicellular eukaryotes," in *Environmental microbiology: Fundamentals and applications* (Dordrecht: Springer), 191–257. doi: 10.1007/978-94-017-9118-2_7

Boudouresque, C. F., Astruch, P., Bănaru, D., Blanfuné, A., Belloni, B., Changeux, T., et al. (2020b). Ecosystem-based quality indices: Valuable tools for environment management. *Vie Milieu – Life Environ.* 70 (3-4), 2–15.

Boudouresque, C. F., Astruch, P., Bănaru, D., Blanfuné, A., Carlotti, F., Faget, D., et al. (2020a). "Global change and the management of Mediterranean coastal habitats: A plea for a socio-ecosystem-based approach," in *Evolution of marine coastal ecosystems under the pressure of global changes* (Cham: Springer International Publishing), 297–320. doi: 10.1007/978-3-030-43484-7_20

Boudouresque, C. F., Astruch, P., Goujard, A., Rouanet, E., Bonhomme, D., and Bonhomme, P. (2019). "The withdrawal of the lower limit of the *Posidonia oceanica* seagrass meadow in the bay of hyères (NW mediterranean): A combination of natural and human-induced recent and ancient phenomena?," in *Proceedings of the 6th Mediterranean symposium on marine vegetation*, Antalya, Turkey, 14-15 January 2019. 35–40.

Boudouresque, C. F., and Denizot, M. (1973). Recherches sur le genre *Peyssonnelia* (Rhodophycées) i. peyssonnelia rosa-marina sp. nov. et *Peyssonnelia bornetii* sp. nov. *Giornale Botanico Italiano* 107, 17–27. doi: 10.1080/11263507309426312

Boudouresque, C. F., Pergent, G., Pergent-Martini, C., Ruitton, S., Thibaut, T., and Verlaque, M. (2016). The necromass of the *Posidonia oceanica* seagrass meadow: Fate, role, ecosystem services and vulnerability. *Hydrobiologia* 781 (1), 25–42. doi: 10.1007/s10750-015-2333-y

Boudouresque, C. F., and Verlaque, M. (2002). Biological pollution in the Mediterranean Sea: invasive versus introduced macrophytes. *Mar. Pollut. Bull.* 44 (1), 32–38. doi: 10.1016/S0025-326X(01)00150-3

Bourcier, M. (1982). Nouvelles localisations et délimitation fine de quelques faciès de la biocénose des fonds détritiques côtiers du PN port-cros. *Travaux Scientifiques du Parc Natl. Port-Cros* 8, 19–24.

Bourcier, M. (1985). Localisation et délimitation de quelques faciès de la biocénose des fonds détritiques côtiers dans la partie nord du PN de port-cros. *Parc Natl. Port-Cros Ed. Sci. Rep. Port-Cros Natl. Park* 11, 181–183.

Bourcier, M. (1988). Macrobenthos de substrat meuble circalittoral autour' de l'île de port-cros. *Parc Natl. Port-Cros Ed. Sci. Rep. Port-Cros Natl. Park* 14, 41–64.

Bourcier, M., and Zibrowius, H. (1973). Red muds dumped in the la cassidaigne (Marseille region), observations with the sp 350 dipping saucer (June 1971), and results of dredgings. *Bull. Signalétique C.N.R.S. 740-1973 34* 11-12), 15190.

Bruno de Sousa, C., Cox, C. J., Brito, L., Pavão, M. M., Pereira, H., Ferreira, A., et al. (2019). Improved phylogeny of brown algae *Cystoseira* (Fucales) from the Atlantic-Mediterranean region based on mitochondrial sequences. *PloS One* 14, e0210143. doi: 10.1371/journal.pone.0210143

Buffoni, G., Bianchi, C. N., Delfanti, R., Di Cola, G., Morri, C., Niccolai, I., et al. (1990). Modello di reti trofiche in biocenosi bentiche. applicazione a biocenosi del golfo di gaeta. *Atti dell'Associazione Italiana di Oceanol. e Limnol.* 8, 227–251.

Burgos, E., Montefalcone, M., Ferrari, M., Paoli, C., Vassallo, P., Morri, C., et al. (2017). Ecosystem functions and economic wealth: Trajectories of change in seagrass meadows. *J. Cleaner Production* 168, 1108–1119. doi: 10.1016/j.jclepro.2017.09.046

Burrows, M. T., Kamenos, N. A., Hughes, D. J., Stahl, H., Howe, J. A., and Tett, P. (2014). "Assessment of carbon budgets and potential blue carbon stores in scotland's coastal and marine environment," in *Scottish Natural heritage commissioned report no. 761* (Scottish Natural Heritage).

Carpine, C. (1958). Recherches sur les fonds à *Peyssonnelia polymorpha* (Zan.) schmitz de la région de marseille. *Bull. l'Institut Océanographique Monaco* 1125, 1–50.

Carpine, C. (1964). Contribution à l'étude bionomique de la méditerranée occidentale (côtes du var et des alpes maritimes, côtes occidentales de corse). fasc. 3: La côte de l'Estérel, de la pointe des lions à la pointe de l'Aiguille (Région A2). *Bull. l'Institut Océanographique Monaco* 63 (1312 A et B), 1–52.

Cerrano, C., Bavestrello, G., Bianchi, C. N., Calcinai, B., Cattaneo-Vietti, R., Morri, C., et al. (2001). "The role of sponge bioerosion in Mediterranean coralligenous accretion," in *Mediterranean Ecosystems* (Milano: Springer), 235–240.

Cerrano, C., Bavestrello, G., Bianchi, C. N., Cattaneo-Vietti, R., Bava, S., Morganti, C., et al. (2000). A catastrophic mass-mortality episode of gorgonians and other organisms in the ligurian Sea (North-western Mediterranean), summer 1999. *Ecol. Lett.* 3, 284293. doi: 10.1046/j.1461-0248.2000.00152.x

Cheminée, A., Feunteun, E., Clerici, S., Cousin, B., and Francour, P. (2014). "Management of infralittoral habitats: Towards a seascape scale approach," in *Underwater seascapes* (Cham: Springer), 161–183. doi: 10.1007/978-3-319-03440-9

Chen, C. T., Carlotti, F., Harmelin-Vivien, M., Lebreton, B., Guillou, G., Vassallo, L., et al. (2022). Diet and trophic interactions of Mediterranean planktivorous fishes. *Mar. Biol.* 169 (9), 1–18. doi: 10.1007/s00227-022-04103-1

Cocito, S., Fanucci, S., Niccolai, I., Morri, C., and Bianchi, C. N. (1990). Relationships between trophic organization of benthic communities and organic matter content in tyrrhenian Sea sediments. *Hydrobiologia* 207 (1), 53–60. doi: 10.1007/BF00041440

Cocito, S., Sgorbini, S., Bianchi, C. N., and Morgigni, M. (1994). R.O.V. monitoring in a dumping site. *Biol. Marina Mediterr.* 1 (1), 275–276.

Connell, S. D., Foster, M. S., and Airoldi, L. (2014). What are algal turfs? towards a better description of turfs. *Mar. Ecol. Prog. Ser.* 495, 299–307. doi: 10.3354/meps10513

Costa, S. (1960). Recherches sur les fonds à *Halarachnion spatulatum* de la baie de marseille. *Vie Milieu* 11, 1–68.

Cresson, P., Chouvelon, T., Bustamante, P., Bănaru, D., Baudrier, J., Le Loc'h, F., et al. (2020). Primary production and depth drive different trophic structure and functioning in French marine ecosystems. *Prog. Oceanogr.* 186 (102343), 1–14. doi: 10.1016/j.pocean.2020.102343

Cresson, P., Ruitton, S., and Harmelin-Vivien, M. (2014). Artificial reefs do increase secondary biomass production: Mechanisms evidenced by stable isotopes. *Mar. Ecol. Prog. Ser.* 509, 15–26. doi: 10.3354/meps10866

Darnaude, A. M. (2005). Fish ecology and terrestrial carbon use in coastal areas: Implications for marine fish production. *J. Anim. Ecol.* 74, 864–876. doi: 10.1111/j.1365-2656.2005.00978.x

Davies, C. E., Moss, D., and Hill, M. O. (2004). *EUNIS habitat classification revised 2004* (European environment agency-European topic centre on nature protection and biodiversity), 127–143.

De Bettignies, T., La Rivière, M., Delavenne, J., Dupré, S., Gaudillat, V., Janson, A.-L., et al. (2021). *Interprétation française des habitats d'Intérêt communautaire marins* (Paris: PatriNat (OFB-CNRS-MNHN), 58.

De Grave, S., and Whitaker, A. (1999). Benthic community re-adjustment following dredging of a muddy-maerl matrix. *Mar. Pollut. Bull.* 38 (2), 102–108. doi: 10.1016/S0025-326X(98)00103-9

Deidun, A., Marrone, A., Gauci, A., Galdies, J., Lorenti, M., Mangano, M. C., et al. (2022). Structure and biodiversity of a Maltese maerl bed: New insight into the associated assemblage 24 years after the first investigation. *Regional Stud. Mar. Sci.* 52, 102262. doi: 10.1016/j.rsma.2022.102262

de Jonge, V. N., Schückel, U., and Baird, D. (2019). Subsets of food webs cannot be used as a substitute to assess the functioning of entire ecosystems. *Mar. Ecol. Prog. Ser.* 613, 49–66. doi: 10.3354/meps12863

Dell'Anno, A., Mei, M. L., Pusceddu, A., and Danovaro, R. (2002). Assessing the trophic state and eutrophication of coastal marine systems: A new approach based on the biochemical composition of sediment organic matter. *Mar. Pollut. Bull.* 44 (7), 611–622. doi: 10.1016/S0025-326X(01)00302-2

Demestre, M., Muntadas, A., Sanchez, P., Garcia-de-Vinuesa, A., Mas, J., Franco, I., et al. (2017). "Bio and anthropogenic disturbance of maërl communities settled on subaqueous dunes on the mar menor continental shelf (Western Mediterranean)," in *Atlas of bedforms in the Western Mediterranean* (Cham: Springer International Publishing), 215–219. doi: 10.1007/978-3-319-33940-5_33

De Ridder, C., and Lawrence, J. M. (1982). "Food and feeding mechanisms: Echinoidea," in *Echinoderm nutrition: 57-1 15*. Eds. M. Jangoux and J. M. Lawrence (Rotterdam: Balkema).

Dutertre, M., Grall, J., Ehrhold, A., and Hamon, D. (2015). Environmental factors affecting maerl bed structure in Brittany (France). *Eur. J. Phycol.* 50 (4), 371–383. doi: 10.1080/09670262.2015.1063698

Enrichetti, F., Bo, M., Morri, C., Montefalcone, M., Toma, M., Bavestrello, G., et al. (2019). Assessing the environmental status of temperate mesophotic reefs: a new, integrated methodological approach. *Ecol. Indic.* 102, 218–229. doi: 10.1016/j.ecolind.2019.02.028

Farriols, M. T., Ordines, F., Somerfield, P. J., Pasqual, C., Hidalgo, M., Guijarro, B., et al. (2017). Bottom trawl impacts on Mediterranean demersal fish diversity: not so obvious or are we too late? *Continental Shelf Res.* 137, 84–102. doi: 10.1016/j.csr.2016.11.011

Fornos, J. J., Ballesteros, E., Massutti, C., and Rodriguez-Perea, A. (1988). Red algae sediments in the Balearic shelf. *Rapports Procès Verbaux Des. Réunions Commission Internationale pour l'Exploration Scientifique la Mer Méditerranée* 31 (2), 86–86.

Foster, M. S., Amado Filho, G. M., Kamenos, N. A., Riosmena-Rodríguez, R., and Steller, D. L. (2013). Rhodoliths and rhodolith beds. *Res. discoveries: revolution Sci. through SCUBA.* 39, 143–155.

Foster, M. S. R., Riosmena-Rodriguez, R., Steller, D. L., and Woelkerling, W. J. (1997). Living rhodolith beds in the gulf of California and their implications. pliocene carbonates and related facies flanking the gulf of California, Baja California, Mexico. *Geol. Soc. America special paper* 318), 127–139.

Fragkopoulou, E., Serrão, E. A., Horta, P. A., Koerich, G., and Assis, J. (2021). Bottom trawling threatens future climate refugia of rhodoliths globally. *Front. Mar. Sci.* 7. doi: 10.3389/fmars.2020.594537

Francour, P. (1989). L'oursin *Centrostephanus longispinus* en méditerranée occidentale: résultats d'une enquête sur sa répartition et son écologie. *Vie Marine H.S. n°10 Actes du VI séminaire Int. sur les Echinodermes* 1988), 138–147.

Francour, P. (1991). "Statut de centrostephanus longispinus en méditerranée," in *Colloque internation. espèces marines à protéger en méditerranée*. Eds. C. F. Boudouresque, M. Avon and V. Gravez (Marseille: GIS Posidonie publ.), 187–202.

Garrabou, J., Coma, R., Bensoussan, N., Bally, M., Chevaldonné, P., Cigliano, M., et al. (2009). Mass mortality in northwestern Mediterranean rocky benthic communities: effects of the 2003 heat wave. *Global Change Biol.* 15 (5), 1090–1103. doi: 10.1111/j.1365-2486.2008.01823.x

Gatti, G., Bianchi, C. N., Morri, C., Montefalcone, M., and Sartoretto, S. (2015). Coralligenous reefs state along anthropized coasts: Application and validation of the COARSE index, based on a rapid visual assessment (RVA) approach. *Ecol. Indic.* 52, 567–576. doi: 10.1016/j.ecolind.2014.12.026

Gautier, Y., and Picard, J. (1957). *Bionomie du banc de magaud (Est des iles d'Hyères)* (Marseille: Recueil des Travaux de la Station Marine d'Endoume), 28–42.

Gayet, G., Baptist, F., Maciejewski, L., Poncet, R., and Bensettiti, F. (2018). *Guide de détermination des habitats terrestres et marins de la typologie EUNIS - version 1.0* (AFB, collection Guides et protocoles), 230.

Giakoumi, S., Halpern, B. S., Michel, L. N., Gobert, S., Sini, M., Boudouresque, C. F., et al. (2015). Towards a framework for assessment and management of cumulative human impacts on marine food webs. *Conserv. Biol.* 29 (4), 1228–1234. doi: 10.1111/cobi.12468

Gianni, F., Manea, E., Cataletto, B., Pugnetti, A., Bergami, C., Bongiorni, L., et al. (2022). Are we overlooking natura 2000 sites? lessons learned from a transnational project in the Adriatic Sea. *Front. Mar. Sci.* 9. doi: 10.3389/fmars.2022.1070373

Giuliani, S., Lamberti, C. V., Sonni, C., and Pellegrini, D. (2005). Mucilage impact on gorgonians in the tyrrhenian Sea. *Sci. Total Environ.* 353 (1-3), 340–349. doi: 10.1016/j.scitotenv.2005.09.023

Gobert, S., Chéry, A., Volpon, A., Pelaprat, C., and Lejeune, P. (2014). "The seascape as an indicator of environmental interest and quality of the Mediterranean benthos: The in situ development of a description index: the LIMA," in *Underwater seascapes* (Cham: Springer International Publishing), 277–291. doi: 10.1007/978-3-319-03440-9_18

Gobert, S., Sartoretto, S., Rico-Raimondino, V., Andral, B., Chery, A., Lejeune, P., et al. (2009). Assessment of the ecological status of Mediterranean French coastal waters as required by the water framework directive using the posidonia oceanica rapid easy index: PREI. *Mar. Pollut. Bull.* 58 (11), 1727–1733. doi: 10.1016/j.marpolbul.2009.06.012

Guarnieri, G., Bevilacqua, S., De Leo, F., Farella, G., Maffia, A., Terlizzi, A., et al. (2016). The challenge of planning conservation strategies in threatened seascapes: Understanding the role of fine scale assessments of community response to cumulative human pressures. *PloS One* 11 (2), e0149253. doi: 10.1371/journal.pone.0149253

Güreşen, A., Güreşen, S. O., and Aktan, Y. (2020). Combined synthetic and biotic indices of *Posidonia oceanica* to qualify the status of coastal ecosystems in the north Aegean. *Ecol. Indic.* 113, 106149. doi: 10.1016/j.ecolind.2020.106149

Halfar, J., Strasser, M., Riegl, B., and Godinez-Orta, L. (2006). "Oceanography, sedimentology and acoustic mapping of a bryomol carbonate factory in the northern gulf of California, Mexico," in *Cool-water carbonates: Depositional systems and palaeoenvironmental controls*, vol. 255 . Eds. H. M. Pedley and G. Carannante (London: Geological Society), 197–215.

Hall-Spencer, J. M. (1998). Conservation issues relating to maerl beds as habitats for molluscs. *J. Conchol. special Publ.* 2, 271–286.

Hall-Spencer, J. M., and Harvey, B. P. (2019). Ocean acidification impacts on coastal ecosystem services due to habitat degradation. *Emerging Topics Life Sci.* 3 (2), 197–206. doi: 10.1042/ETLS20180117

Harmelin, J. G. (1978). Bryozoaires des iles d'Hyères; II: inventaire des fonds détritiques. *Parc Natl. Port-Cros Ed. Travaux Scientifiques du Parc Natl. Port-Cros* 4, 127–148.

Harmelin, J. G. (2017). *Pentapora fascialis*, a bryozoan under stress: Condition on coastal hard bottoms at port-cros island (Port-cros national park, France, Mediterranean) and other sites. *Sci. Rep. Port-Cros Natl. Park* 31, 125–133.

Harmelin, J. G., and Duval, C. (1983). Localisation et dissémination des jeunes de l'oursin *Sphaerechinus granularis* (Lamarck) en méditerranée. *Rapports Procès-verbaux Des. Réunions Commission Internationale pour l'Exploration Scientifique la Mer Mediterranée Monaco* 28, 267–269.

Harmelin, J. G., and Harmelin-Vivien, M. L. (1976). Observations *in situ* des aires de ponte de *Spicara smaris* (Pisces, perciformes, centracanthidae) dans les eaux de port-cros. *Travaux Scientifiques du Parc Natl. Port-Cros* 2, 115–120.

Harmelin-Vivien, M. L., Harmelin, J. G., Chauvet, C., Duval, C., Galzin, R., Lejeune, P., et al. (1985). Evaluation visuelle des peuplements et populations de poisons, méthodes et problèmes. *Rev. d'Ecologie* 40, 467–539.

Harvey, A. S., Harvey, R. M., and Merton, E. (2017). The distribution, significance and vulnerability of Australian rhodolith beds: A review. *Mar. Freshw. Res.* 68 (3), 411–428. doi: 10.1071/MF15434

Holon, F., and Harmelin, J. G. (2014). Bryozoan reef, an unknown Mediterranean habitat? *Int. Bryozool. Assoc. Bull.* 10, 3.

Holon, F., Mouquet, N., Boissery, P., Bouchoucha, M., Delaruelle, G., Tribot, A. S., et al. (2015). Fine-scale cartography of human impacts along French Mediterranean coasts: a relevant map for the management of marine ecosystems. *PloS One* 10 (8), e0135473. doi: 10.1371/journal.pone.0135473

Huvé, H. (1954). Contribution à l'étude des fonds à *Peyssonnelia polymorpha* (Zan.) schmitz de la région de marseille. *Recueil Des. Travaux la Station Mar. d'Endoume* 12, 119–136.

Huvé, H. (1956). Contribution à l'étude des fonds à *Lithothamnium solutum* foslie de la région de marseille. recueil des. *Travaux la Sation Mar. d'Endoume Fr* 18 (1), 105–133.

Jac, C., and Vaz, S. (2020). Abrasion superficielle des fonds par les arts trainants – méditerranée (surface swept area ratio). surface abrasion of seabeds by bottom contacting fishing gears - Mediterranean Sea (surface swept area ratio). *IFREMER* (Marseille), 230. doi: 10.12770/8bed2328-a0fa-4386-8a3e-d6d146cafe54

Jacquotte, R. (1962). Etude des fonds de maërl de méditerranée. *Recueil Des. Travaux la Station Mar. d'Endoume Fr.* 28 (41), 141–235.

James, D. W., Foster, M. S., and O'Sullivan, J. (2006). Bryoliths (Bryozoa) in the gulf of California1. *Pacific Sci.* 60 (1), 117–124. doi: 10.1353/psc.2005.0057

Jódar-Pérez, A. B., Terradas-Fernández, M., López-Moya, F., Asensio-Berbegal, L., and López-Llorca, L. V. (2020). Multidisciplinary analysis of *Cystoseira* sensu lato (SE Spain) suggest a complex colonization of the Mediterranean. *J. Mar. Sci. Eng.* 8 (12), 961. doi: 10.3390/jmse8120961

Joher, S., Ballesteros, E., Cebrian, E., Sánchez, N., and Rodríguez-Prieto, C. (2012). Deep-water macroalgal-dominated coastal detritic assemblages on the continental shelf off mallorca and menorca (Balearic islands, Western Mediterranean). *Botanica Marina* 55 (5), 485–497. doi: 10.1515/bot-2012-0113

Joher, S., Ballesteros, E., and Rodríguez-Prieto, C. (2015). Contribution to the study of deep coastal detritic bottoms: the algal communities of the continental shelf off the Balearic islands, Western Mediterranean. *Mediterr. Mar. Sci.* 16 (3), 573–590. doi: 10.12681/mms.1249

Kamenos, N. A., Moore, P. G., and Hall-Spencer, J. M. (2004). Nursery-area function of maerl grounds for juvenile queen scallops *Aequipecten opercularis* and other invertebrates. *Mar. Ecol. Prog. Ser.* 274, 183–189. doi: 10.3354/meps274183

Katsanevakis, S., Wallentinus, I., Zenetos, A., Leppäkoski, E., Çinar, M. E., Oztürk, B., et al. (2014). Impacts of invasive alien marine species on ecosystem services and biodiversity: a pan-European review. *Aquat. Invasions* 9 (4), 391–423. doi: 10.3391/ai.2014.9.4.01

Kermagoret, C., Claudet, J., Derolez, V., Nugues, M. M., Ouisse, V., Quillien, N., et al. (2019). How does eutrophication impact bundles of ecosystem services in multiple coastal habitats using state-and-transition models. *Ocean Coast. Manage.* 174, 144–153. doi: 10.1016/j.ocecoaman.2019.03.028

Kersting, D. K., Cebrian, E., Verdura, J., and Ballesteros, E. (2017a). Rolling corals in the Mediterranean Sea. *Coral Reefs* 36 (1), 245–245. doi: 10.1007/s00338-016-1498-9

Kersting, D. K., Cebrian, E., Verdura, J., and Ballesteros, E. (2017b). A new *Cladocora caespitosa* population with unique ecological traits. *Mediterr. Mar. Sci.* 18 (1), 38–42. doi: 10.12681/mms.1955

Khoury, C. (1987). Ichtyofaune des herbiers de posidonies du parc national de port-cros: composition, éthologie alimentaire et rôle dans le réseau trophique (Doctoral dissertation, Aix-Marseille 2), 230.

Klein, J., and Verlaque, M. (2008). The *Caulerpa racemosa* invasion: A critical review. *Mar. Pollut. Bull.* 56 (2), 205–225. doi: 10.1016/j.marpolbul.2007.09.043

Klein, J. C., and Verlaque, M. (2009). Macroalgal assemblages of disturbed coastal detritic bottoms subject to invasive species. *Estuarine Coast. Shelf Sci.* 82 (3), 461–468. doi: 10.1016/j.ecss.2009.02.003

Konar, B., Riosmena-Rodriguez, R., and Iken, K. (2006). Rhodolith bed: a newly discovered habitat in the north pacific ocean. *Botanica Marina* 49, 355–359. doi: 10.1515/BOT.2006.044

Laborel, J. (1961). Le concrétionnement algal "coralligène" et son importance geomorphologique en méditerranée. – recueil des travaux de la station marine. *Endoume* 23, 37–60.

Laborel, J., Pérès, J., Picard, M., and Vacelet, J. (1961). Etude directe des fonds des parages de marseille de 30 à 300 m avec la soucoupe plongeante Cousteau. *Bull. l'Institut Océanographique Monaco* 58, 1–5.

Laborel, J., Tailliez, P., and Vacelet, J. (1976). Premières observations dans les eaux du parc national de port-cros à l'aide du sous-marin "Griffon" de la marine nationale. *Travaux Scientifiques du Parc Natl. Port-Cros* 2, 121–130.

Labrune, C., Amouroux, J. M., Sarda, R., Dutrieux, E., Thorin, S., Rosenberg, R., et al. (2006). Characterization of the ecological quality of the coastal gulf of lions (NW mediterranean). a comparative approach based on three biotic indices. *Mar. Pollut. Bull.* 52 (1), 34–47. doi: 10.1016/j.marpolbul.2005.08.005

Labrune, C., Gauthier, O., Conde, A., Grall, J., Blomqvist, M., Bernard, G., et al. (2021). A general-purpose biotic index to measure changes in benthic habitat quality across several pressure gradients. *J. Mar. Sci. Eng.* 9 (6), 654. doi: 10.3390/jmse9060654

Laffoley, D., Maltby, E., Vincent, M. A., Mee, L., Dunn, E., Gilliland, P., et al. (2004). *The ecosystem approach, coherent actions for marine and coastal environments. a report to the UK government* (Peterborough, UK: English Nature), 65.

La Rivière, M., Aish, A., Auby, I., Ar Gall, E., Dauvin, J. C., de Bettignies, T., et al. (2017). *Evaluation de la sensibilité des habitats élémentaires (DHFF) d'Atlantique, de manche et de mer du nord aux pressions physiques* (Paris: Rapport SPN 2017-4. MNHN), 93.

La Rivière, M., Michez, N., Delavenne, J., Andres, S., Fréjefond, C., Janson, A. L., et al. (2021). *Fiches descriptives des biocénoses benthiques de méditerranée* (Paris: UMS PatriNat (OFB-CNRS-MNHN), 660.

Laubier, L. (1966). *Le coralligène des albères* Vol. 43/2 (Paris: Monographie biocénotique. – Annales Institut Océanographique), 137–316.

Ledoyer, M. (1966). Ecologie de la faune vagile des biotopes méditerranéens accessibles en scaphandre autonome. III. données analytiques sur les biotopes de substrat meuble. *Recueil Des. Travaux la Station Mar. d'Endoume* 41 (57), 165–186.

Levin, L. A., and Dayton, P. K. (2009). Ecological theory and continental margins: Where shallow meets deep. *Trends Ecol. Evol.* 24 (11), 606–617. doi: 10.1016/j.tree.2009.04.012

Littler, M. M., and Littler, D. S. (1980). The evolution of thallus form and survival strategies in benthic marine macroalgae: field and laboratory tests of a functional form model. *Am. Nat.* 116 (1), 25–44. doi: 10.1086/283610

Lombardi, C., Taylor, P. D., and Cocito, S. (2014). "Bryozoan constructions in a changing Mediterranean Sea," in *The Mediterranean Sea: Its history and present challenges*. Eds. S. Goffredo and Z. Dubinsky (Dordrecht: Springer), 373–384. doi: 10.1007/978-94-007-6704-1_21

Lopez y Royo, C. L., Casazza, G., Pergent-Martini, C., and Pergent, G. (2010). A biotic index using the seagrass *Posidonia oceanica* (BiPo), to evaluate ecological status of coastal waters. *Ecol. Indic.* 10 (2), 380–389. doi: 10.1016/j.ecolind.2009.07.005

Maciejewski, L., Lepareur, F., Viry, D., Bensettiti, F., Puissauve, R., and Touroult, J. (2016). État de conservation des habitats: propositions de définitions et de concepts pour l'évaluation à l'échelle d'un site natura 2000. *Rev. d'Écologie Terre Vie* 71 (1), 3–20. doi: 10.3406/revec.2016.1862

Mancini, I., Rigo, I., Oprandi, A., Montefalcone, M., Morri, C., Peirano, A., et al. (2020). What biotic indices tell us about ecosystem change: lessons from the seagrass *Posidonia oceanica*. indices application on historical data. *Vie Milieu - Life Environ.* 70 (3-4), 55–61.

Mao, J., Burdett, H. L., McGill, R. A., Newton, J., Gulliver, P., and Kamenos, N. A. (2020). Carbon burial over the last four millennia is regulated by both climatic and land use change. *Global Change Biol.* 26 (4), 2496–2504. doi: 10.1111/gcb.15021

Marion, A. F. (1883). Esquisse d'une topographie zoologique du golfe de marseille. *Cayer cie.* 1 (1), 1–103.

Martin, S., Clavier, J., Chauvaud, L., and Thouzeau, G. (2007). Community metabolism in temperate maerl beds. I. Carbon and carbonate fluxes. *Mar. Ecol. Prog. Ser.* 335, 19–29. doi: 10.3354/meps335019

Martin, C. S., Giannoulaki, M., De Leo, F., Scardi, M., Salomidi, M., Knittweis, L., et al. (2014). Coralligenous and maërl habitats: predictive modelling to identify their spatial distributions across the Mediterranean Sea. *Sci. Rep.* 4 (1), 1–9.

Martin, S., and Hall-Spencer, J. M. (2017). "Effects of ocean warming and acidification on rhodolith/maërl beds," in *Rhodolith/maërl beds: A global perspective* (Cham: Springer International Publishing), 55–85. doi: 10.1007/978-3-3319-29315-8

Meinesz, A., Belsher, T., Thibaut, T., Antolic, B., Mustapha, K. B., Boudouresque, C. F., et al. (2001). The introduced green alga *Caulerpa taxifolia* continues to spread in the Mediterranean. *Biol. Invasions* 3 (2), 201–210. doi: 10.1023/A:1014549500678

Meinesz, A., Boudouresque, C. F., Falconetti, C., Astier, J. M., Bay, D., Blanc, J. J., et al. (1983). Normalisation des symboles pour la représentation et la cartographie des biocénoses benthiques littorales de méditerranée. *Annales l'Institut Océanographique* 59 (2), 155–172.

Michez, N., Dirberg, G., Bellan-Santini, D., Verlaque, M., Bellan, G., Pergent, G., et al. (2011). *Typologie des biocénoses benthiques de méditerranée, liste de référence française et correspondances* (Paris: Rapport SPN–2011 - 13, MNHN), 50.

Michez, N., Fourt, M., Aish, A., Bellan, G., Bellan-Santini, D., Chevaldonné, P., et al. (2014). *Typologie des biocénoses benthiques de méditerranée version 2* (Paris: Rapport SPN–2014 - 33, MNHN), 26.

Monnier, B. (2020). *Quantification et dynamique spatio-temporelle des puits de carbone associés aux herbiers à posidonia oceanica* (Corte: Manuscrit de thèse, Université de Corse Pascal Paoli FRES 3041 – UMR CNRS SPE 6134 Faculté des sciences et techniques) 838, 239.

Monnier, B., Pergent, G., Mateo, M.Á., Carbonell, R., Clabaut, P., and Pergent-Martini, C. (2021). Sizing the carbon sink associated with *Posidonia oceanica* seagrass meadows using very high-resolution seismic reflection imaging. *Mar. Environ. Res.* 170, 105415. doi: 10.1016/j.marenvres.2021.105415

Monnier, B., Pergent, G., Mateo, M.Á., Clabaut, P., and Pergent-Martini, C. (2022). Quantification of blue carbon stocks associated with *Posidonia oceanica* seagrass meadows in Corsica (NW Mediterranean). *Sci. Total Environ.* 838 (1), 155864. doi: 10.1016/j.scitotenv.2022.155864

Montefalcone, M. (2009). Ecosystem health assessment using the Mediterranean seagrass *Posidonia oceanica*: A review. *Ecol. Indic.* 9 (4), 595–604. doi: 10.1016/j.ecolind.2008.09.013

Montefalcone, M., Albertelli, G., Morri, C., and Bianchi, C. N. (2007). Urban seagrass: status of *Posidonia oceanica* off Genoa city waterfront (Italy). *Mar. Pollut. Bull.* 54, 206–213. doi: 10.1016/j.marpolbul.2006.10.005

Montefalcone, M., Morri, C., Parravicini, V., and Bianchi, C. N. (2015b). A tale of two invaders: divergent spreading kinetics of the alien green algae *Caulerpa taxifolia* and *Caulerpa cylindracea*. *Biol. Invasions* 17 (9), 2717–2728. doi: 10.1007/s10530-015-0908-1

Montefalcone, M., Vassallo, P., Gatti, G., Parravicini, V., Paoli, C., Morri, C., et al. (2015a). The exergy of a phase shift: Ecosystem functioning loss in seagrass meadows of the Mediterranean. *Sea. Estuarine Coast. Shelf Sci.* 156, 186–194. doi: 10.1016/j.ecss.2014.12.001

Morri, C., Bavestrello, G., and Bianchi, C. N. (1991). Faunal and ecological notes on some benthic cnidarian species from the Tuscan archipelago and eastern ligurian Sea (western Mediterranean). *Bollettino dei Musei e degli Istituti Biologici dell'Università di Genova* 54-55 (1988-1989), 27–47.

Morri, C., Peirano, A., Bianchi, C. N., and Rodolfo-Metalpa, R. (2000). *Cladocora caespitosa*: A colonial zooxanthellate Mediterranean coral showing constructional ability. *Reef Encounter* 27, 22–25.

Mostajir, B., Amblard, C., Buffan-Dubau, E., de Wit, R., Lensi, R., and Sime-Ngando, T. (2012). *Les Réseaux trophiques microbiens des milieux aquatiques et terrestres*. Ed. J. C. Bertrand, et al (Pau: Presses Universitaires de Pau et des Pays de l'Adour), 28.

Noisette, F., Egilsdottir, H., Davoult, D., and Martin, S. (2013). Physiological responses of three temperate coralline algae from contrasting habitats to near-future ocean acidification. *J. Exp. Mar. Biol. Ecol.* 448, 179–187. doi: 10.1016/j.jembe.2013.07.006

Odum, E. P. (1971). *Fundamentals of Ecology. Third* Edition, W.B. Saunders Co., Philadelphia, 574

Oprandi, A., Bianchi, C. N., Karayali, O., Morri, C., Rigo, I., and Montefalcone, M. (2021). RESQUE: A novel comprehensive approach to compare the performance of different indices in evaluating seagrass health. *Ecol. Indic.* 131, 108118. doi: 10.1016/j.ecolind.2021.108118

Oprandi, A., Mancini, I., Bianchi, C. N., Morri, C., Azzola, A., and Montefalcone, M. (2022). "Indices from the past: relevance in the status assessment of *Posidonia oceanica* meadows," in *Proceedings of the 7th Mediterranean symposium on marine vegetation*. Eds. C. Bouafif and A. Ouerghi (Tunis: SPA/RAC, Tunis), 72–77.

Ordines, F., Ramón, M., Rivera, J., Rodríguez-Prieto, C., Farriols, M. T., Guijarro, B., et al. (2017). Why long term trawled red algae beds off Balearic islands (western Mediterranean) still persist? *Regional Stud. Mar. Sci.* 15, 39–49. doi: 10.1016/j.rsma.2017.07.005

Orekhova, N. A., and Ovsyany, E. I. (2020). Organic carbon and particle-size distribution in the littoral bottom sediments of the laspi bay (the black Sea). *Phys. Oceanogr.* 27 (3), 266–277. doi: 10.22449/1573-160X-2020-3-266-277

Paoli, C., Morten, A., Bianchi., C. N., Morri, C., Fabiano, M., and Vassallo, P. (2016). Capturing ecological complexity: OCI, a novel combination of ecological indices as applied to benthic marine habitats. *Ecol. Indic.* 66, 86–102. doi: 10.1016/j.ecolind.2016.01.029

Pérès, J. M. (1967). The Mediterranean benthos. *Oceanogr. Mar. Biol. - Annu. Rev.* 5, 449–533.

Pérès, J. M. (1982). "Zonations and organismic assemblages," in *Marine ecology, vol. V, ocean management, part 1*. Ed. O. Kinne (Chichester: Wiley), 9–642.

Pérès, J. M., and Picard, J. (1951). Note sur les fonds coralligènes de la région de marseille. – *Arch. Zool. Expérimentale Générale* 88, 24–38.

Pérès, J. M., and Picard, J. (1964). Nouveau manuel de bionomie benthique de la mer méditerranée. *Recueil Des. Travaux la Station Mar. d Endoume* 31 (47), 5–137.

Pergent, G., Agnesi, S., Antonioli, P. A., Babbini, L., Belbacha, S., Ben Mustapha, K., et al. (2015). *Standard methods for inventorying and monitoring coralligenous and rhodoliths assemblages* (Tunis: RAC/SPA, Tunis), 20.

Pergent-Martini, C., Pergent, G., Monnier, B., Boudouresque, C. F., Morri, C., and Valette-Sansevin, A. (2021). Contribution of *Posidonia oceanica* meadows in the context of climate change mitigation in the Mediterranean Sea. *Mar. Environ. Res.* 165, 105236. doi: 10.1016/j.marenvres.2020.105236

Personnic, S., Boudouresque, C. F., Astruch, P., Ballesteros, E., Blouet, S., Bellan-Santini, D., et al. (2014). An ecosystem-based approach to assess the status of a Mediterranean ecosystem, the *Posidonia oceanica* seagrass meadow. *PloS One* 9 (6), e98994. doi: 10.1371/journal.pone.0098994

Petit, A. (2019). Les Aires marines protégées « à la française » un enjeu de politique internationale. *Bull. l'Institut Pierre Renouvin* 1), 161–171. doi: 10.3917/bipr1.049.0161

Piazzi, L., Balata, D., and Cinelli, F. (2007). Invasions of alien macroalgae in Mediterranean coralligenous assemblages. *Cryptogamie-Algologie* 28 (3), 289–302.

Piazzi, L., and Cinelli, F. (2000). Effet' de l'expansion des rhodophyceae introduites *Acrothamnion preissii* et *Womersleyella setacea* sur les communautés algales des rhizomes de *Posidonia oceanica* de méditerranée occidentale. *Cryptogamie Algol.* 21 (3), 291–300. doi: 10.1016/S0181-1568(00)00116-1

Piazzi, L., Gennaro, P., Cecchi, E., Bianchi, C. N., Cinti, M. F., Gatti, G., et al. (2021). Ecological status of coralligenous assemblages: ten years of application of the ESCA index from local to wide scale validation. *Ecol. Indic.* 121, 107077. doi: 10.1016/j.ecolind.2020.107077

Piazzi, L., Gennaro, P., Montefalcone, M., Bianchi, C. N., Cecchi, E., Morri, C., et al. (2019). STAR: An integrated and standardized procedure to evaluate the ecological status of coralligenous reefs. *Aquat. Conservation: Mar. Freshw. Ecosyst.* 29, 189–201. doi: 10.1002/aqc.2983

Piazzi, L., Pardi, G., Balata, D., Cecchi, E., and Cinelli, F. (2002). Seasonal dynamics of a subtidal north-western Mediterranean macroalgal community in relation to depth and substrate inclination. *Botanica Marina* 45, 243–252. doi: 10.1515/BOT.2002.023

Picard, J. (1965). Recherches qualitatives sur les biocénoses marines des substrats meubles dragables de la region marseillaise. *Recueil Des. Travaux la Station Mar. d'Endoume* 52 (36), 1–160 (10).

Pikaver, A. H., Gilbert, C., and Breton, F. (2004). An indicator set to measure the progress in the implementation of integrated coastal zone management in Europe. *Ocean Coast. Manage.* 47, 449–462. doi: 10.1016/j.ocecoaman.2004.06.001

Pinedo, S., Jordana, E., and Ballesteros, E. (2015). A critical analysis on the response of macroinvertebrate communities along disturbance gradients: description of MEDOCC (MEDiterranean OCCidental) index. *Mar. Ecol.* 36, 141–154. doi: 10.1111/maec.12126

Provan, J. I. M., Murphy, S., and Maggs, C. A. (2005). Tracking the invasive history of the green alga codium fragile ssp. *tomentosoides*. *Mol. Ecol.* 14 (1), 189–194. doi: 10.1111/j.1365-294X.2004.02384.x

Quemmerais-Amice, F., Barrere, J., La Rivière, M., Contin, G., and Bailly, D. (2020). A methodology and tool for mapping the risk of cumulative effects on benthic habitats. *Front. Mar. Sci.* 7. doi: 10.3389/fmars.2020.569205

Rastorgueff, P. A., Bellan-Santini, D., Bianchi, C. N., Bussotti, S., Chevaldonné, P., Guidetti, P., et al. (2015). An ecosystem-based approach to evaluate the ecological quality of Mediterranean undersea caves. *Ecol. Indic.* 54, 137–152. doi: 10.1016/j.ecolind.2015.02.014

R core team (2022). *R: A language and environment for statistical computing* (Vienna, Austria: R Foundation for Statistical Computing). Available at: https://www.R-project.org/.

Rees, I. (1999). Lag veneer: a missing piece in the benthic biotopes jigsaw? *Newslett. PMNHS* 2, 24–26.

Rendina, F., Ferrigno, F., Appolloni, L., Donnarumma, L., Sandulli, R., and Fulvio, G. (2020). Anthropic pressure due to lost fishing gears and marine litter on different rhodolith beds off the campania coast (Tyrrhenian Sea, Italy). *Ecol. Questions* 31 (4), 1–17. doi: 10.12775/EQ.2020.027

Reynes, L., Thibaut, T., Mauger, S., Blanfuné, A., Holon, F., Cruaud, C., et al. (2021). Genomic signatures of clonality in the deep water kelp *Laminaria rodriguezii*. *Mol. Ecol.* 30 (8), 1806–1822. doi: 10.1111/mec.15860

Rosenberg, R., Blomqvist, M., Nilsson, H. C., Cederwall, H., and Dimming, A. (2004). Marine quality assessment by use of benthic species-abundance distributions: A proposed new protocol within the European union water framework directive. *Mar. Pollut. Bull.* 49 (9-10), 728–739. doi: 10.1016/j.marpolbul.2004.05.013

Rowe, G., and Wright, G. (1999). The Delphi technique as a forecasting tool: Issues and analysis. *Int. J. Forecasting* 15 (4), 353–375. doi: 10.1016/S0169-2070(99)00018-7

Ruitton, S., Astruch, P., Blanfuné, A., Cabral, M., Thibaut, T., and Boudouresque, C. F. (2020). Bridging risk assessment of human pressure and ecosystem status. *Vie Milieu/Life Environ.* 70 (3-4), 37–53.

Ruitton, S., Boudouresque, C. F., Thibaut, T., Rastorgueff, P. A., Personnic, S., Boissery, P., et al. (2017). *Guide méthodologique pour l'évaluation écosystémique des habitats marins* (Frances: MIO publ.), 161. doi: 10.13140/RG.2.2.23411.02085

Ruitton, S., Personnic, S., Ballesteros, E., Bellan-Santini, D., Boudouresque, C. F., Chevaldonné, P., et al. (2014). "An ecosystem-based approach to assess the status of the Mediterranean coralligenous habitat," in *Proceedings of the 2nd Mediterranean symposium on the conservation of coralligenous and other calcareous bio-concretions*. Eds. C. Bouafif, H. Langar and A. Ouerghi (Tunis: RAC/SPA publ.), 153–158.

Sala, E., Mayorga, J., Bradley, D., Cabral, R. B., Atwood, T. B., Auber, A., et al. (2021). Protecting the global ocean for biodiversity, food and climate. *Nature* 592, 1–6. doi: 10.1038/s41586-021-03371-z

Salomidi, M., Katsanevakis, S., Borja, A., Braeckman, U., Damalas, D., Galparsoro, I., et al. (2012). Assessment of goods and services, vulnerability, and conservation status of European seabed biotopes: A stepping stone towards ecosystem-based marine spatial management. *Mediterr. Mar. Sci.* 13 (1), 49–88. doi: 10.12681/mms.23

Santos, R. O., James, W. R., Nelson, J. A., Rehage, J. S., Serafy, J., Pittman, S. J., et al. (2022). Influence of seascape spatial pattern on the trophic niche of an omnivorous fish. *Ecosphere* 13 (2), e3944. doi: 10.1002/ecs2.3944

Sanz-Lázaro, C., Belando, M. D., Marín-Guirao, L., Navarrete-Mier, F., and Marín, A. (2011). Relationship between sedimentation rates and benthic impact on maerl beds derived from fish farming in the Mediterranean. *Mar. Environ. Res.* 71 (1), 22–30. doi: 10.1016/j.marenvres.2010.09.005

Sartoretto, S., Schohn, T., Bianchi, C. N., Morri, C., Garrabou, J., Ballesteros, E., et al. (2017). An integrated method to evaluate and monitor the conservation state of coralligenous habitats: the INDEX-COR approach. *Mar. Pollut. Bull.* 120, 222–231. doi: 10.1016/j.marpolbul.2017.05.020

Savini, A., Basso, D., Bracchi, V. A., Corselli, C., and Pennetta, M. (2012). Maerl-bed mapping and carbonate quantification on submerged terraces offshore the cilento peninsula (Tyrrhenian Sea, Italy). *Geodiversitas* 34 (1), 77–98. doi: 10.5252/g2012n1a5

Scémama, P., Kermagoret, C., Accornero-Picon, A., Alban, F., Astruch, P., Boemare, C., et al. (2020). A strategic approach to assess the bundle of ecosystem services provided by *Posidonia oceanica* meadows in the bay of marseille. *Vie Milieu/Life Environ.* 70 (3-4), 197–207.

Schiaparelli, S., Castellano, M., Povero, P., Sartoni, G., and Cattaneo-Vietti, R. (2007). A benthic mucilage event in north-Western Mediterranean Sea and its possible relationships with the summer 2003 European heatwave: Short term effects on littoral rocky assemblages. *Mar. Ecol.* 28 (3), 341–353. doi: 10.1111/j.1439-0485.2007.00155.x

Sciberras, M., Rizzo, M., Mifsud, J. R., Camilleri, K., Borg, J. A., Lanfranco, E., et al. (2009). Habitat structure and biological characteristics of maerl bed off the northeastern coast of the Maltese islands (central Mediterranean). *Mar. Biodiversity* 39, 251–264. doi: 10.1007/s12526-009-0017-4

Seitz, R. D., Wennhage, H., Bergström, U., Lipcius, R. N., and Ysebaert, T. (2014). Ecological value of coastal habitats for commercially and ecologically important species. *ICES J. Mar. Sci.* 71 (3), 648–665. doi: 10.1093/icesjms/fst152

Simboura, N., and Zenetos, A. (2002). Benthic indicators to use in ecological quality classification of Mediterranean soft bottom marine ecosystems, including a new biotic index. *Mediterr. Mar. Sci.* 3 (2), 77–111. doi: 10.12681/mms.249

Somaschini, A., Martini, N., Gravina, M. F., Belluscio, A., Corsi, F., and Ardizzone, G. D. (1998). Characterization and cartography of some Mediterranean soft-bottom benthic communities (Ligurian Sea, Italy). *Scientia Marina* 62 (1-2), 27–36.

Souto, J., Reverter-Gil, O., and Fernandez-Pulpeiro, E. (2010). Bryozoa from detritic bottoms in the menorca channel (Balearic islands, western Mediterranean), with notes on the genus *Cribellopora*. *Zootaxa* 2536, 1, 36–52. doi: 10.11646/zootaxa.2536.1.2

Soykan, O., İlkyaz, A. T., Metin, G., and Kinacigil, H. T. (2010). Growth and reproduction of blotched picarel (*Spicara maena* Linnaeus 1758) in the central Aegean Sea, Turkey. *Turkish J. Zool.* 34 (4), 453–459. doi: 10.3906/zoo-0903-29

Stamouli, C., Zenetos, A., Kallianiotis, A., and Voultsiadou, E. (2022). Megabenthic invertebrate diversity in Mediterranean trawlable soft bottoms: A synthesis of current knowledge. *Mediterr. Mar. Sci.* 23 (3), 447–459. doi: 10.12681/mms.29165

Steller, D. L., Riosmena-Rodríguez, R., Foster, M. S., and Roberts, C. A. (2003). Rhodolith bed diversity in the gulf of California: the importance of rhodolith structure and consequences of disturbance. *Aquat. Conservation: Mar. Freshw. Ecosyst.* 13 (S1), S5–S20. doi: 10.1002/aqc.564

Thibaut, T., Blanfuné, A., Boudouresque, C. F., Personnic, S., Ruitton, S., Ballesteros, E., et al. (2017). An ecosystem-based approach to assess the status of Mediterranean algae-dominates shallow rocky reefs. *Mar. Pollut. Bull.* 117, 311–329. doi: 10.1016/j.marpolbul.2017.01.029

Thibaut, T., Blanfuné, A., Verlaque, M., Boudouresque, C. F., and Ruitton, S. (2016). The *Sargassum* conundrum: Very rare, threatened or locally extinct in the NW Mediterranean and still lacking protection. *Hydrobiologia* 781 (1), 3–23. doi: 10.1007/s10750-015-2580-y

Thiriet, P., Cheminée, A., Mangialajo, L., and Francour, P. (2014). "How 3D complexity of macrophyte-formed habitats affect the processes structuring fish assemblages within coastal temperate seascapes?," in *Underwater seascapes* (Cham: Springer), 185–199. doi: 10.1007/978-3-319-03440-9_12

Valette-Sansevin, A., Pergent, G., Buron, K., Pergent-Martini, C., and Damier, E. (2019). Continuous mapping of benthic habitats along the coast of Corsica: A tool for the inventory and monitoring of blue carbon ecosystems. *Mediterr. Mar. Sci.* 20 (3), 585–593. doi: 10.12681/mms.19772

Van der Heijden, L. H., and Kamenos, N. A. (2015). Reviews and syntheses: calculating the global contribution of coralline algae to total carbon burial. *Biogeosciences* 12 (21), 6429–6441. doi: 10.5194/bg-12-6429-2015

Vassallo, P., Bianchi, C. N., Paoli, C., Holon, F., Navone, A., Bavestrello, G., et al. (2018). A predictive approach to benthic marine habitat mapping: Efficacy and management implications. *Mar. Pollut. Bull.* 131, 218–232. doi: 10.1016/j.marpolbul.2018.04.016

Vassallo, P., Paoli, C., Aliani, S., Cocito, S., Morri, C., and Bianchi, C. N. (2020). Benthic diversity patterns and predictors: a study case with inferences for conservation. *Mar. Pollut. Bull.* 150, 110748. doi: 10.1016/j.marpolbul.2019.110748

Velimirov, B., Herndl, G., and Kavka, G. (1984). "Biomass distribution and physiological capabilities of bacteria in the water column above a sea grass system," in *2. colloque international de bacteriologie marine, Brest* (Brest, France: Ifremer), 1–5.

Verlaque, M. (1990). Relations entre *Sarpa salpa* (Linnaeus 1758) (Téléostéen, sparidae), les autres poissons brouteurs et le phytobenthos algal méditerranéen. *Oceanol. Acta* 13 (3), 373–388.

Vidondo, B., and Duarte, C. M. (1995). Seasonal growth of *Codium bursa*, a slow-growing Mediterranean macroalga: *In situ* experimental evidence of nutrient limitation. *Mar. Ecol. Prog. Ser.* 123, 185–191. doi: 10.3354/meps123185

Watanabe, K., Yoshida, G., Hori, M., Umezawa, Y., Moki, H., and Kuwae, T. (2020). Macroalgal metabolism and lateral carbon flows can create significant carbon sinks. *Biogeosciences* 17 (9), 2425–2440. doi: 10.5194/bg-17-2425-2020

Weinberg, S. (1996). *Découvrir la méditerranée* (Avon, France: Nathan Nature), 352.

Wilkie, I. C., Carnevali, M. C., and Andrietti, F. (1996). Mechanical properties of the peristomial membrane of the cidaroid sea-urchin *Stylocidaris affinis*. *J. Zool.* 238 (3), 557–569. doi: 10.1111/j.1469-7998.1996.tb05413.x

Wirtz, P., and Debelius, H. (2003). *Mediterranean And Atlantic invertebrate guide from Spain to Turkey, from Norway to equator* (Hackenheim, Allemagne: ConchBooks), 305.

Word, J. Q. (1978). "The infaunal trophic index," in *Coastal water research project annual report* (El Segundo, CA: southern California coastal water research project), 19–39.

Zenetos, A. (1996). Classification and interpretation of the established mediterranean biocoenoses based solely on bivalve molluscs. *J. Mar. Biol. Assoc. United Kingdom* 76, 403–416. doi: 10.1017/S0025315400030630

Glossary

Life Science Identifiers

Taxa are sorted in order of appearance.

Posidonia oceanica (L.) Delile urn:lsid:marinespecies.org:taxname:145794

Cystoseira C. Agardh urn:lsid:marinespecies.org:taxname:144126

Ericaria Stackhouse urn:lsid:marinespecies.org:taxname:1535414

Gongolaria Boehmer urn:lsid:marinespecies.org:taxname:369694

Osmundaria volubilis R.E.Norris urn:lsid:marinespecies.org:taxname:144841

Lithophyllum racemus (Lamarck) Foslie urn:lsid:marinespecies.org:taxname:145160

Lithothamnion corallioides (P.Crouan & H.Crouan) P.Crouan & H.Crouan urn:lsi:marinespecies.org:taxname:145165

Lithothamnion crispatum Hauck urn:lsid:marinespecies.org:taxname:145166

Lithothamnion minervae Basso urn:lsid:marinespecies.org:taxname:145174

Lithothamnion valens Foslie urn:lsid:marinespecies.org:taxname:145180

Neogoniolithon hauckii (Rothpletz) R.A.Townsend & Huisman urn:lsid:marinespecies.org:taxname:169942

Spongites fruticulosa Kützing urn:lsid:marinespecies.org:taxname:494816

Peyssonnelia crispata Boudouresque & Denizot urn:lsid:marinespecies.org:taxname:145277

Peyssonnelia heteromorpha (Zanardini) Athanasiadis urn:lsid:marinespecies.org:taxname:1311383

Peyssonnelia rosa-marina Boudouresque & Denizot urn:lsid:marinespecies.org:taxname:145285

Peyssonnelia rubra (Greville) J.Agardh urn:lsid:marinespecies.org:taxname:145287

Peyssonnelia squamaria (S.G.Gmelin) Decaisne ex J.Agardh urn:lsid:marinespecies.org:taxname:145288

Sporolithon mediterraneum Heydrich urn:lsid:marinespecies.org:taxname:496041

Pentapora fascialis (Pallas, 1766) urn:lsid:marinespecies.org:taxname:111082

Smittina cervicornis (Pallas, 1766) urn:lsid:marinespecies.org:taxname:111551

Turbicellepora avicularis (Hincks, 1860) urn:lsid:marinespecies.org:taxname:111285

Hornera Lamouroux, 1821 urn:lsid:marinespecies.org:taxname:111041

Cladocora caespitosa (Linnaeus, 1767) urn:lsid:marinespecies.org:taxname:135146

Eunicella singularis (Esper, 1791) urn:lsid:marinespecies.org:taxname:125365

Eunicella verrucosa (Pallas, 1766) urn:lsid:marinespecies.org:taxname:125366

Leptogorgia sarmentosa (Esper, 1791) urn:lsid:marinespcies.org:taxname:125369

Alcyonium palmatum Pallas, 1766 urn:lsid:mariespecies.org:taxname:125334

Pennatula rubra (Ellis, 1764) urn:lsid:marinespecies.org:taxname:128519

Pteroeides griseum (Bohadsch, 1761) urn:lsid:marinespecies.org:taxname:181504

Palinurus elephas (Fabricius, 1787) urn:lsid:marinespecies.org:taxname:107703

Pinna nobilis L. 1758 urn:lsid:marinespecies.org:taxname:140780

Laminaria rodriguezii Bornet urn:lsid:marinespecies.org:axname:145729

Carpomitra costata (Stackhouse) Batters urn:lsid:marinespecies.org:taxname:145910

Codium bursa (Olivi) C.Agardh urn:lsid:marinespecies.org:taxname:145079

Codium vermilara (Olivi) Delle Chiaje urn:lsid:marinespecies.org:taxname:145093

Sphaerococcus coronopifolius Stackhouse urn:lsid:marinespecies.org:taxname:145908

Codium fragile (Suringar) Hariot urn:lsid:marinespecies.org:taxname:145086

Arthrocladia villosa (Hudson) Duby urn:lsid:marinespecies.org:taxname:145306

Sporochnus pedunculatus (Hudson) C.Agardh urn:lsid:marinespecies.org:taxname:145915

Acetabularia acetabulum (L.) P.C.Silva urn:lsid:marinespecies.org:taxname:494795

Padina pavonica (Linnaeus) Thivy urn:lsid:marinespecies.org:taxname:145385

Umbraulva dangeardii M.J.Wynne & G.Furnari urn:lsid:marinespecies.org:taxname:840293

Chrysymenia ventricosa (J.V.Lamouroux) J.Agardh urn:lsid:marinespecies.org:taxname:145845

Sebdenia (J.Agardh) Berthold urn:lsid:marinespecies.org:taxname:144177

Caulerpa cylindracea Sonder urn:lsid:marinespecies.org:taxname:660621

Caulerpa taxifolia (M.Vahl) C.Agardh urn:lsid:marinespecies.org:taxname:144476

Acinetospora crinita (Carmichael) Sauvageau urn:lsid:marinespecies.org:taxname:145398

Chrysonephos lewisii (W.R.Taylor) W.R.Taylor urn:lsid:marinespecies.org:taxname:375956

Nematochrysopsis marina (J.Feldmann) C.Billard urn:lsid:marinespecies.org:taxname:375863

Zosterocarpus oedogonium (Meneghini) Bornet urn:lsid:marinespecies.org:taxname:145476

Pseudochlorodesmis furcellata (Zanardini) Børgesen urn:lsid:marinespecies.org:taxname:144485

Valonia macrophysa Kützing urn:lsid:marinespecies.org:taxname:145883

Womersleyella setacea (Hollenberg) R.E.Norris urn:lsid:marinespecies.orgtaxname:146371

Acrothamnion preissii (Sonder) E.M.Wollaston urn:lsid:marinespecies.org:taxname:144488

Sphaerechinus granularis (Lamarck, 1816) urn:lsid:marinespecies.org:taxname:124427

Stylocidaris affinis (Philippi, 1845) urn:lsid:marinespecies.org:taxname:124268

Centrostephanus longispinus (Philippi, 1845) urn:lsid:marinespecies.org:taxname:124331

Echinus melo Lamarck, 1816 urn:lsid:marinespecies.org:taxname:124294

Cerithium Bruguière, 1789 urn:lsid:marinespecies.org:taxname:137760

Aplysia L., 1767 urn:lsid:marinespecies.org:taxname:137654

Sarpa salpa (L., 1758) urn:lsid:marinespecies.org:taxname:127064

Laevicardium oblongum (Gmelin, 1791) urn:lsid:marinespecies.org:taxname:139006

Acanthocardia deshayesii (Payraudeau, 1826) urn:lsid:marinespecies.org:taxname:138991

Suberites domuncula (Olivi, 1792) urn:lsid:marinespecies.org:taxname:134282

Petta pusilla Malmgren, 1866 urn:lsid:marinespecies.org:taxname:130597

Turritellinella tricarinata (Brocchi, 1814) urn:lsid:marinespecies.org:taxname:1381415

Moerella donacina (L., 1758) urn:lsid:marinespecies.org:taxname:147021

Abra nitida (O. F. Müller, 1776) urn:lsid:marinespecies.org:taxname:141435

Abra prismatica (Montagu, 1808) urn:lsid:marinespecies.org:taxname:141436

Holothuria L., 1767 urn:lsid:marinespecies.org:taxname:123456

Bonellia viridis Rolando, 1822 urn:lsid:marinespecies.org:taxname:110363

Spatangus purpureus O.F. Müller, 1776 urn:lsid:marinespecies.org:taxname:124418

Chaetaster longipes (Bruzelius, 1805) urn:lsid:marinespecies.org:taxname:124004

Echinaster sepositus (Retzius, 1783) urn:lsid:marinespecies.org:taxname:125161

Cliona viridis (Schmidt, 1862) urn:lsid:marinespecies.org:taxname:134146

Spicara maena (L., 1758) urn:lsid:marinespecies.org:taxname:126828

Spicara smaris (L., 1758) urn:lsid:marinespecies.org:taxname:126830

Boops boops (L., 1758) urn:lsid:marinespecies.org:taxname:127047

Chromis chromis (L., 1758) urn:lsid:marinespecies.org:taxname:127000

Anthias anthias (L., 1758) urn:lsid:marinespecies.org:taxname:127031

Scyliorhinus Blainville, 1816 urn:lsid:marinespecies.org:taxname:105729

Serranus hepatus (L., 1758) urn:lsid:marinespecies.org:taxname:127042

Blennius ocellaris L., 1758 urn:lsid:marinespecies.org:taxname:126761

Symphodus cinereus (Bonnaterre, 1788) urn:lsid:marinespecies.org:taxname:273567

Solea Quensel, 1806 urn:lsid:marinespecies.org:taxname:126132

Lophius L., 1758 urn:lsid:marinespecies.org:taxname:125802

Scorpaena scrofa L., 1758 urn:lsid:marinespecies.org:taxname:127248

Dentex dentex (L., 1758) urn:lsid:marinespecies.org:taxname:273962

Pagrus pagrus (L., 1758) urn:lsid:marinespecies.org:taxname:127063

Zeus faber L., 1758 urn:lsid:marinespecies.org:taxname:127427

frontiers | Frontiers in Marine Science

TYPE Original Research
PUBLISHED 08 May 2023
DOI 10.3389/fmars.2023.1134385

Check for updates

OPEN ACCESS

EDITED BY
Monica Montefalcone,
University of Genoa, Italy

REVIEWED BY
Ali Badreddine,
Tyre Coast Nature Reserve, Lebanon
Daniele Ventura,
Sapienza University of Rome, Italy

*CORRESPONDENCE
Flavio Picone
flaviopicone@hotmail.com

RECEIVED 30 December 2022
ACCEPTED 18 April 2023
PUBLISHED 08 May 2023

CITATION
Picone F and Chemello R (2023) Seascape characterization of a Mediterranean vermetid reef: a structural complexity assessment.
Front. Mar. Sci. 10:1134385.
doi: 10.3389/fmars.2023.1134385

COPYRIGHT
© 2023 Picone and Chemello. This is an open-access article distributed under the terms of the Creative Commons Attribution License (CC BY). The use, distribution or reproduction in other forums is permitted, provided the original author(s) and the copyright owner(s) are credited and that the original publication in this journal is cited, in accordance with accepted academic practice. No use, distribution or reproduction is permitted which does not comply with these terms.

Seascape characterization of a Mediterranean vermetid reef: a structural complexity assessment

Flavio Picone[1,2]* and Renato Chemello[2]

[1]National Center for Scientific Research, Research and Service Units (USR) 3278 - Centre de Recherches Insulaires et Observatoire de l'environnement (CRIOBE) - École Pratique des Hautes Études (EPHE)-University of Perpignan Via Domitia (UPVD)-CNRS, Perpignan, France, [2]Department of Earth and Marine Sciences, University of Palermo, Palermo, Italy

In the Mediterranean Sea, vermetid reefs can modify coastal seascapes forming platforms in the intertidal zone of rocky coasts. With their three-dimensional and seaward-expanding structure, these bioconstructions support high biodiversity levels and provide important ecological functions and ecosystem services. In this study, we perform a first structural characterization of a vermetid reef seascape (hereafter, vermetid reefscape) and quantitatively assess the degree of their contribution to the structural complexity of the coastal seascape. Aerial images of a vermetid reef coast were acquired in the Marine Protected Area of Capo Gallo-Isola delle Femmine (Southern Tyrrhenian Sea) by means of unmanned aerial vehicle technology. In the seascape, the *outer reef*, *platform*, and *coast* classes were identified and digitized in GIS environment. The resulting vermetid reefscape was analysed by means of FRAGSTATS software using metrics belonging to the "area-edge", "shape", and "aggregation" categories. To quantitatively assess the structural complexity, the edge density, area-weighted perimeter area ratio, and landscape shape index metrics were applied to the seascapes with and without the vermetid reefs to simulate a sea level rise scenario. In addition, the effect of their presence in terms of coast length (i.e., total edge) was statistically tested using the Wilcoxon signed rank test. The outer reef had the highest total edge value (5,785.6 m) and, at the same time, the lowest class area (1,040 m^2). It was also the patchiest, and the most fragmented and geometrically complex class in the seascape. Overall, the bioconstruction positively contributed to the structural complexity of the seascape with higher values of coastal area (12%), edge density (139%), area-weighted perimeter-area ratio (90%), and landscape shape index (66%). The Wilcoxon test revealed a statistically significant effect of the vermetid reefs presence on the coastal total edge (z = 3.9, p < 0.005), with a large effect size (r = 0.74). The results showed an overall higher structural complexity of the vermetid reefscape, indicating that its loss would lead to a significantly less complex seascape, entailing detrimental effects on the supported biodiversity levels and the valuable ecosystem services provided.

KEYWORDS

Dendropoma, bioconstruction, neglected habitat, habitat structure, seascape ecology, landscape metrics, vermetid reefscape, Mediterranean Sea

1 Introduction

In recent years, seascape ecology rapidly developed as the marine-centric counterpart of the landscape ecology (Turner, 1989; Ray, 1991; Wedding et al., 2011; Bell and Furman, 2017; Pittman et al., 2018), emerging as a new and interdisciplinary science for marine sustainability studies (Pittman et al., 2021). Its applications allow for the exploration of the multi-scale linkages between ecological structure, function, and change in marine environments using a spatially explicit and quantitative approach, with potential to inform management and conservation practices (Pittman et al., 2021). As in the case of the landscape ecology, main focuses are the study of seascape composition (i.e., what and how much is present of each habitat or cover type) and configuration (i.e., the spatial structure or the arrangement of the spatial elements). Changes in configuration are expected to cause changes in ecological functions (Turner, 1989; Turner and Gardner, 2015), hence the importance to assess the relationships between spatial patterns and ecological processes and/or services occurring in the seascape. To do so, seascape ecology has inherited numerous metrics designed to quantify spatial properties in landscapes and analyze spatial patterns (O'Neill et al., 1988; McGarigal, 2002; Cushman et al., 2008; Turner and Gardner, 2015). Their application has proven useful also in the marine realm (Boström et al., 2011; Wedding et al., 2011), especially in coastal seascape research (Bell and Furman, 2017).

So far, the research interest of seascape ecologists has mainly focused on benthic seascapes (Zajac et al., 2000; Brown et al., 2011; Proudfoot et al., 2020), with a number of applications in nearshore and shallow water areas (Pittman et al., 2004; Boström et al., 2011). The attention to coastal seascapes gained momentum along with the research on coastal and marine ecosystem services, which in most cases are provided and therefore more appropriately evaluated and managed at the entire seascape scale (Barbier, 2012; Barbier, 2017). Coastal seascape ecology has been investigating several subtidal and intertidal biogenic habitats across different spatial scales (Robbins and Bell, 1994; Garrabou et al., 1998; Fonseca et al., 2002; Boström et al., 2011; Pittman and Brown, 2011; Furman et al., 2015; Parnell, 2015; Staveley et al., 2017). Among these, marine bioconstructions are of peculiar interest as they modify the biophysical properties of the seascape through their long-lasting and three-dimensional structures that serve as a secondary substrate for the colonization by other marine organisms (Ingrosso et al., 2018). It could be expected that the higher the complexity, size, and stability of these formations, the greater the positive effects on species number and diversity (McCoy and Bell, 1991; Sebens, 1991). Complexity can be defined as "the absolute abundance (per unit area or per unit volume) of individual structural components" for a certain scale of investigation (McCoy and Bell, 1991) and is an important feature of seascape configuration. As such, complexity assessments are used in both two- and three-dimensional seascape analyses. In the case of marine bioconstructions, shape complexity is most commonly investigated relatively to their three-dimensional structure (Burns et al., 2019; Price et al., 2019; Pascoe et al., 2021; Ventura et al., 2021; Carlot et al., 2023), which influences the heterogeneity and therefore the number of microhabitats provided. Irregularities such as holes and crevices provide surfaces with different microclimatic conditions (e.g., humidity, light exposure) and/or shelter from predators compared to the surrounding environment, influencing the number of species that can coexist and resulting in characteristic assemblages of species.

In the Mediterranean Sea, seascape ecology studies on biogenic habitats focused mainly on seagrass meadows (Gatti et al., 2012; Pagès et al., 2014; Pace et al., 2017; Abadie et al., 2018; Rodil et al., 2021) and coralligenous formations (Garrabou et al., 1998; Bracchi et al., 2017; Sini et al., 2019) with many other marine habitats yet to be explored. It is the case of the vermetid reefs, a carbonatic bioconstruction built by the synergistic activity of the encrusting red alga *Neogoniolithon brassica-florida* and gregarious gastropods belonging to the genus *Dendropoma* (Safriel, 1966), namely *D. cristatum*, *D. anguliferum*, *D. lebeche* (Templado et al., 2015), and an undescribed one in the Ionian Sea (Calvo et al., 2009). These formed a cryptic complex of species (Templado et al., 2015) under the name of *Dendropoma petraeum*, which was recently disentangled by Templado et al. (2015).

Vermetid reefs are found at the tide level in rocky shores and can have different morphologies, from simple and thin crusts to broad platforms expanding seawards (Laborel, 1987; Antonioli et al., 1999). Other shapes can result from differential erosive processes, such as the mushroom-like pillars, micro-atolls, and islands (Safriel, 1966; Antonioli et al., 1999). Platforms represent the most complex among the vermetid reef structures (Milazzo et al., 2016), on which the characteristic outer reef, inner edge, and *cuvette* can be identified (Figure 1). The outer reef is the biologically active part of the reef, dense with living *Dendropoma* individuals. It grows upwards and seawards as a crevices-rich and complex structure, often exceeding 50 cm of thickness (Chemello and Silenzi, 2011). The inner edge is a small *Dendropoma* encrustation that can be found at the boundary between the platform and the rocky shore, acting as a superior delimiter of the reef. Compared to its outer counterpart, the inner edge is thinner, mostly vertically developed, and with less dense *Dendropoma* abundances. Enclosed by the two margins is the zone of the *cuvettes*, shallow depressions no deeper than 50 cm that form small pools in low tide and calm water conditions (Molinier and Picard, 1953).

Considering the structural features of the vermetid reefs, a coastal seascape in which they are densely present is supposed to have higher structural complexity and heterogeneity levels compared to seascapes in which they are absent. With their three-dimensional and seaward-expanding structure, vermetid reefs support high biodiversity levels (Safriel and Ben-Eliahu, 1991), providing additional space and microhabitats, reduction of physical disturbances, refuge from predation, and a nursery habitat for many benthic and fish assemblages (Goren and Galil, 2001; Chemello and Silenzi, 2011). In addition to benefitting marine

Abbreviations: CA, Class Area; ED, Edge Density; LSI, Landscape Shape Index; NP, Number of Patches; NRC, No-Reef Coast; PARA AM, Area-Weighted Perimeter-Area Ratio; PD, Patch Density; PLAND, Percentage of Landscape; RC, Reef Coast; SPLIT, Splitting Index; TE, Total Edge; VRS, Vermetid Reef Seascape.

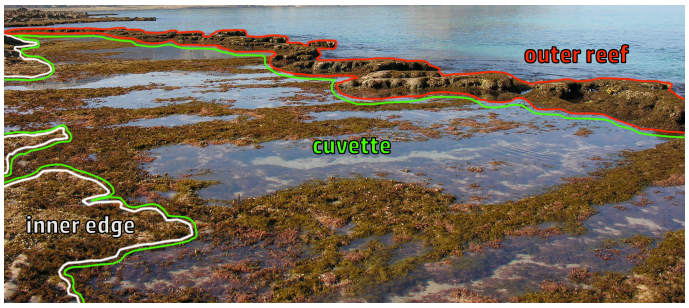

FIGURE 1
Picture of a vermetid reef platform in the northwestern coast of Sicily (Italy). The outer reef, cuvette, and inner edge parts are shown (Photo Credits: R.C.).

biodiversity, the presence of the vermetid reefs in the coastal seascape provides many valuable ecosystem services such as coastal protection, carbon sequestration, and sediment transport regulation (Milazzo et al., 2016).

Despite such ecological importance to Mediterranean coastal seascapes, vermetid reefs are a poorly known and neglected habitat (Picone et al., 2022), whose persistence is at risk. Threatened by a high anthropogenic pressure and the global climate change, local declines and even local losses have been observed and reported in the eastern and central areas of the Mediterranean Sea (Galil, 2013; Badreddine et al., 2019; Bisanti et al., 2022). Ocean warming and acidification negatively impact early life stages of *D. cristatum*, thus impairing the building of new reef surface (Alessi et al., 2019). In addition, considering the slow growth rate of *Dendropoma*, sea level rise is likely one of the most threatening pressures to these bioconstructions (Milazzo et al., 2016). The projected sea level rise under future emissions scenarios (Cooley et al., 2022) would likely lead to the submergence of the reefs, entailing the loss of their structures and key functions in the intertidal zone, with detrimental effects on biodiversity as well as ecosystem services provided. The non-living structures of the submerged reefs would likely continue playing a role in supporting biodiversity in deeper waters, but their original contribution to the structural complexity of the seascape as well as their unique ecological role would be lost.

To our knowledge, no study so far has characterized a coastal seascape with vermetid reefs (hereafter "vermetid reefscape") through the landscape ecology lens. Such approach would provide new insights on the structural properties of the vermetid reefs and set a reference baseline for future studies. In this paper, we provide a first characterization of a vermetid reefscape using landscape ecology metrics, and quantitatively assess the degree of its contribution to the structural complexity of the coastal seascape.

2 Materials and methods

2.1 Study area and data collection

The characterization of the vermetid reefscape was performed in the "Capo Gallo – Isola delle Femmine" Marine Protected Area (CG - 38°C12′37.33"N – 13°C17′10.62"E), along the north-western coast of Sicily (South of Italy). The area is mainly characterized by limestone rocks and shallow rocky coasts along which large vermetid reef platforms can be found. A coast section of 830 m length with a dense presence of reefs was identified and chosen as the study site (Figure 2A). A high-resolution (0.05 m/px) georeferenced aerial image (GeoTIFF) of the study area was produced through unmanned aerial vehicle technology (UAV) by Donnarumma et al. (2021) (Figure 2B). After distributing 24 georeferenced Ground Control Points (GCPs), four flights were performed over the 830 m coastline of the study area and covering a total surface of about 5 ha, using a Hexarotor Skyrobotic SF6, equipped with the SONY DSC-QX100 camera, at 40 m AGL (Above Ground Level) (Figure S1). To make the orthophotomosaic, a total of 700 high quality image frames were produced and processed using the photogrammetric image elaboration software AGISoft Photoscan (Donnarumma et al., 2021).

To characterize the vermetid reefscape, the main classes composing the seascape were identified. Patches of the *outer reef* class were selected as the outer and clearer areas of the bioconstruction, in contrast to the usually adjacent and darker patches of the *cuvette* zone. Due of its main vertical component, the inner edge could not be correctly represented by a 2D-image. For this reason, this portion of the reef was identified together with the *cuvette* zone as single class named the *platform*. For the sake of comprehensiveness and boundaries calculations, the class *sea* was identified in the seascape too. Finally, the *coast* class was selected as the remaining areas between the abovementioned classes and the road bordering the inner parts of the seascape.

Starting from the aerial image of the investigated area, the four seascape classes were manually digitized in GIS environment (QGIS, version 3.16.14) as a polygon vector file. The resulting vermetid reefscape (VRS) was produced considering only those features falling in a 25 m buffer area developed around the coast edge (Figure 3). The produced vector seascape was finally validated through *in situ* measurements.

Starting from the vermetid reefscape, two additional seascape scenarios were produced:

- reef coast (RC), in which outer reef, platform, and coast classes were merged (Figure 4);

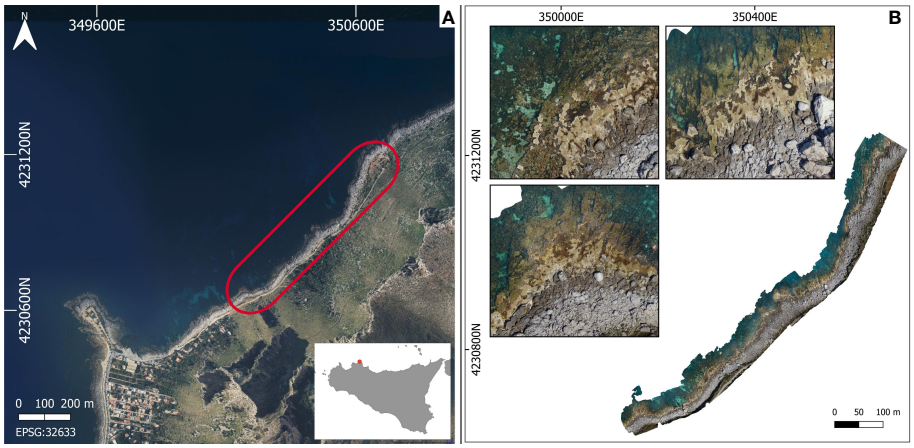

FIGURE 2
(A) Capo Gallo –Isola delle Femmine Marine Protected Area (Sicily, Italy). The red area encloses the investigated coastal seascape. **(B)** Aerial image of the study area, generated through unmanned aerial vehicle technology (Donnarumma et al., 2021).

- no-reef coast (NRC), in which the outer reef and platform classes were removed and only the coast is present (Figure 4). The seascape represents a hypothetical scenario in which the vermetid reefs are not present as a result of their growth rate (Sisma-Ventura et al., 2020) and the local projected sea level rise rates (Lo Presti et al., 2022).

2.2 Characterization of seascape structure and composition

To characterize the structure and composition of the vermetid reefscape, landscape ecology metrics were applied at both the class and the landscape levels using Fragstats (version 4.2.1), a software tool designed to quantify landscape structure (McGarigal and Marks, 1995). The metrics used in this study belonged to the "area-edge", "shape", and "aggregation" categories included in the software tool. The class metrics "total edge" (TE), "class area" (CA), "edge density" (ED), "percentage of landscape" (PLAND), "area-weighted perimeter-area ratio" (PARA AM), "number of patches" (NP), "patch density" (PD), "splitting index" (SPLIT), and "landscape shape index" (LSI) were applied to the classes of the VRS seascape. The landscape version of the same metrics, except for CA, PLAND, NP, and SPLIT, were applied to the RC and NRC seascapes (Table 1).

To use Fragstats, the vector files of the three seascapes (VRS, RC, and NRC) were converted to raster files (GeoTIFF) using a 0.1 m/px resolution. In computing area-edge metrics, no background/boundary interface was counted as edge. The sea class was disabled and no metric was applied to it.

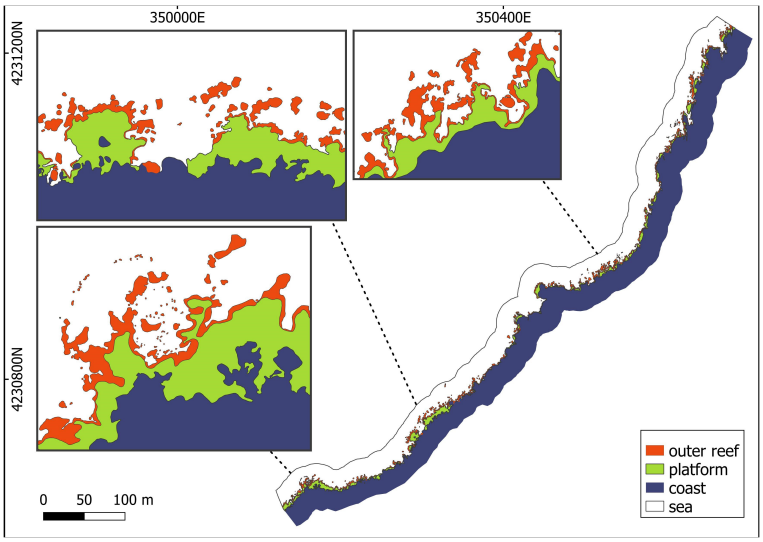

FIGURE 3
Vermetid reefscape (VRS) and its composing classes (i.e., outer reef, platform, coast, and sea) after the digitization of the aerial image of the studied area.

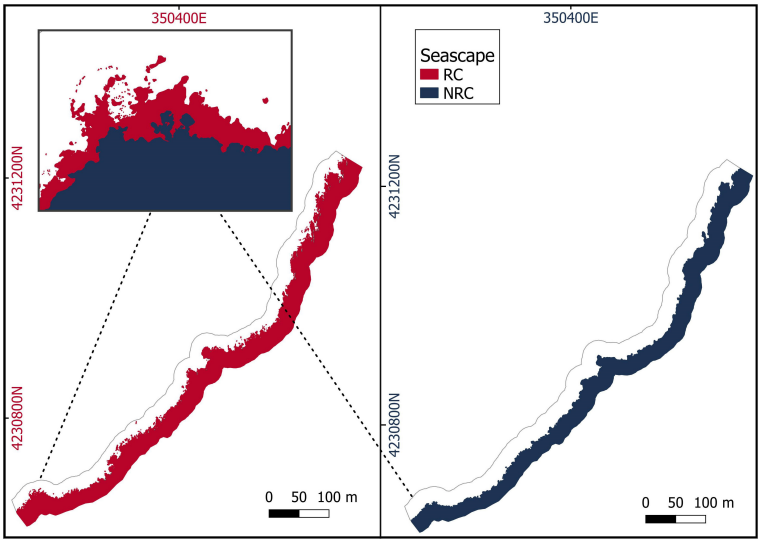

FIGURE 4
Reef coast (RC) seascape, in which the vermetid reef and the coast are merged in a single class, and a hypothetical scenario of the same seascape without the vermetid reefs (no-reef coast - NRC). The magnified image shows the overlapping of the two seascapes.

2.3 Structural complexity comparison in seascape scenarios

To account for the presence of the vermetid reefs in the coastal seascape in terms of added structural complexity, seascapes RC and NRC (i.e., with and without the reef) were compared. As a first explorative approach, a set of landscape metrics previously applied for the seascape analysis was used. The effect of the vermetid reefs on the seascape focused on metrics based on length-area ratios to account for the structural modifications caused by the presence of the bioconstruction in the seascape. The metrics selected for such comparison were edge density (ED), area-weighted perimeter-area ratio (PARA AM), and landscape shape index (LSI). The area (CA) metric was also included as a reference measure. The contribution

TABLE 1 Fragstats metrics applied for the characterization of the seascape structure and composition at class and landscape level.

Category	Metrics	Class level	Landscape level
Area-edge	Total edge (TE)	Total length (m) of edge in the landscape by patch type (class)	Total length (m) of edge in the landscape
	Class area (CA)	Total area (m^2) of each class in the landscape	Not applied
	Edge density (ED)	Total length (m) of edge of a class divided by the total landscape area (m^2)	Total length (m) of edge in the landscape divided by the total landscape area (m^2)
	Percentage of landscape (PLAND)	Proportion of the landscape occupied by a patch type (class)	Not applied
Shape	Area-weighted perimeter-area ratio (PARA AM)	Mean perimeter-area ratio (m/m^2) of all patches of a class. Each patch is weighted by its proportional area representation based on the sum of all patch areas of all classes	Mean perimeter-area ratio (m/m^2) of all patches in the landscape. Each patch is weighted by its proportional area representation based on the sum of all patch areas of the landscape
Aggregation	Number of patches (NP)	Number of patches of the same class in the landscape	Not applied
	Patch density (PD)	Number of patches of a class in the landscape, divided by the area (m^2) of the landscape. It is expressed as number of patches per 100 hectares	Number of patches in the landscape, divided by the area (m^2) of the landscape. It is expressed as number of patches per 100 hectares
	Splitting index (SPLIT)	The total landscape area (m^2) squared divided by the sum of patch area (m^2) squared, summed across all patches of the corresponding patch type	Not applied
	Landscape shape index (LSI)	LSI equals 0.25 times (adjustment for raster format) the total length (m) of the edge between classes and the entire landscape boundary, divided by the square root of the total landscape area (m^2)	LSI equals 0.25 times (adjustment for raster format) the total length (m) of the entire landscape boundary and all edge segments within it, divided by the square root of the total landscape area (m^2)

was calculated as the natural logarithm of the ratios between the RC and the NRC values for each metric, so that a positive value would indicate an increase in the metric output provided by the presence of the vermetid reefs.

Following, a statistical approach was used to test the effect of the "presence of vermetid reefs" factor on the total edge of the coast. The quantity of total edge per unit area was used as a proxy of the overall coast complexity, being it one of the building components of all the used complexity metrics. To do so, RC and NRC coasts were both sampled using a total of 195 adjacent rectangles of 5 m length and 30 m width. The rectangles were created as vector polygons in QGIS and placed continuously along the coast perpendicularly to its profile to avoid the influence of changes in coast orientation on the samples. Once placed, rectangles were then positioned so to include both the RC and the NRC coastal edges. To make the RC samples representative of the reef structure along the coast, different width classes were identified (Figures S2, S3). Reef width was accounted for using reef area in the samples as a proxy (i.e., the greater the area of the reef in the rectangle, the longer its width). Based on the value range obtained from all the 195 RC samples, five classes were produced (Table 2).

For each of the reef classes from 1 to 4, 7 rectangles were randomly sampled, providing that a distance of at least 5 m was guaranteed from each other to respect independence of observations (Figure S1). The corresponding 28 sampling rectangles from the NRC scenario were then selected for the 0 width class, reaching an overall sample size of 56. To test the effect of the "presence of vermetid reefs" factor on the "total edge" variable, the values in the RC and NRC scenarios were paired by sampling rectangle and their difference was tested using a paired statistical test. To choose the appropriate statistical method, the distribution of the total edge data was determined using the Shapiro-Wilk test, which indicated a significant departure from normality ($W = 0.76$, $p < 0.005$). Based on this, the non-parametric Wilcoxon signed rank test was performed. To provide a measure of the magnitude of the factor's effect, the "effect size" (r) was calculated as the ratio between the "z" statistic and the square root of the sample size (N). Ranging from 0 to 1, the effect size value can be considered small (0.10 - < 0.30), moderate (0.30 - < 0.5), or large (≥ 0.5) according to Cohen's classification of effect sizes. In the presence of a significant effect and therefore rejection of the null hypothesis (i.e., no effect of vermetid reefs presence on the total edge of the coast), the effect size would express the degree to which the vermetid reefs contribute to increasing the seascape coastal complexity in terms of added total edge.

3 Results

Among the three classes in the seascape, the outer reef was the one with the highest total edge value (5,785.6 m) and, at the same time, the lowest class area (1,040 m^2). Excluding the sea class, the outer reef accounted for only 3.9% of the total seascape. Opposite are the results of the edge-area metrics for the coast class, which had the lowest total edge (2,248.6), but the highest area (23,710 m^2), representing 89.3% of the seascape. The platform class was, therefore, the second highest class in terms of both total edge (3,511.8 m) and area (1,803 m^2, 6.8%). Accordingly, the highest edge density value was reached by the outer reef (0.12 m/m^2), followed by the platform (0.07 m/m^2) and the coast (0.05 m/m^2) classes (Table 3). In line with these results, the value of the area-weighted perimeter-area ratio for the outer reef class was the highest (55,618), almost three times the platform value (19,544), and more than thirty times compared to the coast (1,479). Aggregation metrics showed the outer reef as the patchiest (NP = 679; PD = 14,193) as well as the most fragmented (i.e., reduced area and smaller patches) class in the seascape (SPLIT = 208,449), followed again by the platform (NP = 103; PD = 2,153; SPLIT = 9,615) and the coast (NP = 7; PD = 146; SPLIT = 4.1). Finally, the same pattern occurred in the case of the landscape shape index, which identified the outer reef as the most geometrically complex among the classes in the seascape (LSI = 44.8), followed by the platform, and the coast (Table 3). The analysis at the landscape level revealed the reef coast seascape (RC) to have higher values than the no-reef coast (NRC) in all the area-edge, shape, and aggregation metrics applied (Table 3). The natural logarithm ratios of the metrics selected for the comparison of the RC and NRC seascapes were all positive, ranging from 0.1 (CA) to 0.87 (ED) (Figure 5). In particular, compared to the NRC scenario, the RC seascape had 12% more coastal area, while the edge density, area-weighted perimeter-area ratio, and landscape shape index were 139%, 90%, and 66% higher, respectively. The Wilcoxon signed rank test revealed a statistically significant effect of the vermetid reefs presence on the coastal total edge ($z = 3.9$, $p < 0.005$), with a large effect size ($r = 0.74$). Total edge values in the RC seascape were significantly higher than in the NRC scenario, with the median score for the RC seascape being 21.9

TABLE 2 Classification of reef width based on the reef area occupied in the rectangle samples of the RC and NRC seascapes.

Width class	Reef area (m^2)	Seascape	Occurrences
0	equal to 0	NRC	195
1	between 0.1 and 9.9	RC	66
2	between 10 and 19.9	RC	77
3	between 20 and 29.9	RC	30
4	equal or higher than 30	RC	22

TABLE 3 Results of the metrics used for the characterization of the seascapes: total edge (TE); class area (CA); edge density (ED); percentage of landscape (PLAND); area-weighted perimeter-area ratio (PARA AM); number of patches (NP); patch density (PD); SPLIT; landscape shape index (LSI).

	Class level			Landscape level	
	outer reef	platform	coast	RC	NRC
TE (m)	5.8e+03	3.5e+03	2.2e+03	5.4e+03	2.3e+03
CA (m^2)	1.0e+03	1.8e+03	2.4e+04	2.7e+04	2.4e+04
ED (m/m^2)	0.12	0.07	0.05	0.11	0.05
PLAND	3.9%	6.8%	89.3%	—	—
PARA AM	5.6e+04	2.0e+04	1.5e+03	1.0e+03	5.3e+02
NP	679	103	7	—	—
PD	1.4e+04	2.1e+03	1.5e+02	3.7e+03	9.8e+01
SPLIT	2.1e+05	9.6e+03	4.1	—	—
LSI	44.8	20.7	5.1	5.5	3.3

compared to 8.5 for the same seascape without the vermetid reefs (Figure 6).

4 Discussion

The use of a UAV remote sensing sampling technique proved a useful tool to investigate the vermetid reefs from a structural perspective, as in the case of other drone-based applications to marine and coastal habitats, including bioconstructions (Collin et al., 2018; Ventura et al., 2018; Jackson-Bué et al., 2021; Tait et al., 2021; Brunier et al., 2022). Such approaches play an increasingly important role not only in detecting and monitoring changes in and impacts to marine and coastal bioconstructions, especially in the face of the threats posed by climate change, but offer also efficient tools to assess the degree to which such impacts affect the generation of many ecosystem services depending on the structural properties of the biogenic formations.

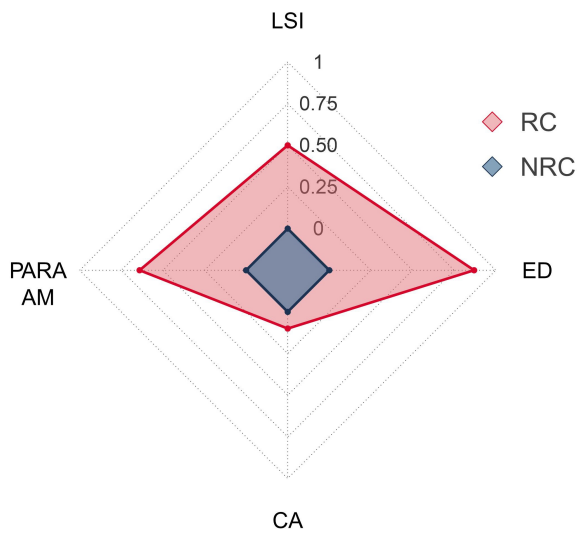

FIGURE 5
Contributions to the structural complexity provided by the presence of the vermetid reefs in the seascape. Values are calculated as the natural logarithm ratios of the area-weighted perimeter-area ratio (PARA AM), landscape shape index (LSI), and edge density (ED) metrics in the seascapes with (RC) and without (NRC) the vermetid reefs. The class area (CA) metric is also included as a reference.

The methodology used in this study allowed a cost-efficient acquisition of high-resolution spatial data, suitable for the analysis of the role played by the vermetid reefs in modifying the structure of the coastal seascape. The visual identification and manual digitization of the seascape classes resulted in a low-cost and time saving method for the classification of a small-scale seascape characterized by a low number of visually discernible classes. If future studies were to be conducted, for instance, on the algal communities living on the vermetid reefs, different techniques would have to be implemented (e.g., Tait et al., 2021). Spectral information and classification algorithms (e.g., support vector machines (SVM), maximum likelihood) would be required to accurately and efficiently perform image classification, especially in the case of highly diverse seascapes with higher number of classes. These automated approaches would require specific training procedures to reach high levels of accuracy, potentially presenting limitations in their applications in the case of an environment characterized by spectral complexity (Brunier et al., 2022).

The analysis of the vermetid reefscape at the class level showed a clear pattern of increasing edge density, perimeter-area ratio of patches, and patchiness from the coast seaward. These features underpin a higher structural complexity of the vermetid reefs and its two constituting classes, the platform and the outer reef. The latter in particular accounts for only about 4% of the seascape surface, which makes it the least represented class, and is configured as a discontinuous, fragmented, and thin stripe between the platform and the sea. Compared to the platform, the outer edge has a six times higher patch density and a more than twenty times higher splitting index, a metric whose value increases as the class area decreases and is subdivided into smaller patches. The disaggregation of the outer reef was also captured by the high

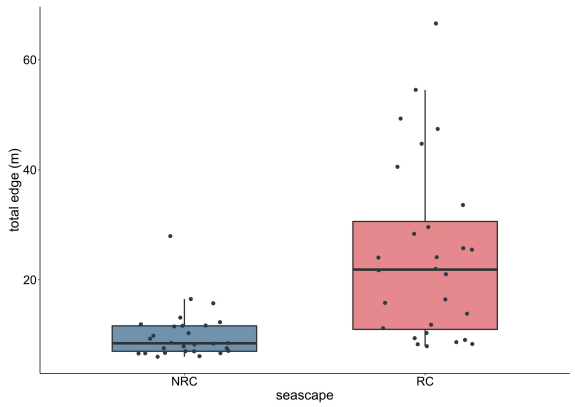

FIGURE 6
Total edge values of the coast samples in the seascapes without (NRC) and with (RC) the vermetid reefs.

value of the landscape shape index that, together with the area-weighted perimeter-area ratio, indicated the outer reef as the most geometrically complex class overall.

The fragmented nature of the outer reef is a peculiar feature of this class of the vermetid reefscape, whose scattered structure results from the interaction of different factors such as hydrodynamics, type of rocky substrate, and reef growth (Safriel, 1966; Antonioli et al., 1999). Anthropogenic stressors acting on this already but naturally fragmented class could have severe impacts on it, drastically lowering the overall complexity and heterogeneity of the vermetid reef. The high perimeter-area ratio makes this class more exposed to potential threats negatively affecting the vitality of the *Dendropoma* individuals. Such scenario would be particularly concerning considering the functional role the outer reef plays in building new reef surface and maintaining the whole bioconstruction alive and expanding. An erosion rate not compensated by a sufficient growth of the outer reef would ultimately lead to the collapse of the entire structure as already reported for the Eastern Mediterranean (Galil, 2013).

The outcomes of the analysis performed at the landscape level were consistent to the ones at the class level, showing overall the same patterns. The presence of the bioconstruction in the RC seascape resulted in a longer coastal edge, a more complex geometric shape, and a patchier configuration of the seascape compared to the NRC scenario in which the vermetid reefs are absent. In the RC seascape, the total edge length was more than doubled compared to the NRC scenario, going from 2.3 to 5.4 km, with an increase in coastal area of about only 11%. The role played by the vermetid reefs in increasing the two-dimensional structural complexity of the seascape stems from their high total edge value per unit area, which positively affects metrics based on a length-area ratio such as perimeter-area ratio, edge density, and landscape shape index.

The comparison of the two seascape scenarios through the logarithmic ratios produced positive values indeed, providing a measure of the degree to which the vermetid reefs contribute to the overall structural complexity of the coastal seascape. The logarithmic responses of edge density, perimeter to area ratio, and landscape shape index were from five to almost nine times higher compared to the area increase. These results once again stress the important role played by the vermetid reef formation in shaping the coastal structure, pointing to features other than just the surface of the reef. The additional area provided by the platform in the intertidal zone is indeed pivotal for the ecological role played by the vermetid reefs, offering a diversified substrate made of crests and *cuvettes* with peculiar microhabitats, which allow the settlement of specific reef communities and the support of high biodiversity levels. Even though the link between platform area and the harboured biodiversity is acknowledged in the literature as the main emergent outcome of the presence of the vermetid reefs, our results showed that the additional area is not their main contribution to the coastal seascape structure. The relatively low coastal area increase (0.1 times) in the RC seascape entailed a 1.4-fold higher coastal total edge, resulting in a seascape characterized by a higher edge density value (Figure 6). The higher values of the perimeter to area ratio and the landscape shape index resulted also from differences in the shape of the vermetid reefscape. The perimeter to area ratio increases as a landscape has more patches with irregular perimeter, while high values of the landscape shape index result from landscapes deviating from a circular shape, with an increase in the amount of internal edges. The two metrics conveyed therefore additional information compared to the edge density, showing that the presence of the vermetid reefs underpinned also higher levels of shape complexity. The results of the Wilcoxon signed rank test confirmed the difference between the two seascapes, showing a statistically significant effect of the presence of the vermetid reefs on the coastal total edge. Moreover, the large effect size (r = 0.74) was consistent with the logarithmic ratio results, showing the high degree to which the vermetid reefs contribute to shaping the coastal seascape.

The loss of the vermetid reefscape as a result of anthropogenic fragmentation and degradation, or even the potential inundation of the reefs according to the sea level rise projections for the next decades (Cooley et al., 2022), would lead to a significantly simpler coastline shape, with a likely less degree of heterogeneity provided to the intertidal zone. Considering the ratio between the current reef growth rate of 0.19 mm/year (Sisma-Ventura et al., 2020) and the sea level rise rate of 1.4 mm/year estimated for the North-Western Sicily (Lo Presti et al., 2022), a scenario of complete inundation of the vermetid reefs is expected to occur between 2060 and 2080. Such changes would increase the competition for space and resources and ultimately lead to lower biodiversity levels (Rilov et al., 2021). In addition, the degradation of the biophysical structures and the ecological functions provided by the vermetid reefscape would involve the loss of many valuable ecosystem services. For instance, simpler, smaller, and more disaggregated patches of vermetid reefs would be less capable of preventing coastal erosion and regulating sediment transport, or acting as seawalls or breakwaters, protecting the coast from currents, waves, and extreme events (Milazzo et al., 2016). Finally, the loss of the outer reef and its living *Dendropoma* individuals would impair reef growth and prevent their CO_2 sequestration from the atmosphere to build new carbonate structures.

The characterization of marine bioconstructions through their structural properties has been increasing in the recent literature,

laying the foundations for the investigation of the links between structure and biodiversity, functions, and services in the marine realm. The seascape approach together with the metrics inherited from the landscape ecology proved a useful set of tools to investigate the role played by the vermetid reefs in shaping the coastal seascape structure, potentially paving the way to applications on other marine bioconstructions.

In conclusion, this paper showed the value of the vermetid reefscape from a structural perspective, pointing to the complexity that would be irreversibly lost at a seascape scale due to the anthropogenic pressures the vermetid reefs will continue facing for the next decades. The study provides a reference for future monitoring and impact assessments on the structure and status of the investigated seascape, representing also a starting point for environmental accounting applications. Future studies on the vermetid reefscape will need to focus on the relationship between the structural complexity and the composition of species assemblages colonizing the reef, investigating the effects of structural changes on the supported biodiversity at different scales. Such investigations would contribute to improving the knowledge on this neglected bioconstruction and its important role in shaping Mediterranean seascapes.

Data availability statement

The raw data supporting the conclusions of this article will be made available by the authors, without undue reservation.

Author contributions

FP: Conceptualization, Methodology, Software, Formal Analysis, Investigation, Data Curation, Writing – Original Draft, Visualization. RC: Conceptualization, Writing – Review & Editing, Supervision. All authors contributed to the article and approved the submitted version.

Acknowledgments

We would like to thank C. Fazio for her contribution to the digitization of the seascape.

Conflict of interest

The authors declare that the research was conducted in the absence of any commercial or financial relationships that could be construed as a potential conflict of interest.

Publisher's note

All claims expressed in this article are solely those of the authors and do not necessarily represent those of their affiliated organizations, or those of the publisher, the editors and the reviewers. Any product that may be evaluated in this article, or claim that may be made by its manufacturer, is not guaranteed or endorsed by the publisher.

Supplementary material

The Supplementary Material for this article can be found online at: https://www.frontiersin.org/articles/10.3389/fmars.2023.1134385/full#supplementary-material

References

Abadie, A., Pace, M., Gobert, S., and Borg, J. A. (2018). Seascape ecology in *Posidonia oceanica* seagrass meadows: linking structure and ecological processes for management. *Ecol. Indic.* 87, 1–13. doi: 10.1016/j.ecolind.2017.12.029

Alessi, C., Giomi, F., Furnari, F., Sarà, G., Chemello, R., and Milazzo, M. (2019). Ocean acidification and elevated temperature negatively affect recruitment, oxygen consumption and calcification of the reef-building *Dendropoma cristatum* early life stages: evidence from a manipulative field study. *Sci. Total. Environ.* 693, 1–10. doi: 10.1016/j.scitotenv.2019.07.282

Antonioli, F., Chemello, R., Improta, S., and Riggio, S. (1999). *Dendropoma* Lower intertidal reef formations and their palaeoclimatological significance (NW Sicily). *Mar. Geol.* 161, 155–170. doi: 10.1016/S0025-3227(99)00038-9

Badreddine, A., Milazzo, M., Abboud-Abi Saab, M., Bitar, G., and Mangialajo, L. (2019). Threatened biogenic formations of the Mediterranean: current status and assessment of the vermetid reefs along the Lebanese coastline (Levant basin). *Ocean. Coast. Manage.* 169, 137–146. doi: 10.1016/j.ocecoaman.2018.12.019

Barbier, E. B. (2012). Progress and challenges in valuing coastal and marine ecosystem services. *Rev. Environ. Econ. Policy* 6, 1–19. doi: 10.1093/reep/rer017

Barbier, E. B. (2017). Marine ecosystem services. *Curr. Biol.* 27, R507–R510. doi: 10.1016/j.cub.2017.03.020

Bell, S. S., and Furman, B. T. (2017). Seascapes are landscapes after all; comment on Manderson, (2016): seascapes are not landscapes: an analysis performed using Bernhard riemann's rules. *ICES Journal of Marine Science* 73, 1831–1838. *ICES. J. Mar. Sci.* 74 (8), 2276–2279. doi: 10.1093/icesjms/fsx070

Bisanti, L., Visconti, G., Scotti, G., and Chemello, R. (2022). Signals of loss: local collapse of neglected vermetid reefs in the western Mediterranean Sea. *Mar. pollut. Bull.* 185, 114383. doi: 10.1016/j.marpolbul.2022.114383

Boström, C., Pittman, S. J., Simenstad, C., and Kneib, R. T. (2011). Seascape ecology of coastal biogenic habitats: advances, gaps, and challenges. *Mar. Ecol. Prog. Ser.* 427, 191–217. doi: 10.3354/meps09051

Bracchi, V. A., Basso, D., Marchese, F., Corselli, C., and Savini, A. (2017). Coralligenous morphotypes on subhorizontal substrate: a new categorization. *Cont. Shelf. Res.* 144, 10–20. doi: 10.1016/j.csr.2017.06.005

Brown, C. J., Smith, S. J., Lawton, P., and Anderson, J. T. (2011). Benthic habitat mapping: A review of progress towards improved understanding of the spatial ecology of the seafloor using acoustic techniques. *Estuar. Coast. Shelf Sci.* 92, 502–520. doi: 10.1016/j.ecss.2011.02.007

Brunier, G., Oiry, S., Gruet, Y., F. Dubois, S., and Barillé, L. (2022). Topographic analysis of intertidal polychaete reefs (*Sabellaria alveolata*) at a very high spatial resolution. *Remote Sens.* 14, 307. doi: 10.3390/rs14020307

Burns, J. H. R., Fukunaga, A., Pascoe, K. H., Runyan, A., Craig, B. K., Talbot, J., et al. (2019). "3D habitat complexity of coral reefs in the northwestern Hawaiian islands is driven by coral assemblage structure," in *The international archives of the photogrammetry, remote sensing and spatial information sciences XLII-2/W10*, 61–67. doi: 10.5194/isprs-archives-XLII-2-W10-61-2019

Calvo, M., Templado, J., Oliverio, M., and MacHordom, A. (2009). Hidden Mediterranean biodiversity: molecular evidence for a cryptic species complex within the reef-building vermetid gastropod *Dendropoma petraeum* (Mollusca: caenogastropoda). *Biol. J. Linn. Soc Lond.* 96, 898–912. doi: 10.1111/j.1095-8312.2008.01167.x

Carlot, J., Vousdoukas, M., Rovere, A., Karambas, T., Lenihan, H. S., Kayal, M., et al. (2023). Coral reef structural complexity loss exposes coastlines to waves. *Sci. Rep.* 13, 1683. doi: 10.1038/s41598-023-28945-x

Chemello, R., and Silenzi, S. (2011). Vermetid reefs in the Mediterranean Sea as archives of sea-level and surface temperature changes. *Chem. Ecol.* 27, 121–127. doi: 10.1080/02757540.2011.554405

Collin, A., Dubois, S., Ramambason, C., and Etienne, S. (2018). Very high-resolution mapping of emerging biogenic reefs using airborne optical imagery and neural network: the honeycomb worm *(Sabellaria alveolata)* case study. *Int. J. Remote Sens.* 39, 5660–5675. doi: 10.1080/01431161.2018.1484964

Cooley, S., Schoeman, D., Bopp, L., Boyd, P., Donner, S., Ghebrehiwet, D. Y., et al. (2022). "Oceans and coastal ecosystems and their services," in *Climate change 2022: impacts, adaptation and vulnerability. contribution of working group II to the sixth assessment report of the intergovernmental panel on climate change*. Eds. H. O. Pörtner, D. C. Roberts, M. Tignor, E. S. Poloczanska, K. Mintenbeck, A. Alegría, et al (Cambridge, UK and New York, NY, USA: Cambridge University Press), 379–550. doi: 10.1017/9781009325844.005

Cushman, S. A., McGarigal, K., and Neel, M. C. (2008). Parsimony in landscape metrics: strength, universality, and consistency. *Ecol. Indic.* 8, 691–703. doi: 10.1016/j.ecolind.2007.12.002

Donnarumma, L., D'Argenio, A., Sandulli, R., Russo, G. F., and Chemello, R. (2021). Unmanned aerial vehicle technology to assess the state of threatened biogenic formations: the vermetid reefs of mediterranean intertidal rocky coasts. *Estuar. Coast. Shelf. Sci.* 251. doi: 10.1016/j.ecss.2021.107228

Fonseca, M. S., Whitfield, P. E., Kelly, N. M., and Bell, S. S. (2002). Modeling seagrass landscape pattern and associated ecological attributes. *Ecol. Appl.* 12, 218–230. doi: 10.1890/1051-0761(2002)012[0218:MSLPAA]2.0.CO;2

Furman, B. T., Jackson, L. J., Bricker, E., and Peterson, B. J. (2015). Sexual recruitment in *Zostera marina*: a patch to landscape-scale investigation. *Limnol. Oceanogr.* 60, 584–599. doi: 10.1002/lno.10043

Galil, B. S. (2013). Going going gone: the loss of a reef building gastropod (Mollusca: caenogastropoda: vermetidae) in the southeast Mediterranean Sea. *Zool. Middle. East.* 59 (2), 179–182. doi: 10.1080/09397140.2013.810885

Garrabou, J., Riera, J., and Zabala, M. (1998). Landscape pattern indices applied to mediterranean subtidal rocky benthic communities. *Landsc. Ecol.* 13, 225–247. doi: 10.1023/A:1007952701795

Gatti, G., Montefalcone, M., Rovere, A., Parravicini, V., Morri, C., Albertelli, G., et al. (2012). Seafloor integrity down the harbor waterfront: the coralligenous shoals off vado ligure (NW Mediterranean). *Adv. Oceanogr. Limnol.* 3, 51–67. doi: 10.1080/19475721.2012.671190

Goren, M., and Galil, B. S. (2001). Fish biodiversity in the vermetid reef of shiqmona (Israel). *Mar. Ecol.* 22, 369–378. doi: 10.1046/j.1439-0485.2001.01750.x

Ingrosso, G., Abbiati, M., Badalamenti, F., Bavestrello, G., Belmonte, G., Cannas, R., et al. (2018). *Mediterranean bioconstructions along the Italian coast. Adv. Mar. Biol.* (Elsevier), 61–136. doi: 10.1016/bs.amb.2018.05.001

Jackson-Bué, T., Williams, G. J., Walker-Springett, G., Rowlands, S. J., and Davies, A. J. (2021). Three-dimensional mapping reveals scale-dependent dynamics in biogenic reef habitat structure. *Remote Sen. Ecol. Conserv.* 7, 621–637. doi: 10.1002/rse2.213

Laborel, J. (1987). Marine biogenic constructions in the mediterranean. a review. *Sci. Rep. Port-Cros. Natl. Park.* 13, 97–126.

Lo Presti, V., Antonioli, F., Casalbore, D., Chiocci, F. L., Lanza, S., Sulli, A., et al. (2022). Geohazard assessment of the north-eastern Sicily continental margin (SW mediterranean): coastal erosion, sea-level rise and retrogressive canyon head dynamics. *Mar. Geophys. Res.* 43 (1), 1–18. doi: 10.1007/s11001-021-09463-9

McCoy, E. D., and Bell, S. S. (1991). "Habitat structure: the evolution and diversification of a complex topic," in *Habitat structure*. Eds. S. S. Bell, E. D. McCoy and H. R. Mushinsky (Dordrecht: Springer Netherlands), 3–27. doi: 10.1007/978-94-011-3076-9_1

McGarigal, K. (2002). "Landscape pattern metrics," in *Encyclopedia of environmetrics*. Eds. A. H. El-Shaarawi and W. W. Piegorsch (Chichester, England: John Wiley & Sons), 1135–1142.

McGarigal, K., and Marks, B. J. (1995). "FRAGSTATS: spatial pattern analysis program for quantifying landscape structure," in *General technical report PNW-GTR-351* (Portland, OR: U.S. Department of Agriculture, Forest Service, Pacific Northwest Research Station). doi: 10.2737/PNW-GTR-351

Milazzo, M., Fine, M., Claudia, E., Marca, L., and Chemello, R. (2016). *Marine animal forests*. Eds. S. Rossi, L. Bramanti, A. Gori and C. Orejas (Cham: Springer International Publishing). doi: 10.1007/978-3-319-17001-5

Molinier, R., and Picard, J. (1953). Notes biologiques à propos d'un voyage d'étude sur les côtes de sicile. *Ann. Inst. Océanogr. Monaco.* 28, 163–188.

O'Neill, R. V., Krummel, J. R., Gardner, R. H., Sugihara, G., Jackson, B., DeAngelis, D. L., et al. (1988). Indices of landscape pattern. *Landsc. Ecol.* 1, 153–162. doi: 10.1007/BF00162741

Pace, M., Borg, J. A., Galdies, C., and Malhotra, A. (2017). Influence of wave climate on architecture and landscape characteristics of *Posidonia oceanica* meadows. *Mar. Ecol.* 38, 1–14. doi: 10.1111/maec.12387

Pagès, J. F., Gera, A., Romero, A., and Alcoverro, T. (2014). Matrix composition and patch edges influence plant–herbivore interactions in marine landscapes. *Funct. Ecol.* 28, 1440–1448. doi: 10.1111/1365-2435.12286

Parnell, P. E. (2015). The effects of seascape pattern on algal patch structure, sea urchin barrens, and ecological processes. *J. Exp. Mar. Biol. Ecol.* 465, 64–76. doi: 10.1016/j.jembe.2015.01.010

Pascoe, K. H., Fukunaga, A., Kosaki, R. K., and Burns, J. H. R. (2021). 3D assessment of a coral reef at Lalo atoll reveals varying responses of habitat metrics following a catastrophic hurricane. *Sci. Rep.* 11, 12050. doi: 10.1038/s41598-021-91509-4

Picone, F., Sottile, G., Fazio, C., and Chemello, R. (2022). The neglected status of the vermetid reefs in the Mediterranean Sea: a systematic map. *Ecol. Indic.* 143, 109358. doi: 10.1016/j.ecolind.2022.109358

Pittman, S. J., and Brown, K. A. (2011). Multi-scale approach for predicting fish species distributions across coral reef seascapes. *PloS One* 6, e20583. doi: 10.1371/journal.pone.0020583

Pittman, S. J., Lepczyk, C. A., Wedding, L. M., and Parrain, C. (2018). "Advancing a holistic systems approach in applied seascape ecology," in *Seascape ecology*. Ed. S. J. Pittman (Hoboken, NJ: Wiley & Sons), 367–389.

Pittman, S. J., McAlpine, C. A., and Pittman, K. M. (2004). Linking fish and prawns to their environment: a hierarchical landscape approach. *Mar. Ecol. Prog. Ser.* 283, 233–254. doi: 10.3354/meps283233

Pittman, S., Yates, K., Bouchet, P., Alvarez-Berastegui, D., Andréfouët, S., Bell, S., et al. (2021). Seascape ecology: identifying research priorities for an emerging ocean sustainability science. *Mar. Ecol. Prog. Ser.* 663, 1–29. doi: 10.3354/meps13661

Price, D. M., Robert, K., Callaway, A., Lo Iacono, C., Hall, R. A., and Huvenne, V. A. I. (2019). Using 3D photogrammetry from ROV video to quantify cold-water coral reef structural complexity and investigate its influence on biodiversity and community assemblage. *Coral. Reefs.* 38, 1007–1021. doi: 10.1007/s00338-019-01827-3

Proudfoot, B., Devillers, R., and Brown, C. J. (2020). Integrating fine-scale seafloor mapping and spatial pattern metrics into marine conservation prioritization. *Aquat. Conserv.: Mar. Freshw. Ecosyst.* 30, 1613–1625. doi: 10.1002/aqc.3360

Ray, G. C. (1991). Coastal-zone biodiversity patterns. *Bioscience* 41, 490–498. doi: 10.2307/1311807

Rilov, G., David, N., Guy-Haim, T., Golomb, D., Arav, R., and Filin, S. (2021). Sea Level rise can severely reduce biodiversity and community net production on rocky shores. *Sci. Total. Environ.* 791, 148377. doi: 10.1016/j.scitotenv.2021.148377

Robbins, B. D., and Bell, S. S. (1994). Seagrass landscapes: a terrestrial approach to the marine subtidal environment. *Trends Ecol. Evol.* 9, 301–304. doi: 10.1016/0169-5347(94)90041-8

Rodil, I. F., Lohrer, A. M., Attard, K. M., Hewitt, J. E., Thrush, S. F., and Norkko, A. (2021). Macrofauna communities across a seascape of seagrass meadows: environmental drivers, biodiversity patterns and conservation implications. *Biodivers. Conserv.* 30, 3023–3043. doi: 10.1007/s10531-021-02234-3

Safriel, U. N. (1966). Recent vermetid formation on the Mediterranean shore of Israel. *Proc. Malacol. Soc Lond.* 37, 27–34.

Safriel, U. N., and Ben-Eliahu, M. N. (1991). "The influence of habitat structure and environmental stability on the species diversity of polychaetes in vermetid reefs," in *Habitat structure. population and community biology series*. Eds. S. S. Bell, D. E. McCoy and H. R. Mushinsy (Dordrecht: Springer Netherlands), 349–369. doi: 10.1007/978-94-011-3076-9_17

Sebens, K. P. (1991). Habitat structure and community dynamics in marine benthic systems. *Habitat Struct.* 211–234. doi: 10.1007/978-94-011-3076-9_11

Sini, M., Garrabou, J., Trygonis, V., and Koutsoubas, D. (2019). Coralligenous formations dominated by *Eunicella cavolini* (Koch 1887) in the NE Mediterranean: biodiversity and structure. *Mediterr. Mar. Sci.* 20, 174–188. doi: 10.12681/mms.18590

Sisma-Ventura, G., Antonioli, F., Silenzi, S., Devoti, S., Montagna, P., Chemello, R., et al. (2020). Assessing vermetid reefs as indicators of past Sea levels in the Mediterranean. *Mar. Geol.* 429, 106313. doi: 10.1016/j.margeo.2020.106313

Staveley, T. A. B., Perry, D., Lindborg, R., and Gullström, M. (2017). Seascape structure and complexity influence temperate seagrass fish assemblage composition. *Ecography. (Cop.).* 40, 936–946. doi: 10.1111/ecog.02745

Tait, L. W., Orchard, S., and Schiel, D. R. (2021). Missing the forest and the trees: utility, limits and caveats for drone imaging of coastal marine ecosystems. *Remote Sens.* 13, 3136. doi: 10.3390/rs13163136

Templado, J., Richter, A., and Calvo, M. (2015). Reef building Mediterranean vermetid gastropods: disentangling the *Dendropoma petraeum* species complex. *Mediterr. Mar. Sci.* 17 (1), 13–31. doi: 10.12681/mms.1333

Turner, M. G. (1989). Landscape ecology: the effect of pattern on process. *Annu. Rev. Ecol. Syst.* 20, 171–197. doi: 10.1146/annurev.es.20.110189.001131

Turner, M. G., and Gardner, R. H. (2015). *Landscape ecology in theory and practice* (New York: Springer New York). doi: 10.1007/978-1-4939-2794-4

Ventura, D., Bonifazi, A., Gravina, M. F., Belluscio, A., and Ardizzone, G. (2018). Mapping and classification of ecologically sensitive marine habitats using unmanned

aerial vehicle (UAV) imagery and object-based image analysis (OBIA). *Remote Sens.* 10, 1331. doi: 10.3390/rs10091331

Ventura, D., Dubois, S. F., Bonifazi, A., Lasinio, G. J., Seminara, M., Gravina, M. F., et al. (2021). Integration of close-range underwater photogrammetry with inspection and mesh processing software: a novel approach for quantifying ecological dynamics of temperate biogenic reefs. *Remote Sens. Ecol. Conserv.* 7, 169–186. doi: 10.1002/rse2.178

Wedding, L. M., Lepczyk, C. A., Pittman, S. J., Friedlander, A. M., and Jorgensen, S. (2011). Quantifying seascape structure: extending terrestrial spatial pattern metrics to the marine realm. *Mar. Ecol. Prog. Ser.* 427, 219–232. doi: 10.3354/meps09119

Zajac, R. N., Lewis, R. S., Poppe, L. J., Twichell, D. C., Vozarik, J., and DiGiacomo-Cohen, M. L. (2000). Relationships among sea-floor structure and benthic communities in long island sound at regional and benthoscape scales. *J. Coast. Res.* 16 (3), 627–640.

frontiers | Frontiers in Marine Science

TYPE Original Research
PUBLISHED 21 July 2023
DOI 10.3389/fmars.2023.1093181

Check for updates

OPEN ACCESS

EDITED BY
Monica Montefalcone,
University of Genoa, Italy

REVIEWED BY
Yanyi Zeng,
Chinese Academy of Fishery Sciences, China
Yibo Liao,
Ministry of Natural Resources, China

*CORRESPONDENCE
Zhijian Jiang
jiangzj1982@scsio.ac.cn
Xiaoping Huang
xphuang@scsio.ac.cn

RECEIVED 08 November 2022
ACCEPTED 23 June 2023
PUBLISHED 21 July 2023

CITATION
Cui L, Jiang Z, Huang X, Liu S and Wu Y (2023) Identification of food sources in tropical seagrass bed food web using triple stable isotopes and fatty acid signatures. *Front. Mar. Sci.* 10:1093181. doi: 10.3389/fmars.2023.1093181

COPYRIGHT
© 2023 Cui, Jiang, Huang, Liu and Wu. This is an open-access article distributed under the terms of the Creative Commons Attribution License (CC BY). The use, distribution or reproduction in other forums is permitted, provided the original author(s) and the copyright owner(s) are credited and that the original publication in this journal is cited, in accordance with accepted academic practice. No use, distribution or reproduction is permitted which does not comply with these terms.

Identification of food sources in tropical seagrass bed food web using triple stable isotopes and fatty acid signatures

Lijun Cui[1,2], Zhijian Jiang[1,2,3,4]*, Xiaoping Huang[1,2,3,4]*, Songlin Liu[1,3,4] and Yunchao Wu[1,3,4]

[1]Key Laboratory of Tropical Marine Bio-resources and Ecology, South China Sea Institute of Oceanology, Chinese Academy of Sciences, Guangzhou, China, [2]University of Chinese Academy of Sciences, Huairou District, Beijing, China, [3]Southern Marine Science and Engineering Guangdong Laboratory, Guangzhou, China, [4]Innovation Academy of South China Sea Ecology and Environmental Engineering, Chinese, Academy of Sciences, Guangzhou, China

Identifying the trophic role of primary producers is the basis of assessing seagrass bed functions but remains difficult due to the underdetermined analysis method. Here, we analyzed the multiple isotopes ($\delta^{13}C$, $\delta^{15}N$, and $\delta^{34}S$ values) and fatty acid markers of food sources and macrobenthos in a tropical seagrass bed in summer and winter, and tried to combine these indicators to resolve the limitation of $\delta^{13}C$ and $\delta^{15}N$ values analysis. We found that the $\delta^{13}C$ and $\delta^{15}N$ values of epiphytes were like that of seagrass and macroalgae, while the $\delta^{34}S$ values of epiphytes and macroalgae were significantly different, and the dominant unsaturated Fatty acid markers of seagrass (18:2n6c and 18:3n3) and epiphytes (16:1n7) were obviously different. These results suggest that the combination of multiple isotopes and Fatty acid markers can effectively distinguish the complex food source. In addition, we also found that multiple isotopes were more suitable to identify the food sources of polychaetes and snails with simple diets, fatty acids were more suitable to identify the food sources of crustaceans with complex diets, but their combination is essential in identifying the diets of macrobenthos since the wide range of isotopic values for omnivores crustaceans and the Fatty acid markers transformation during snails and polychaetes assimilation might mislead us when only isotopes or Fatty acid markers were used. Our findings suggest that in tropical seagrass beds, using multiple isotopes and fatty acid markers together can help reduce the uncertainty caused by single markers variation and thus strengthen the separation of food sources and the diets of different consumer species.

KEYWORDS

trophic role, macrobenthos, sulfur stable isotope, fatty acids, tropical seagrass beds

1 Introduction

Seagrass beds rank among the most valuable ecosystems on the planet, despite only covering 0.15% of global sea surface area (Saderne et al., 2019; Ivajnšič et al., 2022). They are not only highly productive ecosystems, but also support food webs of coastal habitats (Jiang et al., 2019; Unsworth et al., 2019; Canadell and Jackson, 2021). They provide various food sources including seagrass, epiphytes, macroalgae, suspended particulate organic matter (SPOM), and microphytobenthos in the sediment for various fish and invertebrates, and serve as a shelter, habitat, and nursery ground for adult and juvenile faunas (Liu et al., 2020b; Cui et al., 2021a). However, understanding the function of seagrass bed food webs remains to be a challenge since it requires an effective approach to discriminate the food sources and their potential importance in seagrass beds (Abrantes and Sheaves, 2009; Kohlbach et al., 2021).

Integrating carbon and nitrogen stable isotopes into some kind of modeling, especially the Bayesian mixing models, has been widely employed to evaluate the food source contribution of seagrass ecosystems (Paar et al., 2019; Gagnon et al., 2021). This approach is based on the premise that the carbon and nitrogen stable isotopic values of consumer tissues reflect the diets actually assimilated by consumers over time (Weems et al., 2012). Meanwhile, the isotopic ratio enrichment between each trophic level can be predicted. Previous studies suggested that the $\delta^{13}C$ and $\delta^{15}N$ values of organisms generally increase by 0.5-1‰ and 2-5‰ relative to their food sources, respectively (Caut et al., 2009; Sun et al., 2020). However, this approach only provides two-dimensional discrimination, which may fail to identify the trophic base of the seagrass bed food webs, especially for tropical seagrass bed food webs, since they usually have more diversified primary producers and the isotopic values of food sources are often similar (Nakamoto et al., 2019). For example, in tropical seagrass ecosystems, the isotopic values of seagrass are usually close to those of epiphytes (Mittermayr et al., 2014; Cui et al., 2021a). In addition, the temporal variances in environmental factors may also result in similar stable isotopic values between seagrass and other food sources (Fritts et al., 2018). Therefore, it is essential to improve this approach.

Recent studies showed that the sulfur stable isotope composition has been successfully used in identifying the consumer diets of saltmarsh food webs (Jinks et al., 2020; Lippold et al., 2020). In saltmarsh ecosystems, the $\delta^{34}S$ values of food sources can be clearly separated (seawater column: ~+20‰, anaerobic sediments: ~-24‰, (Valiela et al., 2018b) because different primary producers usually acquire sulfur from different sources. For example, rooted marine vascular plants obtain sulfur most from anaerobic sediments, whereas other food sources, such as algae, obtain sulfur mostly from seawater sulfate. These factors result in a clear dissimilation in their $\delta^{34}S$ values (Fritts et al., 2018). Similarly, the $\delta^{34}S$ values of rooted seagrass may be also clear dissimilation from that of macroalgae or epiphytes in seagrass beds. Therefore, the sulfur isotopic composition may be proper as a third index (besides $\delta^{13}C$ and $\delta^{15}N$) to help us discriminate the food sources of seagrass bed food webs. However, in tropical seagrass beds with various food sources, the $\delta^{34}S$ values of primary producers are also largely affected by local sulfur cycling (Guiry et al., 2021). For example, in tropical seagrass beds with various food sources, some food sources (e.g., epiphytes, macroalgae, and phytoplankton) obtain sulfur from seawater sulfate and may have similar isotopes (Valiela et al., 2018b), and the $\delta^{34}S$ values of sediment may be more enriched or depleted under microbial metabolisms (e.g., microbial sulfate reduction and microbial sulfide oxidation) (Pellerin et al., 2019). Therefore, the ambiguities associated with similar isotopes in tropical seagrass beds may not be completely overcome by only using carbon, nitrogen, and sulfur stable isotopic composition.

Fatty acid markers may be another helpful tool to overcome the isotopic uncertainties since many primary producers can synthesize high levels of specific fatty acids as their unique identity indicators, and laboratory experiments have proven that the transfer of specific fatty acid markers is conservative in the process of fish diets (Xu et al., 2020). However, we still cannot ignore whether these specific fatty acid markers are similar in primary producers of seagrass beds, and whether they will be affected by the ability of macrobenthos to metabolize and transform fatty acids. Therefore, to overcome the limitation of only using carbon and nitrogen in the modeling, adding the analysis of sulfur isotopes and fatty acids biomarkers may be a promising approach for food web studies in tropical seagrass beds.

Macrobenthos are the key components of the seagrass bed food webs. They not only rely on various primary producers, but also serve as primary food sources for other higher faunas. Therefore, in this study, we made an attempt to identify whether stable isotopes and fatty acids biomarkers can effectively discriminate food sources in complex, tropical seagrass beds, and to explore whether this combination can reliably identify the diets of different macrobenthos.

2 Materials and methods

2.1 Study area

The study region is placed in Xincun Bay, which is located in the southeast coast of Lingshui County, Hainan Island, South China Sea (Figure 1). This bay is an almost entirely closed bay with only one narrow channel connecting to the South China Sea in the southwest. According to previous surveys, the Xincun seagrass bed is a mixed seagrass bed, which occupies an area of approximately 175 ha and is mainly distributed in the shallow waters of southern Xincun Bay (Huang et al., 2006; Huang et al., 2019). Seagrass species in this bay include *Enhalus acoroides*, *Thalassia hemprichii*, *Cymodocea rotundata*, *Halodule uninervis*, and *Halophila ovalis*, with *E. acoroides* and *T. hemprichii* as the dominant species (Huang et al., 2006; Huang et al., 2019).

2.2 Sampling design, field collection, and sample processing

According to the abundance and distribution of seagrass, samples for analysis were collected at stations S1, S2, and S3 (Figure 1) during low tide in summer (August 2018) and winter (January 2019). At each station, one to three samples were collected depending on the abundance and distribution of sampling

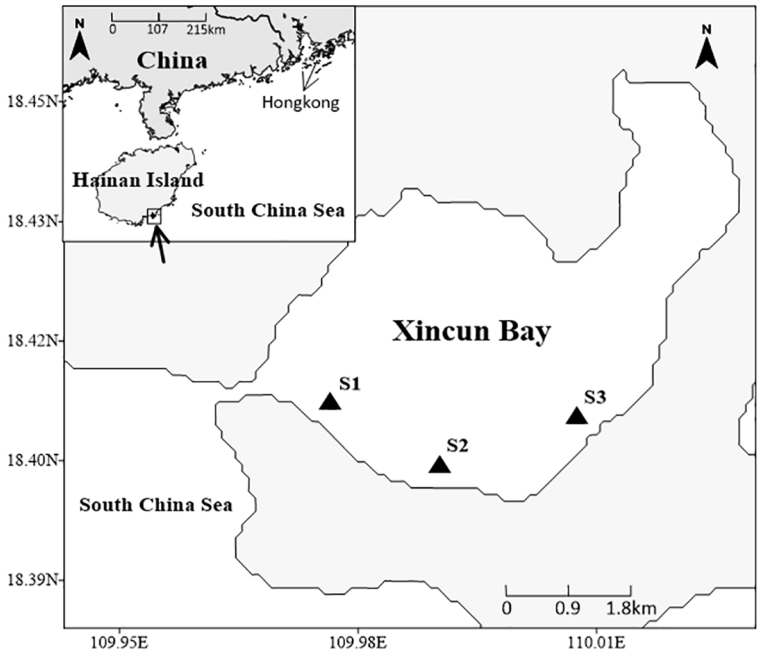

FIGURE 1
Sampling sites in Xincun Bay, Hainan Island, South China Sea.

organisms. Seagrass (*E. acoroides* and *T. hemprichii*) and macroalgae *Ulva lactuca* were collected by hand and washed with distilled water to remove attachments. For seagrass epiphytes, we applied the commonly used scraping method (i.e., removed carefully from the surface of seagrass leaves using a scalpel blade), because of the wideness of seagrass leaves: from 0.8 to 2.1 cm width (Huang et al., 2019), and the relatively high biomass of epiphytes (Cui et al., 2021b). Suspended particulate organic matter (SPOM) samples were obtained by filtering surface seawater onto pretreated (heated 2h at 450°C) Whatman GF/F filters. For sediment organic matter (SOM) samples, only the upper 1cm of the surface sediment layer was collected using a spade. For macroinvertebrates, crustaceans were collected by trammel nets, gastropods were sampled by hand, and polychaetes were sampled by sieving sediments through the 5mm mesh screen. Live invertebrates were put into containers with filtered seawater and kept for 24h to evacuate gut contents. Afterward, the gastropods and crustaceans were sorted, identified, and taken muscle. All the samples were placed in plastic polyethylene bags and stored in a freezer at -20°C (< 1 week) for their transportation to the laboratory.

In the laboratory, samples were freeze-dried at -40°C for 48h, and grounded into a fine homogeneous powder. Before stable isotope analysis, epiphytes, SPOM, and SOM were acidified to remove the effect of inorganic carbon on the $\delta^{13}C$ ratio of these samples. SPOM samples were acidified by exposure to hydrochloric acid (HCl) vapor for 24h. Epiphytes and SOM were acidified with a 1 mol/L solution until there were no bubbles. Subsequently, all acidified samples were rinsed with distilled water, freeze-dried again, and stored in the centrifuge tube for subsequent analysis.

Homogenized powder samples and SPOM were transferred to tin capsules, and $\delta^{13}C$, $\delta^{15}N$, and $\delta^{34}S$ values of samples were measured using a continuous-flow isotope-ratio mass spectrometer (Delta V Advantage, Thermo Fisher Scientific, Waltham, MA, USA) attached to an elemental analyzer (Flash EA 1112, Thermo Fisher Scientific, Milan, Italy). $\delta^{13}C$, $\delta^{15}N$, and $\delta^{34}S$ values were expressed in ‰ relative to the standard reference materials (Vienna Pee Dee Belemnite for $\delta^{13}C$ values, atmospheric N_2 for $\delta^{15}N$ values and Vienna Canyon Diablo Troilite for $\delta^{34}S$ values) using the standard δ notation:

$$\delta X(‰) = [(R_{sample}/R_{standard}) - 1] \times 1000 \quad (1)$$

where X is $\delta^{13}C$, $\delta^{15}N$ or $\delta^{34}S$ ratio, and R is $^{15}N/^{14}N$, $^{13}C/^{12}C$ or $^{34}S/^{32}S$. The detection limits for $\delta^{13}C$, $\delta^{15}N$ and $\delta^{34}S$ values were<0.2‰,<0.2‰, and<0.3‰, respectively.

Fatty acids were extracted using a method modified from (Folch et al., 1957). Briefly, a 2:1(v/v) chloroform and methanol mixed solution was used to extract the lipids of each sample (about 0.2-1mg), and a 0.9% sodium chloride solution was used to separate the lipids solution from the mixed solution. The sample was then concentrated using a rotary evaporator to obtain total lipid. The resulting total lipid samples were methylated with 0.5mol/L sodium hydroxide-methanol solution, derivatized with boron trifluoride-methanol solution, extracted with hexane and stratified with saturated sodium chloride to obtain fatty acid methyl ester (FAMEs) samples. To quantification the fatty acid, mixtures of FAMEs: internal standard methyl nonadecanoate (1:1) were run on a Gas Chromatograph (GC-7890B, Agilent Technologies, Inc. USA) attached to a Mass Spectrometer Detector (MSD-5977A, Agilent Technologies, Inc. USA). Helium was the carrier gas, and the thermal gradient was set as from 125°C to 227°C at 2°C min^{-1}. Fatty acid profile identifications were performed by comparison to relative retention times of a known standard (GAQSIQ, 2008).

2.3 Statistical analyses

The contribution proportion of each source to macroinvertebrate diets was estimated based on $\delta^{13}C$, $\delta^{15}N$ or $\delta^{34}S$ values using the Bayesian stable isotope mixing model SIMMR (Parnell and Inger, 2019), which is a package in R (Team, 2019). Here, the food sources were divided into four groups mainly including seagrass (including *E. acoroides* and *T. hemprichii*), epiphytes (including epiphytes attached to *E. acoroides* and *T. hemprichii*), macroalgae (*U. lactuca*), and SPOM. SOM was excluded from SIMMR since that SOM is a mixture of other primary food sources (i.e., seagrass, epiphytes, macroalgae, and POM) (Xu et al., 2018). The $\delta^{34}S$ values of SPOM were not detected due to the relatively small amount of collected material and were not used in this model. The trophic enrichment factors (TEFs) in this Bayesian mixing model were $\delta^{13}C$ of 0.4 ± 1.3‰ and $\delta^{15}N$ of 2.3 ± 1.61‰ for snails, bivalves and polychaetes (Mascart et al., 2018; Débora et al., 2020), and $\delta^{13}C$ of 0.5 ± 0.8‰ and $\delta^{15}N$ of 3.2 ± 0.26‰ for crustaceans (Mittermayr et al., 2014; Riccialdelli et al., 2017; Beesley et al., 2020). This SIMMR model was based on normal (100,000) interactions, and outputs of the contributional proportion were expressed as mean value, 2.5%, 25%, 50%, 75% and, 99% confidence intervals (CI).

To explore whether the variation of multiple stable isotope ratios ($\delta^{13}C$, $\delta^{15}N$, and $\delta^{34}S$) was greatest amongst food sources (i.e., seagrass, epiphytes, macroalgae, SPOM, and SOM) or between seasons (i.e. summer and winter), all data were firstly checked the normality and/or homogeneity of variance using the Shapiro-Wilk test and Levene's test, respectively. Subsequently, a two-way ANOVAs was performed. Meanwhile, a *post-hoc* test (Tukey's HSD) was also applied in order to identify the specific differences among food source types. Furthermore, we also performed a one-way ANOVA or Mann-Whitney *U*-test to evaluate the seasonal changes of each food source in detail. Similarly, two-way ANOVAs were performed in order to test the significant differences amongst consumer groups (snails, crustaceans, bivalves, and polychaetes) and between seasons. The variations in the fatty acid markers of food sources and consumers were tested by a distance-based permutational analysis of variance (PERANOVA). This analysis used Euclidean distance resemblance calculated from untransformed data. In addition, to visualize multivariate patterns we generated a generalized discriminant analysis using Canonical Analysis of Principal Coordinates (CAP) (Anderson and Willis, 2003). To explore which fatty acid markers contributed most to the differences among food sources, we correlated the fatty acid data with the canonical axes. ANOVA analyses were performed with SPSS version 22 (IBM Corporation, Chicago, IL, USA), PERMANOVA and CAP were performed with PRIMER v6 software (Clarke and Gorley, 2006).

3 Result

3.1 Multiple stable isotopes of food sources and macrobenthos

The main food sources in Xincun seagrass bed displayed a wide range of $\delta^{13}C$ and $\delta^{34}S$ values (Figure 2), which correspondingly ranged from -18.6 ± 0.9‰ for winter SPOM to -8.4‰ for summer macroalgae (Appendix S1-Table A1), and from 5.6 ± 2.5‰ for winter SOM to 17.4 ± 0.2‰ for winter macroalgae, respectively. In contrast, the $\delta^{15}N$ values showed a narrow range, ranging from 5.5 ± 0.2‰ for winter SPOM to 8.6 ± 0.4‰ for summer macroalgae. Two-way ANOVA analysis showed distinct differences among the five food sources for $\delta^{13}C$, $\delta^{15}N$, and $\delta^{34}S$ values, while the clear distinction between seasons could only be found in $\delta^{13}C$ and $\delta^{34}S$ values (Table 1). *Post-hoc* test indicated that the difference in $\delta^{13}C$ values among the food sources was driven by the OM (organic matter, including SPOM and SOM), which differed from the seagrass, epiphytes, and macroalgae, respectively (Figure 2 and Appendix S1-Table A2). Whereas, significant differences in the $\delta^{15}N$ values only existed in seagrass versus macroalgae, epiphytes versus SPOM, and macroalgae versus OM, respectively. By contrast, all other food sources were significantly different for $\delta^{34}S$ values.Multiple stable isotope ($\delta^{13}C$, $\delta^{15}N$ and $\delta^{34}S$) values of macrobenthos were significantly different among groups (snail, crustaceans, bivalves and polychaetes, Two-way ANOVA, $\delta^{13}C$: $F_3 = 19.56$, $p = 0$, $\delta^{15}N$: $F_3 = 20.90$, $p = 0$, $\delta^{34}S$: $F_3 = 10.22$, $p = 0$), whereas there were no significant differences between seasons (Two-way ANOVA, $\delta^{13}C$: $F_1 = 0.33$, $p = 0.565$, $\delta^{15}N$: $F_1 = 0.03$, $p = 0.861$, $\delta^{34}S$: $F_1 = 8.19$, $p = 0.01$). In contrast to the food sources, macrobenthos had a reduced range in the $\delta^{13}C$ and $\delta^{34}S$ values, which ranged from -15.8 ± 0.2‰ (crustaceans *Calappa xp* in winter) to -7.3 ± 0.5‰ (snail *Notosinister subaura* in winter) for $\delta^{13}C$ values and from 8.8 ± 1.9‰ (polychaetes *Arenicola cristata* in summer) to 18.3 ± 0.5‰ (crustaceans *Calappa xp* in winter) for $\delta^{34}S$ values, redpectively. However, for $\delta^{15}N$ values, macrobenthos showed a larger range than that of food sources, ranging from 8‰ (snail *Notosinister subaura* in summer) to 12.1 ± 0.7‰ (crustaceans *Menippe rumphii* summer).

3.2 Fatty acid composition of food sources and macrobenthos

A total of twenty-one fatty acids were used for the profiles of food sources and macrobenthos (Appendix-Table A3). For food sources, percentages of saturated fatty acids accounted for greater than 50% of total fatty acids composition. PERANOVA of the total fatty acid data showed significant differences among food sources and between seasons (Table 1). CAP on total fatty acids showed that seagrass was significantly distinct from epiphytes and OM along the first axis, and the epiphytes were clearly separated from the macroalgae and OM along the second axis (Figure 3A), while SPOM had a greater overlap with SOM. When only poly-unsaturated fatty acids were considered (Figures 3B, 4), Fatty acids 18:2n6c and 18:3n3 for seagrass, 18:1n9c and 16:1n7 for epiphytes, and 18:1n9t, 20:1, 20:5n, 22:6n3, 18:3n6, and 14:1n5 for OM, were significantly higher than those of the other food sources. Macroalgae showed some certain degree of dispersed fatty acid profiles with relatively high levels of 15:1n5 in summer, and 18:1n9c in summer and winter, although these fatty acids also showed similarly high levels in seagrass and epiphytes.

For consumers, the percentages of saturated fatty acids still accounted for a larger proportion (55-75%) than unsaturated fatty

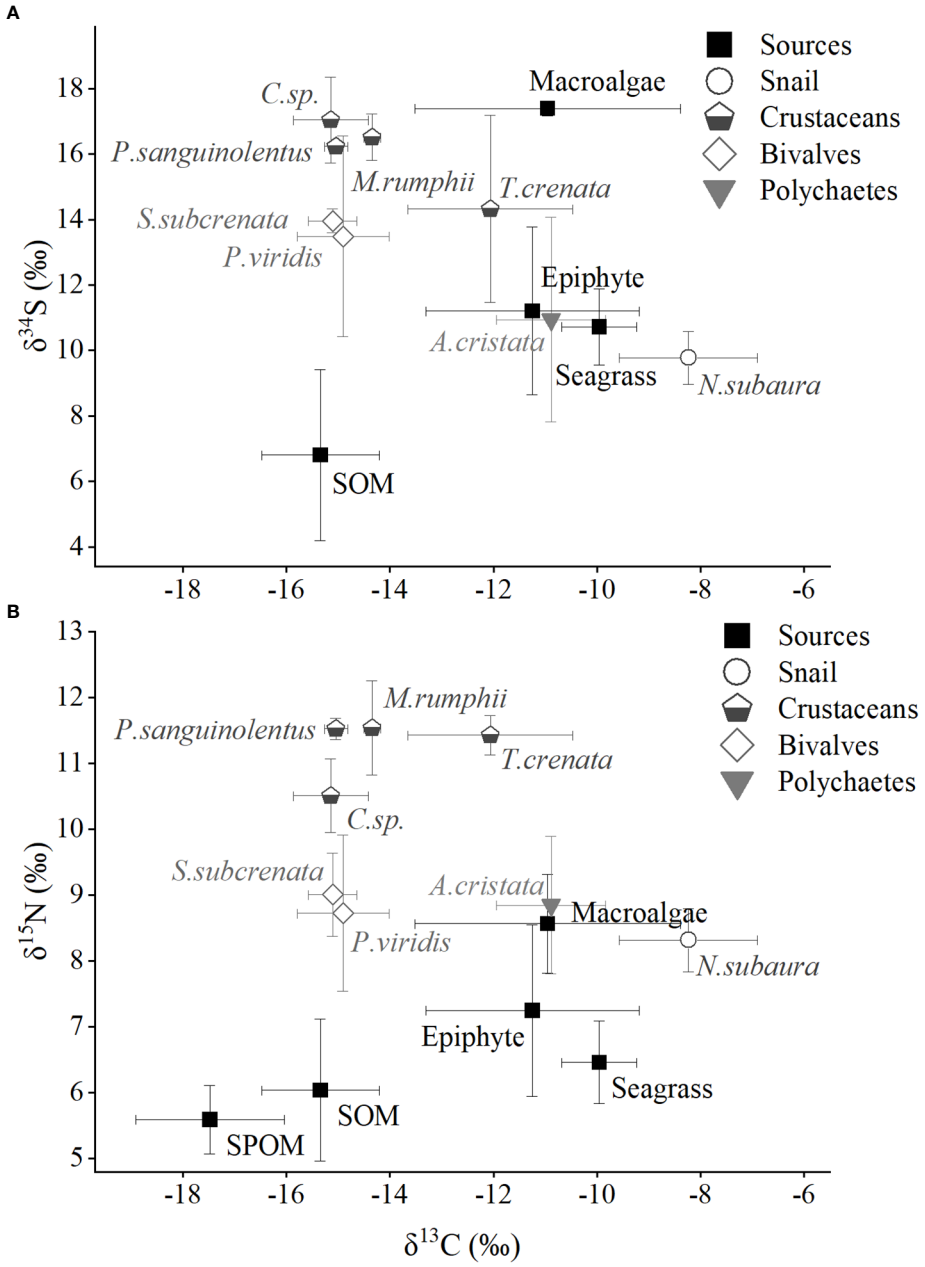

FIGURE 2
Annual mean values (including summer and winter) of isotopic signatures (**A**, $\delta^{13}C$ and $\delta^{15}N$; **B**, $\delta^{13}C$ and $\delta^{34}S$) for food sources and macroinvertebrates in Xincun seagrass bed. SPOM and SOM represent suspended particulate organic matter and sediment organic matter, respectively. The detailed labels of macroinvertebrates are given in Appendix-Table A1.

acids (26-47%), but it was lower than that of food sources (Appendix-Table A3). Significant differences in total fatty acids were also evident among groups (Table 1), while differences between seasons were not significant. Especially, for poly-unsaturated fatty acids, gastropods, crustaceans, and polychaetes had a high level of 18:1n9c and 20:5n3, while bivalves contained a high level of 16:1n7 and 22:6n3. In addition, the levels of 18:2n6c and 18:3n3 in snails and polychaetes were higher than those of other macrobenthos.

3.3 Isotopic mixing model

The SIMMR mixing models showed that the contribution of the food sources to most macrobenthos was relatively similar between seasons in this seagrass bed (Figure 5). For the snail *Notosinister subaura* and the polychaete *Arenicola cristata*, seagrass contributed the highest to their diet, with the corresponding mean value of 30-35% and 29-31%, respectively, while epiphytes contributed subordinately, with the corresponding mean value of 25-26% and

10.3389/fmars.2023.1093181

TABLE 1 Results of two-way ANOVA of multiple stable isotopic compositions ($\delta^{13}C$, $\delta^{15}N$, and $\delta^{34}S$) for food sources and consumers, and PERANOVA of fatty acids for food sources and consumers, (ns, no significant difference $p < 0.05$).

Source	df	MS	F	*p*
Food sources				
$\delta^{13}C$				
Species (type)	4	76.464	36.793	< 0.001
Seasons	1	15.628	7.52	**0.010**
Species×Seasons	4	10.241	4.928	**0.003**
Residual	31	2.078		
$\delta^{15}N$				
Species (type)	4	8.748	9.274	< 0.001
Seasons	1	2.537	2.689	0.111
Species×Seasons	4	0.675	0.716	0.588
Residual	31	0.943		
$\delta^{34}S$				
Species (type)	3	116.304	33.974	< 0.001
Seasons	1	9.177	2.681	0.113
Species×Seasons	3	9.709	2.836	0.057
Residual	27	3.423		
Total fatty acids				
Species (type)	4	1191.1	19.6	**0.001**
Seasons	1	316.5	5.2	**0.004**
Species×Seasons	4	205.0	3.4	**0.001**
Residual	24	60.8450		
Consumers				
$\delta^{13}C$				
Species (type)	3	48.635	28.333	< 0.001
Seasons	1	0.24	0.14	0.712
Species×Seasons	3	4.659	2.714	0.065
Residual	26	1.717		
$\delta^{15}N$				
Species (type)	3	17.682	25.399	< 0.001
Seasons	1	0.048	0.069	0.794
Species×Seasons	3	1.117	1.604	0.213
Residual	26	0.696		
$\delta^{34}S$				
Species (type)	3	57.691	13.512	< 0.001
Seasons	1	44.533	10.437	**0.003**
Species×Seasons	3	6.061	1.420	0.259
Residual	26	4.267		
Total fatty acids				

(Continued)

TABLE 1 Continued

Source	df	MS	F	*p*
Groups	3	450.1	3.512	**0.001**
Seasons	1	110.0	0.858	0.486
Groups×Seasons	3	122.2	0.953	0.496
Residual	18	128.2		

Numbers in bold indicate a significant result ($p < 0.05$).

24-29%, respectively. For the crustaceans, SPOM contributed significantly to *Calappa sp* and *Menippe rumphii* in summer, while macroalgae and SPOM were the main contributors to their diets in winter. The diet of *Portunus sanguinolentus* and *Thalamita crenata* had significantly seasonal variation, with a high contribution of epiphytes to *P.sanguinolentus* (67%) and macroalgae (42%) to *T.crenata* in summer, as well as the high contribution of macroalgae to their diets in winter (Figure 5). While for the bivalves *Perna viridis* and *Scapharca subcrenata*, SPOM showed a consistently high contribution to their diets in both seasons (mean value, 34-44% and 33-41%, respectively).

4 Discussion

4.1 Differences in the multiple stable isotopes and fatty acids among food sources

In the present study of tropical primary produces, the main variance of food sources for stable isotopes and fatty acids was amongst source types rather than seasons, except for the obvious seasonal variation in $\delta^{13}C$ values of macroalgae. In particular, the significant difference in $\delta^{13}C$ values between seagrass and OM allows this indicator to distinguish between vascular and organic matter. However, the wide range of $\delta^{13}C$ (from -14‰ to -7.9‰) and $\delta^{15}N$ (from 4.1‰ to 8.8‰) values for epiphytes overlapped with that of seagrass, which suggested the difficulty in using these biomarkers to identify the diets of consumers. The epiphytes attached to seagrass are mainly composed of bryozoans, diatoms *Cocconeis scutellum*, red algae, brown algae, small crustose coralline alga *Pneophyllum lejolisii*, bacteria, and fungi (Kharlamenko et al., 2001). The variation of environmental factors caused by stations (e.g. salinity and nutrient availability) and seasons (e.g. temperature and light) may lead to differences in the composition of epiphytes, and thus result in a large isotopic range (Nichols et al., 1985; Gacia et al., 2009; Liu et al., 2017). Similarly, the wide range of $\delta^{13}C$ values for macroalgae, overlapped with that of seagrass, might also be caused by these variations in environmental factors. This is mainly because the macroalgae *Ulva* sp. have been proven to be capable of both C3 and C4 photosynthesis (Valiela et al., 2018a), which may be affected by environmental factors (Xu et al., 2012). However, the $\delta^{15}N$ values of seagrass and macroalgae were significantly different, which indicated that we can use this indicator to distinguish macroalgae from seagrass. This may be reasonable because macroalgae are generally considered to assimilate significantly sufficient amounts of dissolved inorganic nitrogen from highly nutritious seawater columns in a shorter time

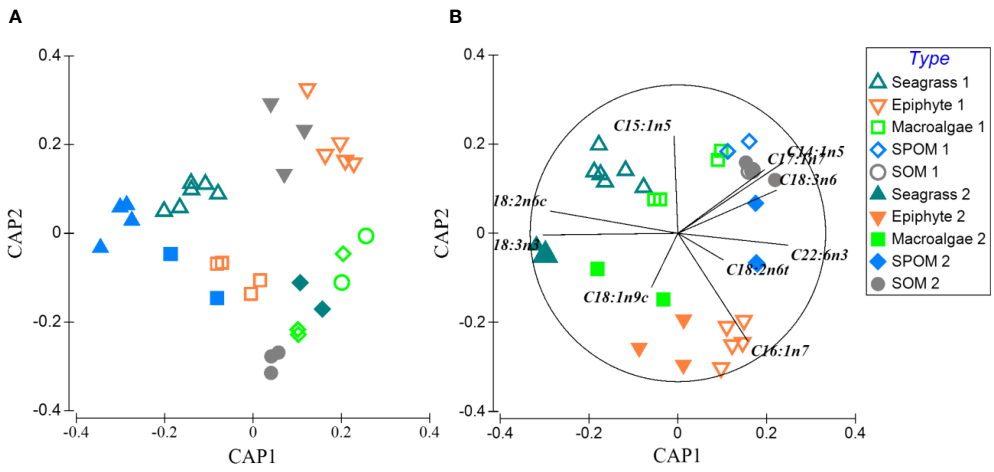

FIGURE 3
Constrained ordination (canonical analysis of principal coordinates, CAP) of total fatty acid composition from 5 sources in winter and summer of Xincun Bay. Hollow (1) and solid (2) symbols represent sources in summer and winter, respectively. **(A, B)** display the result of clustering results of total fatty acid composition from 5 sources, and principal component of the 5 sources, respectively.

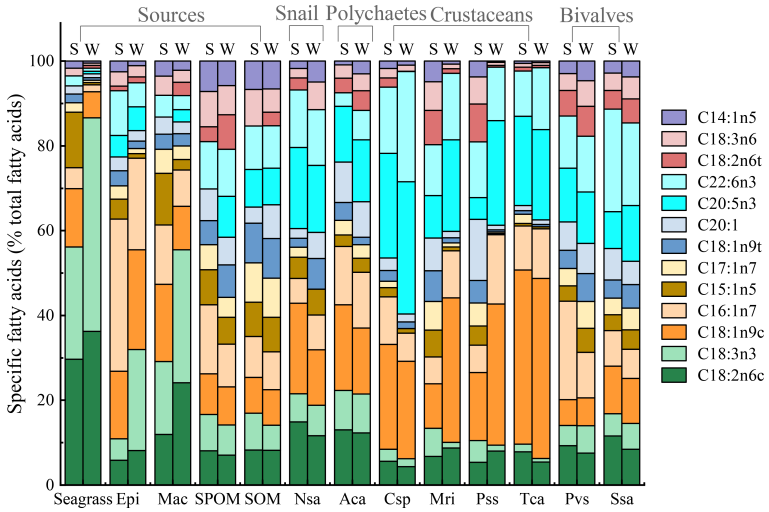

FIGURE 4
The percentages of specific fatty acids (% of total fatty acids) for the food sources and macroinvertebrates in summer (S) and winter (W) in the Xincun seagrass bed. Epi, Epiphyte; Mac, Macroalgae; Nsa, *Notosinister subaura*; Aca, *Arenicola cristata*; Cxp, *Calappa xp*; Mri, *Menippe rumphii*; Pss, *Portunus sanguinolentus*; Tca, *Thalamita crenata*; Pvs, *Perna viridis*; Ssa, *Scapharca subcrenata*.

than seagrass and OM (Gartner et al., 2002; Thornber et al., 2008), and previous study have shown that this area was subject to considerable anthropogenic nitrogen source input (Liu et al., 2020a).

Sulfur isotope was considered to be the most likely biomarker to effectively distinguish food sources since different food sources have distinct sulfur sources (Moncreiff and Sullivan, 2001). In the present study, significant differences in the $\delta^{34}S$ values of food sources among food sources helped distinguish food sources. In particular, the obvious difference in $\delta^{34}S$ values between macroalgae and epiphytes can make up for the limitation in the use of $\delta^{13}C$ and $\delta^{15}N$ values. Algae usually obtain more sulfur from seawater sulfate ($\delta^{34}S$ =20‰) than seagrass, which results in enriched $\delta^{34}S$ values (Moncreiff and Sullivan, 2001). In our study, the $\delta^{34}S$ values of macroalgae were the most enriched, which was similar to those of macroalgae in other seagrass beds (Holmer and Nielsen, 2007; Oduro et al., 2012). However, similar to $\delta^{13}C$ and $\delta^{15}N$ values, the $\delta^{34}S$ values of epiphytes and seagrass also exhibited significant overlap. This obvious overlap might be attributed to the difference in the composition of epiphytes among stations or the resuspension of benthic microalgae in some stations (Jorge and Van Beusekom, 1995; Kasim and Mukai, 2006), which led to great changes in the sulfur isotopes of epiphytes, ranging from 5.8‰ (close to the $\delta^{34}S$

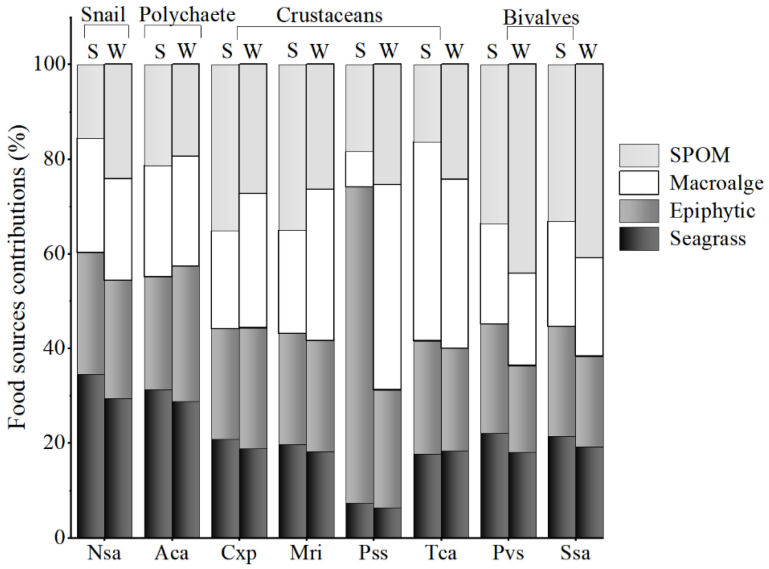

FIGURE 5
Mean relative contributions of food sources to the diets of macroinvertebrates in summer (S) and winter (W) in the Xincun seagrass bed. Nsa, *Notosinister subaura*; Aca, *Arenicola cristata*; Csp, *Calappa* sp.; Mri, *Menippe rumphii*; Pss, *Portunus* sp.; Tca, *Thalamita crenata*; Pvs, *Perna viridis*; Ssa, *Scapharca subcrenata*. The detailed outputs of contribution proportion calculated by SIMMR are given in Supporting information Table A5.

values of 6.8‰ SOM in this area) to 15.5‰. In addition, significant seasonal differences in $\delta^{34}S$ values of seagrass and epiphytes may also increase the overlapping probability of their $\delta^{34}S$ values. Therefore, the combination of multiple stable isotopes cannot completely distinguish the food sources in this area.

In comparison to the multiple stable isotope data, the fatty acid compositions of food sources are generally considered to be significantly different (Crawley et al., 2009; Madgett et al., 2019). In our study, all food sources were rich in saturated fatty acids (61%-77%), especially 16:0, which was similar to the research results in other seagrass beds (Crawley et al., 2009; Park et al., 2013). In contrast, the unsaturated fatty acid compositions among food sources were clearly distinct. The much higher level of 18:2n6c and 18:3n3 in seagrass, 16:1n7 in epiphytes and 18:1n9t, 20:1, 20:5n3, 22:6n3 18:2n6t,18:2n6 and 14:1n5 in OM can effectively separate seagrass, epiphytes, and OM from each other. It is worth noting that 20:5n3 and 22:6n3 were also abundant in epiphytes. The unsaturated fatty acids 16:1n7, 20:5n3, and 22:6n3 are generally biosynthesized by diatoms (Coelho et al., 2011) and have been used as benthic diatom biomarkers (Kharlamenko et al., 2001; Belicka et al., 2012; Jankowska et al., 2018). Therefore, diatoms mainly originated from the resuspension of SOM might have an important effect on the component of epiphytes, which can also explain the wide range of $\delta^{13}C$ values for epiphytes and the overlap in $\delta^{15}N$ and $\delta^{34}S$ values for epiphytes and SOM in this area. In addition, the fatty acid compositions of macroalgae were also similar to that of seagrass and epiphytes, with a high level of 18:2n6c and 18:3n3. Such fatty acid composition characteristics of seagrass and macroalgae were also evidenced in other temperate bays (Meziane and Tsuchiya, 2000; Lebreton et al., 2011). The most likely explanation was that macroalgae and seagrass are in the same lineage with the same suite of photosynthetic pigments and similar biochemical pathways (Galloway et al., 2012). These characteristics limit us to distinguish seagrass and macroalgae based on their specific fatty acid compositions.

4.2 Application of multiple stable isotopes and fatty acids markers in different macrobenthos

Despite the combination of multiple stable isotopes and fatty acid biomarkers can make a clear distinction for food sources, caution is still required with interpretations of field-based biomarker studies, as some factors such as growth rates, metabolism, and mixed diets will affect the isotope values and fatty acid compositions of consumers (Hanson et al., 2010; Pecquerie et al., 2010). In this study, the accuracy of using multiple stable isotopes and fatty acid biomarkers to identify the diets of different trophic groups was significantly different. The filter-feeder bivalves are the only trophic group, of which diets can be accurately identified by the stable isotopes and fatty acid biomarkers. This has been proved by the similar $\delta^{13}C$ values for these bivalves (*P. sanguinolentus* and *S. subcrenata*) and OM, and the high level of OM FA markers 18:2n6c, 22:6n3, and 20:5n3 for these bivalves, which all indicated the significant OM contribution to their diets. However, for the grazer snail *N. subaura*, its $\delta^{13}C$, $\delta^{15}N$, and $\delta^{34}S$ values significantly overlapped with that of seagrass and epiphytes. This indicated that their main food sources were more likely to be seagrass, which was also confirmed by the SIMMR results. Accordingly, the seagrass FA marker 18:2n6c in the snail was indeed higher than that of other consumers, whereas, the most abundant fatty acid composition in the snail was OM indicators 20:5n3 and 22:6n3, which may mislead us to identify the diet of this snail. The most likely reason is that there are some transformations in the process of assimilation of fatty acids by the snails. Evidence to date indicates that some primary consumers, such as herbivores, have the ability to convert C18 fatty acids to 20:5n3 and 22:6n3 (Caramujo et al., 2008; McLeod et al., 2013), therefore a high level of 20:5n3 and 22:6n3 in these consumers may be transformed by the seagrass biomarker 18:2n6c. Similarly, although the $\delta^{13}C$, $\delta^{15}N$, and $\delta^{34}S$ values of deposit feeder polychaete *A. cristata* were more similar to that of seagrass and epiphytes, the level of 18:2n6c in the polychaete was not clearly higher than that of other unsaturated fatty acids (i.g., 20:5n3 and 20:6n3), which indicated that the polychaete may also have the ability to convert these fatty acids.

Most crustaceans are known to be omnivores or generalized predators and have mixed diets, therefore there may be great obscure when using $\delta^{13}C$ and $\delta^{15}N$ values to identify their diets (Reaka-Kudla, 2001). In this study, the $\delta^{13}C$ values of predators *P. sanguinolentus* and *M. rumphii* overlapped more with those of OM in both seasons, which is often mistakenly believed that their carbon sources were mainly OM in both seasons (Fan et al., 2011; Du et al., 2019). The mixing model also showed a high POM contribution to their diets. Whereas, their $\delta^{13}C$ values were also located in the middle of OM and epiphytes, which also indicated they might feed on OM and epiphytes together. This possibility has also been confirmed by their fatty acid composition. The high level of OM FA marker 18:2n6c in summer, and OM FA markers (20:5n3, 22:6n3, and 18:2n6t) and epiphytes FA markers (18:1n9c and 16:1n7) in winter indicated that their food sources were OM in summer and OM and epiphytes in winter, respectively. Some researchers also suggested that OM and epiphytes had a high contribution to the predator crustaceans (Ning et al., 2019; Paar et al., 2019).

Similarly, it is also difficult to accurately distinguish the diets of omnivores crab *C.* sp. and *T. crenata* because of their wide range of $\delta^{13}C$ and $\delta^{15}N$ values. The SIMMR results showed the relative average coverage contribution of each food source to *C.* sp. and the high contribution of macroalgae to *T. crenata*. Relatively higher levels of epiphytes FA marker 16:1n7 and OM FA markers 20:5n3 and 22:6n3 in these omnivores indicated a mixed diets contribution of epiphytes and OM. Nevertheless, the significantly high level of FA marker 18:1n9 in the omnivores during summer suggested that their chief food source was probably macroalgae. Therefore, it is necessary to further distinguish epiphytes from macroalgae by the $\delta^{34}S$ values. Considering the trophic fraction of $\delta^{34}S$ values was from 0 to 1.9 (McCutchan et al., 2003; Mittermayr et al., 2014), and the higher $\delta^{34}S$ values of macroalgae were higher than that of these omnivores. Therefore, the food sources of these omnivores were more likely to be epiphytes and OM.

Overall, for diverse primary producers in our tropical seagrass bed food webs study, multiple stable isotopes usually change obviously among primary producer species and seasons within a region. This characteristic would affect the application of multiple isotopes to identify the food sources of dispersed consumers.

Whereas, for snails, polychaetes and bivalves, multiple isotopes usually could discriminate their food sources, because limited mobile ability induced their diets to be often relatively single and fixed within a period and region (Fukumori et al., 2008; Tue et al., 2012; Cui et al., 2021b). By contrast, fatty acids generally provide clearer separation of primary producer species than multiple stable isotopes by providing specific FA biomarkers for each food source. This characteristic would allow FAs to identify the food sources of crustaceans with complex diets. However, the specific FA marker of each species might be the same due to they might have the same suite of photosynthetic pigments and similar biochemical pathways (i.e., seagrass and macroalgae in this study) (Galloway et al., 2012), and its dynamic is always linked with the metabolic conditions of the consumers (i.e., snails in this study). Therefore, using both types of biomarkers together may reduce the uncertainty caused by natural variation and thus strengthen the separation of food sources and the diets of different consumer species. Further study is needed to apply multiple isotopes and fatty acids into the mixing model to quantify the diet contribution of consumers. In addition, in our study, most consumers have a high level of diatom biomarkers, which indicated microphytobenthos might also be their important food source. Therefore, further study in seagrass ecosystems is also needed to consider microphytobenthos as an independent carbon source.

5 Conclusions

Our study has evaluated various food sources and macrobenthos in a tropical seagrass bed, and has shown that the combination of multiple stable isotopes and fatty acids is essential in identifying the diets of consumers. We showed that the use of a combination of multiple stable isotopes and fatty acids can effectively distinguish different food sources, among which multiple stable isotopic compositions (particularly $\delta^{13}C$ and $\delta^{34}S$) can distinguish seagrass and epiphytes from other food sources, while the application of fatty acid markers can distinguish seagrass from epiphytes. In addition, we evaluated for the first time the feasibility of applying this combination to identify the food sources of macrobenthos in tropical seagrass beds. Our results indicated that multiple stable isotopic compositions are more useful than fatty acid markers in identifying the diets of grazers snails and deposit feeder polychaetes due to the transformation in the process of fatty acids assimilation. In contrast, fatty acid markers are more useful in identifying the diets of predatory crustaceans due to their mixed diets. Whereas the identification of omnivorous crustaceans food sources requires the combination of multiple stable isotopes and fatty acids biomarkers due to their wide range of isotope values. The bivalves are the only consumer that can be effectively evaluated by both stable isotopes and fatty acids biomarkers.

Data availability statement

The original contributions presented in the study are included in the article/Supplementary Material. Further inquiries can be directed to the corresponding authors.

Ethics statement

The animal study was reviewed and approved by the South China Sea Institute of Oceanology, Chinese Academy of Sciences.

Author contributions

LC: Conceptualization, Methodology, Investigation, Formal analysis, Visualization, Writing - original draft. ZJ: Conceptualization, Investigation, Writing - review & editing. XH: Supervision, Conceptualization Writing - review & editing, Funding acquisition. SL: Investigation, Writing – review. YW: Investigation. All authors contributed to the article and approved the submitted version.

Funding

This research was supported by Nansha District Science and Technology Plan Project Incentive Fund, National Natural Science Foundation of China (nos. 41730529, U1901221, 42176158), Key Special Project for Introduced Talents Team of Southern Marine Science and Engineering Guangdong Laboratory (Guangzhou) (GML2019ZD0405), the Natural Science Fund of Guangdong (2019A1515010552, 2020A1515010907, 2018A030310043), and the Science and Technology Planning Project of Guangdong Province, China (2020B1212060058).

Acknowledgments

The authors thank Shouhui Dai and Qiming Chen for performing the stable isotope analyses.

Conflict of interest

The authors declare that the research was conducted in the absence of any commercial or financial relationships that could be construed as a potential conflict of interest.

Publisher's note

All claims expressed in this article are solely those of the authors and do not necessarily represent those of their affiliated organizations, or those of the publisher, the editors and the reviewers. Any product that may be evaluated in this article, or claim that may be made by its manufacturer, is not guaranteed or endorsed by the publisher.

Supplementary material

The Supplementary Material for this article can be found online at: https://www.frontiersin.org/articles/10.3389/fmars.2023.1093181/full#supplementary-material

References

Abrantes, K., and Sheaves, M. (2009). Food web structure in a near-pristine mangrove area of the Australian wet tropics. *Estuarine Coast. Shelf Sci.* 82, 597–607. doi: 10.1016/j.ecss.2009.02.021

Anderson, M. J., and Willis, T. J. (2003). Canonical analysis of principal coordinates: a useful method of constrained ordination for ecology. *Ecology* 84, 511–525. doi: 10.1890/0012-9658(2003)084[0511:CAOPCA]2.0.CO;2

Beesley, L. S., Pusey, B. J., Douglas, M. M., Gwinn, D. C., Canham, C. A., Keogh, C. S., et al. (2020). New insights into the food web of an Australian tropical river to inform water resource management. *Sci. Rep.* 10, 14294. doi: 10.1038/s41598-020-71331-0

Belicka, L. L., Burkholder, D., Fourqurean, J. W., Heithaus, M. R., MacKo, S. A., and Jaff, R. (2012). Stable isotope and fatty acid biomarkers of seagrass, epiphytic, and algal organic matter to consumers in a pristine seagrass ecosystem. *Mar. Freshw. Res.* 63, 1085–1097. doi: 10.1071/MF12027

Canadell, J. G., and Jackson, R. B. (2021). *Ecosystem collapse and climate change: an introduction* (Cham: Springer International Publishing). doi: 10.1007/978-3-030-71330-0_1

Caramujo, M. J., Boschker, H. T. S., and Admiraal, W. (2008). Fatty acid profiles of algae mark the development and composition of harpacticoid copepods. *Freshw. Biol.* 53, 77–90. doi: 10.1111/j.1365-2427.2007.01868.x

Caut, S., Angulo, E., and Courchamp, F. (2009). Variation in discrimination factors (Δ15N and Δ13C): the effect of diet isotopic values and applications for diet reconstruction. *J. Appl. Ecol.* 46, 443–453. doi: 10.1111/j.1365-2664.2009.01620.x

Clarke, K., and Gorley, R. (2006). PRIMER v6: user Manual/Tutorial. *Primer-E Ltd.: Plymouth UK.* 1–182.

Coelho, H., Lopes da Silva, T., Reis, A., Queiroga, H., Serôdio, J., and Calado, R. (2011). Fatty acid profiles indicate the habitat of mud snails hydrobia ulvae within the same estuary: mudflats vs. seagrass meadows. *Estuarine Coast. Shelf Sci.* 92, 181–187. doi: 10.1016/j.ecss.2011.01.005

Crawley, K. R., Hyndes, G. A., Vanderklift, M. A., Revill, A. T., and Nichols, P. D. (2009). Allochthonous brown algae are the primary food source for consumers in a temperate, coastal environment. *Mar. Ecol. Prog. Ser.* 376, 33–44. doi: 10.3354/meps07810

Cui, L., Jiang, Z., Huang, X., Chen, Q., Wu, Y., Liu, S., et al. (2021a). Eutrophication reduces seagrass contribution to coastal food webs. *Ecosphere* 12:e03626. doi: 10.1002/ecs2.3626

Cui, L., Jiang, Z., Huang, X., Wu, Y., Liu, S., Chen, Q., et al. (2021b). Carbon transfer processes of food web and trophic pathways in a tropical eutrophic seagrass meadow. *Front. Mar. Sci.* 8. doi: 10.3389/fmars.2021.725282

Débora, R., de, C., Carlos, B. M. A., Marcelo, Z. M., and Paulo, S. P. (2020). Trophic diversity and carbon sources supporting fish communities along a pollution gradient in a tropical river. *Sci. Total Environ.* 738, 139878. doi: 10.1016/j.scitotenv.2020.139878

Du, J., Chen, Z., Xie, M., Chen, M., Zheng, X., Liao, J., et al. (2019). Analysis of organic carbon sources in tropical seagrass fish: a case study of the east coast of Hainan Province. *Mar. Biol. Res.* 15, 513–522. doi: 10.1080/17451000.2019.1673896

Fan, M., Huang, X., Zhang, D., Zhang, J., Jiang, Z., and Zeng, Y. (2011). Food sources of fish and macro-invertebrates in a tropical seagrass bed at Xincun Bay, Southern China. *Shengtai Xuebao/ Acta Ecologica Sin.* 31, 31–38 (in Chinese).

Folch, J., Lees, M., and Sloane stanley, G. H. (1957). A simple method for the isolation and purification of total lipides from animal tissues. *J. Biol. Chem.* 226, 497–509. doi: 10.1016/s0021-9258(18)64849-5

Fritts, A. K., Knights, B. C., Lafrancois, T. D., Bartsch, L. A., Vallazza, J. M., Bartsch, M. R., et al. (2018). Spatial and temporal variance in fatty acid and stable isotope signatures across trophic levels in large river systems. *River Res. Appl.* 34, 834–843. doi: 10.1002/rra.3295

Fukumori, K., Oi, M., Doi, H., Takahashi, D., Okuda, N., Miller, T. W., et al. (2008). Bivalve tissue as a carbon and nitrogen isotope baseline indicator in coastal ecosystems. *Estuarine Coast. Shelf Sci.* 79, 45–50. doi: 10.1016/j.ecss.2008.03.004

Gacia, E., Costalago, D., Prado, P., Piorno, D., and Tomas, F. (2009). Mesograzers in posidonia oceanica meadows: an update of data on gastropod-epiphyte-seagrass interactions. *Botanica Marina* 52, 439–447. doi: 10.1515/BOT.2009.054

Gagnon, K., Gustafsson, C., Salo, T., Rossi, F., Gunell, S., Richardson, J. P., et al. (2021). Role of food web interactions in promoting resilience to nutrient enrichment in a brackish water eelgrass (Zostera marina) ecosystem. *Limnol. Oceanogr.* 66, 2810–2826. doi: 10.1002/lno.11792

Galloway, A. W. E., Britton-Simmons, K. H., Duggins, D. O., Gabrielson, P. W., and Brett, M. T. (2012). Fatty acid signatures differentiate marine macrophytes at ordinal and family ranks. *J. Phycol.* 48, 956–965. doi: 10.1111/j.1529-8817.2012.01173.x

GAQSIQ (2008). *Determination of total fat, saturated fat, and unsaturated fat in foods: hydrolytic extraction-gas chromatography* (Beijing: Standards Press of China).

Gartner, A., Lavery, P., and Smit, A. J. (2002). Use of δ15N signatures of different functional forms of macroalgae and filter-feeders to reveal temporal and spatial patterns in sewage dispersal. *Mar. Ecol. Prog. Ser.* 235, 63–73. doi: 10.3354/meps235063

Guiry, E., Noël, S., and Fowler, J. (2021). Archaeological herbivore δ13C and δ34S provide a marker for saltmarsh use and new insights into the process of 15N-enrichment in coastal plants. *J. Archaeol. Sci.* 125:14750-14760. doi: 10.1016/j.jas.2020.105295

Hanson, C. E., Hyndes, G. A., and Wang, S. F. (2010). Differentiation of benthic marine primary producers using stable isotopes and fatty acids: implications to food web studies. *Aquat. Bot.* 93, 114–122. doi: 10.1016/j.aquabot.2010.04.004

Holmer, M., and Nielsen, R. M. (2007). Effects of filamentous algal mats on sulfide invasion in eelgrass (Zostera marina). *J. Exp. Mar. Biol. Ecol.* 353, 245–252. doi: 10.1016/j.jembe.2007.09.010

Huang, X., Huang, L., Li, Y., Xu, Z., Fong, C. W., Huang, D., et al. (2006). Main seagrass beds and threats to their habitats in the coastal sea of South China. *Chin. Sci. Bull.* 51, 136–142. doi: 10.1007/s11434-006-9136-5

Huang, X., Jiang, Z., Liu, S., Yu, S., Wu, Y., Zhang, J., et al. (2019). *Study on ecology of tropical seagrass in China* (Beijing: Science China Press (in Chinese).

Ivajnšič, D., Orlando-Bonaca, M., Donša, D., Grujić, V. J., Trkov, D., Mavrič, B., et al. (2022). Evaluating seagrass meadow dynamics by integrating field-based and remote sensing techniques. *Plants* 11, 1196. doi: 10.3390/plants11091196

Jankowska, E., De Troch, M., Michel, L. N., Lepoint, G., and Włodarska-Kowalczuk, M. (2018). Modification of benthic food web structure by recovering seagrass meadows, as revealed by trophic markers and mixing models. *Ecol. Indic.* 90, 28–37. doi: 10.1016/j.ecolind.2018.02.054

Jiang, Z., Zhao, C., Yu, S., and Liu, S. (2019). Contrasting root length, nutrient content and carbon sequestration of seagrass growing in offshore carbonate and onshore terrigenous sediments in the South China Sea. *Sci. Total Environ.* 662, 151–159. doi: 10.1016/j.scitotenv.2019.01.175

Jinks, K. I., Rasheed, M. A., Brown, C. J., Olds, A. D., Schlacher, T. A., Sheaves, M., et al. (2020). Saltmarsh grass supports fishery food webs in subtropical Australian estuaries. *Estuarine Coast. Shelf Sci.* 238, 106719. doi: 10.1016/j.ecss.2020.106719

Jorge, V. N., and Van Beusekom, J. E. E. (1995). Wind- and tide-induced resuspension of sediment and microphytobenthos from tidal flats in the Ems estuary. *Limnol. Oceanogr.* 40, 776–778. doi: 10.4319/lo.1995.40.4.0776

Kasim, M., and Mukai, H. (2006). Contribution of benthic and epiphytic diatoms to clam and oyster production in the Akkeshi-ko estuary. *J. Oceanogr.* 62, 267–281. doi: 10.1007/s10872-006-0051-9

Kharlamenko, V. I., Kiyashko, S. I., Imbs, A. B., and Vyshkvartzev, D. I. (2001). Identification of food sources of invertebrates from the seagrass Zostera marina community using carbon and sulfur stable isotope ratio and fatty acid analyses. *Mar. Ecol. Prog. Ser.* 220, 103–117. doi: 10.3354/meps220103

Kohlbach, D., Hop, H., Wold, A., Schmidt, K., Smik, L., Belt, S. T., et al. (2021). Multiple trophic markers trace dietary carbon sources in barents sea zooplankton during late summer. *Front. Mar. Sci.* 7. doi: 10.3389/fmars.2020.610248

Lebreton, B., Richard, P., Galois, R., Radenac, G., Pfléger, C., Guillou, G., et al. (2011). Trophic importance of diatoms in an intertidal Zostera noltii seagrass bed: evidence from stable isotope and fatty acid analyses. *Estuarine Coast. Shelf Sci.* 92, 140–153. doi: 10.1016/j.ecss.2010.12.027

Lippold, A., Aars, J., Andersen, M., Aubail, A., Derocher, A. E., Dietz, R., et al. (2020). Two decades of mercury concentrations in barents sea polar bears (Ursus maritimus) in relation to dietary carbon, sulfur, and nitrogen. *Environ. Sci. Technol.* 54, 7388–7397. doi: 10.1021/acs.est.0c01848

Liu, S., Deng, Y., Jiang, Z., Wu, Y., Huang, X., and Macreadie, P. I. (2020a). Nutrient loading diminishes the dissolved organic carbon drawdown capacity of seagrass ecosystems. *Sci. Total Environ.* 740, 140185. doi: 10.1016/j.scitotenv.2020.140185

Liu, S., Jiang, Z., Zhang, J., Wu, Y., Huang, X., and Macreadie, P. I. (2017). Sediment microbes mediate the impact of nutrient loading on blue carbon sequestration by mixed seagrass meadows. *Sci. Total Environ.*, 599–600 1479–1484. doi: 10.1016/j.scitotenv.2017.05.129

Liu, S., Trevathan-Tackett, S. M., Ewers Lewis, C. J., Huang, X., and Macreadie, P. I. (2020b). Macroalgal blooms trigger the breakdown of seagrass blue carbon. *Environ. Sci. Technol.* 54, 14750–14760. doi: 10.1021/acs.est.0c03720

Madgett, A. S., Yates, K., Webster, L., McKenzie, C., and Moffat, C. F. (2019). Understanding marine food web dynamics using fatty acid signatures and stable isotope ratios: improving contaminant impacts assessments across trophic levels. *Estuarine Coast. Shelf Sci.* 227, 106327. doi: 10.1016/j.ecss.2019.106327

Mascart, T., De Troch, M., Remy, F., Michel, L. N., and Lepoint, G. (2018). Seasonal dependence on seagrass detritus and trophic niche partitioning in four copepod eco-morphotypes. *Food Webs* 16, e00086. doi: 10.1016/j.fooweb.2018.e00086

McCutchan, J. H., Lewis, W. M., Kendall, C., and McGrath, C. C. (2003). Variation in trophic shift for stable isotope ratios of carbon, nitrogen, and sulfur. *Oikos* 102, 378–390. doi: 10.1034/j.1600-0706.2003.12098.x

McLeod, R. J., Hyndes, G. A., Hurd, C. L., and Frew, R. D. (2013). Unexpected shifts in fatty acid composition in response to diet in a common littoral amphipod. *Mar. Ecol. Prog. Ser.* 479, 1–12. doi: 10.3354/meps10327

Meziane, T., and Tsuchiya, M. (2000). Fatty acids as tracers of organic matter in the sediment and food web of a mangrove/intertidal flat ecosystem, Okinawa, Japan. *Mar. Ecol. Prog. Ser.* 200, 49–57. doi: 10.3354/meps200049

Mittermayr, A., Fox, S. E., and Sommer, U. (2014). Temporal variation in stable isotope composition (δ13C, δ15N and δ34S) of a temperate Zostera marina food web. *Mar. Ecol. Prog. Ser.* 505, 95–105. doi: 10.3354/meps10797

Moncreiff, C. A., and Sullivan, M. J. (2001). Trophic importance of epiphytic algae in subtropical seagrass beds: evidence from multiple stable isotope analyses. *Mar. Ecol. Prog. Ser.* 215, 93–106. doi: 10.3354/meps215093

Nakamoto, K., Hayakawa, J., Kawamura, T., Ohtsuchi, N., Yamada, H., Kitagawa, T., et al. (2019). Seasonal fluctuation in food sources of herbivorous gastropods in a subtropical seagrass bed estimated by stable isotope analysis. *J. Mar. Biol. Assoc. United Kingdom* 99, 1119–1125. doi: 10.1017/S0025315418001108

Nichols, P. D., Klumpp, D. W., and Johns, R. B. (1985). A study of food chains in seagrass communities iii. stable carbon isotope ratios. *Mar. Freshw. Res.* 36, 683–690. doi: 10.1071/MF9850683

Ning, J., Du, F., Wang, X., Wang, L., and Li, Y. (2019). Trophic connectivity between intertidal and offshore food webs in Mirs Bay, China. *Oceanologia* 61, 208–217. doi: 10.1016/j.oceano.2018.10.001

Oduro, H., Van Alstyne, K. L., and Farquhar, J. (2012). Sulfur isotope variability of oceanic DMSP generation and its contributions to marine biogenic sulfur emissions. *Proc. Natl. Acad. Sci. United States America* 109, 9012–9016. doi: 10.1073/pnas.1117691109

Paar, M., Lebreton, B., Graeve, M., Greenacre, M., Asmus, R., and Asmus, H. (2019). Food sources of macrozoobenthos in an Arctic kelp belt: trophic relationships revealed by stable isotope and fatty acid analyses. *Mar. Ecol. Prog. Ser.* 615, 31–49. doi: 10.3354/meps12923

Park, H. J., Choy, E. J., Lee, K., and Kang, C. (2013). Trophic transfer between coastal habitats in a seagrass-dominated macrotidal embayment system as determined by stable isotope and fatty acid signatures. *Mar. Freshw. Res.* 64, 1169–1183. doi: 10.1071/MF12327

Parnell, A., and Inger, R. (2019) *Stable isotope mixing models in R with simmr*. Available at: https://cran.r-project.org/web/packages/simmr/vignettes/simmr.html.

Pecquerie, L., Nisbet, R. M., Fablet, R., Lorrain, A., and Kooijman, S. A. L. M. (2010). The impact of metabolism on stable isotope dynamics: a theoretical framework. *Philos. Trans. R. Soc. B: Biol. Sci.* 365, 3455–3468. doi: 10.1098/rstb.2010.0097

Pellerin, A., Antler, G., Holm, S. A., Findlay, A. J., Crockford, P. W., Turchyn, A. V., et al. (2019). Large Sulfur isotope fractionation by bacterial sulfide oxidation. *Sci. Adv.* 5, 1–7. doi: 10.1126/sciadv.aaw1480

Reaka-Kudla, M. L. (2001). Crustaceans. *Encyclopedia Biodivers.: Second Edition* 1, 396–418. doi: 10.1016/B978-0-12-384719-5.00165-9

Riccialdelli, L., Newsome, S. D., Fogel, M. L., and Fernández, D. A. (2017). Trophic interactions and food web structure of a subantarctic marine food web in the Beagle Channel: Bahía Lapataia, Argentina. *Polar Biol.* 40, 807–821. doi: 10.1007/s00300-016-2007-x

Saderne, V., Geraldi, N. R., Macreadie, P. I., Maher, D. T., Middelburg, J. J., Serrano, O., et al. (2019). Role of carbonate burial in Blue Carbon budgets. *Nat. Commun.* 10, 1–9. doi: 10.1038/s41467-019-08842-6

Sun, H., Li, Y., Hao, Y., Zhu, Y., Yang, R., Wang, P., et al. (2020). Bioaccumulation and trophic transfer of polybrominated diphenyl ethers and their hydroxylated and methoxylated analogues in polar marine food webs. *Environ. Sci. Technol.* 54, 15086–15096. doi: 10.1021/acs.est.0c05427

Team, R. C. (2019). *R: a language and environment for statistical computing* (R Foundation for Statistical Computing, Vienna, Austria).

Thornber, C. S., DiMilla, P., Nixon, S. W., and McKinney, R. A. (2008). Natural and anthropogenic nitrogen uptake by bloom-forming macroalgae. *Mar. pollut. Bull.* 56, 261–269. doi: 10.1016/j.marpolbul.2007.10.031

Tue, N. T., Hamaoka, H., Sogabe, A., Quy, T. D., Nhuan, M. T., and Omori, K. (2012). Food sources of macro-invertebrates in an important mangrove ecosystem of Vietnam determined by dual stable isotope signatures. *J. Sea Res.* 72, 14–21. doi: 10.1016/j.seares.2012.05.006

Unsworth, R. K. F., Nordlund, L. M., and Cullen-Unsworth, L. C. (2019). Seagrass meadows support global fisheries production. *Conserv. Lett.* 12, 1–8. doi: 10.1111/conl.12566

Valiela, I., Liu, D., Lloret, J., Chenoweth, K., and Hanacek, D. (2018a). Stable isotopic evidence of nitrogen sources and C4 metabolism driving the world's largest macroalgal green tides in the Yellow Sea. *Sci. Rep.* 8, 1–12. doi: 10.1038/s41598-018-35309-3

Valiela, I., Pascual, J., Giblin, A., Barth-Jensen, C., Martinetto, P., Otter, M., et al. (2018b). External and local controls on land-sea coupling assessed by stable isotopic signatures of mangrove producers in estuaries of Pacific Panama. *Mar. Environ. Res.* 137, 133–144. doi: 10.1016/j.marenvres.2018.03.003

Weems, J., Iken, K., Gradinger, R. , and Wooller, M. J. (2012). Carbon and nitrogen assimilation in the Bering Sea clams Nuculana radiata and Macoma moesta. *J. Exp. Mar. Biol. Ecol.*, 430–431, 32–42. doi: 10.1016/j.jembe.2012.06.015

Xu, W.-Z., Cheung, S. G., Zhang, Z.-N., and Shin, P. K. S. (2018). Dual isotope assessment of trophic dynamics of an intertidal infaunal community with seasonal shifts in food sources. *Mar. Biol.* 165, 21. doi: 10.1007/s00227-017-3278-7

Xu, J., Fan, X., Zhang, X., Xu, D., Mou, S., Cao, S., et al. (2012). Evidence of coexistence of C3 and C4 photosynthetic pathways in a green-tide-forming alga, ulva prolifera. *PloS One* 7, 1–10. doi: 10.1371/journal.pone.0037438

Xu, H., Turchini, G. M., Francis, D. S., Liang, M., Mock, T. S., Rombenso, A., et al. (2020). Are fish what they eat? a fatty acid's perspective. *Prog. Lipid Res.* 80, 101064. doi: 10.1016/j.plipres.2020.101064

Frontiers in Marine Science

Explores ocean-based solutions for emerging global challenges

The third most-cited marine and freshwater biology journal, advancing our understanding of marine systems and addressing global challenges including overfishing, pollution, and climate change.

Discover the latest Research Topics

See more →

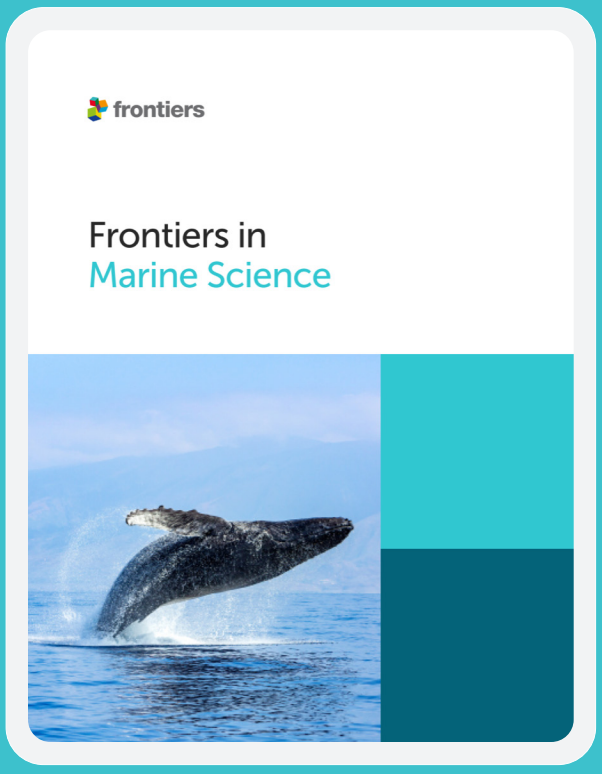

Frontiers

Avenue du Tribunal-Fédéral 34
1005 Lausanne, Switzerland
frontiersin.org

Contact us

+41 (0)21 510 17 00
frontiersin.org/about/contact